MOLECULAR MECHANISM OF NECROPTOSIS IN MACROPHAGES

SAHIL YADAV

Thesis Submitted to the University of Ottawa

In partial fulfillment of the requirements for the PhD in Microbiology and Immunology

Department of Biochemistry, Microbiology, and Immunology

Faculty of Medicine

University of Ottawa

ABSTRACT

Regulated cell death plays a vital role in tissue homeostasis and development. Recent studies have highlighted necroptosis, a programmed cell death mode combining features of necrosis and apoptosis, as having diverse biological impacts. The necroptosis pathway involves activating receptor-interacting protein kinases (RipK-1 and -3), which form a complex with mixed-lineage kinase domain-like protein (MLKL). This complex translocates to the plasma membrane, inducing its rupture. This study reveals that ARF6 targets the RipK1-dependent ripoptosome and necrosome cell death pathways without impacting apoptosis susceptibility. ARF6 regulates the maturation of the endo-lysosomal compartment, promoting cIAP1/2 degradation and facilitating RipK1 phosphorylation towards cell death pathways. This finding unveils a new signaling event preceding RipK1 phosphorylation, which is necessary for activating RipK1-dependent cell death pathways. The research also demonstrates that necroptosis program initiation activates RipK1, leading to MAPK pathway upregulation and increased inflammatory cytokine expression, independent of cell death. This inflammatory response is counterbalanced by type I interferon expression during necrosome activation. The crosstalk between IFNAR1 signalling, the MAPK pathway, and post-transcriptional regulation through ZFP36 plays a crucial role in balancing inflammatory responses and cell death. Furthermore, the study provides compelling evidence for IFNAR1 signalling's critical role in necroptosis. *Ifnar1*-deficient macrophages exhibit significant resistance to necroptosis induced by various stimuli. IFNAR1 signaling is crucial for the proper functioning of the ISGF3 complex and the expression and activation of MLKL, a key necroptosis executioner. Surprisingly, restoring MLKL expression in *Ifnar1*-deficient cells did not fully reverse their necroptosis resistance, suggesting additional mechanisms at play. Further investigation revealed that IFNAR1 signaling is essential for the appropriate translocation of phosphorylated MLKL to the plasma membrane, a critical step in necroptosis execution. These findings significantly advance our understanding of the molecular mechanisms underlying necroptosis and highlight the complex interplay between different pathways that lead to programmed cell death pathways in macrophages. Deregulation of necroptosis is associated with pathological conditions such as cancer, neurodegenerative diseases, inflammatory diseases, and critical response against many viruses, including pox, herpes, and influenza. This research aims to identify potential therapeutic targets that can be exploited in chronic inflammatory conditions and viral infections.

PREFACE

This thesis contains original research that was published in *Cell Death & Disease*.

Yadav, Sahil, Rayan El Hamra, Norah A. Alturki, Ardeshir Ariana, Avni Bhan, Kate Hurley, Matthias Gaestel, Perry J. Blackshear, Alexandre Blais, and Subash Sad. "Regulation of Zfp36 by ISGF3 and MK2 Restricts the Expression of Inflammatory Cytokines during Necroptosis Stimulation." *Cell Death & Disease* ***15***, no. 8 (2024): 1-16. Accessed February 28, 2025. https://doi.org/10.1038/s41419-024-06964-4

Specific contributions are listed below:

- S. Y. designed and performed nearly all experiments, analyzed data, and wrote the thesis. N. A. extracted RNA for Microarray Analysis. Dr. Alexandre Blais's laboratory performed and provided all the reagents and microarray slides used for gene expression profiling. R. H. and A. B. performed the gene expression profiling. Dr. Rayan Russell's laboratory performed the MLKL transduction. A. A. and S. S. conceptualized the study, designed experiments, and cooperated in writing the manuscript and data analysis.
- The experimental protocol [BMIb 4456 (Replacing BMI3486)] used was approved by the University of Ottawa Animal Care Committee.
- Flow cytometry experiments were conducted at the Flow Cytometry & Virometry Core facility at the University of Ottawa.
- Cell Imaging experiments were conducted at the Cell Biology and Image Acquisition Core (RRID: SCR_021845) funded by the University of Ottawa, Ottawa, Natural Sciences and Engineering Research Council of Canada, and the Canada Foundation for Innovation.
- The work was funded by grants from the Canadian Institutes of Health Research (CIHR) (# PJT-185880) to Dr. Subash Sad and partially by the intramural research program of the NIEHS, NIH (Dr. P. Blackshear)

➢ All figures in the introduction section were created with https://www.biorender.com/.

ACKNOWLEDGEMENTS

I would like to express my profound gratitude to my advisor, Dr. Subash Sad, for granting me the opportunity to pursue my PhD in his laboratory. Your unwavering support, both in science and life, has been invaluable. Your mentorship has honed my critical thinking skills, and I am grateful for the insightful anecdotes, sage advice, and enriching discussions we have shared over time. Thank you for challenging me, pushing my limits, and bringing the best out of me.

My sincere appreciation extends to Dr. Ardeshir Ariana for his steadfast support and guidance throughout my project.

I thank my thesis advisory committee members, Dr. Tommy Alain, Dr. Seung-Hwan Lee, Dr. Shawn T. Beug, and Dr. Jim Sun, for their rigorous questioning and invaluable input as my thesis evolved. I also extend my gratitude to my comprehensive examiner, Dr. Lisheng Wang, for his valuable advice. Your collective support and encouragement over the years have been instrumental to this project.

To all past and present members of the Sad Lab with whom I have had the privilege of working, I offer my heartfelt thanks. Each of you has been a wellspring of inspiration, collaboration, and support, significantly contributing to my scientific training and research. Our time together has been immensely rewarding and made this journey a pleasant one.

I am grateful to the members of ACVS for imparting essential mouse-handling skills and diligently caring for the mice crucial to my project.

A special note of thanks goes to Christ Church Cathedral Cricket Club and its members for adding joy and balance to this journey.

Lastly, I extend my deepest appreciation to my family, siblings, and close friends. Your unconditional love, unwavering support, and countless sacrifices have been my foundation, enabling me to pursue and achieve my dreams. You have truly been my pillar of strength throughout this journey.

TABLE OF CONTENTS

LIST OF ABBREVIATIONS

ADP	Adenosine Diphosphate
AIF	Apoptosis-Inducing Factor
AIM2	Absent in Melanoma 2
AKT	Protein Kinase B
ALR	Absent in Melanoma 2-Like Receptors
ANOVA	Analysis of Variance
AP	Anchored Protein
APAF1	Apoptotic Protease Activating Factor 1
APC	Antigen Presenting Cell
APO	Apolipoprotein
ARE	Adenylate-Uridylate-Rich Element
ARF/Arf	ADP-Ribosylation Factor
ATF	Activating Transcription Factor
BAFF	B-Cell Activating Factor
BAK	Bcl-2-Anatagonist Killer
BAX	Bcl-2-Associated X Protein
BCA	Bicinchoninic Acid
BCL	B-Cell Lymphoma Protein 2
BCR	B Cell Receptor
BH3	BH3 Domain
BID	BH3 Interacting-Domain Death Agonist
BMDM	Bone Marrow-Derived Macrophage
BMI	Biochemistry Microbiology and Immunology
BMM	Bone Marrow Macrophage
BP	Birinapant
cFLIP	Cellular FLICE (caspase-8/a–h)-Like Inhibitory Protein
cIAP	Cellular Inhibitor of Apoptosis
CHX	Cycloheximide
CMV	Cytomegalovirus
CRISPR	Clustered Regularly Interspaced Short Palindromic Repeats
CYLD	Cylindromatosis
DAI	DNA-dependent Activator of Interferon-regulatory factors
DAMP	Danger Associated Molecular Pattern
DD	Death Domain
DGE	Differential Gene Expression
DIABLO	Direct Inhibitor of Apoptosis-Binding Protein with Low pI
DISC	Death-Inducing Signaling Complex
DMSO	Dimethyl Sulfoxide

DNA	Deoxyribonucleic Acid
DNM	Dynamin
DR	Death Receptor
DUB	Deubiquitinating Enzyme
EFA6	Exchange Factor for Arf 6
ELISA	Enzyme-linked Immunosorbent Assay
EMR	Emricasan
ERK	Extracellular signal–Regulated Kinase
FACS	Fluorescence-Activated Cell Sorting
FADD	Fas-Associated protein with Death Domain
FAS	Fas cell surface death receptor
FBS	Fetal Bovine Serum
FLICE	FADD-Like Interleukin-1 beta-converting enzyme
GAPDH	Glyceraldehyde-3-phosphate dehydrogenase
GAS	Gamma Activated Site
GDP	Guanosine Diphosphate
GEF	Guanine nucleotide Exchange Factor
GFP	Green Fluorescent Protein
GPI	Glycosylphosphatidylinositol
GSEA	Gene Set Enrichment Analysis
GTP	Guanosine Triphosphate
HIV	Human Immunodeficiency Virus
HMGB1	High Mobility Group Box 1 Protein
HOIL1	Heme-Oxidized IRP2 ubiquitin Ligase 1
HOIP	HOIL-1-Interacting Protein
IAP	Inhibitor of Apoptosis
IETD	Isoleucine-Glutamic Acid-Threonine-Aspartic Acid
eIF2	Eukaryotic Initiation Factor 2
eIF4A	Eukaryotic initiation factor 4A
IF4E	Eukaryotic Translation Initiation Factor 4E
IFN	Interferon
IFNAR	Interferon α/β Receptor
IFNAR1	Interferon α/β Receptor 1
IFN-I	Type-I Interferon
IkB	Inhibitor of kappa B
IKK	Inhibitor of Nuclear Factor Kappa-B Kinase
IL-6	Interleukin 6
IL-10	Interleukin 10
IP	Immunoprecipitation
IRF	Interferon Regulatory Factor
ISG	Interferon Stimulated Gene

ISGF3	Interferon-Stimulated Gene Factor 3
ISRE	Interferon-Stimulated Response Element
JAK1	Janus Kinase 1
JNK	c-Jun N-terminal Kinase
LBP	Lipopolysaccharide Binding Protein
LDL	Low-Density Lipoprotein
LPS	Lipopolysaccharide
LUBAC	Linear ubiquitin chain assembly complex
MAPK	Mitogen-Activated Protein Kinases
MCSF	Macrophage Colony Stimulating Factor
MEKK3	Mitogen-Activated Protein Kinase Kinase 3
MFI	Mean Fluorescence Intensity
MLKL	Mixed Lineage Kinase domain-Like Protein
MOMP	Mitochondrial Outer Membrane Permeabilization
MTT	3-(4,5-dimethylthiazol-2-yl)-2,5-diphenyltetrazolium bromide
MyD88	Myeloid Differentiation Primary Response Gene 88
NADPH	Nicotinamide Adenine Dinucleotide Phosphate
NCBI	National Center for Biotechnology Information
NEMO	NFκB Essential Modulator
NFκB	Nuclear Factor Kappa-light-chain-enhancer of Activated B Cells
NIK	NFκB Inducing Kinase
NLR	NOD-Like Receptor
NLRP3	NLR Family Pyrin Domain Containing 3
NOD	Nucleotide-binding Oligomerization Domain
OAS1	2'-5'-Oligoadenylate Synthetase 1
p38	MAPK p38 Mitogen-Activated Protein Kinase
p65	NFκB Subunit 65 of nuclear factor kappa-light-chain-enhancer of activated B cells
PAGE	Polyacrylamide Gel Electrophoresis
PAMP	Pathogen-Associated Molecular Pattern
PARP	Poly (ADP-ribose) polymerase
PBS	Phosphate Buffered Saline
PCD	Programmed Cell Death
PE	Phycoerythrin
PI3K	Phosphoinositide 3-kinase
PIP	Phosphatidylinositol Phosphate
PIP2	Phosphatidylinositol 4,5-bisphosphate
PIP5K	Phosphatidylinositol-4-phosphate 5-kinase
PKC	Protein Kinase C
PLD	Phospholipase D
PolyI:C	Polyinosinic-polycytidylic Acid

PML	Promyelocytic Leukemia
PRR	Pattern Recognition Receptor
R8	RPMI with 8% Fetal Bovine Serum
PVDF	Polyvinylidene Fluoride
RANK	Receptor Activator of Nuclear Factor Kappa-B
RHIM	Rip Homotypic Interaction Motif Domain
RIG	Retinoic acid-Inducible Gene
RING	Really Interesting New Gene
RipK	Receptor Interacting Protein Kinase 1 /3
RNA	Ribonucleic Acid
ROS	Reactive Oxygen Species
RPMI	Roswell Park Memorial Institute Medium
RRID	Research Resource Identifier
SAPK	Stress-Activated Protein Kinase
SDS	Sodium Dodecyl Sulfate
SEM	Standard Error of the Mean
SLE	Systemic Lupus Erythematosus
SMAC	Secondary Mitochondrial Activator of Cell Death
SMARTP	Simple Modular Architecture Research Tool
STAT	Signal Transducers and Activators of Transcription
STING	Stimulator of Interferon Genes
TAB1	Transforming Growth Factor-Beta Activated Kinase 1 Binding protein 1
TAK1	Transforming Growth Factor-Beta-Activated Kinase 1
TCR	T Cell Receptor
TGF	Transforming Growth Factor
TICAM1	TIR Domain Containing Adaptor Molecule 1
TIR	Toll/Interleukin-1 Receptor
TIRAP	Toll-Interleukin 1 Receptor (TIR) Domain Containing Adaptor Protein
TLR	Toll Like Receptor
TNF	Tumor Necrosis Factor
TNFR	Tumor Necrosis Factor Receptor
TORC1	Target Of Rapamycin Complex 1
TRADD	TNFR Associated Death Domain Protein
TRAF	TNFR Associated Factor 2
TRAIL	TNF Related Apoptosis Inducing Ligand
TRAM	TRIF Related Adaptor Molecule
TRIF	TIR-domain Containing Adapter Inducing IFN-ß
TTP	Tristetraprolin
TYK2	Tyrosine Kinase 2
WT	Wild Type
XAF1	XIAP Associated Factor 1

XIAP	X-Linked Inhibitor of Apoptosis
ZBP1	Z-DNA Binding Protein 1
ZFP36	Zinc Finger Protein 36
Z-VAD-FMK	Benzyloxycarbonyl-Val-Ala-Asp (OMe)-Fluoromethylketone
2BM	2 Beta Mercaptoethanol

LIST OF FIGURES

LIST OF TABLES

1. INTRODUCTION

Cell death is the event in which a biological cell ceases to carry out its functions, either as a natural process for removing unwanted or damaged cells or as a result of injury or disease. It is also a fundamental physiological process in all organisms, playing a crucial role in embryonic development, organ maintenance, and the regulation of autoimmunity within the body. Cell death was considered an undesirable yet unavoidable consequence of dysfunctional cells for a long time, as damage inevitably triggered inflammation. Regulated cell death, orchestrated by specialized molecular machinery and called programmed cell death (PCD), plays a crucial role in health and disease. Over the past few decades, scientific research has unveiled a diverse array of cell death mechanisms that are genetically encoded within cells. These programmed cell death pathways serve a critical function: they act as cellular quality control systems, eliminating cells that are either no longer needed or have sustained severe damage. By removing these potentially harmful cells, these mechanisms play a crucial role in protecting the integrity of surrounding tissues and maintaining overall cellular health.

In recent years, we have gained more comprehension of the mechanism of cell death and have clarified the different types of "programmed cell death", and identified some key genes in these processes (Shen et al., 2023). While significant progress has been made in understanding various cell death mechanisms in recent years, several unexplored areas and unanswered questions remain in this field. Notably, the interconversion between different modes of cell death and their potential applications in disease contexts have not been extensively investigated. Impaired or malfunctioning PCD mechanisms have been linked to a spectrum of serious health conditions, including compromised immune function, disorders affecting the nervous system, persistent inflammatory states, developmental abnormalities of the neural system, and autoimmune disorders. The latter may be triggered by prolonged activation of T cells in the context of chronic inflammation, leading to excessive cell death and subsequent immune dysregulation (Lockshin & Zakeri, 2007). This highlights the critical role that regulated cell death plays in maintaining overall health and preventing disease.

PCD has emerged as a rapidly evolving and intensively investigated area of biological research, attracting significant scientific attention and resources. Research has uncovered diverse forms of

PCD, with apoptosis and necroptosis emerging as the two primary mechanisms, each leading to distinct cellular outcomes. Apoptosis, the first identified form of PCD and the most widely researched form of cell death, is characterized by its highly regulated nature and lack of inflammatory response, as apoptotic cells are cleared without triggering immune activation. Decades later, researchers discovered necroptosis, a distinct type of regulated cell death that, unlike apoptosis, induces inflammation while maintaining controlled execution, blending features of both necrosis and apoptosis (Shlomovitz et al., 2018). While apoptosis and necroptosis can be triggered by similar stimuli, such as death receptors and intracellular sensors, they follow distinct regulatory mechanisms and lead to markedly different physiological outcomes. Necroptosis, a regulated form of cell death, plays a dual role in physiology and pathology. While it can trigger harmful inflammatory responses leading to tissue damage, chronic diseases, and tumor progression, necroptosis also serves as a crucial defense mechanism against pathogens and tumors through its pro-inflammatory effects. This duality highlights necroptosis as a "double-edged sword" in biological processes (Ye et al., 2023). While apoptosis has been extensively studied for decades, necroptosis research has gained significant momentum in recent years, revealing its distinct mechanisms and physiological roles, though it remains less comprehensively understood compared to apoptosis. In 2005, researchers identified necroptosis as a distinct form of programmed cell death, characterized by its non-apoptotic nature and activation by TNFα when caspase-8 is inhibited or absent (Degterev et al., 2005). Necroptosis exhibits the key morphological characteristics of necrosis, such as swollen organelles, absence of nuclear fragmentation, plasma membrane disruption, and release of cellular contents, despite being a regulated form of cell death (D. Chen et al., 2016). Necroptosis expands our understanding of programmed cell death beyond apoptosis. A deeper comprehension of necroptosis regulation is crucial for managing this inflammatory cell death pathway in diverse pathological conditions, including cancer, sepsis, rheumatoid arthritis, Alzheimer's disease, multiple sclerosis, and atherosclerosis, potentially leading to novel therapeutic approaches (G. Zhang et al., 2022). The precise molecular pathways governing necrosome formation, its role in triggering inflammation, and the subsequent execution of necroptotic cell death remain incompletely understood. Further research is needed to elucidate the intricate signaling cascades and regulatory mechanisms involved in this complex process of programmed necrosis.

1.1. The Immune System

The immune system is a complex network of cells, tissues, and organs that work together to defend the body against harmful invaders. This sophisticated defense mechanism has evolved to recognize and neutralize a wide variety of pathogens, including bacteria, viruses, parasites, and fungi, as well as other potentially dangerous substances. Our knowledge of the immune system and its protective mechanisms against infections is rapidly expanding, with ongoing research continually unveiling new insights into its complex functions and interactions.

The immune system employs a two-tiered defense strategy against pathogens: innate and adaptive immunity. Innate immunity acts as the first line of defense, providing rapid, non-specific responses to invading pathogens without developing immunological memory. In contrast, adaptive immunity offers a more targeted, antigen-specific defense that takes longer to activate but develops a memory for faster future responses (Marshall et al., 2018). These two systems are not isolated but work in tandem, complementing each other to provide comprehensive protection. Deficiencies in either system can lead to increased susceptibility to infections or improper immune reactions. This synergistic relationship between innate and adaptive immunity, along with physical and chemical barriers, forms the foundation of the body's defense mechanisms against pathogens.

Innate immunity encompasses four defensive barriers: anatomical (skin and mucous membranes), physiological (temperature, pH, and chemical mediators), cellular (endocytosis and phagocytosis), and inflammatory responses, collectively forming a multi-layered protection against pathogens (Chaplin, 2003). When encountering a novel pathogen, the innate immune system provides the initial recognition and response, subsequently triggering the activation of the adaptive immune system for a more targeted defense. The innate immune system serves as the body's initial defense against infections, utilizing specialized pattern recognition receptors (PRRs) to detect both pathogen-associated molecular patterns (PAMPs) and damage-associated molecular patterns (DAMPs) (D. Li & Wu, 2021). Upon recognition, these receptors trigger direct activation of immune cells, initiating a rapid and broad-spectrum immune response to combat invading pathogens. Six distinct groups of PRRs have been identified: Toll-like receptors (TLRs), RIG-I-like receptors (RLRs), NOD-like receptors (NLRs), C-type lectin receptors (CLRs), cGAS-STING pathway components, and AIM2-like receptors (ALRs), each playing unique roles in innate

immune recognition of PAMPs and specific response against them (Wicherska-Pawłowska et al., 2021). Activation of these receptors initiates a signaling cascade that results in enhanced production of type I interferons, proinflammatory cytokines (such as IL-1, IL-6, and TNF), and other inflammatory mediators, collectively amplifying the immune response (L. Chen et al., 2017). Beyond triggering IFN-I and proinflammatory cytokine production, the immune system can combat infections through the direct elimination of infected cells via programmed cell death mechanisms such as necroptosis, pyroptosis, or autophagy (Akira et al., 2006; Riera Romo et al., 2016). The release of DAMPs triggers recognition by PRRs, activating intracellular signaling cascades that lead to the production of cytokines and chemokines, ultimately inducing a state of "sterile inflammation" in the absence of pathogens (Gong et al., 2020). The recognition of PAMPs or DAMPs by PRRs initiates downstream signaling in innate immune cells, promoting pathogen elimination and subsequently activating the adaptive immune response. PRRs are found both on the surface and within various immune cells (including macrophages, dendritic cells, NK cells, mast cells, neutrophils, and eosinophils) as well as non-immune cells (such as epithelial cells, endothelial cells, and fibroblasts), enabling widespread pathogen detection throughout the body (Akira et al., 2006).

Unlike the rapid response of the innate immune system, the adaptive immune system takes longer to develop and mount a targeted defense against pathogens but offers more specific and long-lasting protection. The adaptive immune system comprises a diverse array of cells, factors, and mechanisms that utilize specialized receptors to identify and react to specific antigens, whether they originate from external sources like pathogens and allergens, or internal sources such as tumors and self-tissues. T cells and B cells, collectively known as lymphocytes, form the cornerstone of the adaptive immune system, serving as its primary cellular components (Dupuis-Girod et al., 2003). The adaptive immune system's T cell populations are divided into CD4+ helper T cells, which orchestrate immune responses through various mechanisms, and CD8+ cytotoxic T cells, which primarily eliminate target cells, while B cells produce antibodies and serve as antigen-presenting cells to activate T cells (Cooper, 2015). Antibodies bind specifically to target antigens, interfering with pathogenic processes like cellular attachment, potentially preventing pathogen entry, and providing sterilizing immunity against intracellular pathogens (L. L. Lu et al., 2018). Lymphocytes communicate through two primary methods: the release of soluble proteins

(including cytokines and chemokines) and direct cell-to-cell interactions via surface ligands and receptors.

1.1.1. Monocytes and Macrophages

Monocytes, the largest leukocytes in the bloodstream, are crucial components of the immune system, bridging innate and adaptive immunity through their diverse functions and ability to differentiate into macrophages and dendritic cells. Monocytes and macrophages are mononuclear phagocytes. Macrophages are differentiated forms of monocytes that have left the bloodstream and entered various tissues throughout the body, where they play crucial roles in immune defense, tissue homeostasis, and inflammation. Given their significant roles in various physiological and pathological processes, there is considerable research interest in developing strategies to modulate macrophage function for therapeutic purposes.

Macrophages, key players in immune function and tissue maintenance, have diverse origins and developmental pathways that have been extensively studied, revealing their complex lineage and versatile roles in health and disease. Many tissue-resident macrophages have an embryonic origin, arising from progenitors in the yolk sac and fetal liver during early development (Bajgar & Krejčová, 2023). In addition to embryonic-derived macrophages, a significant population of macrophages originates from hematopoietic stem cells in the bone marrow (Virolainen, 1968). These cells differentiate into monocytes, which can then be recruited to tissues and differentiate into macrophages in response to various stimuli, particularly during inflammation or tissue injury (Alabdulaali et al., 2023) **(Figure 1)**. Macrophages can adopt various activation states along a spectrum, with M1 (pro-inflammatory) and M2 (anti-inflammatory) representing the extremes (Ricketts et al., 2021). However, this binary classification is an oversimplification, as macrophages exist on a continuum of activation states with diverse functional properties (Yan et al., 2024). Macrophages can rapidly switch between different functional phenotypes in response to changing microenvironmental signals (R. Yuan et al., 2023). This flexibility allows them to adapt to the evolving needs of tissue repair, inflammation resolution, or pathogen clearance. The plasticity of macrophages is closely linked to their metabolic adaptations. Different activation states are associated with distinct metabolic profiles, which in turn influence their functional capabilities (Kolliniati et al., 2021). Macrophages play a pivotal role in innate immunity by orchestrating

various homeostatic and evolutionary host defense mechanisms. These versatile cells also contribute to diverse biological processes, including the regulation of reactive oxygen species (ROS) levels, maintenance of iron homeostasis, facilitation of tissue repair following injury, and the modulation of multiple metabolic functions (L. Chen et al., 2017; T. Zhao et al., 2022). Macrophages perform three critical functions essential for immune responses: immunomodulation, phagocytosis, and antigen presentation. These capabilities enable them to orchestrate effective immune reactions across a spectrum of pathophysiological conditions, making them indispensable components of the immune system (Pidwill et al., 2020).

Macrophages play a crucial role in the interplay between cell death and inflammation, with their functions and responses significantly impacting both processes. This correlation is evident in various physiological and pathological conditions. Macrophages are key players in the clearance of apoptotic cells, a process known as efferocytosis. This process is essential for maintaining tissue homeostasis and resolving inflammation (Schilperoort et al., 2023). When macrophages efficiently clear apoptotic cells, it typically leads to an anti-inflammatory response, promoting the resolution of inflammation and tissue repair. However, if apoptotic cells are not cleared efficiently, they can undergo secondary necrosis, releasing DAMPs that can trigger inflammation (Clarke et al., 2010). This highlights the importance of timely and effective macrophage-mediated clearance of apoptotic cells in preventing excessive inflammation. The polarization state of macrophages significantly influences their role in inflammation. Macrophages are associated with pro-inflammatory responses and increased production of inflammatory cytokines such as TNFα, IL-6, and IL-1β (Atri et al., 2018). Macrophage cell death, particularly necroptosis, plays a crucial role in inflammation and various inflammation-related diseases. This complex interplay has significant implications for disease progression and potential therapeutic approaches. Necroptosis is a regulated form of necrotic cell death. Necroptosis is activated by inflammatory stimuli, particularly tumor necrosis factor-α (TNFα) (Han et al., 2022). The death of macrophages through necroptosis can release DAMPs, further promoting inflammation. The intricate relationship between macrophage cell death, particularly necroptosis, and inflammation plays a pivotal role in various diseases. Targeting these processes offers promising strategies for developing new treatments for inflammation-related disorders.

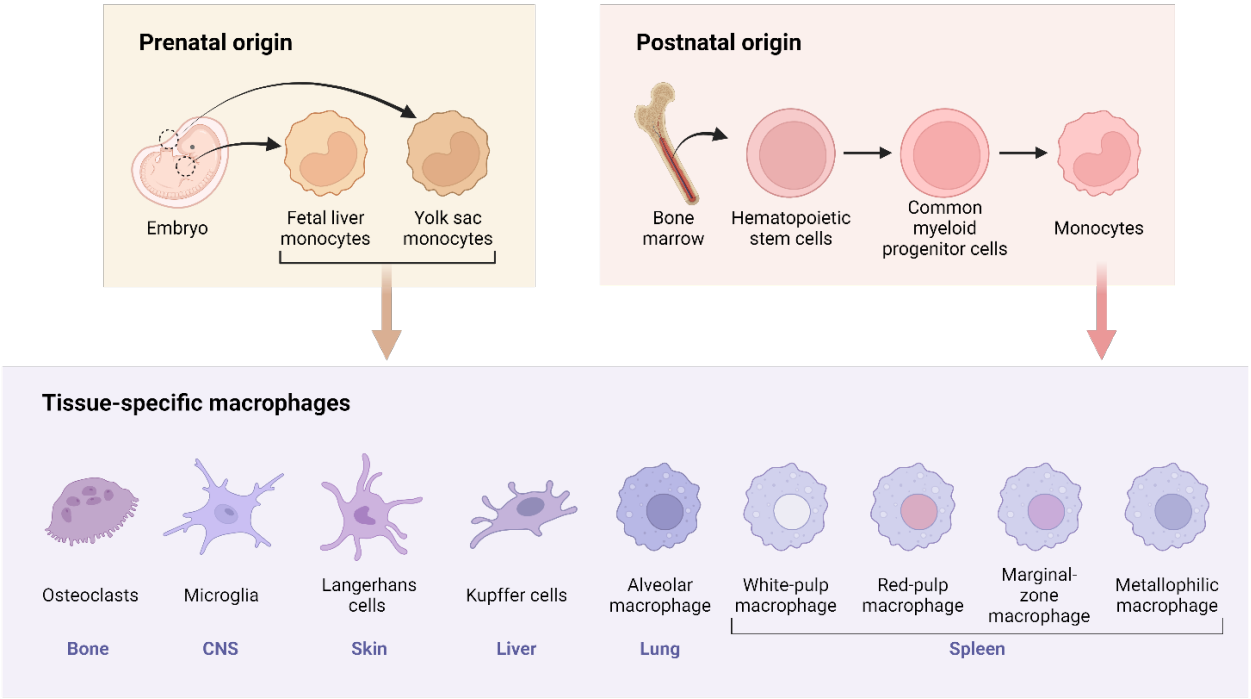

Figure 1. Origin and Development of Macrophages

Macrophages are immune cells that originate from two primary sources during development and throughout life: embryonic precursors and bone marrow-derived monocytes. Their omnipresence across tissues enables them to perform specialized functions tailored to their microenvironment, making them indispensable for both health and disease. They have a critical role in maintaining tissue homeostasis, immune defense, and development.

1.2. Endocytosis

Endocytosis is a cellular process that occurs at the cell surface, involving the internalization of plasma membrane components, including proteins and lipids. This mechanism allows cells to sample their external environment and regulate various processes that originate at the cell surface. Endocytosis can be categorized into three primary forms: phagocytosis, which involves the engulfment of large particles; pinocytosis, the uptake of fluids and dissolved substances; and receptor-mediated endocytosis, a highly selective process for internalizing specific molecules. Early studies in cell biology revealed the intimate connection between endocytosis and receptor-mediated signaling pathways.

Macrophages, key players in the immune system, utilize receptor-mediated endocytosis as a crucial mechanism for cellular uptake and signaling. This process involves the specific binding of ligands to cell surface receptors, triggering the internalization of the receptor-ligand complex. In macrophages, receptor-mediated endocytosis serves multiple functions, including the uptake of pathogens, cellular debris, and various molecules such as LDL cholesterol (B. Liu et al., 2007). This pathway not only facilitates the clearance of potentially harmful substances but also plays a vital role in antigen presentation, cell signaling, and the regulation of immune responses (Montaner et al., 1999). Receptor internalization begins when ligands bind to the receptor, recruiting molecules like clathrin and adapters. This triggers plasma membrane invagination, forming vesicles that are then severed by dynamin. These vesicles, containing ligand-receptor complexes, travel through various subcellular compartments such as early endosomes, late endosomes, and lysosomes (Mani & Singh, 2023). The GTPase dynamin plays a crucial role in endocytosis by functioning as a molecular scissor (Gundu et al., 2022). Endocytosis can be classified into two main categories based on the involvement of dynamin.

1.2.1. Dynamin-Dependent Endocytosis

The 100-kDa GTPase dynamin is vital for various vesicle-related processes, including receptor-mediated endocytosis, synaptic vesicle recycling, caveolae internalization, and potentially, Golgi-associated vesicle trafficking (Hinshaw, 2000). Dynamins play a crucial role in the extensively researched processes of clathrin- and caveolin-mediated endocytosis (Casamento & Boucrot,

2020) **(Figure 2)**. Dynamins is classified as Dynamin 1 (DNM1), Dynamin 2 (DNM2), and Dynamin 3 (DNM3) are distinguished and categorized according to their unique domain architectures (Singh et al., 2017). At membrane invagination sites, dynamins assemble into helical structures, activating their GTPase function. This process facilitates the internalization of encapsulated cargo during clathrin- and caveolae-mediated endocytosis, a crucial phase in cellular uptake (Henley et al., 1998; Heymann & Hinshaw, 2009). Dynamins also play a vital role in the endocytic uptake of various cellular components, including essential nutrients and key receptors such as the interleukin-2 receptor and epidermal growth factor receptor (Basquin et al., 2013). Beyond their role in endocytosis, dynamins and their associated proteins contribute to additional cellular processes, including the scission of phagosomes and the modulation of mitochondrial fusion and fission events (Gundu et al., 2022).

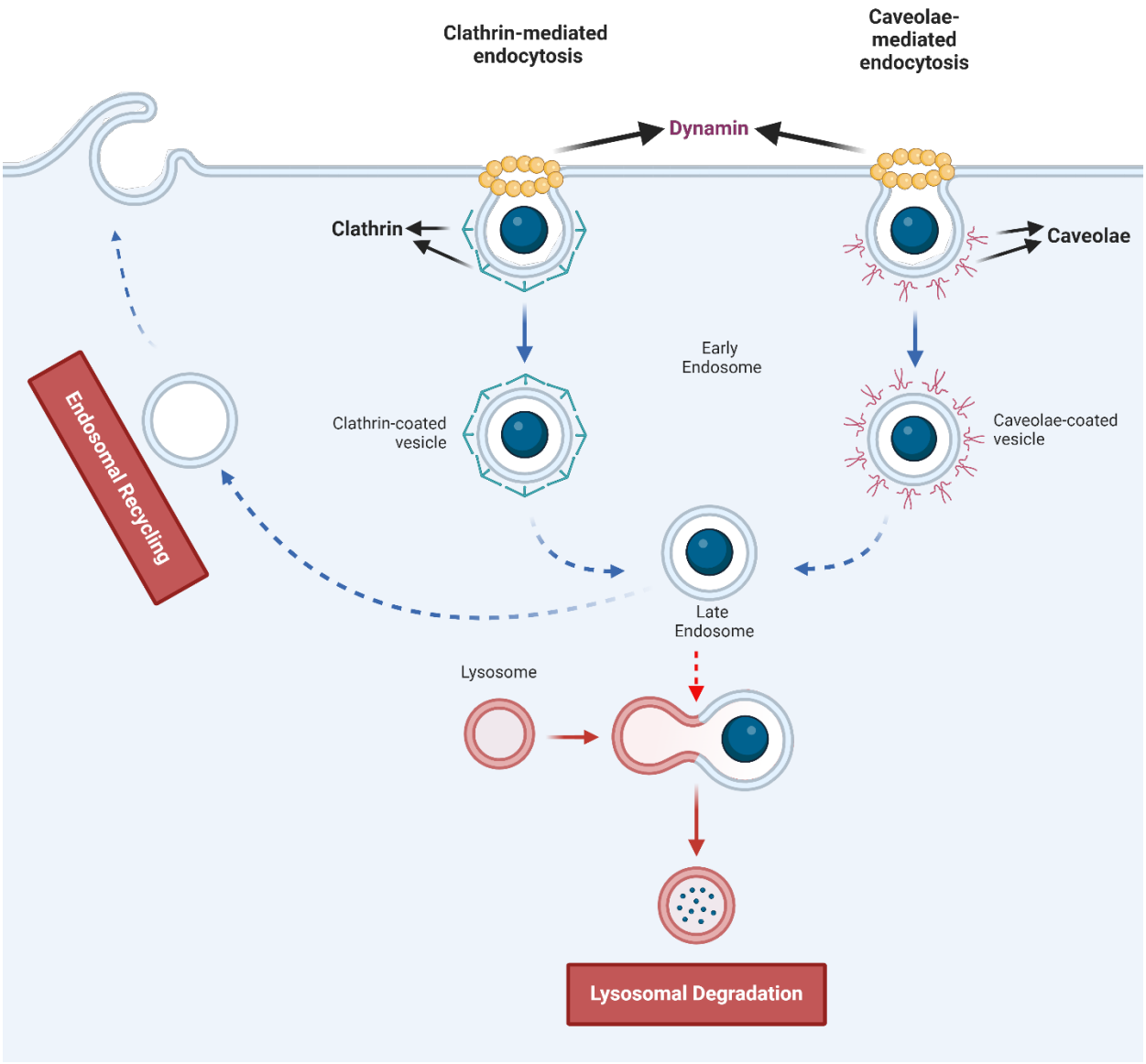

Figure 2. Dynamin-Dependent Endocytosis

1.2.2. Dynamin-Independent Endocytosis

Recent research has illuminated novel pathways of endosome internalization and trafficking that operate independently of dynamin. These pathways involve actin-associated proteins, small GTPases (like ARF6 and Cdc42) (Peters et al., 1995; Thottacherry et al., 2019), flotillins (F. Zhao et al., 2011), secondary messengers (such as calcium) (C. Zhang et al., 2004), pinocytosis (a process of cell drinking where the cell internalizes extracellular fluid via endocytosis) (Brandt, 1958), and entosis (a non-apoptotic cell death program with a cell-in-cell (CIC) cytological feature. Entosis is often referred to as a cannibalistic quality of cells, where those detached from adherent junctions are engulfed by other healthy cells. (Krishna & Overholtzer, 2016) are the essential components driving these cellular processes **(Figure 3)**. The Clathrin-Independent Carrier/Glycosylphosphatidylinositol (GPI)-anchored protein (AP)-enriched endosomal Compartments (CLIC/GEEC-CG) endocytosis pathway represents a unique, clathrin- and dynamin-independent internalization route for GPI-APs-enriched early endosomal compartments. Cdc42 is one of the key regulators for CG endocytosis (Mayor et al., 2014). It plays a crucial role in maintaining plasma membrane integrity, facilitating morphogen signaling during Drosophila development, and enabling the uptake of various molecules, including T-cell receptors and bacterial toxins (Hemalatha et al., 2016; Rossatti et al., 2019). Flotillins are conserved membrane-associated proteins that form distinct microdomains in the plasma membrane, facilitating various cellular functions. These proteins, flotillin-1, and flotillin-2, are involved in a unique form of endocytosis that is distinct from clathrin- and caveolin-mediated pathways (F. Zhao et al., 2011). This pathway is significant in processes such as T-cell signaling, cholesterol uptake, and neuronal function (Ge et al., 2011; Giri et al., 2007). Calcium plays a crucial role in regulating various forms of endocytosis by influencing synaptic transmission, membrane integrity, and diverse cell signaling events through its interactions with calcium sensors and its effects on membrane dynamics (C. Zhang et al., 2004).

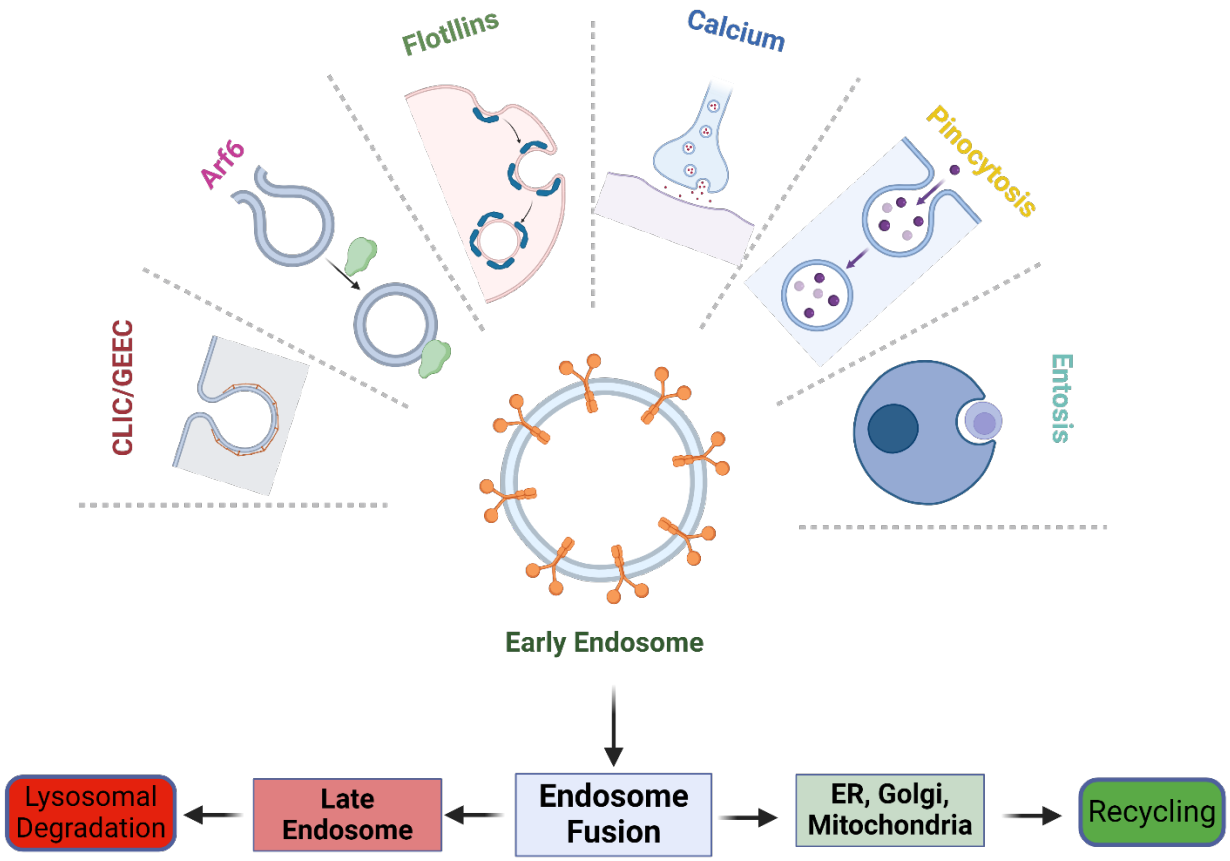

Figure 3. Multiple Mechanism that promotes Dynamin-Independent Endocytosis

1.2.3. ARF6

ADP-ribosylation factors (ARFs) are a group of Ras family GTPases that are divided into three classes (Randazzo et al., 2000). Class I ARFs (ARF1, ARF2, ARF3): These proteins (97% sequence homology) are primarily involved in the secretory pathway and lipid metabolism (Kahn et al., 2006). Class II ARFs (ARF4, ARF5): Their functions are less understood, though recent research has revealed Arf4's role in endosomal recycling (Nakai et al., 2013). Class III ARF (ARF6): this well-studied member is known for its significant role in regulating membrane trafficking and endocytosis (D'Souza-Schorey & Chavrier, 2006).

The effects of ARF6 on membrane trafficking were indeed first observed in 1995 (Peters et al., 1995). ARF6 is distributed across the plasma membrane, cytosol, and endosomal membranes, featuring an N-terminal myristoylation site. Its association with membranes is regulated by its GTP-bound state (active); ARF6 attaches to membranes in the GTP-bound state and detaches upon GTP hydrolysis (inactive) (Radhakrishna et al., 1999). This observation laid the foundation for understanding the role of ARF6 in regulating membrane trafficking between the plasma membrane and endosomes. ARF6, the sole member of class III ARFs, stands out in both sequence and function from its family members. It uniquely participates in both clathrin-mediated and clathrin-independent endocytosis, as well as in endosomal trafficking and recycling processes that occur independently of the Golgi apparatus **(Figure 4)** (Gaschet & Hsu, 1999). It activates phosphatidylinositol-4-phosphate 5-kinase (PIP5K), leading to increased production of phosphatidylinositol-4,5-bisphosphate (PIP2), which is essential for Clathrin-Mediated Endocytosis (CME) (Okada et al., 2015). ARF6 activation has also been found to be influenced by the GTP hydrolysis activity of dynamin II (Okada et al., 2015). ARF6 recruits nucleoside diphosphate kinase Nm23-H1 as a GTP source for dynamin-mediated fission during endocytosis (Van Acker et al., 2019). It interacts with dynamin2 (Dyn2) through guanine nucleotide exchange factors (GEFs) EFA6B and EFA6D, forming a Dyn2-EFA6-ARF6 axis that regulates CME (Okada et al., 2015). ARF6 also mediates cargo internalization and transportation in ARF6-enriched vesicles in a Clathrin and dynamin-independent manner (Van Acker et al., 2019). ARF6-GTP hydrolysis to ARF6-GDP and removal of PIP2 are required for cargo progression through this pathway (Van Acker et al., 2019). It facilitates the recycling of various proteins, including integrins and Rac1, from recycling endosomes to the plasma membrane. It activates phospholipase D (PLD),

leading to increased phosphatidic acid (PA) production, which further enhances PIP2 synthesis. ARF6 plays a crucial role in pathogen phagocytosis, immune signaling through Toll-like receptors, and NADPH oxidase activation, while also being exploited by various pathogens to either inhibit phagocytosis or facilitate their intracellular entry (Van Acker et al., 2019).

ARF6 plays a critical role in both the MyD88-dependent and Trif-dependent signaling pathways following TLR4 engagement. In the MyD88-dependent pathway, ARF6 stimulates PIP 5-kinase to produce PIP2, which serves as a binding site for Mal. This Mal-PIP2 interaction facilitates the recruitment of MyD88 to the activated TLR4 complex (Kagan & Medzhitov, 2006). For the Trif-dependent pathway, ARF6 promotes the internalization of the activated receptor complex. It facilitates the uptake of LPS and the transport of TRAM and may also be involved in the internalization of the TLR4 complex itself (Husebye et al., 2010) **(Figure 4 A)**.

ARF6 modulates actin cytoskeleton remodeling, which is essential for endocytic vesicle formation and movement (Schweitzer et al., 2011). It regulates the recycling of internalized receptors back to the plasma membrane, influencing receptor resensitization and signaling (E. Macia et al., 2012). It impacts various cellular processes, including cell motility, cytokinesis, and cholesterol homeostasis, through its effects on endocytic trafficking (Schweitzer et al., 2011). In summary, ARF6 is a key regulator of receptor-mediated endocytosis. Its activity influences receptor internalization, trafficking, recycling, initiating and sustaining immune responses and has broad implications for cellular function and signaling.

Despite its well-established importance in cellular trafficking and signaling, the role of ARF6 in cell death remains largely unexplored. Recent studies have begun to shed light on this aspect, suggesting that ARF6 may be involved in regulating apoptosis and other forms of programmed cell death. For instance, research has shown that ARF6 deficiency can render naive T cells more susceptible to apoptosis during TCR-induced activation (Sumiyoshi et al., 2021). Additionally, ARF6 has been linked to autophagy, a process that can influence cell survival and death (George et al., 2016; Moreau et al., 2012).

In silico analysis of amino acid sequence of ARF6 reveals key structural features typical of proteins involved in intracellular cargo shuttling. Specifically, an N-terminal myristoylation site is

identified, which is crucial for membrane association. This is followed by a polybasic region, characterized by a cluster of positively charged amino acids (D'Souza-Schorey & Stahl, 1995). Together, these elements form a bipartite membrane-targeting signal **(Figure 4 B)**. This structural arrangement enables ARF6 to reversibly interact with membranes, facilitating its role in vesicular trafficking and membrane dynamics. The myristoylation site allows for the covalent attachment of a lipid moiety, enhancing ARF6's affinity for membranes, while the polybasic region likely interacts with negatively charged phospholipids on membrane surfaces. The presence of these features aligns with ARF6's known functions in regulating endosomal recycling, membrane trafficking, and actin remodeling at the plasma membrane. These structural elements allow Arf6 to cycle between membrane-bound and cytosolic states, a crucial aspect of its function in coordinating various cellular processes. The contribution of ARF6 and other endocytic pathways in the activation of various cell death pathways has not been evaluated.

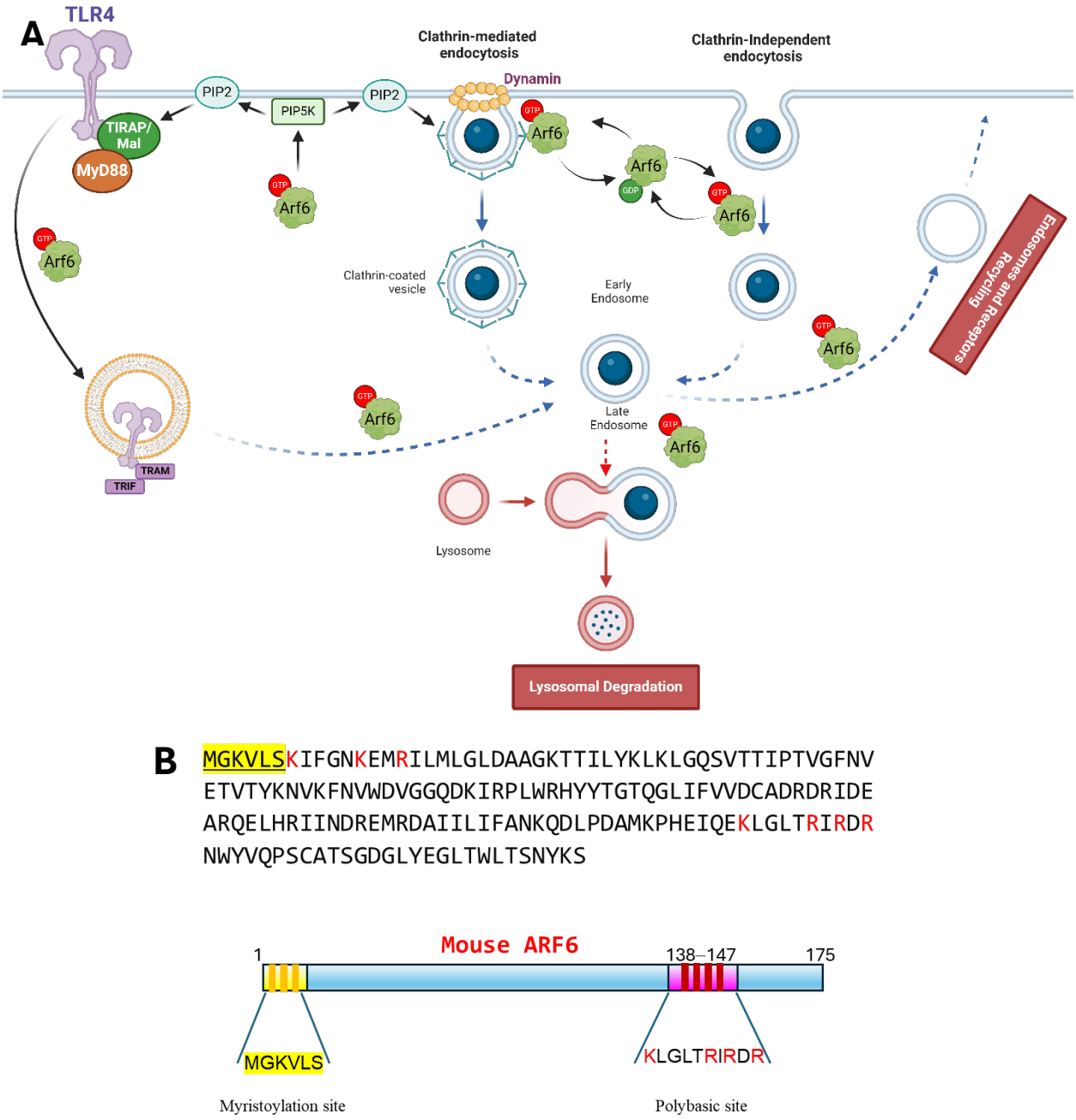

Figure 4. ARF6-Mediated Endocytosis

A The role of ARF6 in endocytosis, intracellular trafficking, and recycling upon clathrin-mediated endocytosis and clathrin-independent endocytosis. **B** The bipartite protein shuttling motif in ARF6 is depicted by the myristoylation site at the N-terminus (consensus sequence of MGXXXS/T), followed by a polybasic motif.

1.3. Cell Death

Cell death is a fundamental biological process that is essential for maintaining tissue homeostasis, regulating development, and shaping immune responses. Once thought to be a simple, binary event, our understanding of cell death has evolved dramatically in recent years, revealing a complex landscape of interconnected pathways and mechanisms. Cell death has traditionally been categorized into two main types: necrosis and programmed cell death (PCD). PCD is a regulated process that unfolds through a sequence of molecular events triggered by specific physiological or developmental cues. In contrast, Necrosis (Non-Programmed Cell Death) is considered as an uncontrolled form of cell death, which typically occurs during severe cellular injury or trauma (Kanduc et al., 2002) **(Figure 5)**. But now, the field of cell death research has expanded beyond the classical dichotomy of apoptosis and necrosis to include several regulated forms of cell death.

Recent scientific advances have reshaped our understanding of necrosis, challenging its conventional portrayal as a solely passive and accidental form of cell death. New research reveals that necrosis can also be a regulated process that is governed by specific cellular signaling pathways under certain circumstances. This controlled form of necrotic cell death is now recognized as programmed necrosis, with "necroptosis" emerging as its most prominent example. This paradigm shift suggests that necrosis is not always a chaotic response to severe cellular damage. Instead, it can be a precisely orchestrated cellular event, initiated and executed through intricate molecular mechanisms. The activation of these pathways depends on the nature and intensity of the stimuli affecting the cell. Consequently, necrosis now occupies a more nuanced position in cell biology, encompassing both uncontrolled and regulated forms of cell death, each triggered by distinct cellular conditions and external factors.

1.3.1. Programmed Cell Death (PCD)

Programmed cell death (PCD) plays a crucial role in the development and maintenance of multicellular organisms by orchestrating the elimination of unnecessary or potentially harmful cells (Ellis et al., 1991). PCD can be divided into several distinct types based on morphological features, biochemical mechanisms, and functional characteristics. Recent scientific advances have revealed a diverse landscape of PCD, with researchers now recognizing over 20 distinct forms (W.

Park et al., 2023). This expanding repertoire of PCD mechanisms highlights the complexity and sophistication of cellular regulation in response to various stimuli and physiological conditions. PCD is broadly classified into two main categories: those that rely on caspase enzymes for execution, and those that proceed independently of caspase activity (S. L. Fink & Cookson, 2005). This distinction highlights the diverse molecular mechanisms underlying different forms of PCD.

Apoptosis is the most well-characterized form of PCD, featuring distinctive morphological changes such as cell shrinkage and nuclear fragmentation. It is primarily mediated by caspases, particularly caspase-3, -6, and -7 (Lomphithak & Fadeel, 2023). Pyroptosis is an inflammatory form of PCD that is associated with caspase-1 activation and the processing and release of mature IL-1β and IL-18. It is driven by inflammatory caspases (caspase-1, -4, -5, -11) and gasdermin proteins (Kowalski et al., 2023) **(Figure 5)**.

Necroptosis is a controlled form of cell death that exhibits necrotic characteristics and is orchestrated by receptor-interacting protein kinases. This pathway is typically activated when caspase-mediated cell death mechanisms are suppressed, serving as an alternative means of eliminating cells under specific conditions (Dhuriya & Sharma, 2018) **(Figure 5)**.

Other major caspase-independent forms of cell death are Parthanatos (mediated by PARP-1 hyperactivation and AIF release) (Fatokun et al., 2014), Ferroptosis (Iron-dependent cell death characterized by lipid peroxidation) (Cao & Dixon, 2016), and Autophagic cell death (Excessive autophagy leading to cell demise) (Yonekawa & Thorburn, 2013).

Recent genetic and biochemical research has uncovered a surprising level of adaptability in the utilization of PCD pathways. These studies demonstrate significant versatility in the molecular mechanisms governing PCD, highlighting a complex and dynamic regulatory network that can adjust to various cellular contexts and stimuli.

PCD pathways are orchestrated by distinct protein complexes that initiate and execute specific cellular demise mechanisms. The apoptosome, inflammasome, ripoptosome, and necrosome are key assemblies in this process. The apoptosome activates caspases in apoptosis, while the inflammasome triggers pyroptosis through caspase-1 activation and gasdermin D pore formation. The necrosome mediates necroptosis via RipK1/RipK3 signaling and MLKL activation. The

ripoptosome serves as a molecular switch between apoptosis and necroptosis, depending on caspase-8 activity. These complexes form intricate signaling hubs that determine cell fate in response to various stimuli, highlighting the sophisticated regulation of PCD pathways in cellular homeostasis and disease contexts.

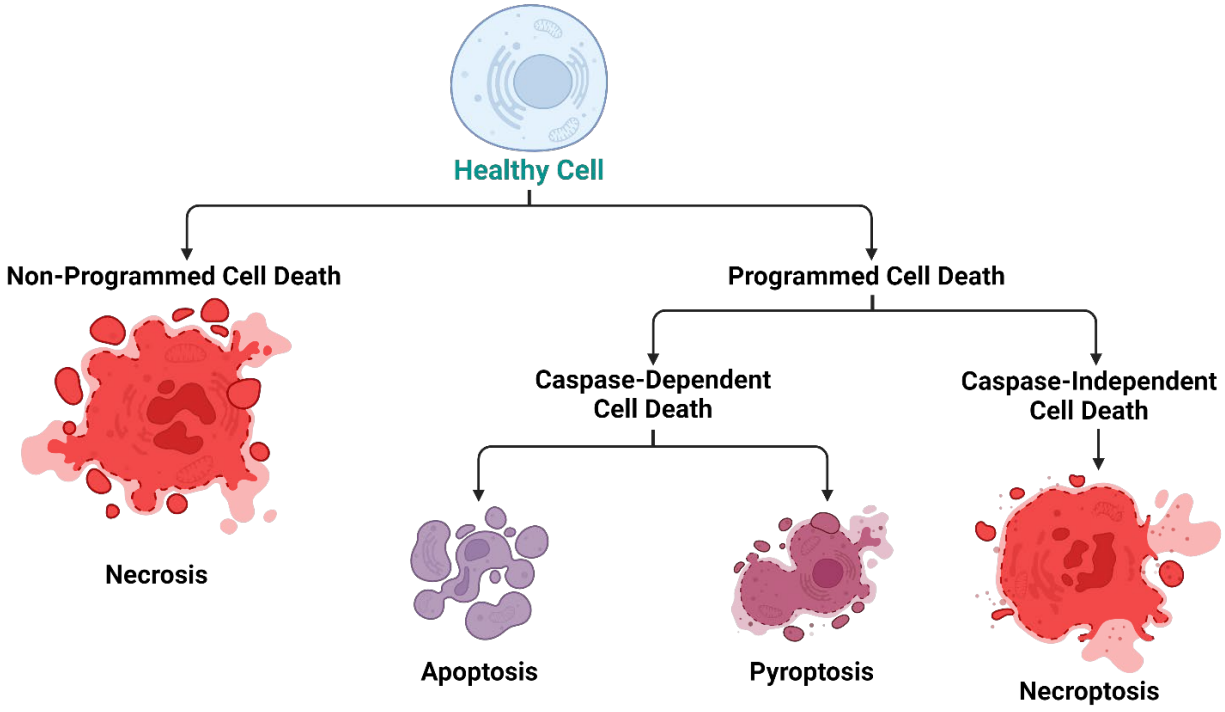

Figure 5. Modes of Cell Death

Cell death can be broadly categorized into programmed and non-programmed forms. Non-programmed cell death is primarily necrosis, resulting from acute cellular injury. Programmed cell death is further divided into caspase-dependent types (e.g., apoptosis, pyroptosis) and caspase-independent types (e.g., necroptosis). This classification highlights the diverse regulated mechanisms by which cells can die in response to various stimuli or conditions.

1.3.1.1. Apoptosis

Apoptosis is a fundamental biological process of PCD that plays crucial roles in development, homeostasis, and disease. As a key mechanism for eliminating unwanted or damaged cells, apoptosis is tightly regulated and involves distinct molecular pathways. Apoptosis involves intricate and elaborate molecular processes characterized by a series of energy-requiring events that unfold in a precise, cascading manner. Current research has identified two primary apoptotic pathways: the extrinsic (death receptor) pathway and the intrinsic (mitochondrial) pathway **(Figure 6)**. Recent evidence suggests that these pathways are not entirely independent but interconnected, with molecules from one pathway capable of influencing the other. This interconnection highlights the complexity of apoptotic regulation and the potential for crosstalk between different cell death mechanisms (Igney & Krammer, 2002).

Intrinsic apoptosis is a form of regulated cell death that is triggered by various internal or external cellular stressors, such as DNA damage, endoplasmic reticulum stress, oxidative stress, loss of growth factors, or disruptions to the microtubule network. The pivotal event in this process is the permeabilization of the mitochondrial outer membrane (MOMP) (Galluzzi et al., 2016). MOMP is regulated by various pro-apoptotic and anti-apoptotic proteins belonging to the BCL2 family. When activated, the intrinsic apoptosis pathway leads to the release of pro-apoptotic factors from the mitochondria, including cytochrome C and the Second Mitochondria-derived Activator of Caspase (SMAC), also known as DIABLO. Other key players in this process include p53, which can upregulate pro-apoptotic proteins like Bax, and inhibitors of apoptosis (IAP) proteins, which can suppress caspases (Loiben et al., 2022). These factors contribute to the formation of the apoptosome, which activates caspase-9 and, subsequently caspase-3, leading to cellular degradation (Q. Li et al., 2007) **(Figure 6)**.

The extrinsic apoptotic pathway is typically initiated when specific ligands bind to their corresponding death receptors (DRs) on the cell surface (Aggarwal et al., 2012). The key DRs involved in extrinsic apoptosis are: FAS (CD95/APO-1), TNF-R1 (TNFRSF1A), TRAIL-R1 (DR4/TNFRSF10A), and TRAIL-R2 (DR5/TNFRSF10B) (Wajant, 2002). When ligands bind to death receptors, causing them to trimerize or form larger complexes, it triggers the assembly of multi-protein structures like the death-inducing signaling complex (DISC) and complex II. The

DISC then activates initiator caspases, primarily caspase-8 and caspase-10, which in turn cleave and activate effector caspases like caspase-3 (Wohlfromm et al., 2024). These effector caspases are responsible for the proteolytic cleavage of cellular proteins, ultimately resulting in the characteristic morphological and biochemical changes associated with apoptosis. The extrinsic pathway can also crosstalk with the intrinsic (mitochondrial) pathway through the cleavage of the pro-apoptotic protein Bid by caspase-8, amplifying the apoptotic signal (Kim et al., 2007) **(Figure 6)**.

This interconnected network of signaling events ensures efficient and controlled elimination of cells, making the extrinsic apoptosis pathway a critical component in various physiological processes and a potential target for therapeutic interventions in diseases such as cancer.

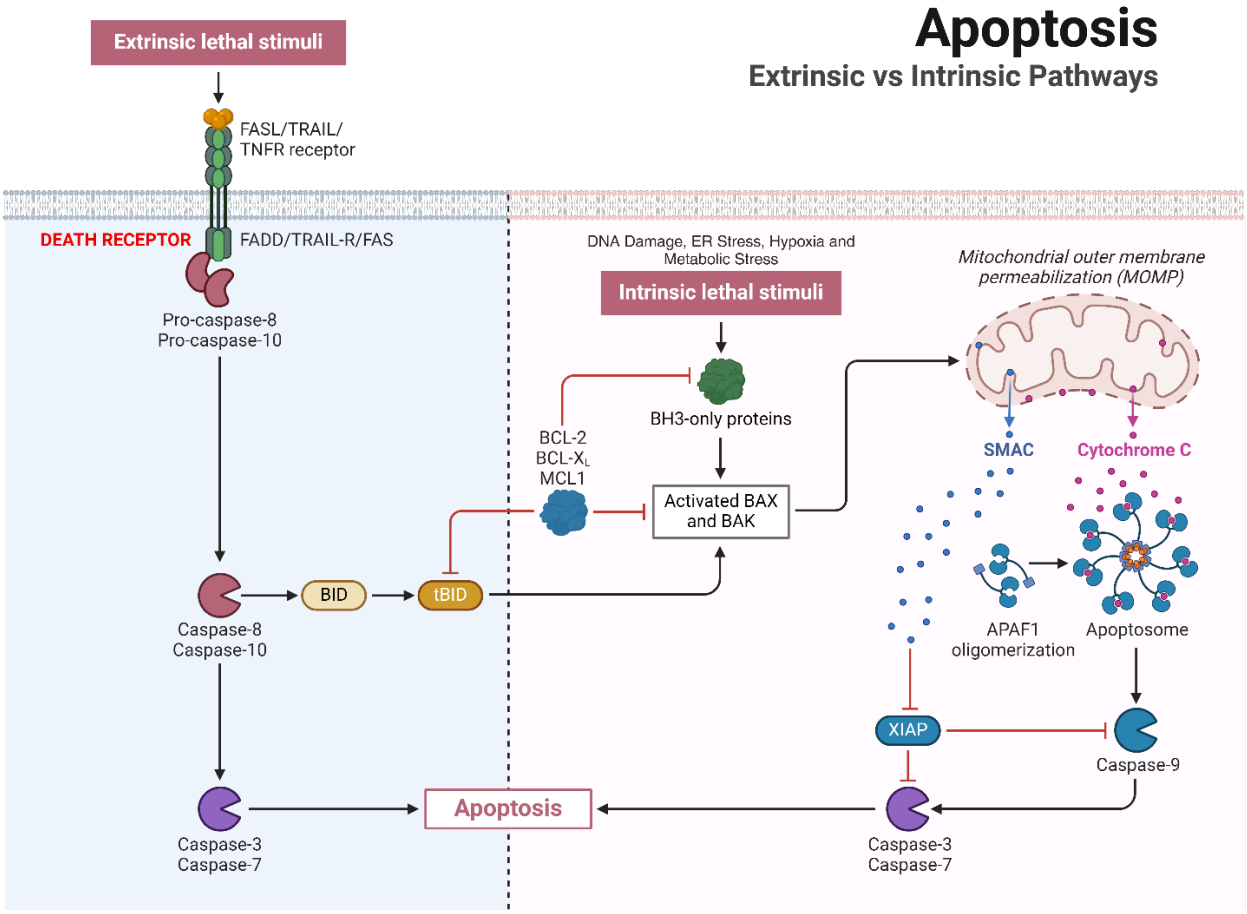

Figure 6. Apoptosis

Apoptosis, a form of programmed cell death, can be initiated through two main pathways: extrinsic and intrinsic. The extrinsic pathway begins when death receptors like tumour necrosis factor (TNF)-related apoptosis-inducing ligand (TRAIL) receptor (TRAIL-R) or FAS bind to their respective ligands, activating initiator caspases (8 and 10) via adaptor proteins such as FAS-associated death domain protein (FADD). These initiator caspases then activate effector caspases (3 and 7), leading to apoptosis. The intrinsic pathway is triggered by cellular stress, which activates BCL-2 homology domain 3 (BH3)-only proteins. These proteins promote BAX and BAK activity, causing mitochondrial outer membrane permeabilization (MOMP). MOMP is counteracted by anti-apoptotic BCL-2 family proteins. Following MOMP, cytochrome c is released into the cytosol, where it interacts with apoptotic protease activating factor 1 (APAF1) to form the apoptosome, activating caspase-9. Caspase-9 then activates caspases 3 and 7. Additionally, the second mitochondria-derived activator of caspases (SMAC) is released from mitochondria, inhibiting the caspase inhibitor X-linked inhibitor of apoptosis protein (XIAP). The two pathways can intersect when caspase-8 cleaves the BH3-only protein BH3-interacting death domain agonist (BID), allowing it to promote MOMP.

1.3.1.2. TNFR signaling- Balancing Life and Death in Macrophages

Macrophages are crucial immune cells that serve dual roles: defending against pathogens and maintaining tissue homeostasis. They accomplish these tasks by utilizing PRRs to detect PAMPs/ and DAMPs. Most PRRs, when activated, stimulate the production of TNF, a versatile cytokine that plays a significant role in immune responses and cellular regulation. Tumor necrosis factor-alpha (TNF) is a versatile cytokine with wide-ranging effects on various cell types, inducing diverse cellular responses, including the expression of pro-inflammatory genes, proliferation, differentiation, and programmed cell death mechanisms like apoptosis and necroptosis (Veldhuis et al., 1991). TNFα exists in two forms. Type I is a soluble variant released by proteolytic cleavage of the transmembrane region, which mainly circulates in the body and activates TNFR1. Type II is a transmembrane variant that is expressed on the cell surface and can bind to both TNFR1 and TNFR2 but mainly TNFR2. Both forms contain the characteristic TNF homology domain (THD) (Nascimento et al., 2007). THD plays a crucial role in both the transmembrane and soluble forms of TNF, enabling their trimerization and interaction with TNF receptor 1 (TNFR1) and TNF receptor 2 (TNFR2) (Farajzadeh et al., 2017). THD enables trimerization and receptor binding in both its membrane-bound and soluble forms. TNFR1, a death receptor, contains a cytoplasmic death domain (DD), while TNFR2 lacks a DD and primarily interacts with TNF receptor-associated factors (TRAFs) (Tartaglia et al., 1993; Xie, 2013). These structural differences lead to distinct signaling pathways and cellular responses when activated by TNF. TNFR2 contains a C-terminal motif that recruits TRAF2 (TNF receptor-associated factor) and associated proteins TRAF1 and cIAP1/2 (cellular inhibitor of apoptosis protein), promoting NFκB signaling and kinase activation without inducing cell death (Wajant et al., 2003). In contrast, TNFR1 utilizes death domain-containing proteins to trigger apoptosis or necroptosis while also activating NFκB and MAP kinase pathways (Brenner et al., 2015).

1.3.1.2.1. Formation of the Core Signaling Complexes

The interaction between TNFα and TNFR1 initiates a cascade of molecular events crucial for signal transduction. Upon binding, TNFα induces the formation of TNFR1 trimers, which serves as a pivotal step in the signaling process. This trimerization of the receptor molecules sets the stage for the subsequent assembly of a key signaling complex **(Figure 7)**. The newly formed TNFR1

trimers provide a platform for the recruitment and organization of various signaling proteins on the intracellular portion of the receptor. This cytoplasmic domain of TNFR1 becomes a focal point for the aggregation of these proteins, forming a core signaling complex that is essential for transmitting the extracellular signal into the cell.

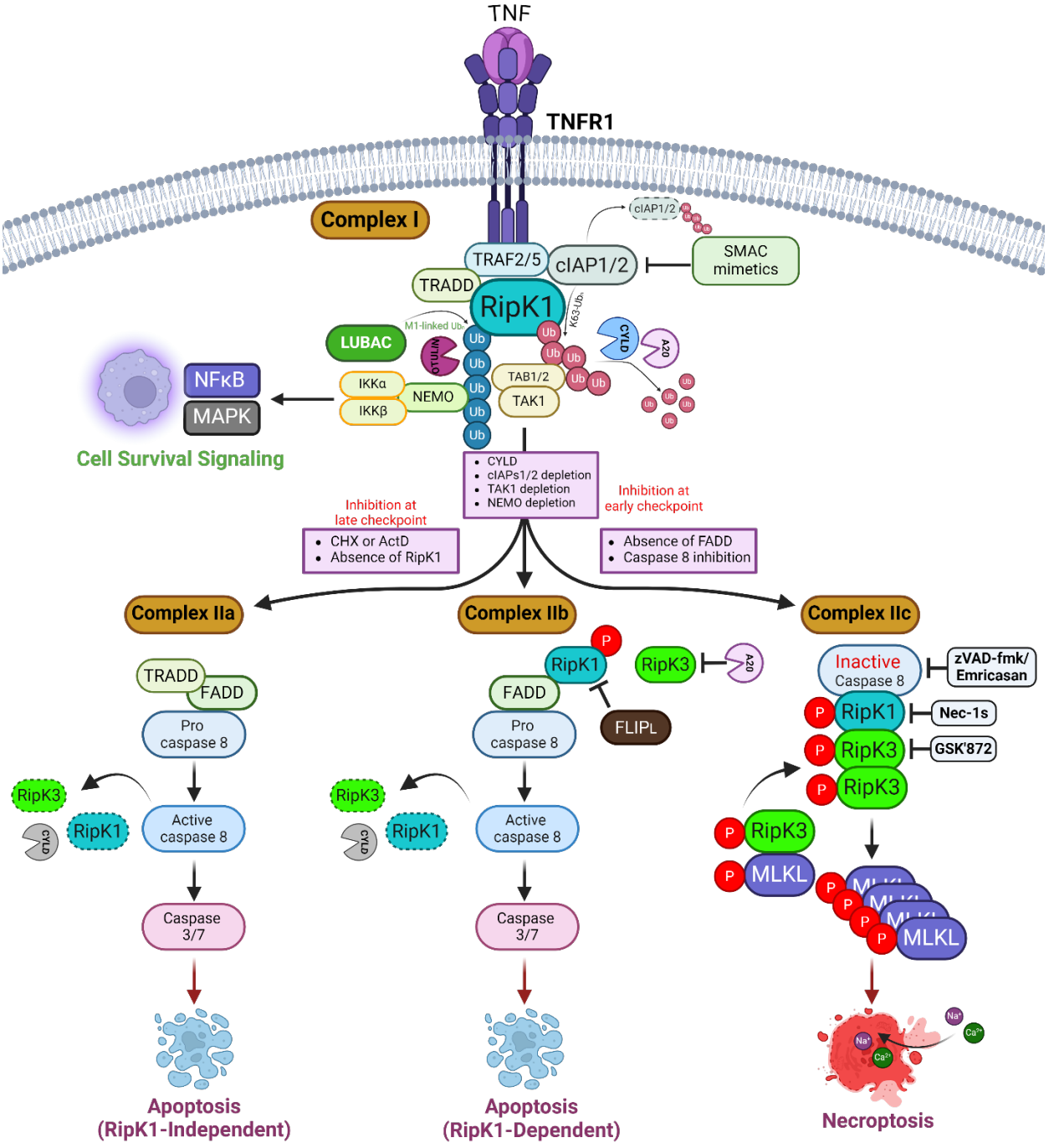
TNF
TNFR1
Complex I
cIAP1/2
TRAF2/5
cIAP1/2
SMAC mimetics
TRADD
RipK1
M1-linked Ub
K63-Ub
LUBAC
OTULIN
CYLD
A20
NFκB
MAPK
IKKα
IKKβ
NEMO
TAB1/2
TAK1
Ub
Cell Survival Signaling
CYLD
cIAPs1/2 depletion
TAK1 depletion
NEMO depletion
Inhibition at late checkpoint
CHX or ActD
Absence of RipK1
Inhibition at early checkpoint
Absence of FADD
Caspase 8 inhibition
Complex IIa
Complex IIb
Complex IIc
TRADD
FADD
Pro caspase 8
RipK3
RipK1
CYLD
Active caspase 8
Caspase 3/7
P
FLIPL
Inactive Caspase 8
zVAD-fmk/ Emricasan
Nec-1s
GSK'872
MLKL
Apoptosis (RipK1-Independent)
Apoptosis (RipK1-Dependent)
Necroptosis
Na+
Ca2+

Figure 7. The Main Signalling Events Downstream of TNFR Activation

The signaling pathway begins with the assembly of complex I upon TNF binding to TNFR1. This complex serves as a crucial platform for subsequent events and consists of several key proteins: TNFR1, TNFR1-associated death domain (TRADD), receptor-interacting serine/threonine-protein kinase 1 (RipK1), TNFR-associated factor 2 (TRAF2), cellular inhibitor of apoptosis protein 1/2 (cIAP1/2), and linear ubiquitin chain assembly complex (LUBAC). Within complex I, RipK1 undergoes ubiquitination, which plays a pivotal role in determining the cell's fate. This ubiquitination can be of two types: Lys63-linked ubiquitylation by cIAP1/2 or M1-linear ubiquitylation by LUBAC. The ubiquitination process leads to the recruitment of additional factors, including transforming growth factor-β (TGFβ)-activated kinase (TAK1), TAK1-binding protein 1 (TAB1), TAB2, NF-κB essential modulator (NEMO), and the inhibitor of the NF-κB kinase-α (IKKα)–IKKβ complex. These recruited factors typically trigger canonical NF-κB and MAPK signaling, promoting cell survival. The pathway can diverge from this point, leading to different outcomes depending on various factors and cellular conditions. In the presence of cycloheximide (CHX), a translational inhibitor, TNF stimulation results in the formation of complex IIa. This cytosolic complex is characterized by the disappearance of RipK1 and the interaction between TRADD and FAS-associated death domain (FADD). This interaction activates caspase 8 and effector caspases such as caspase 3 and caspase 7, ultimately leading to RipK1-independent apoptotic. Under conditions where cIAP1/2 are inhibited (e.g., by SMAC mimetics), knocked down, or when TAK1 or NEMO are inhibited or depleted, complex IIb forms. This complex consists of RipK1, RipK3, FADD, and caspase 8, and promotes RipK1-kinase-activity-dependent apoptosis. It's worth noting that heteromeric pro-caspase 8–FLICE-like inhibitory protein long isoform ($FLIP_L$) can inhibit necroptosis, likely by cleaving RipK1, RipK3, and Cylindromatosis (CYLD). In scenarios where RipK3 expression is sufficient and pro-caspase 8 and $FLIP_L$ are inhibited or have reduced expression, complex IIc (also known as the necrosome) forms. This complex formation involves the association of RipK1 and RipK3, followed by a series of auto- and transphosphorylation events. Activated RipK3 then phosphorylates and recruits mixed lineage kinase domain-like protein (MLKL). This process culminates in the formation of a supramolecular protein complex at the plasma membrane, ultimately leading to necroptosis. Various inhibitors and modulators can influence these pathways. SMAC mimetics are being developed to impair survival signaling and sensitize cells to death triggers in cancer treatment. Z-VAD-FMK or Emricasan acts as a pan-caspase inhibitor. Necrostatin-1s (Nec-1s) RipK1 kinase activity, and RipK3 inhibitor GSK′872 thus blocking necroptotic signaling.

1.3.1.2.1.1. Complex I– Cell Survival Signaling

TNFR1 trimerization enables its death domain to recruit TRADD (TNFR1-associated death domain), which serves as a scaffold for the signaling complex (H. Hsu et al., 1995). TRADD then orchestrates downstream signaling by recruiting TRAF2/5 (TNF receptor-associated factor), and RipK1 (serine/threonine-protein kinase 1) (Siegmund et al., 2023). Subsequently, TRAF2 facilitates the recruitment of E3 ligases cIAP1/2 (Shu et al., 1996). cIAPs modify RipK1 and other complex components by adding the K63, K11, and K48 poly-ubiquitin chains, creating binding sites for LUBAC (Linear Ubiquitin Chain Assembly Complex) and stabilizing Complex I. LUBAC further modifies RipK1 with M1 ubiquitin chains, enabling the recruitment of TAK1 (Transforming Growth Factor-β- Activated Kinases-1) via TAB2- (TAK1-Binding Protein) and the IKK (Inhibitor of Kappa B Kinases) complex. The ubiquitin modifications serve as scaffolds for additional signaling components, culminating in the formation of Complex I **(Figure 7)**. This complex activates NF-κB and MAPK pathways that promote cytokine production and cell survival (Vince et al., 2009).

1.3.1.2.1.1.1. NFκB Signaling

NF-κB, a key transcription factor, orchestrates various innate and adaptive immune responses and acts as a central mediator of inflammation (Mulero et al., 2019). This versatile regulator influences multiple aspects of immune function, including cytokine production, cell survival, and inflammatory processes (Vicioso et al., 2021). NF-κB proteins are typically retained in the cytoplasm through interaction with inhibitory proteins, primarily members of the IκB (Inhibitor of Nuclear factor Kappa B) family (S.-C. Sun, 2011). NF-κB activation occurs through two main pathways: the canonical and noncanonical (alternative) pathways (Vallabhapurapu & Karin, 2009). Despite their distinct signaling mechanisms, both pathways play crucial roles in regulating immune and inflammatory responses.

The canonical NF-κB pathway is rapidly activated by diverse stimuli, including cytokine receptors, PRRs, TNFR superfamily members, TCR, and BCR ligands (T- and B-cell receptors) (H. Zhang & Sun, 2015). The IKK complex consists of two catalytic subunits (IKKα and IKKβ) and a regulatory subunit NEMO (NF-κB essential Modulator) or IKKγ. This complex can be activated

by a wide range of stimuli, including cytokines, growth factors, mitogens, microbial components, and stress agents (S.-C. Sun & Ley, 2008). The diverse array of activators allows the IKK complex to integrate various cellular signals and initiate appropriate NF-κB-mediated responses. Activation of IKK leads to the phosphorylation of IκBα at two N-terminal serine residues. This phosphorylation event triggers the ubiquitin-dependent degradation of IκBα in the proteasome. Consequently, canonical NF-κB members, primarily p50/RelA and p50/c-Rel dimers, rapidly and transiently translocate to the nucleus (Hayden & Ghosh, 2008). This process results in the activation of NF-κB-mediated transcription of genes **(Figure 8)**.

In contrast, the noncanonical NF-κB pathway is a slow and sustainable response to a distinct set of stimuli, primarily ligands of specific TNFR superfamily members, including LTβR, BAFFR, CD40, and RANK (S.-C. Sun, 2012). The noncanonical NF-κB pathway employs a distinct activation mechanism that does not require IκBα degradation. Instead, this pathway relies on the processing of the NF-κB2 precursor protein, p100, to generate the active p52 subunit (S.-C. Sun, 2011). NIK (NF-κB-inducing Kinase) is the key signaling molecule in the noncanonical NF-κB pathway. It activates and cooperates with IKKα to phosphorylate p100, leading to its ubiquitination and processing. This process degrades p100's C-terminal IκB-like structure, generating mature p52. The resulting p52/RelB complex then translocates to the nucleus, activating noncanonical NF-κB signaling (H. Zhang & Sun, 2015) **(Figure 8)**.

Functionally, the canonical NF-κB pathway plays a central role in regulating diverse aspects of immune responses, while the noncanonical NF-κB pathway acts as a complementary signaling axis. This noncanonical pathway collaborates with the canonical pathway to regulate specific immune system functions.

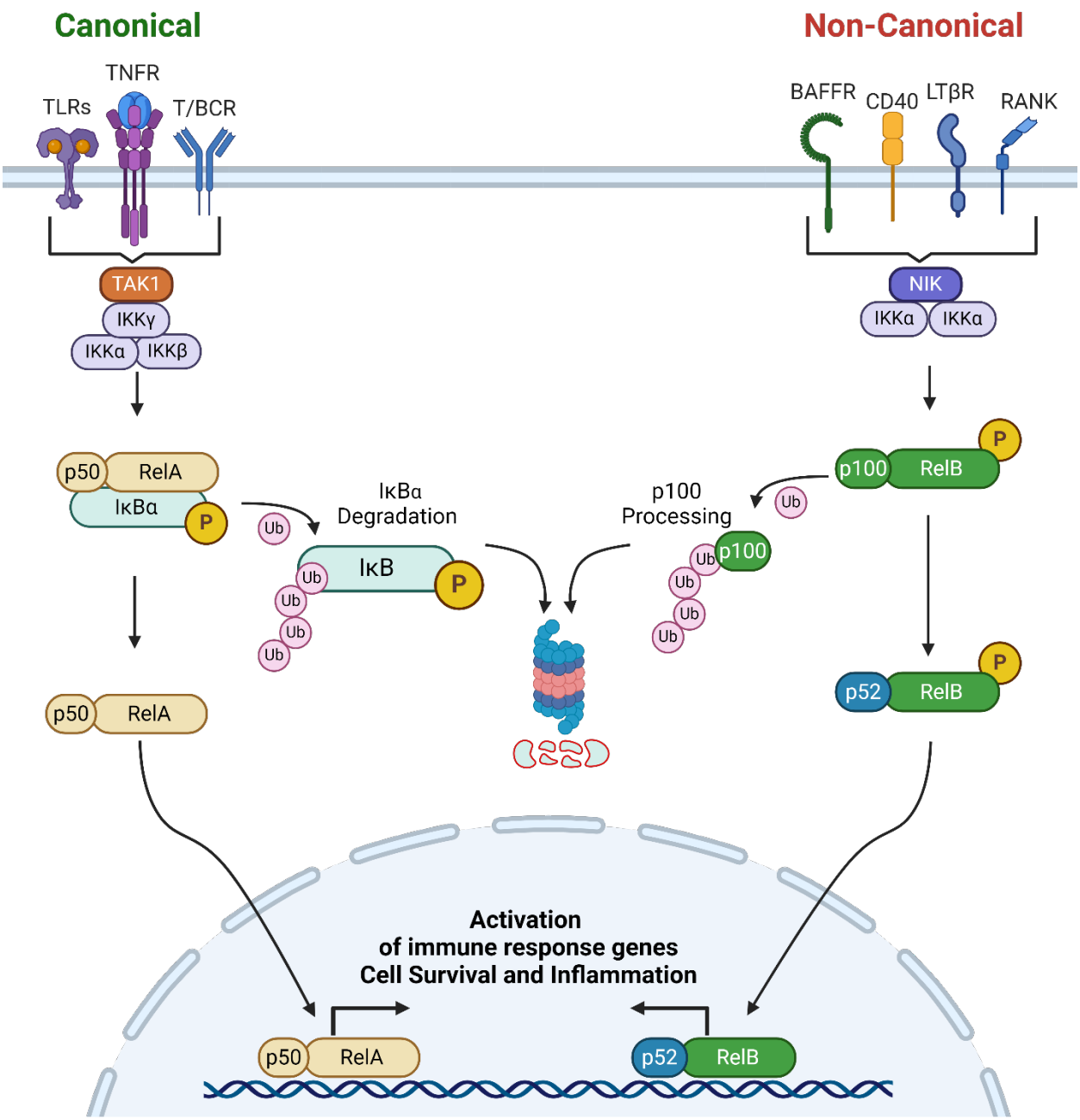
Canonical
Non-Canonical
TNFR
TLRs
T/BCR
BAFFR
CD40
LTβR
RANK
TAK1
IKKγ
IKKα
IKKβ
NIK
IKKα
IKKα
p50
RelA
IκBα
P
Ub
IκBα
Degradation
IκB
p100
Processing
p100
p100
RelB
p52
RelB
p50
RelA
Activation
of immune response genes
Cell Survival and Inflammation
p50
RelA
p52
RelB

Figure 8. Canonical and Non-canonical NF-κB Signaling

The canonical NF-κB pathway is activated by a wide array of signals, including those from both innate and adaptive immune receptors. This pathway involves a series of steps: Tak1 activates the IKK complex, which then phosphorylates IκBα, leading to its degradation. This process results in the swift and temporary nuclear translocation of the archetypal NF-κB heterodimer, RelA/p50. In contrast, the non-canonical NF-κB pathway is initiated by signals from a specific subset of TNFR members, triggering phosphorylation-induced processing of p100. This alternative pathway relies on NIK and IKKα but operates independently of the trimeric IKK complex. The outcome of this pathway is the sustained activation of the RelB/p52 complex.

1.3.1.2.1.1.2. MAPK Signaling

The mitogen-activated protein kinase (MAPK) pathway serves as a crucial signal transduction mechanism, converting external stimuli into internal cellular responses. This pathway acts as a molecular bridge, relaying information from the cell surface to the nucleus, thereby orchestrating various cellular processes in response to environmental cues (J. Macia et al., 2009). Three major MAPK families have been identified: ERK (Extracellular Signal-regulated Kinase), JNK/SAPK (Jun Kinase), and p38 MAPK (Cuschieri & Maier, 2005).

The extracellular signal-regulated kinase (ERK) signaling pathway is a crucial intracellular signaling cascade that plays a vital role in regulating various cellular processes, including proliferation, differentiation, survival, and apoptosis (Nakamura et al., 2021). ERK1/2 plays a crucial role in cellular signaling by phosphorylating and activating a diverse set of transcription factors, which in turn regulate the expression of genes that are important in various cellular processes. These transcription factors include Elk-1, c-FOS, c-Jun, p53, NF-κB/IκBα, and Est1/2 (Cook et al., 2017) **(Figure 9)**. The activation of these transcription factors by ERK1/2 can lead to different outcomes depending on the cellular context and the specific combination of factors activated. For example, phosphorylation of c-FOS and c-Jun can promote cell cycle progression, while activation of p53 may induce cell cycle arrest or apoptosis (Ahmed et al., 2006).

JNK is encoded by three genes (α, β, and γ) with 12 possible isoforms resulting from alternative splicing (Yarza et al., 2016). JNK phosphorylates several transcription factors, such as c-Jun, ATF-2, and p53, leading to increased expression of genes with AP-1 sites in their promoters (Y. R. Chen et al., 1996). The JNK pathway is involved in various cellular processes, including transformation, differentiation, and apoptosis (Y.-R. Chen et al., 1996) **(Figure 9)**.

The family in mammals is activated by a diverse array of cellular stressors, including ultraviolet radiation, thermal shock, hyperosmotic conditions, endotoxins, protein synthesis inhibitors, inflammatory cytokines (such as interleukin-1 and TNFα), and specific mitogenic factors (Ichijo, 1999). $p38^{MAPK}$ is a member of the MAPK family that exists in four distinct isoforms in mammalian cells: p38α, p38β, p38γ, and p38δ. These isoforms, while structurally similar, exhibit unique patterns of substrate phosphorylation and activation, leading to diverse cellular responses

(Cuadrado & Nebreda, 2010). Interferon (IFN) signaling requires p38 MAPK, which phosphorylates and activates cytosolic phospholipase A2, while IFN-α/-γ-induced $p38^{MAPK}$ activation leads to Stat1 phosphorylation on Ser727 (Goh et al., 1999). The $p38^{MAPK}$ pathway is activated by upstream kinases MKK3, MKK4, and MKK6. Following activation, p38 phosphorylates MAPK-activated protein kinases 2 and 3 (MK2 and MK3), which are ubiquitously expressed and primarily found in the nucleus **(Figure 9)**. Once activated, MK2 and MK3 regulate various cellular functions, including actin cytoskeleton remodeling, cell motility, inflammatory cytokine production, gene transcription, and cell cycle progression (Cargnello & Roux, 2011).

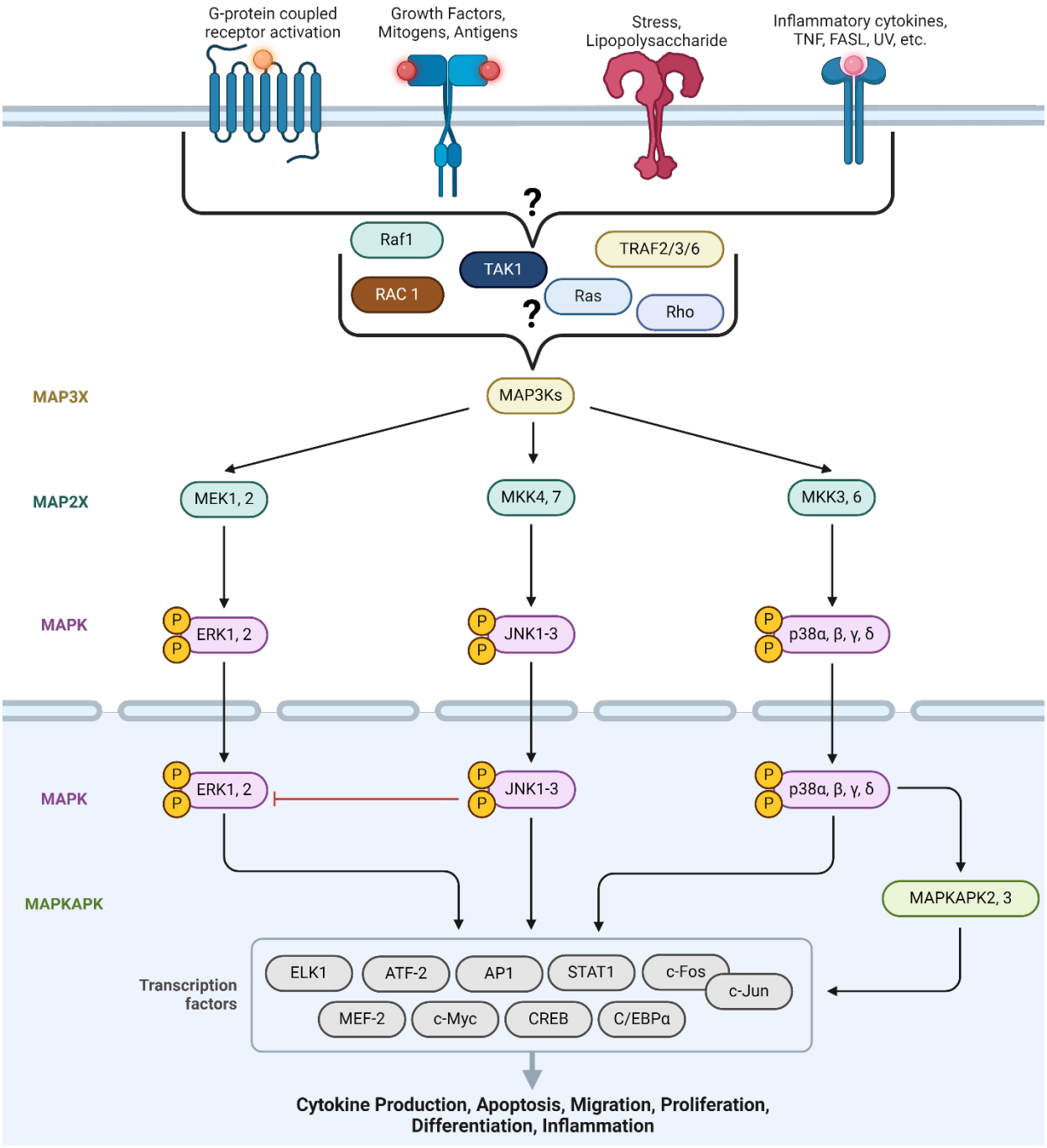

Figure 9. Schematic Diagram of the MAPK Signaling Pathways

1.3.1.2.1.1.3. p38^{MAPK}-MK2-TTP Axis

The p38^{MAPK} is activated through dual phosphorylation on threonine-180 and tyrosine-182 residues, a process mediated by upstream MAP2Ks, specifically MKK3 and MKK6 (Raingeaud et al., 1995). Upon activation, p38^{MAPK} orchestrates cellular responses by phosphorylating various targets. This results in the amplification of inflammatory processes through increased production and secretion of pro-inflammatory cytokines (Ronkina et al., 2010). The p38^{MAPK} phosphorylates several targets, with MK2 being a key substrate that coordinates most of the processes. This p38 MAPK-MK2 signaling pathway plays a critical role in mediating cellular responses to stress and inflammatory stimuli. MK2 activation occurs through phosphorylation at Thr-222, Ser-272, and Thr-334 by p38^{MAPK} α and β isoforms (Freshney et al., 1994). MK2 phosphorylates various substrates but acts as a crucial regulator of RNA-binding proteins, thereby exerting indirect control over gene expression at the translational level (Gaestel, 2006; Menon & Gaestel, 2018). Cytokine mRNAs often contain adenylate-uridylate-rich elements (AREs) in their 3' untranslated regions. These AREs serve as binding sites for regulatory proteins, enabling posttranscriptional control of cytokine production by modulating mRNA stability and translation efficiency (Anderson, 2008). Zinc finger protein 36 (Zfp36), also described as Tristetraprolin (TTP), is an ARE-binding protein that negatively regulates the expression of various cytokines and chemokines by destabilizing mRNAs and inhibiting their translation through interactions with AREs (Ross et al., 2015). Under normal conditions, TTP is expressed at low levels in all tissues. However, inflammatory stimuli such as lipopolysaccharide (LPS) and various cytokines such as TNFα trigger both transcriptional and posttranscriptional upregulation of TTP expression in macrophages (Tiedje et al., 2012). Interferons (IFNs) contribute significantly to the resolution of inflammation by stimulating the expression of TTP. The induction of TTP by IFNs requires both the activation of the transcription factor STAT1 by IFN signaling and the concurrent activation of p38^{MAPK} by stress signals, illustrating a dual-control mechanism for TTP expression. Once induced, TTP acts to destabilize mRNAs of several pro-inflammatory cytokines, including TNFα, IL-6, and others (Sauer et al., 2006). This mechanism establishes a negative feedback loop that helps to dampen the inflammatory response and promote its resolution. During the early inflammatory response, TTP expression is rapidly upregulated and undergoes transient phosphorylation at multiple sites. Specifically, the p38^{MAPK}-activated kinases MK2 directly phosphorylate TTP at two key sites, S52 and S178 (Ronkina et al., 2019). This phosphorylation plays a crucial role in inhibiting the activity

of TTP and, consequently, its regulation of inflammatory cytokine production. Stress activates $p38^{MAPK}$, triggering a phosphorylation cascade: $p38^{MAPK}$ phosphorylates MK2, which then phosphorylates TTP, transmitting the stress signal. TTP phosphorylation enables its binding to 14-3-3 proteins. These 14-3-3 proteins function as molecular chaperones, maintaining specific conformations of various target proteins, including the phosphorylated TTP (Chrestensen et al., 2004). TTP's association with 14-3-3 proteins disrupt its ability to recruit the exosome complex. This disruption prevents the normal degradation process, resulting in increased stability of mRNAs containing AU-rich elements (AREs) (Stoecklin et al., 2004) **(Figure 10)**. The precise molecular details underlying this process remain to be fully uncovered.

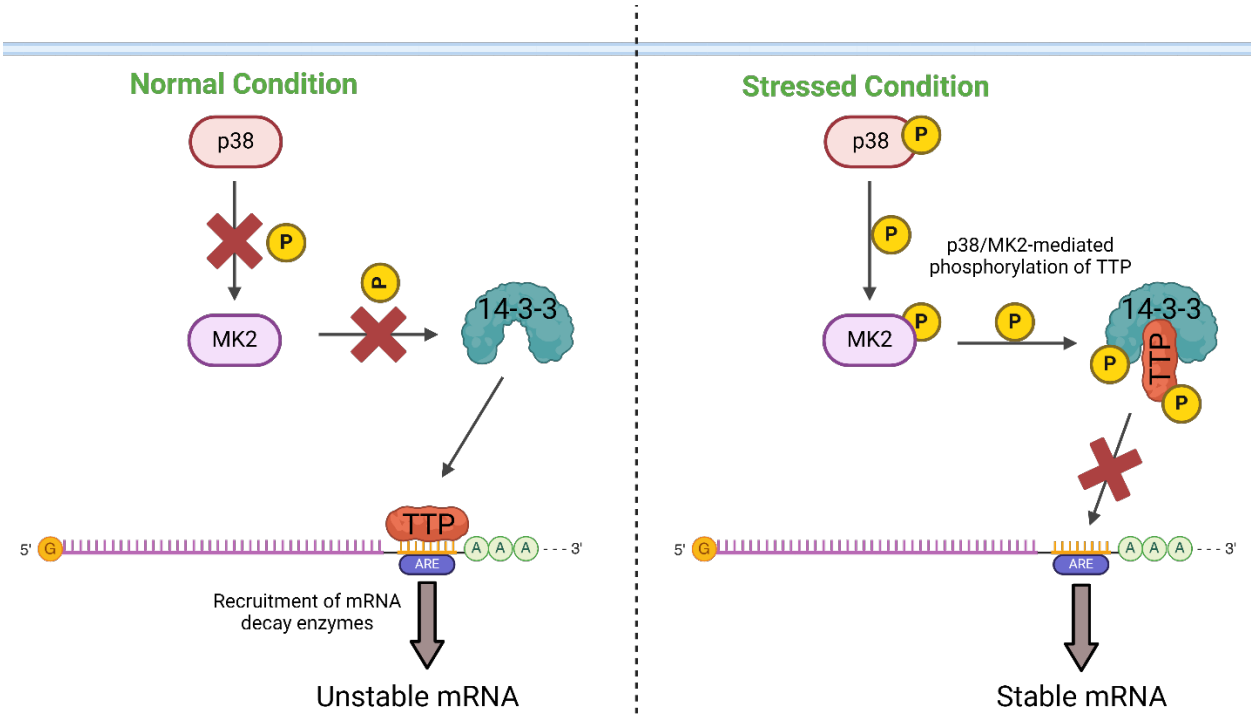

Figure 10. Overview of the p38-MK2-TTP Axis

Under normal cellular conditions, the p38 MAPK pathway remains inactive, allowing TTP (Tristetraprolin) to freely bind to the ARE (AU-rich element) in the 3'UTR of ARE-containing mRNAs. This binding enables TTP to recruit mRNA decay enzymes, promoting the degradation of these transcripts. However, when cells encounter stress stimuli, the p38 MAPK pathway becomes activated, triggering a phosphorylation cascade. This cascade culminates in the phosphorylation of TTP, which subsequently leads to its sequestration by 14-3-3 proteins. The 14-3-3 proteins are a family of regulatory molecules that function as molecular chaperones, capable of stabilizing specific conformations of various target proteins. In this context, the 14-3-3-mediated sequestration of TTP effectively prevents it from interacting with the ARE, thus altering the fate of ARE-containing mRNAs.

1.3.1.2.1.2. Complex II – Cell Death Signaling

The formation of signaling complexes in cell death pathways is critically dependent on the ubiquitination status of RipK1. While the assembly of Complex I requires complete ubiquitination of RipK1, the formation of Complex II is facilitated by partial or incomplete ubiquitination of RipK1. This differential ubiquitination serves as a molecular switch, determining whether the cell death signaling proceeds through Complex I or Complex II pathways (H. Li et al., 2006). When RipK1 is incompletely ubiquitinated, it detaches from the initial signaling complex I and participates in different signaling pathways.

1.3.1.2.1.2.1. Complex IIa- RipK1-Independent Apoptosis

Cylindromatosis (CYLD), induced by NF-κB, initiates Complex IIa formation by de-ubiquitinating RipK1, thus creating a negative feedback loop for NF-κB activation (Trompouki et al., 2003). CYLD's association with TRAF2 removes K63 and M1 poly-ubiquitin chains from RipK1, enabling its dissociation from the TNFR1 complex (Kovalenko et al., 2003). Recent findings indicate that CYLD's primary role is likely in regulating RipK1 activation within Complex II, rather than facilitating the transition from Complex I to Complex II (Moquin et al., 2013). Upon release into the cytosol, RipK1 participates in the assembly of Complex IIa by binding with TRADD, FADD (Fas-Associated Death Domain), and pro-caspase 8 (L. Wang et al., 2008). These proteins may collectively serve as a nucleation point to recruit additional RipK1 and RipK3 molecules (J. Li et al., 2012). Noteworthy, TNFR1-induced $p38^{MAPK}$ activation leads to MK2-mediated phosphorylation of RipK1 (on serine 320 in humans or 321 in mice) in both TNFR1-associated and free cytosolic forms, inhibiting RipK1's ability to act as a nucleation point for cytosolic complexes containing kinase-active RipK1 (Jaco et al., 2017; J. Li et al., 2012). When protein synthesis is blocked by cycloheximide (CHX) and IKK inhibitors, the consequent suppression of the NF-κB pathway allows Caspase-8 to become active. The active Caspase-8 inactivates RipK1 and RipK3 through proteolytic cleavage, initiating proapoptotic caspase activation (Vanlangenakker, Bertrand, et al., 2011) and which initiates the activation of pro-caspases -3 and -7, leading to RipK1-independent apoptotic cell death (Elmore, 2007) **(Figure 7)**.

1.3.1.2.1.2.2. Complex IIb- RipK1-Dependent Apoptosis

The formation of Complex IIb can be triggered by insufficient ubiquitination of RipK1, which occurs when cIAP1/2 is depleted or degraded (e.g. by SMAC- Mitochondria- Derived Activator of Caspase Mimetics or genotoxic stress), resulting in reduced or absent K63 poly-ubiquitin chains on RipK1 (Tenev et al., 2011; L. Wang et al., 2008) or inhibition of TAK1 or NEMO (Dondelinger et al., 2013). The binding of SMAC to cIAPs triggers the auto-ubiquitination of cIAPs, resulting in the subsequent degradation of cIAPs (Du et al., 2000). The lack of K63-linked ubiquitination destabilizes RipK1 in the core signaling complex, causing it to dissociate from TNFR1, like the initial stages of Complex IIa formation. RipK1 reassembles in the cytosol, forming a complex called the Ripoptosome, which includes FADD, pro-caspase 8, and RipK3 (Tenev et al., 2011). cIAP1, cIAP2, XIAP, and $FLIP_L$ act as negative regulators of the Ripoptosome complex. C-FLIP is an anti-apoptotic protein (cellular- FADD-like-1β-Converting Enzyme) that exists in multiple forms: the long-form (c-FLIPL), the short form (c-FLIPS), and various splice variants known as $c\text{-}FLIP_R$ (Safa, 2013). Contrary to $c\text{-}FLIP_L$, which inhibits Ripoptosome formation, $c\text{-}FLIP_S$ surprisingly facilitates its assembly. The Caspase-8: $c\text{-}FLIP_L$ heterodimer in Complex IIb cleaves RipK1 and RipK3, potentially preventing necrosome formation. In contrast, the enzymatically inactive Caspase-8: $c\text{-}FLIP_S$ heterodimer cannot cleave RipK1/3, thus favoring necroptosis induction. The specific c-FLIP isoforms present in the Ripoptosome play a crucial role in determining the cell death pathway, directing it toward either Rip1-dependent apoptosis or necroptosis (Feoktistova et al., 2011) **(Figure 7)**.

1.3.1.2.1.2.3. Complex IIc- Necrosome

Following caspase 8 activation in Complex IIa and IIb, the activated caspase degrades RipK1 and RipK3 in the cytosolic compartment. However, when caspase-8 activity is suppressed, either endogenously by $cFLIP_S$ (Feoktistova et al., 2011)or exogenously by pan-caspase inhibitors like zVAD or Emricasan (EMR) (Brumatti et al., 2016; Ito et al., 2016), it leads to the phosphorylation of RipK3.(J. Li et al., 2012). Also, A20 inhibits RipK3-driven necroptosis when caspases are active by preventing RipK3 ubiquitination and leading to the disruption of the RipK1-RipK3 complex (Gurung et al., 2015). The necrosome, an amyloid-like structure, forms when RipK1 recruits RipK3 via their RIP homotypic interaction motif (RHIM). This RipK1-RipK3 complex then

facilitates the recruitment and phosphorylation of mixed-lineage kinase domain-like (MLKL) protein, a key step in the necroptosis pathway (L. Sun et al., 2012). Upon phosphorylation, MLKL proteins assemble into tetrameric structures and migrate to the plasma membrane causing cell lysis and inflammation (Cai et al., 2014) **(Figure 7)**.

1.3.1.3. Necroptosis

In 2005, researchers identified necroptosis as a distinct form of cell death, triggered by TNFα when caspase-8 is inactive, representing a non-apoptotic pathway of programmed cell death (Degterev et al., 2005). Necroptosis exhibits key morphological characteristics of necrosis, such as swollen organelles, intact nuclei, ruptured plasma membranes, and the release of cellular contents (Seo et al., 2021). TNF-induced necroptosis stands out as the most extensively studied form of regulated necrosis, a non-apoptotic cell death pathway (Vanden Berghe et al., 2014). The discovery of necrostatins, particularly necrostatin-1, which inhibits RipK1 and blocks TNF-induced necrosis, sparked a surge in necroptosis research (Degterev et al., 2008).

Necroptosis serves as a crucial backup mechanism when apoptosis is inhibited or compromised. It helps eliminate damaged or infected cells that cannot undergo apoptosis, maintain tissue homeostasis, and defend against pathogens (Loftus et al., 2022). Necroptosis is also predominantly associated with pathological conditions characterized by pronounced inflammation, including Crohn's disease, ischemia-reperfusion injury, amyotrophic lateral sclerosis, toxic epidermal necrolysis, and multiple sclerosis, among others (Conrad et al., 2016). Necroptosis is a tightly regulated form of programmed cell death that acts as a double-edged sword in human physiology and disease. On one hand, it serves as a crucial host defense mechanism, leveraging its robust pro-inflammatory properties to eliminate pathogen-infected or malignant cells, thereby contributing to antimicrobial immunity and tumor suppression. However, this same inflammatory potency can become detrimental, as necroptosis is also capable of triggering uncontrolled inflammatory cascades that result in severe tissue injury, chronic disease progression, and, in some cases, even promote tumor growth and metastasis. The dual nature of necroptosis—protective in some contexts and destructive in others—underscores its complex role in health and disease, highlighting the importance of carefully targeting this pathway in therapeutic strategies (Kaczmarek et al., 2013).

Necroptosis was first identified in fibroblasts, specifically in L929 mouse fibrosarcoma cells. This discovery laid the groundwork for understanding the basic mechanisms of this form of programmed cell death (Degterev et al., 2005). As research progressed, the focus shifted towards immune cells, particularly macrophages, due to their critical role in inflammation and immune responses (He et al., 2009; Kaiser et al., 2013; D.-W. Zhang et al., 2009).

Various external stressors can initiate necroptosis, such as tissue damage from ischemia-reperfusion, excessive calcium influx, pharmacological agents, changes in osmotic pressure, and elevated temperatures (Vanlangenakker et al., 2012; X. Yu et al., 2013; F. Yuan et al., 2022; W. Zhang et al., 2022). These stressors initiate necroptosis through multiple signaling pathways that involve specific ligand-receptor interactions. The key pathways include TNFα binding to TNFR (L. Sun et al., 2012), Fas ligand interacting with FAS (Estlack et al., 2014), Death Receptor 3 (DR3) (Bittner et al., 2016), interferon-gamma (IFN-γ) and IFNAR1 (Hos et al., 2017), double-stranded RNA activating Toll-Like Receptor 3 (TLR3) (Upton et al., 2019), Toll-Like Receptor 4 (TLR4) (Kaiser et al., 2013), and double-stranded DNA binding to Z-DNA binding protein 1 (ZBP1, also known as DNA-dependent activator of IFN-regulatory factors - DAI) (Jiao et al., 2020). These diverse ligand-receptor interactions initiate distinct signaling cascades that converge on necroptotic cell death, underscoring the complex and multifaceted nature of stimuli capable of triggering this regulated form of necrosis **(Figure 11)**.

Necroptosis is characterized by its ability to provoke and amplify inflammatory responses (Davidovich et al., 2014). Research using animal models has demonstrated that necroptosis plays a crucial role in the development and progression of various inflammatory disorders. In the absence of pathogens, cells undergoing death can initiate inflammatory responses by releasing DAMPs, a group of endogenous signaling molecules (Pasparakis & Vandenabeele, 2015). The scientific community widely agrees that necroptosis directly incites inflammation through the substantial release of DAMPs as the cell breaks down.

The precise early molecular mechanisms that determine whether a cell undergoes apoptosis or necroptosis remain elusive. Although necroptosis is known to aggravate numerous inflammatory conditions, the specific pathways governing the resulting inflammatory responses are not yet fully understood. This study aims to elucidate the early molecular switches determining cell fate

between apoptosis and necroptosis and unravel the intricate pathways regulating inflammatory responses triggered by necroptosis in various diseases, including Alzheimer's disease, amyotrophic lateral sclerosis (ALS), ischemic injuries (e.g., stroke, myocardial infarction), and multiple sclerosis (Atri et al., 2018; Gong et al., 2020, 2020; D. Li & Wu, 2021).

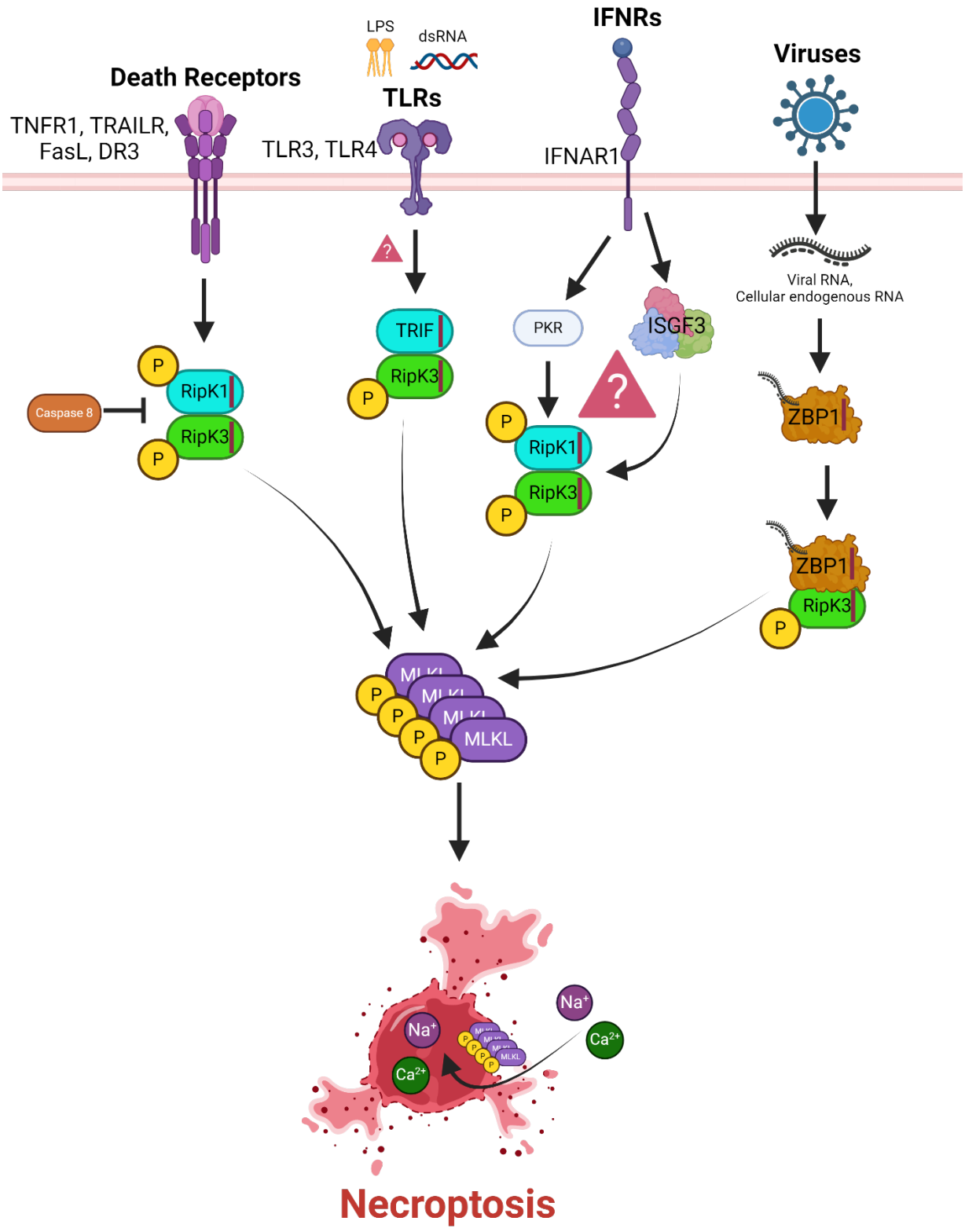

Figure 11. Multiple Stimuli that Lead to Necroptosis

1.3.1.3.1. Molecular Mechanism of Necroptosis

It is well established that during the execution of necroptosis, three crucial components of the pathway - RIP1, RIP3, and MLKL - undergo phosphorylation. RipK1 has emerged as a major signaling hub downstream of several immune receptors, where it regulates the cell's fate through kinase-dependent and -independent mechanisms (Silke et al., 2015). Within complex I, RipK1 undergoes extensive phosphorylation at multiple sites (Delanghe et al., 2020). Various research groups have reported that MK2 phosphorylates RipK1 at S321 and S336 (S320 and S335 in humans) within its intermediate domain (Geng et al., 2017). Notably, the MK2 phosphorylation sites S321 and S336 on RipK1 are located close to its Caspase-8 cleavage site (D324), suggesting a potential interplay between MK2-mediated phosphorylation and Caspase-8-induced proteolytic inactivation of RipK1 (Menon et al., 2017). RipK1's kinase activity in cell death signaling remains enigmatic, with auto-phosphorylation as its only known function. This self-modification may trigger structural changes in RipK1, facilitating its association with FADD and RipK3 to promote cell death. RipK1 undergoes auto-phosphorylation at multiple sites, including S14/15, S20 (in humans), S161, S166, and T169 (in mice) (Heger et al., 2018; Oberbeck et al., 2019). The exact mechanisms triggering RipK1 autophosphorylation and its specific role in the necroptotic process remain to be fully elucidated. The RHIM (RIP homotypic interaction motif), a hydrophobic β-sheet region, facilitates the interaction between RipK1 and RipK3. The RHIM is present in several other adaptor proteins crucial for innate immunity and cell death signaling, including TRIF (TIR domain-containing adaptor-inducing interferon-β) (Meylan et al., 2004) and DAI (DNA-dependent activator of IFN regulatory factors, also known as ZBP1 or DLM-1) (Kaiser et al., 2008). The N-terminal regions of both RipK1 and RipK3 are characterized by the presence of Ser/Thr kinase domains (KDs). RipK1 phosphorylates RipK3 at specific sites, with Ser227 in human RipK3 (corresponding to Thr231/Ser232 in mouse RipK3) being crucial for the recruitment and activation of mixed-lineage kinase domain-like (MLKL) (L. Sun et al., 2012). While RipK3 contains multiple phosphorylated serine/threonine residues, the functional significance of these additional phosphorylation sites in RipK3 activation remains less clear (W. Chen et al., 2013). RipK3 triggers necroptosis by activating MLKL. Activated RipK3 phosphorylates MLKL at specific residues: T357 and S358 in human MLKL and S345 in mouse MLKL (Rodriguez et al., 2016). Phosphorylation triggers MLKL tetramerization and exposes its four-helix bundle domain. MLKL

then translocates to the plasma membrane, where its conformation changes, enhancing its membrane-binding capacity. Research has yielded diverse explanations for how MLKL translocation leads to cell death. At the membrane, MLKL interacts with phosphatidylinositol phosphate (PIP) and cardiolipin (CL). Oligomerized MLKL can engage with TRPM7 channels, facilitating the influx of extracellular Ca2+, which ultimately results in plasma membrane disruption (Cai et al., 2014). The MLKL complex, once localized to the plasma membrane, can enhance sodium ion influx, either directly or by interacting with other membrane proteins. This increased sodium influx elevates intracellular osmotic pressure, ultimately causing cell swelling and rupture of the plasma membrane (X. Chen et al., 2014). The rupture of the plasma membrane results in the release of damage-associated molecular patterns (DAMPs), triggering inflammation and leading to the release of pro-inflammatory cytokines, further amplifying the inflammatory response (X. Wu et al., 2024).

1.3.1.3.2. Ubiquitination and Deubiquitination

Protein stability and function are modulated by the dynamic processes of ubiquitination and deubiquitination, which play crucial roles in diverse cellular activities such as DNA repair, cell death, gene transcription, and cell cycle regulation (Dagar et al., 2023). PCD is controlled by intracellular proteins subject to various post-translational modifications, particularly mono- and polyubiquitination. Ubiquitination dynamically influences protein abundance, location, and function. This reversible process, counteracted by deubiquitinases, balances deubiquitination to determine cellular outcomes during stress.

Ubiquitination is a post-translational modification where the 76-amino acid protein ubiquitin is covalently attached to target proteins through a cascade involving E1 (ubiquitin-activating), E2 (ubiquitin-conjugating), and E3 (ubiquitin ligase) enzymes (Hershko & Ciechanover, 1998). Ubiquitin chains can be added on different lysine residues (K6, K11, K27, K29, K33, K48, or K63) (Kwon & Ciechanover, 2017). K48-linked ubiquitination primarily targets proteins for proteasomal degradation, while K63-linked ubiquitination regulates non-proteolytic functions such as kinase activation, signaling, and DNA repair (Swatek & Komander, 2016). Deubiquitination is the reversal of ubiquitination, mediated by deubiquitinases (DUBs). DUBs regulate protein fate by removing ubiquitin chains, inhibiting ubiquitination processes, and editing

ubiquitin chains, thus maintaining cellular ubiquitin homeostasis and modulating protein degradation and signaling. The human genome encodes approximately 100 deubiquitinases (DUBs) categorized into seven families: USPs, UCHs, OTUs, MJDs, JAMM/MPN+, MINDYs, and ZUFSP, each with distinct structural and functional characteristics (Abdul Rehman et al., 2016).

Upon activation, TNFR1 engages RipK1 and TRADD, followed by TRADD's recruitment of TRAF2/5, which subsequently attracts cIAP1/2 to the complex (Bertrand et al., 2008). RipK1 is post-translationally modified by various E3 ligases, deubiquitinases, and kinases, which function as cell fate determinants, regulating the inflammatory and death-signaling pathways (Annibaldi et al., 2018). cIAP1/2, functioning as RING finger E3 ligases, attach K63- and K48-linked ubiquitin chains to various components of Complex I, including RipK1 to stabilize it in complex I. This process is followed by the recruitment of LUBAC, another E3 ligase, which then adds M1-linked ubiquitin chains to RipK1 (Gerlach et al., 2011; Keusekotten et al., 2013). The K63-linked and M1-linked ubiquitin chains on RipK1 serve as docking sites for the TAK1 and IKK complexes, leading to the activation of MAPK and NF-κB signaling pathways, respectively. cIAP1 also attaches K11-linked ubiquitin chains to RipK1, which further promotes the recruitment of the IKK complex (Dynek et al., 2010). Recent research has demonstrated that the deubiquitinase OTULIN removes M1-linked ubiquitin chains from RipK1 during necroptosis (Douglas & Saleh, 2019). When RipK1 is deubiquitinated by CYLD or fails to be ubiquitinated upon recruitment to Complex I (such as during IAP depletion), the signaling pathway shifts towards the formation of Complex IIa or IIb, respectively (Bertrand et al., 2008; Kovalenko et al., 2003). Mass spectrometric analysis of HT29 cells revealed that RipK1's K115 residue is specifically ubiquitinated during TNFα-induced necroptosis (de Almagro et al., 2017). This site appears to be the primary location for M1- and K63-linked ubiquitin chains during necroptosis (de Almagro et al., 2015). While the K115 mutation reduces necroptosis, it remains unclear how both chain types coexist at this site and whether they have pro- or anti-necroptotic effects. The precise roles of these ubiquitin modifications in regulating necroptosis require further investigation. The cellular context determines whether Complex IIa or IIb will trigger apoptosis or necroptosis. Research indicates that RipK3 ubiquitination plays a role in promoting necroptosis. A20 inhibits RipK3 function by attaching K48-linked ubiquitin chains to its K5 residue, thereby preventing RipK1-RipK3 complex

formation and protecting cells from necroptosis (Onizawa et al., 2015). Other E3 ligases also suppress necroptosis by altering RipK3's ubiquitination status. For instance, Pellino-1 catalyzes K48-linked ubiquitination of active RipK3 (Choi et al., 2018).

Understanding the early events of ubiquitination and deubiquitination in necroptosis plays a crucial role in elucidating the regulation of this cell death pathway. These post-translational modifications serve as important checkpoints that determine whether cells undergo necroptosis or survive. By elucidating these early events, we can gain a more comprehensive understanding of necroptosis regulation, potentially leading to new therapeutic strategies for diseases involving aberrant necroptotic signaling.

1.3.1.3.3. TLR-Mediated Necroptotic Pathways

Pathogen sensors detect microbial patterns, activating host defenses through immune factors. These sensors, while protective, can also promote inflammation and autoimmunity. Recent research highlights their role in determining infected cell fate through various regulated death pathways, serving as a primary mechanism for eliminating infected cells (Lamkanfi & Dixit, 2010). Toll-like receptors (TLRs) were the first pattern recognition receptors (PRRs) to be discovered (Akira et al., 2006). These receptors recognize various pathogen-associated molecular patterns, including peptidoglycan (sensed by TLR2), double-stranded RNA (TLR3), lipopolysaccharide (TLR4), flagellin (TLR5), and unmethylated CpG DNA motifs (TLR9). TLR3 and TLR4 distinctively use the TRIF adapter for signaling, while TLR4 and all other TLRs also utilize MyD88. Like TNF family death receptors, TLRs not only promote the expression of cytokines including interferons, but they also play a crucial role in determining cell fate, including the induction of apoptosis and programmed necrosis (He et al., 2011; Kaiser & Offermann, 2005). Research has consistently demonstrated that the engagement of TLR3/4 can trigger necroptosis in primary macrophages when caspase activity is inhibited (Legarda et al., 2016; Linkermann & Green, 2014; McComb et al., 2014; Robinson et al., 2012).

TLR4-mediated necroptosis has emerged as a prominent focus in current research due to its unique and complex signaling mechanisms. As the only Toll-like receptor utilizing both MyD88 (myeloid differentiation primary response protein 88) and TRIF (Toll/IL-1R domain-containing adaptor-

inducing IFN-β) adaptor proteins, TLR4 activates multiple signaling cascades, making it an intriguing subject for studying intricate cellular responses.

The activation of TLR4 by LPS involves a multi-step process that converts bacterial LPS aggregates into monomers at the cell surface. Serum LBP initiates this by binding to LPS micelles, typically followed by CD14-mediated extraction of LPS monomers. CD14 then delivers these monomers to the TLR4/MD-2 complex, concentrating them near the receptor and enabling activation (Gioannini et al., 2005; Iovine et al., 2002; B. Yu & Wright, 1996). TLR4/MD-2 activation occurs when two agonistic LPS molecules bind, causing dimerization of TLR4 ectodomains into an "M-shape". This configuration brings the intracellular TIR domains of TLR4 into proximity, enabling interactions with TIR domains and activating two downstream pathways (Meng et al., 2011; B. S. Park et al., 2009). First, the MyD88-dependent pathway is initiated when Mal (MyD88 adaptor-like, also called TIRAP) is recruited to the plasma membrane. There, Mal serves as a bridge between MyD88 and the activated receptor, facilitated by its Toll-IL-1 receptor (TIR) interaction domain (Yamamoto et al., 2002). Apart from the TIR domain, TIRAP also carries a domain enriched in basic and aromatic residues that interact with phosphatidylinositols (PIs) and phosphatidylserine (PS) (Bonham et al., 2014). The TLR4-bound TIRAP recruits MyD88, which further recruits E3 ubiquitin ligase TRAF6, which triggers a signaling cascade involving TAK1 kinase and leading to the signaling cascade that activates key transcription factors, notably NF-κB and AP-1 (via MAPK) (Y.-C. Lu et al., 2008) **(Figure 12)**. These activated transcription factors then trigger the production of various pro-inflammatory cytokines such as TNFα (Takeda & Akira, 2004). Second, the MyD88-independent pathway is activated when TLR4 is internalized into endosomes. Simultaneously, TIRAP and MyD88 dissociate from the membrane, allowing TLR4 to bind in the endosome to a second set of TIR-containing adaptor proteins, TRAM and TRIF (Marongiu et al., 2019). In this situation, TRAM (Trif-related adaptor molecule) acts as a bridging adaptor that facilitates the interaction of TRIF with TLR4 (Oshiumi et al., 2003). This internalization facilitates the binding of TRAM to TLR4. TRAM then recruits Trif (TIR-domain-containing adaptor-inducing interferon-β), which leads to interferon-regulatory factors -3 and -7 (IRF3 and IRF7) activation by TBK1 and then dissociates from TRIF, dimerizes, and translocates to the nucleus (S. Liu et al., 2015). Ultimately, this cascade results in the production of type I interferons (Fitzgerald et al., 2003; Oshiumi et al., 2003) **(Figure 12)**.

TLR3/4 signaling, mediated by TRIF through its C-terminal RHIM domain interaction with RipK1 or RipK3 (Meylan et al., 2004), can lead to three distinct cellular outcomes. First, it can activate NF-κB (Vivarelli et al., 2004), a process partially reliant on RipK1. Second, it can initiate apoptosis via Caspase-8 (Feoktistova et al., 2011)which is influenced by RipK1 engagement. Third, when Caspase-8 activity is inhibited, TLR3 signaling can induce necroptosis (He et al., 2011)dependent on both RipK1 and RipK3. TLR4-mediated necroptosis is a critical process in immune responses and inflammatory conditions due to its role in triggering TNF and IFN secretion. This pathway amplifies inflammatory responses through a positive feedback loop, where necroptosis releases DAMPs that further stimulate cytokine production. TNF can trigger further necroptosis in neighboring cells, while IFN can prime cells for enhanced responsiveness to subsequent stimuli. The intricate relationship between TLR4-mediated necroptosis and TNF/IFN secretion presents both challenges in managing inflammatory disorders and opportunities for developing targeted therapies.

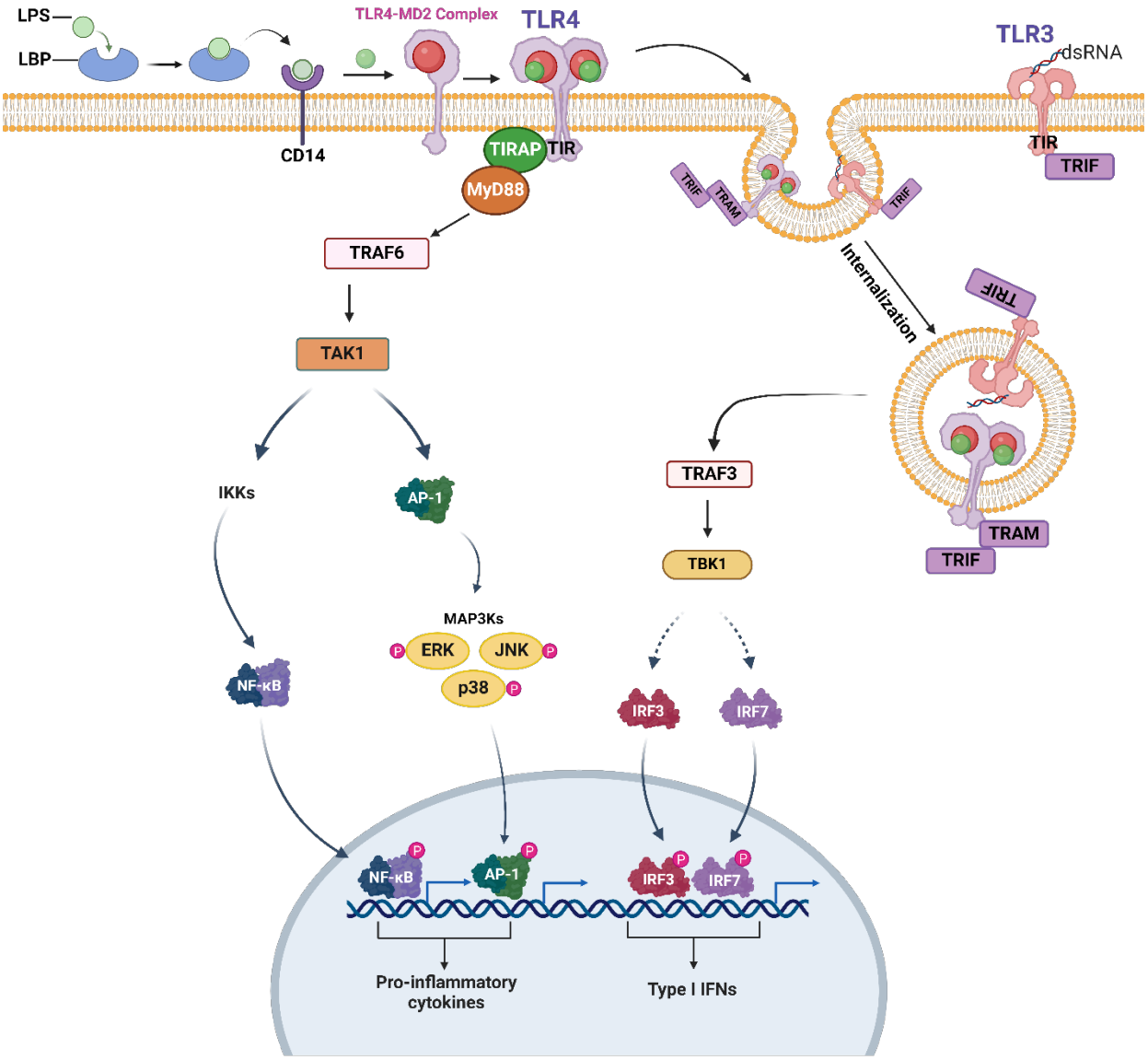

Figure 12. Toll-Like Receptor (TLR) -3 and -4 Signalling Pathways

1.3.1.3.4. Necroptosis Regulation through Interferons

Interferons (IFNs) are a family of cytokines that play a crucial role in the body's defense against viral infections and the surveillance of malignant cells. These widely expressed molecules are categorized into three main classes: type I, type II, and the newly discovered type III interferons. As the first line of defense against viruses, IFNs exhibit potent antiviral properties and can inhibit cell growth (Pestka et al., 1987). Type I interferons comprise a diverse group, including IFN-α, IFN-β, and IFN-ω, all of which interact with a shared cell-surface receptor. In contrast, IFN-γ stands alone as the sole type II interferon, activating signaling pathways by binding to its distinct receptor on the cell surface (Pestka et al., 2004).

Type I interferons (IFN-I) are key regulators of inflammatory processes and have been implicated in the pathogenesis of numerous inflammatory disorders. While the influence of IFN-I on immune and inflammatory responses through various signaling pathways is well-documented, a comprehensive review of their critical regulatory roles in specific pathways and related inflammatory diseases is currently lacking. Worldwide, a substantial portion of the population is affected by diverse inflammatory conditions, including infectious diseases, systemic lupus erythematosus (SLE), rheumatoid arthritis (RA), systemic sclerosis (SSc), juvenile dermatomyositis (JDM), periodontitis, autoimmune disorders, and chronic infections (K. Chen et al., 2017; Fernandez-Ruiz & Niewold, 2022). The role of IFN-I in inflammatory processes is intricate and paradoxical, acting as a double-edged sword. It can either suppress pro-inflammatory responses or, conversely, induce excessive inflammatory responses (Ivashkiv & Donlin, 2014). IFN-I's are pleiotropic cytokines with three primary functions: inducing an anti-viral state in infected cells to control pathogens, regulating innate immunity by enhancing antigen presentation and natural killer cell function, and activating adaptive immunity to develop high-affinity immune responses and memory (Gallucci et al., 2021; Mayer-Barber & Yan, 2017; Pasrija & Naime, 2021).

The IFN-I receptor consists of a heterodimer formed by IFNAR1 and IFNAR2. When IFN-I (either IFN-α or IFN-β) binds to this ubiquitous receptor, it triggers multiple signaling cascades, including the activation of JAK/STAT, NF-κB, and PI3K pathways (Hervas-Stubbs et al., 2011). The binding of type I interferons to their receptor, IFNAR, initiates a signaling cascade by activating two associated protein tyrosine kinases: Janus kinase 1 (JAK1) and tyrosine kinase 2 (TYK2). In the

canonical IFNα/β signaling pathway, these activated kinases phosphorylate cytosolic STAT1 and STAT2 molecules. This phosphorylation triggers the dimerization of STAT1 and STAT2, which then translocate to the nucleus and interact with IRF9 to form the ISGF3 complex. ISGF3 subsequently binds to specific DNA sequences called IFN-stimulated response elements (ISREs) that are located in the promoter regions of interferon-stimulated genes (ISGs), thereby activating their transcription **(Figure 13)**. This process results in the expression of numerous genes that mediate the cellular response to interferon stimulation (Ivashkiv & Donlin, 2014).

Recent studies have identified LPS-induced expression interferon as a key factor in triggering necroptosis. Macrophages obtained from mice lacking the IFNAR1 gene exhibit significant resistance to necroptosis (McComb et al., 2014). The study revealed that IFN-β triggers necroptosis in macrophages via the ISGF3 (IFN-stimulated gene factor 3) signaling pathway. ISGF3 is a transcriptional complex consisting of three components: STAT1, STAT2, and IRF9. Type I interferon plays a crucial role in TNF-induced auto necroptosis of macrophages by upregulating the expression of essential necroptosis signaling components, particularly TNFR2 and MLKL (Legarda et al., 2016). Recent research has further emphasized the significance of IFN signaling in necroptosis. MLKL expression is notably enhanced by interferon exposure (Knuth et al., 2018). In macrophages, constitutive interferon signaling is crucial for initiating necroptosis through the intrinsic activity of the cGAS/STING pathway, which senses cytosolic DNA. This process has been shown to promote the maintenance of MLKL expression at a critical level necessary for necroptosis to occur (Sarhan et al., 2019).

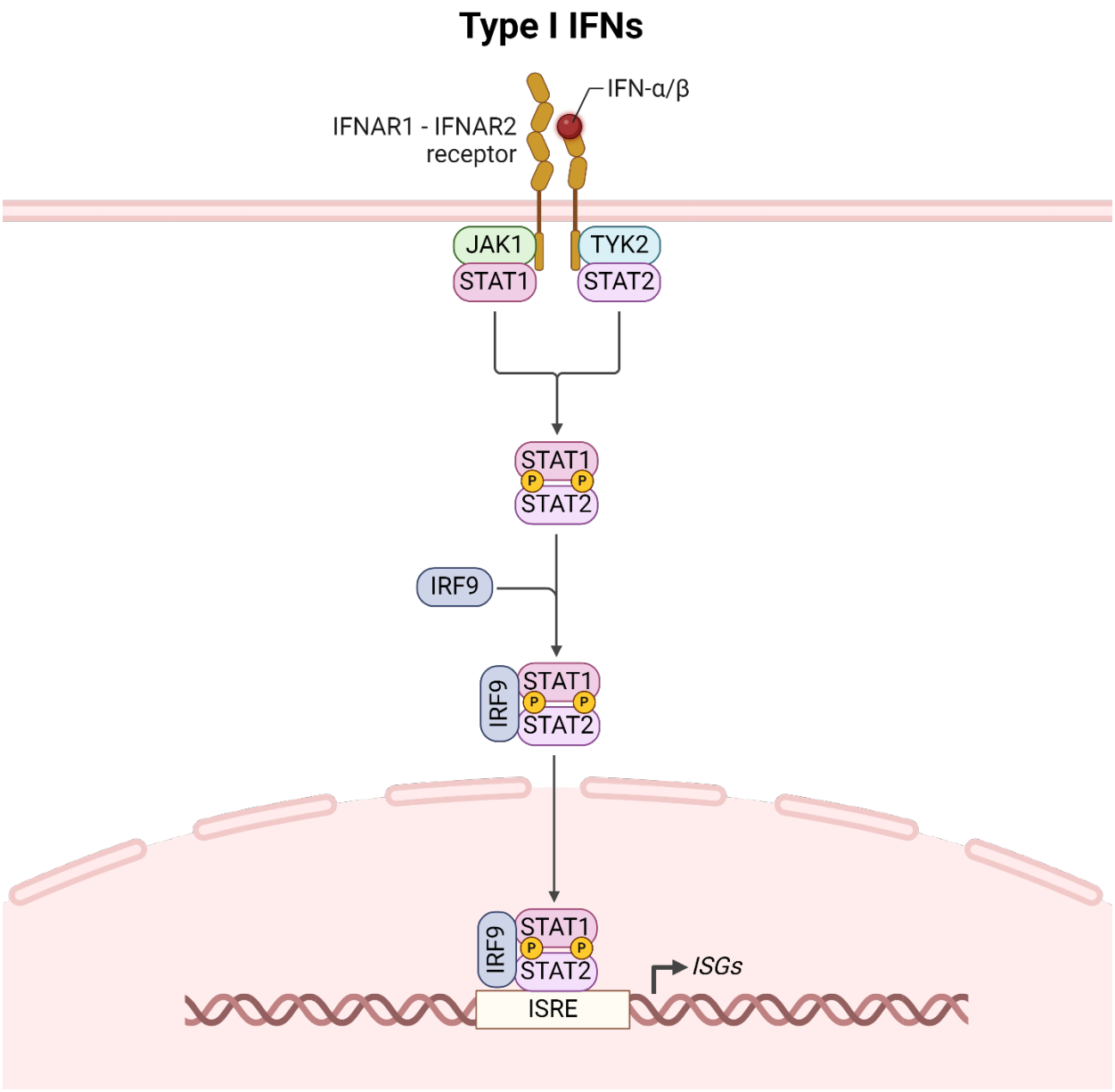

Figure 13. Type 1 IFN Signaling Pathway

2. THESIS SUMMARY

2.1. RATIONALE

Phosphorylation of receptor-interacting protein kinase-1 (RipK1) is indeed a critical initiating event in necroptosis, but several molecular events likely precede this step and are not yet fully elucidated. In addition, previous research from our lab has shown that the absence of type I interferon significantly reduces necroptosis susceptibility in macrophages (McComb et al., 2014; Robinson et al., 2012), though the exact mechanism remains unclear. Elucidating the early stages of necroptosis, including receptor endocytosis and role of interferon signaling, is essential for comprehending the full mechanism of this programmed cell death pathway. While necroptosis is linked to various inflammatory diseases, the precise molecular mechanisms connecting necroptosis signaling to inflammation remain elusive. A critical question is whether the inflammatory response is triggered solely after cell rupture or can occur independently of cellular disintegration. The molecular pathways driving necroptosis and inflammation in macrophages are still incompletely understood.

Unraveling these pathways is crucial for developing targeted therapies and will be the focus of this research. By investigating the intricate relationships between receptor internalization, necroptosis signaling, type 1 interferon signaling, and inflammatory responses, we aim to provide novel insights into the regulation of cell death and inflammation.

2.2. HYPOTHESIS

ARF6 plays a crucial role in facilitating the transition from Complex I to the necrosome formation and subsequent necroptosis, while IFNAR1 signaling regulates cytokine expression and amplifies necroptotic responses at later stages of necrosome signaling, leading to enhanced cell death in macrophages.

2.3. OBJECTIVES

The thesis is structured around three interconnected objectives:

2.3.1. Aim 1: Deciphering the early events of necroptosis in macrophages.

2.3.2. Aim 2: Delineating the role of necroptosis signaling on the inflammatory response.

2.3.3. Aim 3: Deciphering the mechanism of necroptosis induction by IFNAR1 signaling.

3. MATERIALS AND METHODS

3.1. Ethics Approval and Consent to Participate

Experiments were conducted in accordance with the Canadian Council on Animal Care (CCAC) guidelines and were approved by the University of Ottawa Animal Care Committee. The experimental protocol used was BMIe3590, and BMIb 4456 (Replacing BMI-3486).

3.2. Mice

All mice used in the study were maintained in specific pathogen-free conditions at the University of Ottawa Animal facility, adhering to CCAC guidelines and approved protocols. Experiments utilized age and sex-matched mice, predominantly on a C57BL/6 genetic background unless otherwise specified. C57BL6/J (Jax #000664), *Ifnar1*$^{-/-}$ (Jax #020288), *Ticam1*$^{-/-}$ (Jax #005037), *MyD88*$^{-/-}$ (Jax #009088), *Stat1*$^{-/-}$ (Jax #012606), *Stat2*$^{-/-}$ (Jax #023309) were obtained from Jackson Labs (Bar Harbor, USA). *Mk2*$^{-/-}$ mice were obtained from Dr. Matthias Gaestel (Kotlyarov et al., 1999) (Hannover Medical School). *Zfp36*$^{-/-}$ mice were obtained from Dr. Perry Blackshear (Taylor et al., 1996) (National Institute of Environmental Sciences, NIH, USA). *RipK3*$^{-/-}$ was a kind gift from Dr. Vishva Dixit (Genentech, San Francisco, CA, USA). *Irf9*$^{-/-}$ mice were obtained from Dr. Karen Mossman (McMaster University). *MyD88*$^{-/-}$*Ticam1*$^{-/-}$ and *Ifnar1*$^{-/-}$*Mk2*$^{-/-}$ -double knockouts were obtained by crossing the single knockout mice. Mice of both sexes were randomly assigned to experimental groups to ensure unbiased group distribution. This approach eliminated sex-based selection preferences while maintaining randomization across all study conditions.

3.3. Generation of Bone Marrow-Derived Macrophages:

Primary murine BMMs were generated by culturing bone marrow cells with M-CSF as described in our previous publication (Sadh et al., 2020). In brief, the mice were sacrificed, and bone marrow was harvested from the femur, tibia, and hip bones. The bone marrow cells were cultured in RPMI 1640 media (Gibco #31800089) supplemented with 8% fetal bovine serum (Gibco) (R8), 50 µg/mL gentamicin (Gibco #15750060), and 5 ng/mL macrophage colony-stimulating factor (BioLegend #576404) in a 5% CO_2 incubator. After 7 days, macrophages were harvested for use.

3.4. ARF6 Inhibitory Peptide and RNA interference:

ARF6 inhibitory peptide was obtained from Gene Script synthesis services, with a sequence length of 31 amino acids- GKVLSKIFGNKEMRIRQIKIWFQNRRMKWKK with an N-terminal myristoyl group as described previously (Van Acker et al., 2014). The Accell SMARTPool Mouse ARF6 siRNA (#E-043217-00-0005) was purchased from DharmaconTM. BMDMs were transfected with siRNA using Lipofectamine® RNAiMAX Transfection Reagent (Invitrogen #13778030) as per the manufacturer's instructions. After 72-96h, the transfected cells were used for the experiments.

3.5. Cell Line:

RAW264.7 cells were cultured in RPMI 1640 media (Gibco #31800089) supplemented with 8% fetal bovine serum (Gibco) (R8), 50 µg/mL gentamicin (Gibco #15750060) in a 5% CO_2 incubator. For dissociating the cells TrypLE™ was used (Gibco #12604013).

3.6. Generation of RAW264.7 *Arf6* Knockout Cells:

RAW264.7 *Arf6* knockout cells were generated using ARF6sgRNA CRISPR/Cas9 All-in-one Non-Viral Vector Set (Mouse) obtained from Applied Biological Materials Inc. (ABM #12260134). Cells were transfected with 1µg of each of the three plasmids using Amaxa™ SF Cell Line 4D-Nucleofector™ X Kit (Lonza #V4XC-2024), in the 4D-Nucleofector™ X Unit as per manufacturer's instructions. Transfected GFP-positive cells were sorted using the Sony SH800 Cell Sorter with a 100 µM sorting chip. Single GFP-positive cell was seeded in individual wells of a 96-well plate to establish knockout populations. Multiple clones were obtained using this method. The expression level of the ARF6 protein was analyzed by western blotting in each clone. Clones with no detectable ARF6 protein expression were selected. After performing initial experiments on all knockout clones, one clone was randomly selected for further studies.

3.7. Reagents:

Ultrapure LPS (*E. coli* 0111: B4) was obtained from Millipore Sigma (L4524). Poly I:C was obtained from Sigma-Aldrich (#P1530). Mouse IFN-β was obtained from PBL Assay Science (#12410). Recombinant mouse IFN-β1 (#581302) was obtained from BioLegend. Recombinant mouse TNFα was obtained from R&D Systems (#410-MT-010/CF). Actinomycin-D was obtained from MP Biomedicals (#02194525-CF). SMAC- IAPs inhibitor- Birinapant (TL32711) (#A4219) and Pan-caspase inhibitor Z-VAD-FMK (#A1902) were obtained from ApexBio. Pan-caspase inhibitor Emricasan (EMR) (#S7775), $p38^{MAPK}$ inhibitor- Ralimetinib (LY2228820) dimesylate, (#S1494) and the MK2 inhibitor III (#S6930), STAT3 inhibitor- BP-1-102 (#S7769), RipK3 inhibitor GSK872 (#S8465), and IKK2 inhibitor- LY2409881 (#S7697) were obtained from Selleckchem. RipK1 inhibitor II, 7-Cl-O-Nec-1 (#5042970001), NF-κB activation inhibitor II (#481408), DNA synthesis inhibitor- Gliotoxin (#G9893), and Topoisomerase II inhibitor- Etoposide (#341205) were obtained from Millipore Sigma.

3.8. Cell Culture and Viability:

Cells were stimulated in 96-well and 24-well tissue culture plates with various reagents as indicated. In some experiments, cells were co-treated with different inhibitors and agonists before stimulation and incubated for specified time points before assessing cell viability or collecting protein lysates.

Cell death was assessed by quantifying neutral red uptake, as described previously (Ariana et al., 2020; McComb et al., 2014; Rijal et al., 2018). In brief, cells were incubated with neutral red dye (1:20) (Millipore Sigma #N2889) until viable cells became visibly red. The cells were then washed once with PBS to remove any free dye and lysed with a solubilization solution to release the accumulated dye within live cells. The absorbance of the solubilized dye was quantified by colorimetric analysis at 570 nm using a FilterMax F5 microplate reader (Molecular Devices).

Cell viability was measured using a 3-[4,5-dimethylthiazol-2-yl]-2,5-diphenyltetrazolium bromide (MTT) assay (Mosmann, 1983). The MTT reagent was diluted with R8 media at a final concentration of 0.5 mg/mL and incubated at 37 °C. After 2 h, DMSO was added to solubilize MTT

crystals, and absorbance was measured at a wavelength of 570 nm with a reference wavelength of 650 nm on a Molecular Devices FilterMax plate reader.

For cell death analyses by imaging, cells were stained with Hoechst (2.5 μg/mL; Invitrogen #33342) and propidium iodide (1:10 dilution; BD Pharmingen #550825) and incubated at 37 °C for 20-30 min. Cells were then washed twice with PBS before evaluation by immunofluorescence microscopy using a Zeiss AxioObserver.D1 microscope. To count live versus dead cells, we employed a Python-based automated image analysis pipeline that leverages OpenCV for image processing, and NumPy for computation. Samples were converted to grayscale and binarized via Otsu's method to highlight and distinguish features of interest from the background. External contours were calculated using OpenCV's contour detecting algorithm, which sets to retrieve only the external contours and approximate the contour shapes to reduce the number of points. For each detected contour, the minimal enclosing circle was measured, providing the center and radius of the circular features in the sample. Each point is then calculated and circled on the original sample for manual verification.

3.9. Western Blotting:

Cells were stimulated as described and cell extracts were reconstituted in SDS lysis buffer containing 1% β-mercaptoethanol and heated immediately at 95 °C for 5 min. Lysates were separated by SDS-PAGE and transferred to the PVDF membrane. Immunoblot analysis was performed using the following antibodies: ARF6 (3A-1) (Santa Cruz #sc-7971), p-RipK1^{S166} (Cell Signaling #31122), p-RipK1^{S321} (Cell Signaling #83613), RipK1 (BD Biosciences #610459), p-RipK3$^{T231/S232}$ (Cell Signaling #91702), RipK3 (ProSci #2283), p-MLKL^{S345} (Cell Signaling #37333), MLKL (Millipore Sigma #MABC604), cIAP 1& 2 (MBL Life Science #CY-P1041), CYLD (Cell Signaling #8462), Cleaved Caspase-8 (Cell Signaling #9429), Cleaved Caspase-3 (Cell Signaling #9664), TRAF2 (#4712), A20 (Cell Signaling #5630), FADD (Enzo #ADI-AAM-212-E), TRIF (TICAM1) (GeneTex #GTX13810), p-STAT1^{Y701} (Cell Signaling #9167), p-STAT1^{S727} (Cell Signaling #9177), STAT1 (Cell Signaling #9172), p-STAT2^{Y689} (Millipore Sigma #ABE541), STAT2 (Cell Signaling #72604), p-STAT3^{Y705} (Cell Signaling #9131), p-STAT3^{S727} (Cell Signaling #94994), STAT3 (Cell Signaling #12640), IRF9 (Millipore Sigma #MABS1920), p-IRF-3^{S396} (Cell Signaling #4947), IRF-3 (Cell Signaling #4302) p-

MK2^{T334} (Cell Signaling #3007), MK2 (Cell Signaling #3042), p-SAPK/JNK$^{T183/Y185}$ (Cell Signaling #9251, SAPK/JNK (Cell Signaling #9252), p-p44/42 MAPK (Erk1/2)$^{T202/Y204}$ (Cell Signaling #4370), p44/42 MAPK (Erk1/2) (Cell Signaling #4695), p-p38 MAPK$^{T180/Y182}$ (Cell Signaling #9211), p38 MAPK (Cell Signaling #8690), p-TAK1^{S412} (Cell Signaling #9339), p-IKKα/β$^{S176/180}$ (Cell Signaling #2697), IKKβ (Cell Signaling #8943), p-NF-κB^{S536} (Cell Signaling #3033), NF-κB (Cell Signaling #8242), PI3 Kinase p110α (Cell Signaling #4249), p-P70 S6 Kinase^{T389} (Cell Signaling #9234), P70 S6 Kinase (Cell Signaling #2708), p-eIF4E^{S209} (Cell Signaling #9741), p-4E-BP1$^{T37/46}$ (Cell Signaling #2855), 4E-BP1 (Cell Signaling #9644), p-AKT^{T308} (Cell Signaling #9275), AKT (Cell Signaling #9272), Tristetraprolin (TTP) (Cell Signaling #71632), β- Actin (Cell Signaling #3700), and GAPDH (Cell Signaling #97166). The densitometric quantification of western blot signals was performed using ImageJ software.

3.10. Immunoprecipitations:

Cell lysates were immunoprecipitated with Dynabeads^{TM} Co-Immunoprecipitation kit (Invitrogen, #14321D) with the following antibodies: RipK1 (BD Biosciences #610459), and RipK3 (ProSci Inc #2283) as per manufacturer's instructions. Bound proteins were eluted and subsequently analyzed using the standard western blot protocol. The densitometric quantification of western blot signals was performed using ImageJ software.

3.11. Cell fractionation:

Cell lysates were collected using a Subcellular Protein Fractionation kit (ThermoFisher Scientific, #78840). Membrane and cytoplasm samples were separated and extracted as per the manufacturer's instructions. Protein normalization was performed using the BCA Protein Assay Kit (ThermoFisher Scientific, #A53225) as per the manufacturer's instructions. Extracted proteins were subsequently analyzed using the standard western blot protocol. The densitometric quantification of western blot signals was performed using ImageJ software.

3.12. Cytokine measurement:

Supernatants were collected from 96-well plates and the expression of cytokines was assessed using the mouse TNFα (BD OptEIA #555268), mouse IL-6 (BD OptEIA #555240), mouse IL-10

(BD OptEIA #555252), mouse IL-12p70 (BD OptEIA #555256), and mouse IFN-β (R&D System #DY8234-05) according to the manufacturer's instructions. The absorbance was detected at 450–570 nm on a FilterMax F5 multimode microplate reader (Molecular Devices).

The expression of IFN-I was also measured using a reporter cell line. ISRE-L929 cells were seeded at 5×10^4 cells per well in a 96-well tissue culture plate and incubated at 37°C with 50µl of culture supernatants for 4 h. Using the luciferase assay system kit (Promega #E1500), a Molecular Devices Emax plate reader measured the luminescence, and data were analyzed by SoftMax Pro.

3.13. Flow Cytometric Analysis:

Cells were seeded in 6-well plates and stimulated with different reagents as described. After specific time intervals cells were detached using a cell lifter in PBS and then washed with FACS buffer (PBS containing 1% FBS). For cell surface receptors analysis, the cells were preincubated with an anti-mouse CD16/CD32 Ab (Fc blocking; BD BioSciences #553143) for 20 min and then stained with the following Abs: APC anti-mouse TLR4 (BioLegend #145405), PE anti-mouse IFNAR1 (Invitrogen #12-5945-82), and PE anti-mouse TNFR1 (BioLegend #113003) for 30min. Then, the cells were washed with FACS buffer and acquired on the flow cytometer (BD LSRFortessa). For phagocytosis, pHrodo Deep Red *E. coli* BioParticles (ThermoFisher Scientific #P35361) were prepared according to the manufacturer's instructions. Particles were opsonized using normal mouse serum (diluted 1:4 in PBS) for 25 minutes at 37°C and shaking at 250 rpm. Bioparticles were added to cells and samples were acquired at different time intervals on BD-LSRFortessa immediately after the infection. For lysosomal activity, cells were treated with 1X LysoView dye (Biotium #70067) for different time intervals. Then, the cells were washed with FACS buffer and acquired on the flow cytometer (BD LSRFortessa). All the data was analyzed using FlowJo™ software.

3.14. Microscopy:

Cells were seeded in 8-well slides (Ibidi #80826) and stimulated with different reagents as described for immunofluorescence staining. For lysosome detection, 1X LysoView dye (Biotium #70067) and for the detection of endosomes, 1X ECGreen-Endocytosis Detection (Dojindo #E296) were used. The nucleus was stained with Hoechst (300nM; Invitrogen #33342) for 5 min.

To determine the internalization of LPS after stimulation, cells were incubated for different time intervals with 100ng/ml of fluorophore-labeled LPS from *Escherichia coli* Serotype 055:B5, Alexa Fluor 594 conjugate (ThermoFisher Scientific #L23353). A Membrite® 405/430 (Biotium #30092) Fix cell surface staining kit was used to stain the membranes of cells as per the manufacturer's instructions. Images were acquired using a 63X, 1.4NA, Oil, Plan-Apochromat objective of Zeiss Observer O7 epifluorescence microscope, and images were analyzed using ImageJ software.

3.15. Quantitative RT-PCR

Total RNA was extracted using the RNeasy Mini Kit (Qiagen) as per the manufacturer's instructions. cDNA synthesis was performed using the iScript cDNA Synthesis Kit (Bio-Rad Laboratories Inc) according to the manufacturer's instructions, and samples were stored at −20 °C until use. Quantitative real-time PCR was performed using the Bio-Rad CFX384 Touch Real-Time PCR System (Bio-Rad Laboratories Inc) in conjunction with SYBR Green PCR Master Mix (ThermoFisher Scientific Inc).

The primers used were as follows:

Table 1. Primers used for qRT-PCR

Gene	Forward primer sequence (5'-3')	Reverse primer sequence (5'-3')
Cxcl1	TGAGCTGCGCTGTCAGTG	AGAAGCCAGCGTTCACCAGA
Ifnβ1	ATGGTGGTCCGAGCAGAGAT	CCACCACTCATTCTGAGGCA
Zfp36	TTTCCCCTTCTGCCTTCTCT	TGGTGCTGGGGGTAGTAGAC
IL-12p35	ATGTGTCAATCACGCTACCTCC	TCAGGCGGAGCTCAGATAGCC
IL-12p40	GTCCTCAGAAGCTAACCATCTCC	CCAGAGCCTATGACTCCATGTC
Mlkl	CTGGCAGAGAACGAATCTTGG	TGCTCCCAGCAATAAGTTGA
Xaf1	TGTGCCTTTCTTTCTCCCCC	CAGAGGCCAAACATGGAGGG
TNFα	GAGAAGTTCCCAAATGGCCTCCC	GTATGAGATAGCAAATCGGCTGACGC
Actin	GATCAAGATCATTGCTCCTCCTG	AGGGTGTAAAACGCAGCTCA

3.16. Gene Expression Profiling and Analysis

Bone marrow-derived macrophages were treated with IFNβ (10 ng/mL) or LPS (10 ng/mL) with or without zVAD (50μM). Cells were harvested 6 h post-treatment and RNA was collected using the RNeasy Mini Kit (Qiagen). Reverse transcription of total RNA (200 ng) was conducted using the Agilent Low-input Quick Amp single color labeling kit. Labeled cRNA was hybridized to Agilent-028005 SurePrint G3 Mouse GE 8x60K Microarray (GPL10787). Exported probe data was filtered using a script in R (4.3.3). Probes with expression greater than background in at least 50% of arrays were retained. The background-subtracted data was quantile-normalized and probes representing low-expressed genes were removed from the analysis. Differential expression testing was performed in R (4.3.3) by considering genotype and treatment in the differential expression analysis design. The p-value was evaluated using the Benjamini–Hochberg procedure."

Gene set enrichment analysis (GSEA) was conducted with all differentially expressed genes, using the R cluster Profiler package with the parameters minGSSize = 10, maxGSSize = 6000, pvalueCutoff = 1.0, pAdjustMethod = 'BH', and Eps = 0. The p-value was adjusted using the Benjamini–Hochberg procedure. Gene sets with adj.Pval < 0.05 were considered significant if the NES was > 1.5, or < −1.5. The gene sets that are most significantly enriched in WT cells upon necroptosis induction ('TNFα signaling pathway' and 'Inflammatory Response LPS') were selected for further analysis. Gene set enrichment plots were used to determine the leading-edge genes enriched in each pathway. Heatmaps of the leading-edge genes were generated using median-centered $\log_2$FC differential expression values.

3.17. Analysis of ChIP-Seq Data

ChIP-seq data was retrieved from the NCBI SRA (GSE115435) (Platanitis et al., 2019)and decompressed into a fastq file format using fasterq-dump. Adapter contamination and low-quality sections of the raw reads were removed using fastp. The trimmed reads were aligned on the Mus musculus mm10 genome using the STAR aligner. Duplicate read pairs were marked using Picard and replicates were merged into a single bam file using samtools. SSP was utilized to determine chromatin fragment length and bamCoverage was used to calculate read density. The resulting bigWig files were loaded on the integrative genomics viewer for analysis.

3.18. Transduction of RAW264.7 *Ifnar1*$^{-/-}$ Cells with MLKL:

RAW *Ifnar1*$^{-/-}$ cells produced by Ilia (a previous summer student in our lab). MLKL gene sequence fragmented with P2A-T2A, G418, and CMV forward promoter for Vector Backbone pLV-mCherry (Addgene #36084) to form a plasmid. Virus precipitation was performed using a Virus Precipitation Kit (Benchmark Bioscience #P-100/P-250) as per the manufacturer's instructions. Then the viruses were assembled in the packaging cells- 293A (or 293T) with the MLKL plasmid and produced. After that Virus particles were left with polybrene for overnight incubation to increase the efficacy of gene transfer. RAW *Ifnar1*$^{-/-}$ cells were then infected with MLKL plasmid viruses and cell selection was performed using the G418 antibiotic treatment. Cells were treated with the antibiotic until no cell died and after that healthy cells were recovered and allowed to grow. For further confirmation cells were sorted using the Sony SH800 Cell Sorter with a 100 µM sorting chip.

3.19. Statistical Analyses:

All graphs show the average results taken from at least three independent experiments. Error bars show the standard error of the mean, and statistical significance between groups was determined using the student's *t*-test or ANOVA using the GraphPad Prism software. The Brown–Forsythe test is used to test for equality of variances. Statistical evaluation of GSEA and differential gene expression (DGE) was performed in R. Specifically, the calculated P-values following DGE analysis and GSEA were adjusted using the Benjamini–Hochberg (B-H) procedure.

3.20. Data Availability:

All the original high throughput microarray data has been deposited at GEO (GSE134549).

4. RESULTS

4.1. Aim 1: Early events of necroptosis in macrophages.

4.1.1. Inactivation of ARF6 leads to resistance against necroptosis

Necroptosis can be triggered when TLRs such as TLR4 and TLR3, or cytokine receptors like TNF and IFNAR1, are engaged under conditions where caspase activity is suppressed (Degterev et al., 2008). This suppression of caspase activity can occur naturally through FLIP or artificially using pan-caspase inhibitors like zVAD-fmk (Y.-S. Chen et al., 2022; Guo et al., 2016). In these circumstances, instead of undergoing apoptosis, cells initiate the necroptotic pathway, leading to a form of programmed necrotic cell death. We aimed to uncover the signaling events that occur prior to RipK1 phosphorylation, which is considered the first detectable step in necroptosis activation. Previous studies have demonstrated that necroptosis triggered by TLR stimulation partly relies on TRIF signaling. Moreover, when both TRIF and MyD88 signaling pathways are absent, cells become completely resistant to necroptosis induction (Ariana et al., 2020). This information suggests that these adaptor proteins play crucial roles in the early stages of the necroptotic signaling cascade, potentially acting upstream of RipK1 phosphorylation. We proposed that the ARF6 GTPase might participate in the signaling events prior to RipK1 phosphorylation that promotes necroptosis signaling. This idea stems from the necessity of receptor endocytic events in promoting TLR signaling and the role of ARF6 in shuttling between the plasma membrane and endo-lysosomal compartments. As a member of the Ras superfamily of small GTPases, ARF6 could potentially trigger the necroptotic signaling cascade by facilitating TLR endocytosis.

Bone marrow-derived macrophages (BMDMs) underwent cell death when exposed to LPS and the caspase inhibitor zVAD **(Figure 14 A)**. This cell death was prevented by Nec-1, which inhibits RipK1 kinase activity. Notably, an ARF6-inhibitory peptide also significantly reduced cell death **(Figure 14 A)**, correlating with decreased phosphorylation of RipK3 and MLKL **(Figure 14 B)**, suggesting that ARF6 may play a role in promoting necroptosis signaling. ARF6 knockdown using siRNA **(Figure 14 C)** significantly protected the cells from necroptosis induced by either LPS **(Figure 14 D)** or poly I:C **(Figure 14 E)** treatment. These findings collectively indicate that ARF6 is involved in the necroptotic signaling pathway triggered by TLR stimulation in the absence of caspase activity.

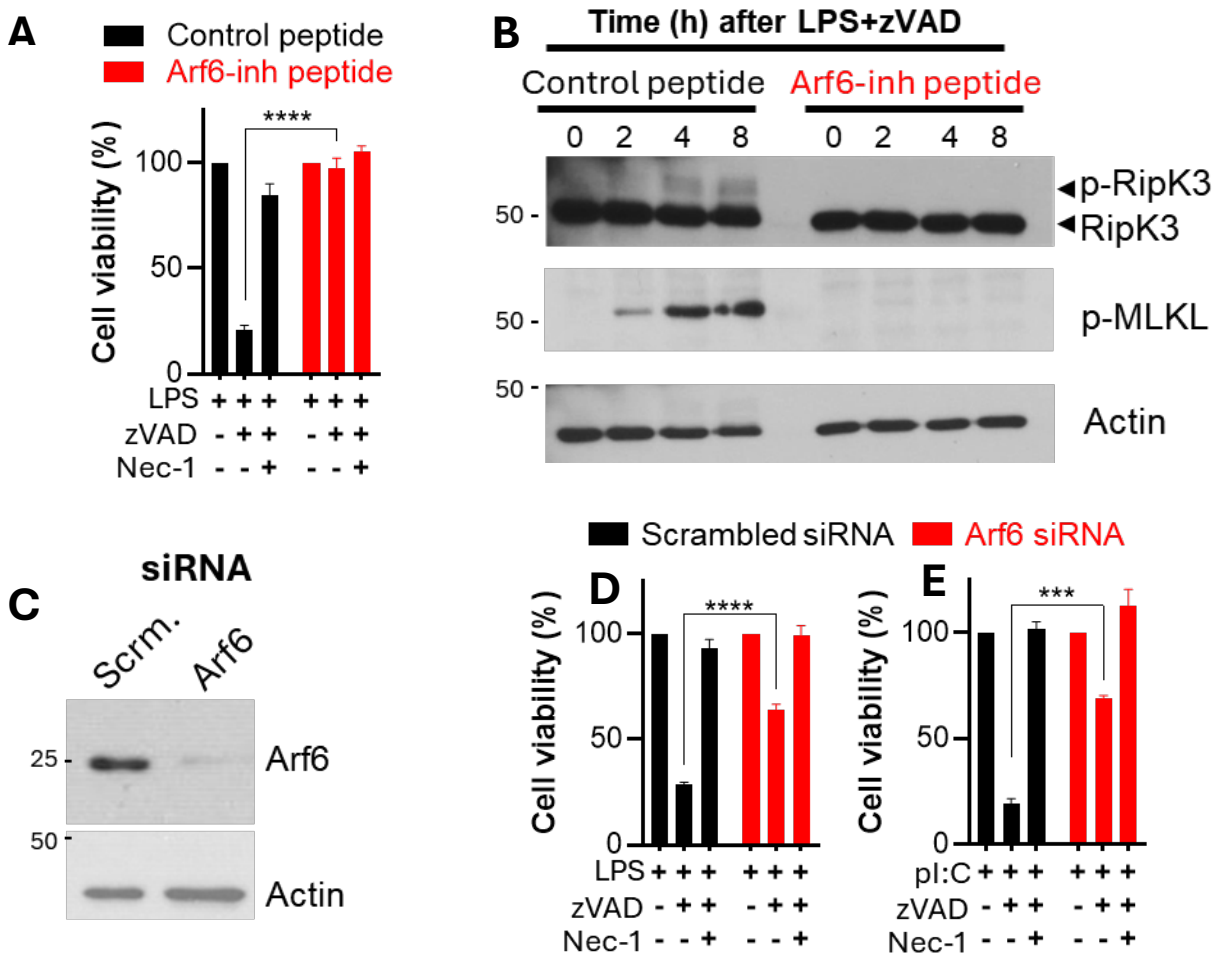

Figure 14. Inhibition and gene silencing of ARF6 leads to resistance against necroptosis

A, B WT BMDMs were treated with 5μM of the ARF6 inhibitory peptide for 3h. After that, cells were treated with LPS (100ng/mL), zVAD-fmk (25μM), and Nec-1 (10μM), and the impact on cell viability was evaluated at 24h by Neutral Red uptake **(A).** The activation of signaling proteins was evaluated by western blot analysis of the cell extracts collected at various time intervals **(B)**. **C-E** WT BMDMs were treated with 1μM of scrambled siRNA or ARF6 siRNA for 72h. After that, the expression level of ARF6 was evaluated by western blotting **(C)**, and cells were treated with LPS (100ng/mL), pI:C (1μg/mL), zVAD-fmk (25μM), and Nec-1 (10μM). The impact on cell viability was evaluated at 24h by Neutral Red uptake **(D, E)**. Graphs depict mean ± SEM. Each experiment was repeated at least three times. (***P< 0.001, ****P< 0.0001).

To precisely investigate the role of ARF6 in necroptosis signaling, we used the CRISPR-Cas9 approach to generate *Arf6* knockout macrophages using the RAW264.7 macrophage cell line. The success of the knockout was evaluated through Western blotting of cell extracts, which allowed the assessment of ARF6 expression in various clones **(Figure 15 A)**. Treatment of BMDMs with LPS and the pan-caspase inhibitor Q-VD-OPh or the caspase-8 inhibitor (zIETD-fmk) does not induce necroptosis (Ariana et al., 2020). Although zVAD-fmk is a pan-caspase inhibitor, it blocks the caspase-8–cFLIPs heterodimer more efficiently than the zIETD-fmk or Q-VD-OPh, hence favoring necroptosis (Hughes et al., 2016; Oberst et al., 2011). Recently, it has been reported that the caspase inhibitor Emricasan (EMR) promotes necroptosis at reduced concentrations due to its increased specificity towards caspase-8, which results in better inhibition of the cFLIP-caspase-8 heterodimers (Brumatti et al., 2016). Consequently, EMR was chosen over zVAD-fmk for subsequent experiments.

All clones with successful deletion of *Arf6* **(Figure 15 A)** demonstrated significant resistance to LPS-induced necroptosis **(Figure 15 B)**. The clone A2 was chosen for further experimentation since it showed the greatest resistance to necroptosis activation.

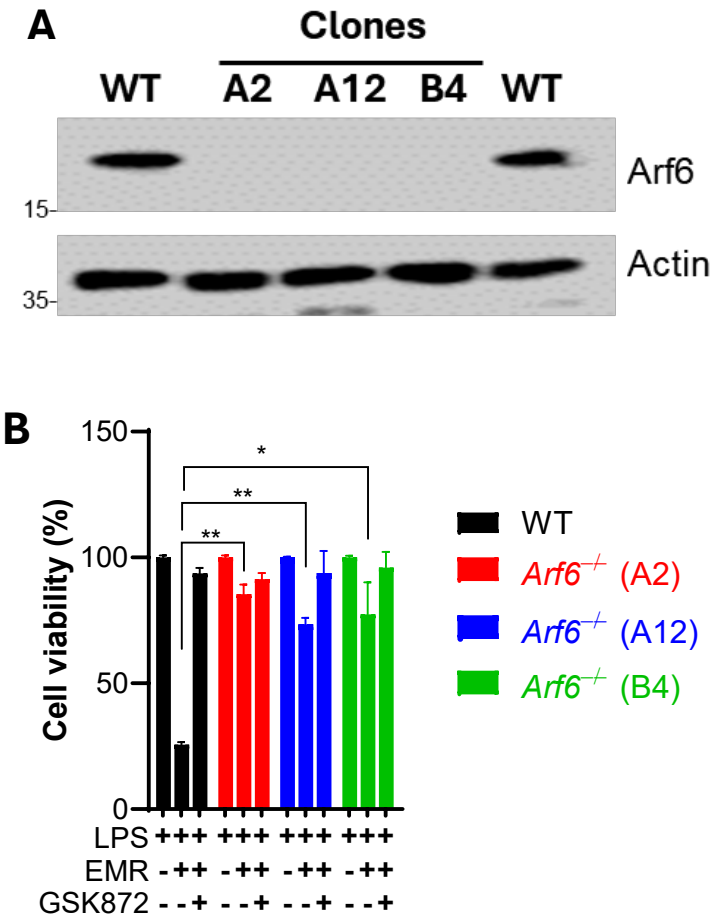

Figure 15. Generation and selection of *Arf6* knockout clones

A The expression of ARF6 was evaluated in various CRISPR-Cas9 clones of *Arf6*$^{-/-}$ RAW264.7 cells by performing western blot analysis. **B** WT and *Arf6*$^{-/-}$ RAW264.7 clones were treated with LPS (100ng/mL), EMR (10µM), and GSK872 (10 µM), and the impact on cell viability was evaluated at 24h by Neutral Red uptake. Graphs depict mean ± SEM. Each experiment was repeated at least three times. (**P< 0.01).

Arf6$^{-/-}$ cells showed markedly reduced necroptosis when treated with LPS or pI:C in the presence of EMR **(Figure 16 A)**. The RipK3 inhibitor GSK872 rescued cell death, confirming necroptosis as the mode of cell death. Necroptosis in WT cells was undetectable at 6h post-LPS+EMR stimulation **(Figure 16 B)** but progressed at later time points **(Figure 16 C).** At 18h post-LPS+EMR treatment **(Figure 16 D, E),** most WT cells incorporated PI, indicating compromised membrane integrity, while *Arf6*$^{-/-}$ cells strongly resisted cell death.

LPS+EMR-induced necroptosis in WT cells **(Figure 16 F)** was associated with activating phosphorylation (S166) of RipK1 and phosphorylation of downstream targets RipK3 and MLKL. In contrast, activation of RipK1, RipK3, and MLKL was undetectable in *Arf6*$^{-/-}$ cells. However, the inhibitory phosphorylation (S321) of RipK1, mediated by MK2 downstream of p38MAPK, remained unaffected in *Arf6*$^{-/-}$ cells **(Figure 16 F)**.

The lack of RipK1 S166 phosphorylation in *Arf6*$^{-/-}$ cells suggests that ARF6 plays a crucial role in promoting initial necroptosis signaling events prior to RipK1 phosphorylation.

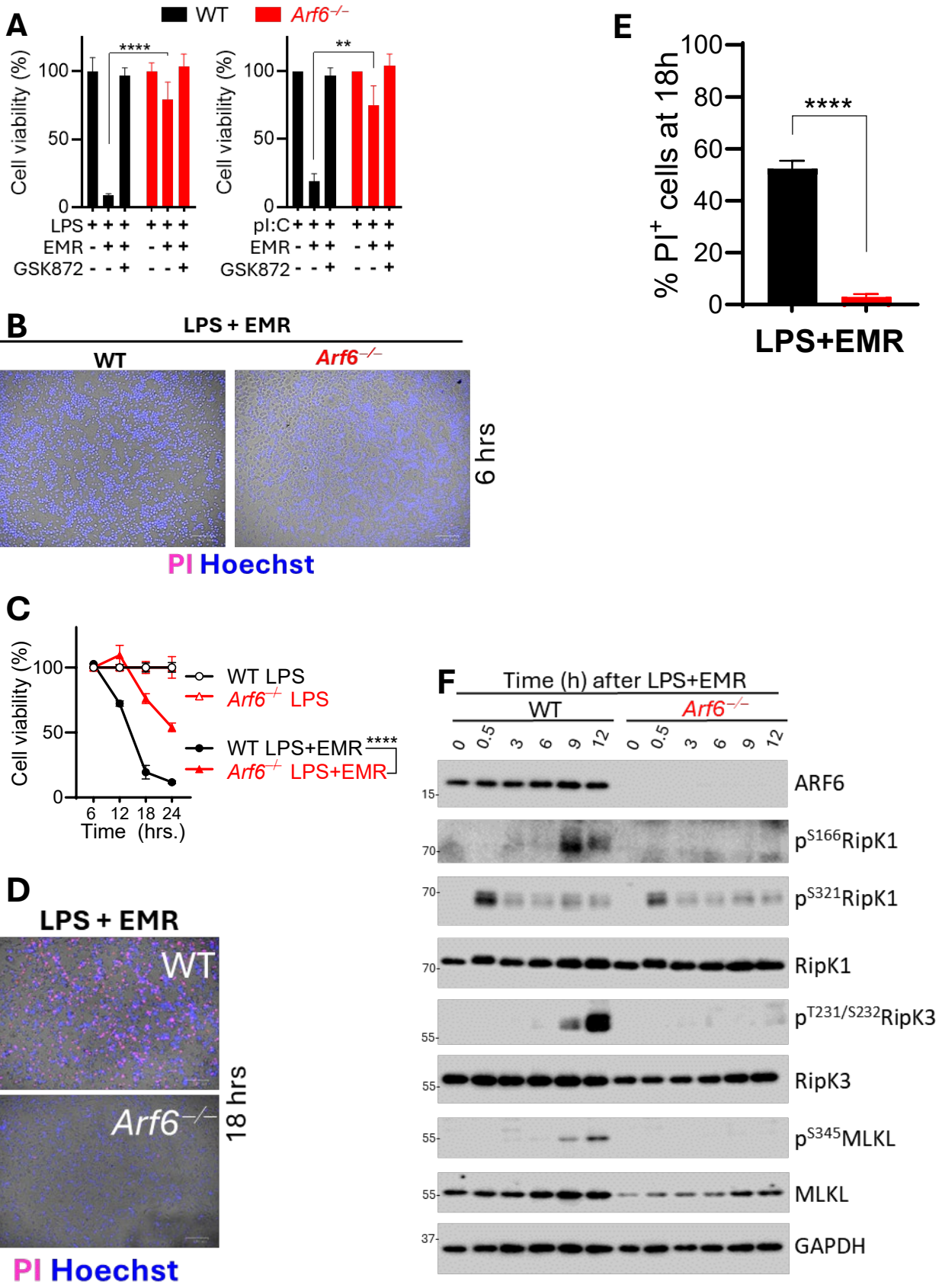
A
WT
Arf6−/−
Cell viability (%)
****
**
LPS
pI:C
EMR
GSK872
B
LPS + EMR
WT
Arf6−/−
6 hrs
PI Hoechst
C
Cell viability (%)
WT LPS
Arf6−/− LPS
WT LPS+EMR
Arf6−/− LPS+EMR
****
Time (hrs.)
D
LPS + EMR
WT
Arf6−/−
18 hrs
PI Hoechst
E
% PI+ cells at 18h
****
LPS+EMR
F
Time (h) after LPS+EMR
WT
Arf6−/−
ARF6
pS166RipK1
pS321RipK1
RipK1
pT231/S232RipK3
RipK3
pS345MLKL
MLKL
GAPDH

Figure 16. Knocking out the *Arf6* gene leads to resistance against necroptosis and inactivation of key necroptotic proteins

A WT and *Arf6*$^{-/-}$ RAW264.7 cells were treated with LPS (100ng/mL), pI:C (1µg/mL), EMR (10µM), and GSK872 (10µM) and the impact on cell viability was evaluated at 24h by Neutral Red uptake. **B** WT and *Arf6*$^{-/-}$ RAW264.7 cells (A2 clone) were treated with LPS (100ng/mL) and EMR (10µM) and the impact on cell viability was evaluated at 6h by staining the cells with PI and Hoechst. **C-E** WT and *Arf6*$^{-/-}$ RAW264.7 cells were treated with LPS (100ng/mL) and EMR (10µM). The impact on cell viability was evaluated at different time points by Neutral Red uptake **(C)** and by staining the cells with PI and Hoechst at 18h **(D, E)**. **F** Western blot analysis was performed on cell extracts collected at different time points. Graphs depict mean ± SEM. Each experiment was repeated at least three times. (**P< 0.01, ***P< 0.001, ****P< 0.0001).

4.1.2. ARF6 promotes the activation of IRF3 without impacting the endocytosis of TLR4

Since ARF6 regulates membrane traffic and communication between various intracellular compartments in some circumstances (Van Acker et al., 2019), we evaluated whether ARF6 promoted the endocytosis of TLR4 during necroptosis stimulation. During the stimulation of cells with LPS+EMR, the cell surface expression of TLR4 was progressively reduced in WT cells, confirming the endocytosis of TLR4 **(Figure 17 A)**. Similar results were obtained when cells were stimulated with LPS alone **(Figure 17 B)**. However, the cell surface expression of TLR4 was also reduced in *Arf6*$^{-/-}$ cells to the same degree as WT cells **(Figure 17 A)**. These observations suggest that ARF6 may not be essential for the endocytosis of TLR4 during stimulation with LPS or LPS + EMR. To further investigate the role of ARF6 in TLR4 signaling, we examined the activation of downstream pathways. There was a minor reduction in the activation of NF-κB in *Arf6*$^{-/-}$ cells in comparison to WT cells **(Figure 17 C)**. This slight difference in NF-κB activation indicates that ARF6 might play a subtle role in modulating this pathway. Activation of TAK1, which participates in the NF-κB and MAPK pathways, was not influenced by ARF6 **(Figure 17 C)**, suggesting that ARF6 does not directly regulate TAK1-dependent signaling cascades. On the other hand, the activation of IRF3 was highly reduced in *Arf6*$^{-/-}$ cells following treatment with LPS+EMR **(Figure 17 D)**. Since TRIF signaling leads to the activation of IRF3 following TLR4 engagement, these results indicate that ARF6 promotes TRIF signaling during necrosome activation downstream of TLR4 endocytosis. These findings reveal a complex relationship between ARF6 and TLR4 signaling, highlighting the importance of ARF6 in modulating specific downstream pathways during necroptosis stimulation.

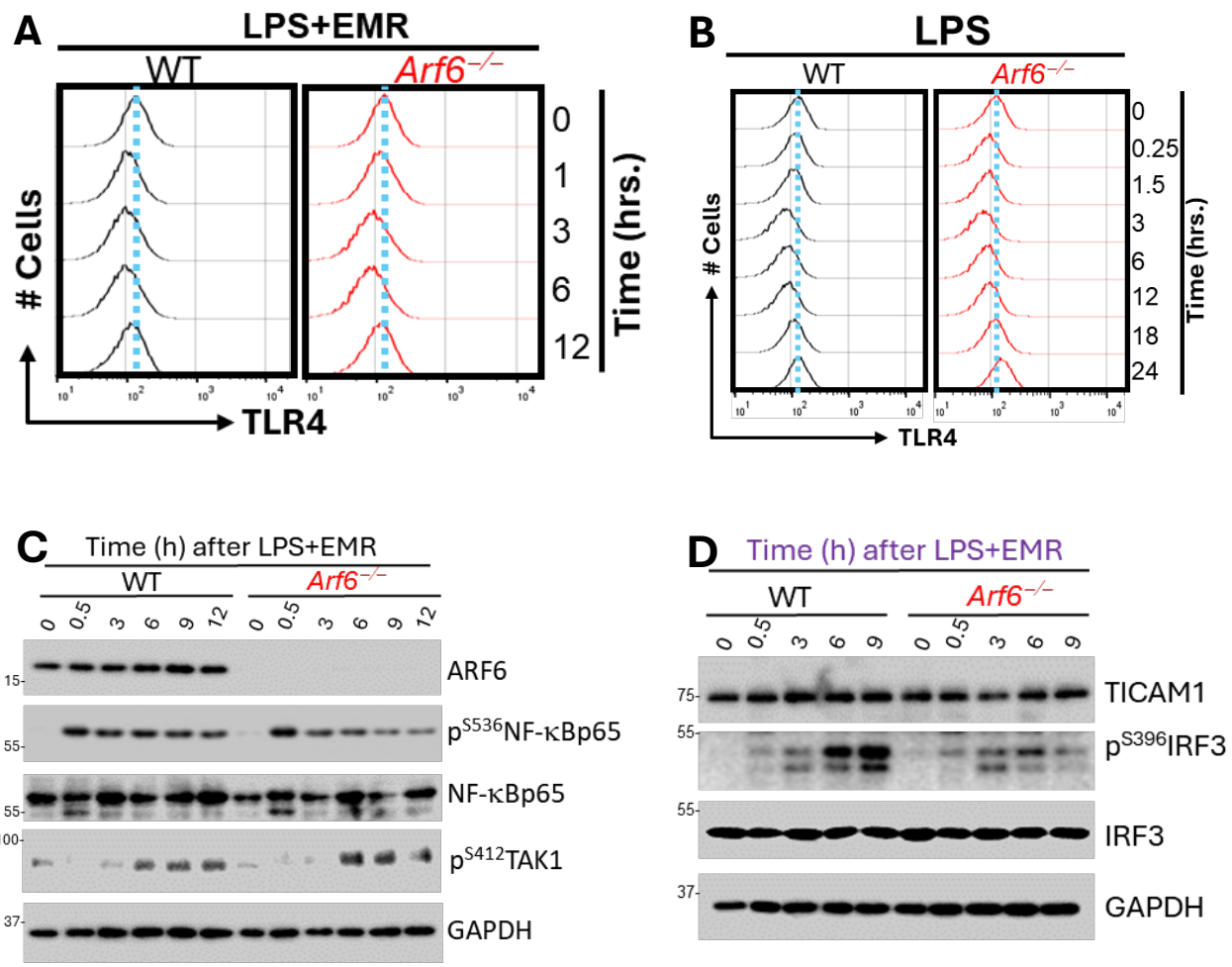

Figure 17. ARF6 promotes the activation of IRF3 without impacting the endocytosis of TLR4

A, B WT and *Arf6*$^{-/-}$ cells were treated with LPS (100ng/mL) + EMR (10μM) and LPS (100ng/mL) for different time intervals as shown. After that, cells were stained with an anti-TLR4 antibody. **C, D** Histograms of stained cells are shown. Cell extracts were collected at various time intervals, and the activation of signaling proteins was evaluated by western blot analysis**.** Each experiment was repeated at least three times.

During the stimulation of cells with LPS alone, ARF6 played a significant role in promoting the secretion of interleukin-10 (IL-10). However, its impact on the expression of other cytokines was relatively minor **(Figure 18 A)**. This observation suggests that ARF6 has a specific impact on IL-10 production in response to LPS stimulation.

Interestingly, when the cells were treated with a combination of LPS and EMR (LPS+EMR) to induce necroptosis activation, the influence of ARF6 on cytokine secretion became more pronounced compared to stimulation with LPS alone. In this scenario, the absence of ARF6 had a broader and more significant effect on the cytokine profile. Specifically, in *Arf6*-deficient cells, there was a notable reduction in the secretion of all the cytokines tested **(Figure 18 B, C)**. This finding indicates that ARF6 promotes cytokine production during necroptosis activation induced by LPS+EMR stimulation.

Since the MAPK pathway plays a key role in promoting cytokine production during TLR signaling, we evaluated whether ARF6 impacts the activation of various key members of the MAPK pathway during necroptosis stimulation. The persistence, but not the initial activation of $p38^{MAPK}$ and its downstream kinase MK2, was compromised in $Arf6^{-/-}$ cells (**Figure 18 D**). The persistence of JNK and ERK1/2 was also compromised in $Arf6^{-/-}$ cells (**Figure 18 D**). The activation of STAT3 was compromised during necroptosis stimulation of $Arf6^{-/-}$ cells relative to WT cells (**Figure 18D**). Activation of STAT3 was highly dependent on $p38^{MAPK}$ activity as treatment of cells with a $p38^{MAPK}$ inhibitor resulted in the potent reduction of STAT3 activation in WT cells during necroptosis stimulation (**Figure 18 E**). Inhibition of STAT3 resulted in a reduction in the level of IL-6 but not TNFα in WT cells (**Figure 18 F**).

Overall, these results showed that ARF6 promotes IRF3 activation and sustained MAPK pathway activation during necroptosis, influencing cytokine production and STAT3 activation, without impacting the endocytosis of TLR4. These results indicate that ARF6 promotes signaling in the macrophages downstream of TLR4 endocytosis.

.

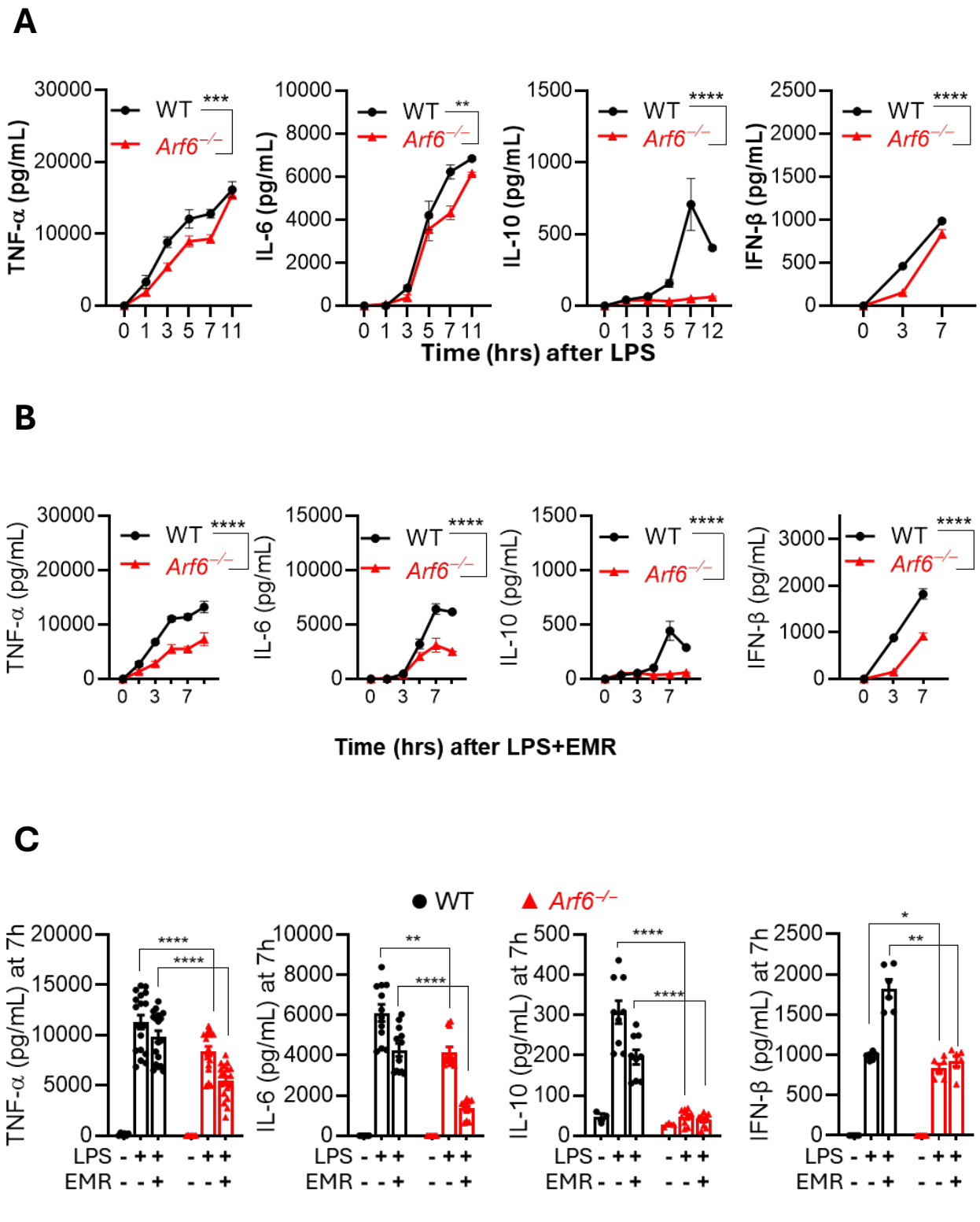
A
TNF-α (pg/mL)
IL-6 (pg/mL)
IL-10 (pg/mL)
IFN-β (pg/mL)
WT
Arf6−/−
Time (hrs) after LPS
B
Time (hrs) after LPS+EMR
C
TNF-α (pg/mL) at 7h
IL-6 (pg/mL) at 7h
IL-10 (pg/mL) at 7h
IFN-β (pg/mL) at 7h
LPS
EMR

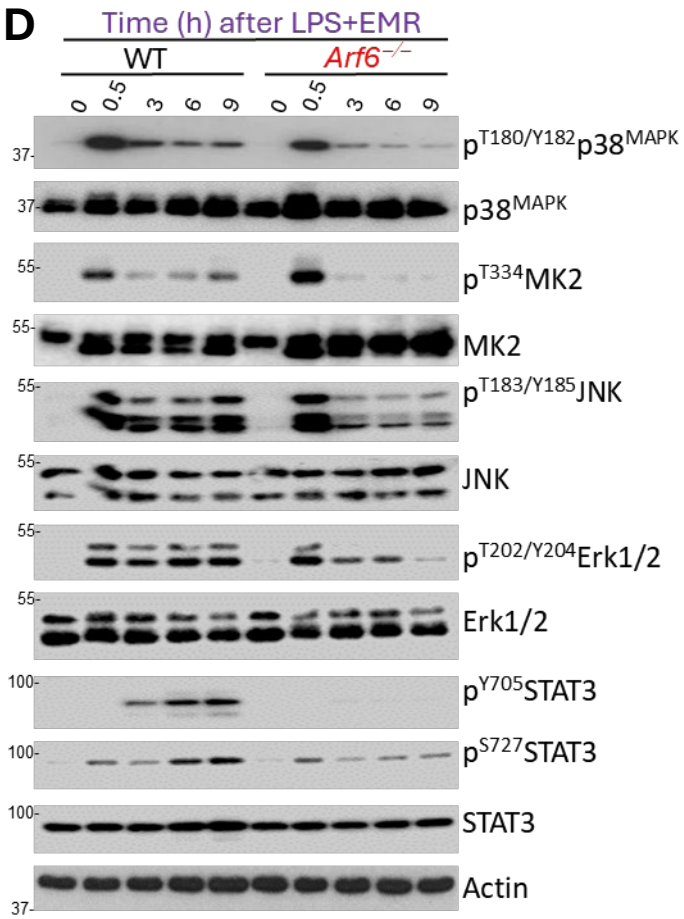
D
Time (h) after LPS+EMR
WT
Arf6−/−
0 0.5 3 6 9 0 0.5 3 6 9
37-
pT180/Y182p38MAPK
37-
p38MAPK
55-
pT334MK2
55-
MK2
55-
pT183/Y185JNK
55-
JNK
55-
pT202/Y204Erk1/2
55-
Erk1/2
100-
pY705STAT3
100-
pS727STAT3
100-
STAT3
37-
Actin

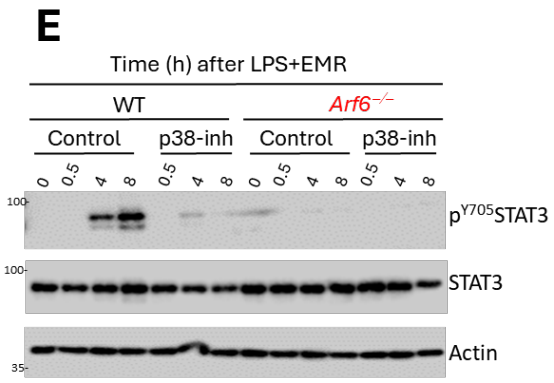
E
Time (h) after LPS+EMR
WT
Arf6−/−
Control
p38-inh
Control
p38-inh
0 0.5 4 8 0.5 4 8 0 0.5 4 8 0.5 4 8
100-
pY705STAT3
100-
STAT3
35-
Actin

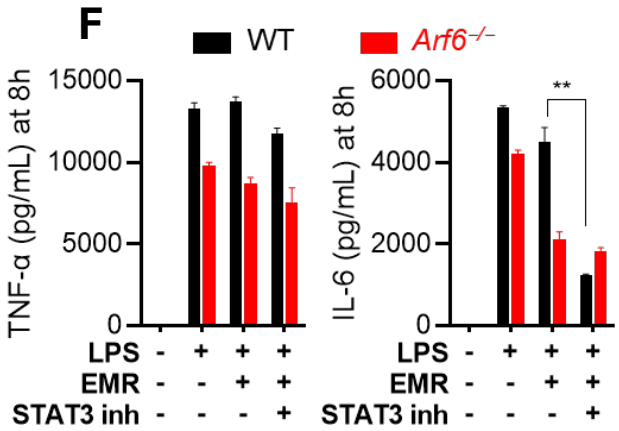
F
WT
Arf6−/−
TNF-α (pg/mL) at 8h
15000
10000
5000
0
IL-6 (pg/mL) at 8h
6000
4000
2000
0
**
LPS - + + +
EMR - - + +
STAT3 inh - - - +
LPS - + + +
EMR - - + +
STAT3 inh - - - +

Figure 18. ARF6 promotes cytokine production during TLR4-dependent necroptosis stimulation

A-C WT and *Arf6*$^{-/-}$ cells were treated with LPS (100ng/mL) and LPS (100ng/mL) + EMR (10µM) for different time intervals, as shown. The expression of different cytokines was measured in WT and *Arf6*$^{-/-}$ cells at various time intervals by ELISA after stimulation with LPS (100ng/mL) **(A)**, LPS (100ng/mL) + EMR (10µM) **(B)**, and at 7h following treatment with LPS (100ng/mL) or with LPS (100ng/mL) + EMR (10µM) **(C)**. Cell extracts were collected at various time intervals, and the activation of signaling proteins was evaluated by western blot analysis **(D)**. **E, F** WT, and *Arf6*$^{-/-}$ cells were treated with LPS (100ng/mL), EMR (10µM), and STAT3 inhibitor (10µM). The impact on the expression of p^{Y705}STAT3 was evaluated by western blot analysis at different time intervals **(E)**, and the impact on cytokine expression was evaluated at 8h by ELISA. **(F)**. Graphs depict mean ± SEM. Each experiment was repeated at least three times. (*P< 0.05, **P< 0.01, ***P< 0.001, ****P< 0.0001).

4.1.3. ARF6 promotes type I interferon signaling during necroptosis stimulation

We considered the possibility that the endocytosis of the type I interferon receptor (IFNAR1) may be impacted in *Arf6*$^{-/-}$ cells due to reduced secretion of IFN-β during necroptosis activation by LPS+EMR (**Figure 18 B**). The cell surface expression of IFNAR1 was rapidly reduced in WT cells following necroptosis stimulation by LPS+EMR, confirming the rapid internalization of IFNAR1 (**Figure 19 A**). In contrast, the internalization of cell surface IFNAR1 was reduced in *Arf6*$^{-/-}$ cells (**Figure 19 A**), implying that ARF6 promotes the internalization of IFNAR1 but not TLR4 during necroptosis stimulation by LPS+EMR. The activation of STAT1 and STAT2 was slightly reduced in *Arf6*$^{-/-}$ cells (**Figure 19 B**), which correlated with the reduced secretion of IFN-β (**Figure 18 B**) and decreased IFNAR1 internalization (**Figure 19 A**).

Overall, these results indicate that ARF6 signaling primarily promotes the activation of IRF3 during stimulation by LPS+EMR, with a minor impact on the activation of the NF-κB pathway. Reduced cytokine expression by *Arf6*$^{-/-}$ cells could explain the reduced persistence of the MAPK pathway.

We tested whether the reduced secretion of IFN-β by *Arf6*$^{-/-}$ cells due to poor IRF3 activation was responsible for the increased resistance of these cells to necroptosis. We stimulated the cells with IFN-β+EMR instead of LPS+EMR and tested the impact on necroptosis. We observed that *Arf6*$^{-/-}$ cells were resistant to necroptosis induced by IFNβ+EMR treatment (**Figure 19 C-E**). Commensurate with poor necroptosis, the activation of RipK1, RipK3, and MLKL was compromised in *Arf6*$^{-/-}$ cells following IFN-β+EMR treatment (**Figure 19 F**). As was observed with the LPS-induced necroptosis signaling (**Figure 16 F**), the inhibitory phosphorylation (S321) of RipK1 was partially reduced in *Arf6*$^{-/-}$ cells in comparison to the necroptosis-activating phosphorylation (S166) of RipK1, which was abrogated (**Figure 19 F**). These results suggest that the resistance of *Arf6*$^{-/-}$ cells to necroptosis cannot be solely related to the reduced expression of cytokines during TLR signaling.

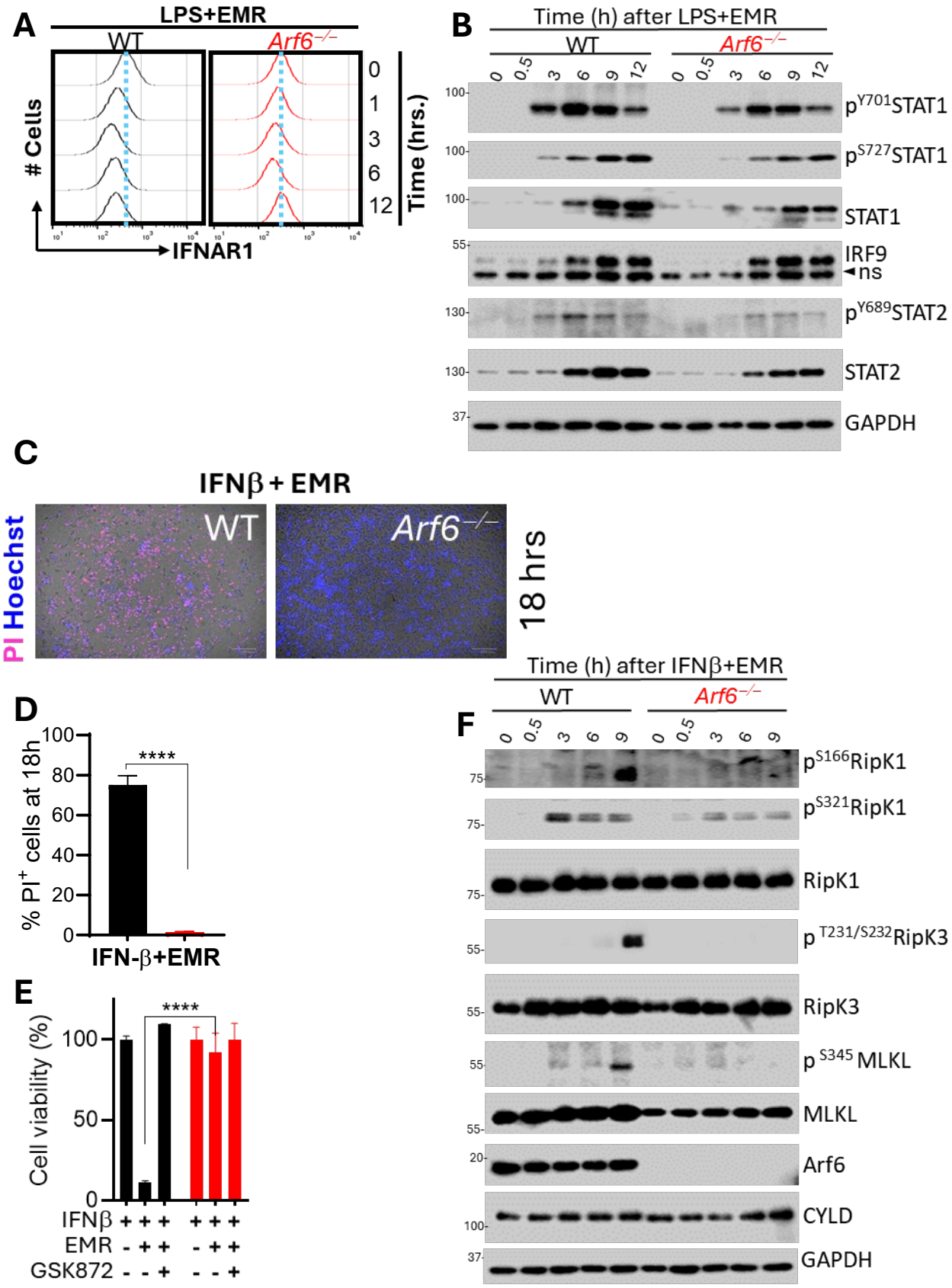
A
LPS+EMR
WT
Arf6−/−
Cells
IFNAR1
Time (hrs.)
0
1
3
6
12
B
Time (h) after LPS+EMR
WT
Arf6−/−
0 0.5 3 6 9 12 0 0.5 3 6 9 12
100-
pY701STAT1
pS727STAT1
STAT1
55-
IRF9
ns
130-
pY689STAT2
STAT2
37-
GAPDH
C
IFNβ + EMR
PI Hoechst
WT
Arf6−/−
18 hrs
D
% PI+ cells at 18h
****
IFN-β+EMR
E
Cell viability (%)
****
IFNβ + + + + + +
EMR - + + - + +
GSK872 - - + - - +
F
Time (h) after IFNβ+EMR
WT
Arf6−/−
0 0.5 3 6 9 0 0.5 3 6 9
75-
pS166RipK1
pS321RipK1
RipK1
55-
pT231/S232RipK3
RipK3
pS345MLKL
MLKL
20-
Arf6
CYLD
GAPDH

Figure 19. ARF6 promotes type I interferon signaling during necroptosis stimulation

A WT and *Arf6*$^{-/-}$ cells were treated with LPS (100ng/mL) and EMR (10μM) for different time intervals, as shown. After that, cells were stained with an anti-IFNAR1 antibody. Histograms of stained cells are shown. **B** Cell extracts were collected at various time intervals, and the activation of signaling proteins was evaluated by western blot analysis. **C-F** WT and *Arf6*$^{-/-}$ cells were treated with IFNβ (10ng/mL) and EMR (10μM). The impact on cell viability was evaluated at 18h by staining the cells with PI and Hoechst **(C, D)** and at 24h by Neutral Red uptake **(E)**. Cell extracts were collected at various time intervals, and the activation of signaling proteins was evaluated by western blot analysis **(F)**. Graphs depict mean ± SEM. Each experiment was repeated at least three times. (****P< 0.0001).

Arf6$^{-/-}$ cells exhibited significantly reduced secretion of pro-inflammatory cytokines TNFα and IL-6 when stimulated with IFN-β+EMR **(Figure 20 A, B)** or IFN-β alone **(Figure 20 C)**. This observation suggests a crucial role for ARF6 in promoting the expression of inflammatory cytokines in response to cytokine stimulation. Upon stimulation with IFN-β+EMR, WT cells displayed the expected phosphorylation of STAT1 and STAT2. *Arf6*$^{-/-}$ cells showed a light-reduction in the activation of these crucial signaling molecules **(Figure 20 D)**. Interestingly, the impact of ARF6 deficiency on cytokine expression was more pronounced compared to the relatively smaller effect observed on STAT1/2 activation, indicating the potential involvement of additional regulatory mechanisms. Furthermore, the activation of STAT3, another transcription factor that promotes inflammatory response, was also diminished in *Arf6*$^{-/-}$ cells **(Figure 20 D)**. To elucidate the specific contribution of STAT3 to the inflammatory response, inhibition studies were conducted. STAT3 inhibition partially reduced TNFα secretion in response to IFN-β+EMR treatment **(Figure 20 E)**, highlighting its importance in the cytokine production cascade. We further investigated the role of ARF6 in receptor dynamics. Notably, *Arf6*$^{-/-}$ cells demonstrated reduced internalization of the IFNAR1 receptor following necroptosis stimulation by IFN-β+EMR **(Figure 20 F)**. This reduced receptor internalization of IFNAR1 provides a mechanistic explanation for the observed reduction in STAT1 and STAT2 activation in *Arf6*$^{-/-}$ cells **(Figure 20 D)**, as receptor internalization is often crucial for efficient signal transduction. In stark contrast to the relatively modest impact on STAT1/2 activation, the MAPK pathway activation was severely compromised in *Arf6*$^{-/-}$ cells during necroptosis stimulation by IFN-β+EMR **(Figure 20 G)**. This finding suggests that ARF6 plays a more critical role in MAPK signaling compared to the STAT pathway in the context of necroptosis.

Taken together, these results highlight the multifaceted role of ArRF in necroptosis signaling. ARF6 emerges as a key player in promoting IFNAR1 internalization, enhancing both STAT and MAPK pathway activation, and crucially regulating necroptosis signaling induced by both LPS+EMR and IFN-β+EMR stimuli. The absence of ARF6 leads to a cascade of cellular events, including reduced cytokine secretion and increased resistance to necroptosis.

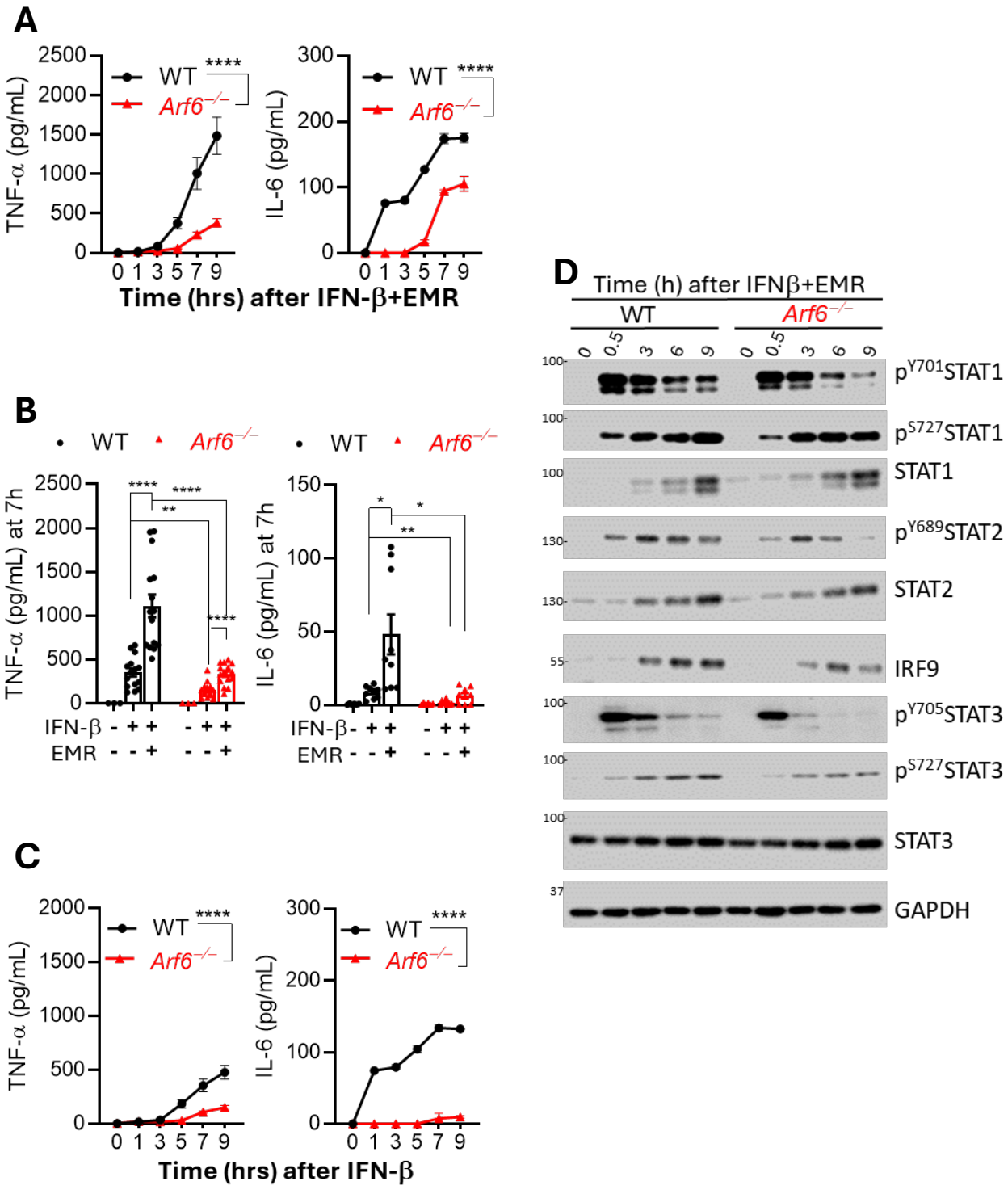
A
TNF-α (pg/mL)
IL-6 (pg/mL)
WT
Arf6−/−
****
Time (hrs) after IFN-β+EMR
B
TNF-α (pg/mL) at 7h
IL-6 (pg/mL) at 7h
IFN-β
EMR
C
Time (hrs) after IFN-β
D
Time (h) after IFNβ+EMR
pY701STAT1
pS727STAT1
STAT1
pY689STAT2
STAT2
IRF9
pY705STAT3
pS727STAT3
STAT3
GAPDH

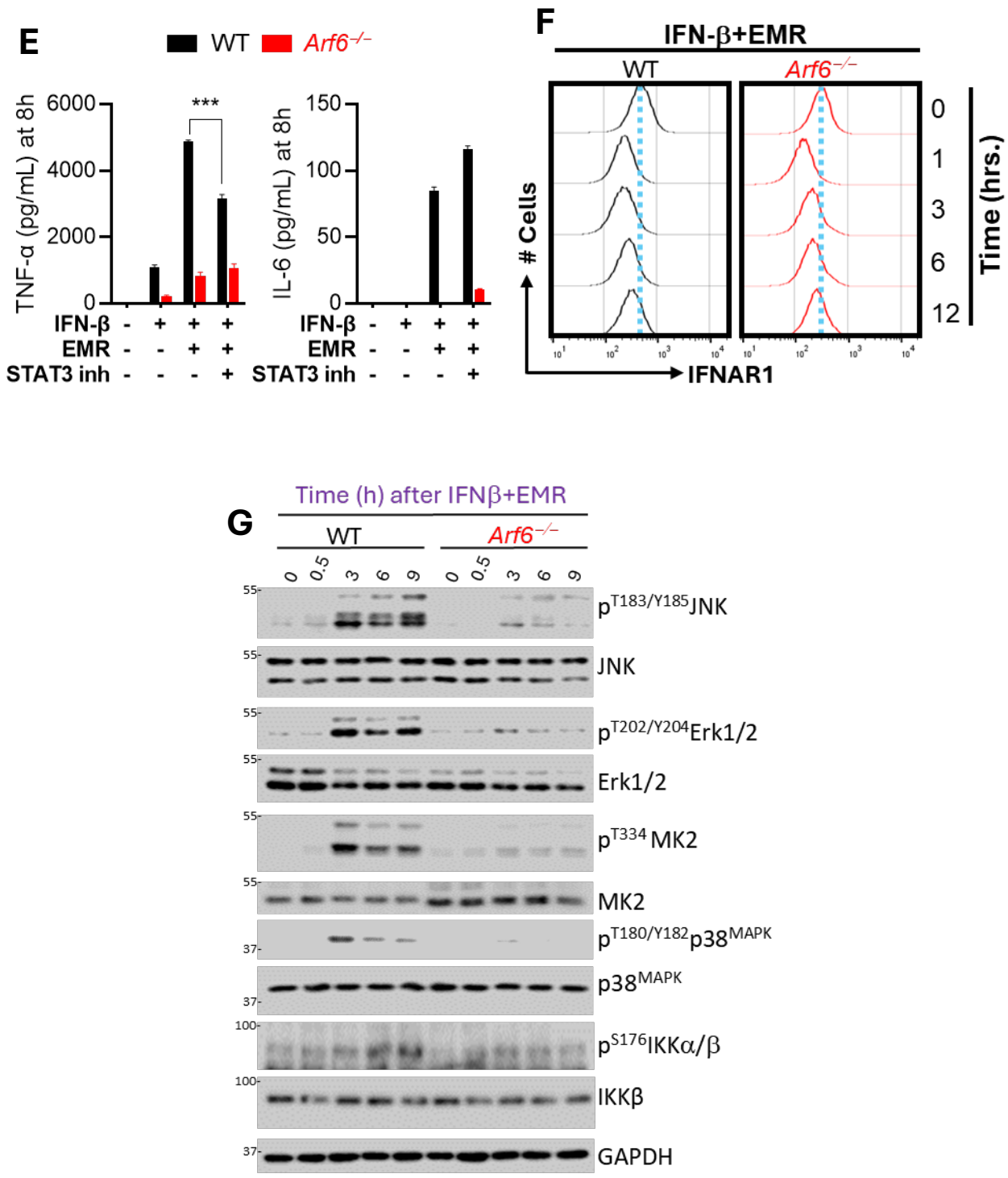
E
WT
Arf6−/−
TNF-α (pg/mL) at 8h
6000
4000
2000
0
***
IL-6 (pg/mL) at 8h
150
100
50
0
IFN-β - + + +
EMR - - + +
STAT3 inh - - - +
F
IFN-β+EMR
WT
Arf6−/−
Cells
IFNAR1
0
1
3
6
12
Time (hrs.)
G
Time (h) after IFNβ+EMR
WT
Arf6−/−
0 0.5 3 6 9 0 0.5 3 6 9
55
pT183/Y185JNK
JNK
pT202/Y204Erk1/2
Erk1/2
pT334 MK2
MK2
37
pT180/Y182p38MAPK
p38MAPK
100
pS176IKKα/β
IKKβ
GAPDH

Figure 20. ARF6 promotes IFNβ-induced cytokine production

A-B The expression level of TNFα and IL-6 in cell supernatants was measured in WT and *Arf6*$^{-/-}$ cells with IFNβ (10ng/mL) and EMR (10μM) at various time intervals **(A)** and 7h post-treatment **(B)** by ELISA. **C** The expression level of TNFα and IL-6 in cell supernatants was measured in WT and *Arf6*$^{-/-}$ cells at various time intervals with IFNβ (10ng/mL) by ELISA. **D, G** WT, and *Arf6*$^{-/-}$ cells were treated with IFNβ (10ng/mL) and EMR (10μM). Cell extracts were collected at various time intervals, and the activation of signaling proteins was evaluated by western blot analysis. **E** WT and *Arf6*$^{-/-}$ cells were treated with IFNβ (10ng/mL), EMR (10μM), and STAT3 inhibitor (10μM), and the impact on the expression of TNFα and IL-6 was analyzed at 8h by ELISA. **F** WT and *Arf6*$^{-/-}$ cells were treated with IFNβ (10ng/mL) and EMR (10μM). At various time intervals, cells were stained with an anti-IFNAR1 antibody. Histograms of surface IFNAR1 expression at different time intervals are shown. Graphs depict mean ± SEM. Each experiment was repeated at least three times. (*P< 0.05, **P< 0.01, ***P< 0.001, ****P< 0.0001).

4.1.4. The lysosomal compartment is impaired in *Arf6*-deficient cells

Our investigation into the reduced activation of IRF3, a downstream effector of TRIF signaling, in *Arf6*$^{-/-}$ cells led us to explore potential alterations in the endo-lysosomal compartment. We employed two distinct experimental approaches to address the role of ARF6 in the endo-lysosomal compartment.

Firstly, we utilized neutral red staining to evaluate lysosomal accumulation in unstimulated cells. Neutral red is a dye that selectively accumulates in lysosomes, providing a visual indicator of lysosomal content and function. Our observations revealed a marked reduction in neutral red accumulation within *Arf6*$^{-/-}$ cells compared to WT cells **(Figure 21A)**. This finding suggests a potential impairment in lysosomal function or quantity in the absence of ARF6.

Secondly, we conducted a time-course experiment to measure the accumulation of pHrodo-labeled *Escherichia coli* (*E. coli*) bioparticles in both WT and *Arf6*$^{-/-}$ cells. pHrodo exhibits increased fluorescence intensity as the pH decreases during phagosomal maturation. We assessed the fluorescence intensity at various time intervals following the introduction of the labeled bioparticles **(Figure 21B and C)**. The results indicated a significant reduction in pHrodo fluorescence intensity within *Arf6*$^{-/-}$ cells compared to their WT counterparts. This observation indicates that the *Arf6*-deficient cells may have impaired lysosomal acidification or altered kinetics of phagosome-lysosome fusion. The diminished fluorescence could be attributed to either a delay in the trafficking of the bioparticles to the lysosomes or a reduction in the acidity of the lysosomal compartments in *Arf6*$^{-/-}$ cells.

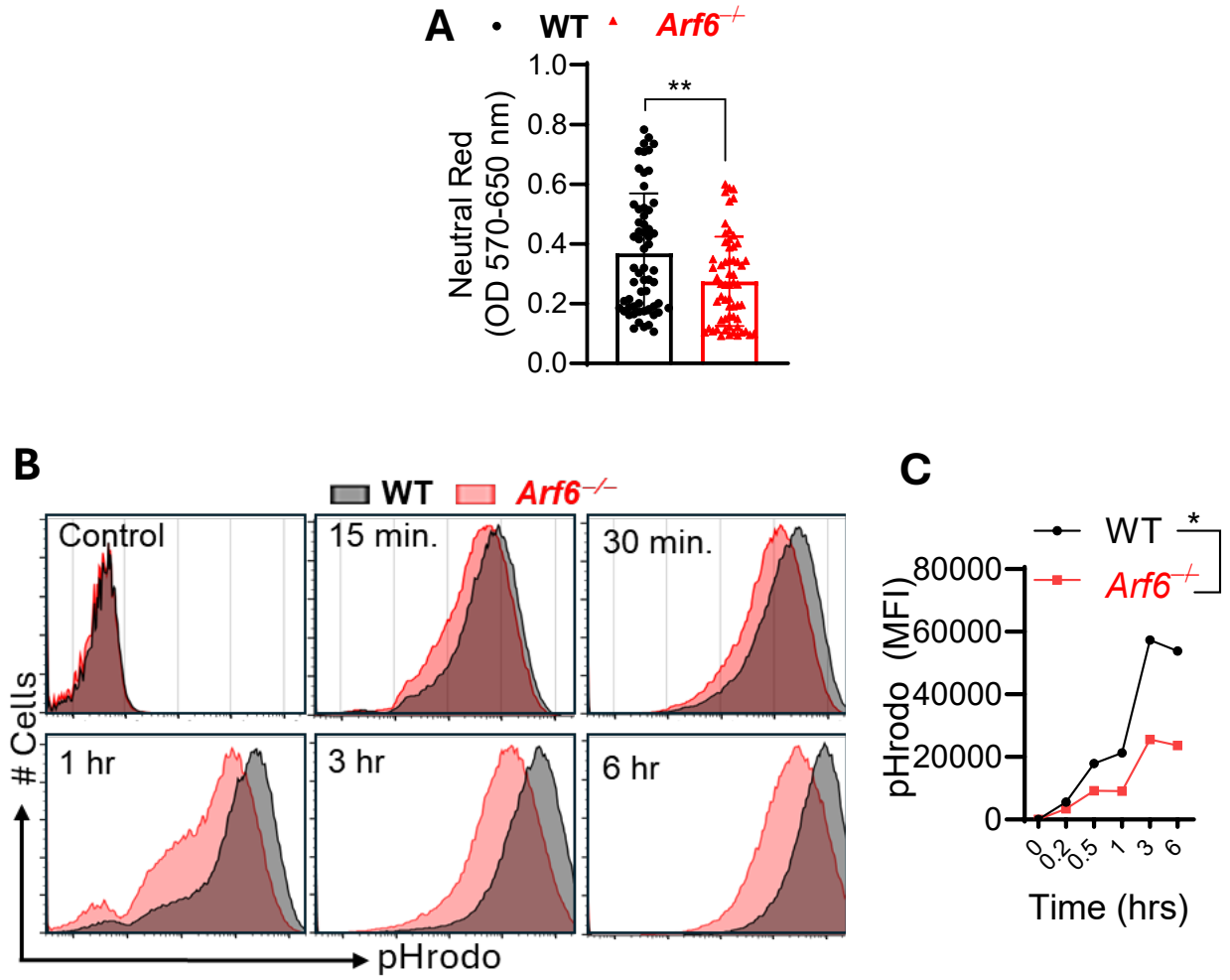

Figure 21. ARF6 deficiency impairs Endo-Phago-Lysosomal function

The uptake of Neutral Red by lysosomes was evaluated by measuring the optical density following the incorporation of the dye. **B, C** WT, and *Arf6*$^{-/-}$ cells were incubated with the pHrodo Deep Red *E. coli* at different intervals. The graphs represent the histogram of stained cells **(B)** and the pHrodo MFI values **(C)**. Graphs depict mean ± SEM. Each experiment was repeated at least three times. (*P< 0.05, **P< 0.01).

We conducted a comprehensive analysis of lysosomal function and cellular trafficking in *Arf6*$^{-/-}$ cells using various fluorescent markers and stimulation conditions. To visualize lysosomes and late endosomes, we stained cells with LysoView, a pH-sensitive dye that accumulates in acidic lysosomal compartments. Our results revealed a significant reduction in LysoView staining in *Arf6*$^{-/-}$ cells compared to wild-type controls, both at 30 minutes and 6 hours post-staining, in the absence of any external stimulation **(Figure 22 A, C, E, F)**. This finding suggests an inherent impairment in lysosomal function or acidification in *Arf6*-deficient cells at basal conditions.

To further investigate the role of ARF6 in lysosomal dynamics during cellular stress, we stimulated the cells with a combination of LPS + EMR. This necroptosis-inducing treatment resulted in an overall increase in lysosomal staining across both genotypes. However, the *Arf6*$^{-/-}$ cells consistently exhibited reduced LysoView fluorescence intensity compared to their wild-type counterparts, even under stimulated conditions **(Figure 22 B, D, E, F)**. This observation indicates that the lysosomal impairment in *Arf6*$^{-/-}$ cells persists during necroptosis induction, suggesting a fundamental role for ARF6 in maintaining lysosomal integrity and function.

To dissect the specific cellular processes affected by ARF6 deficiency, we performed additional experiments focusing on endocytic trafficking. We utilized fluorophore-labeled LPS to track its internalization and found that *Arf6*$^{-/-}$ cells showed no impairment in LPS uptake compared to wild-type cells **(Figure 22 G)**. This result indicates that the initial steps of endocytosis remain intact in the absence of ARF6. Furthermore, we employed EC-Green staining to visualize early endosomes and observed no discernible differences between *Arf6*$^{-/-}$ and WT cells **(Figure 22 H)**.

To gain insights into the trafficking of internalized LPS, we examined its colocalization with LysoView-positive compartments. In WT cells, we observed substantial colocalization between internalized LPS and LysoView, indicating efficient delivery of LPS to lysosomes. However, this colocalization was markedly reduced in *Arf6*$^{-/-}$ cells **(Figure 22 I)**. We attribute this reduction primarily to the impairment in lysosomal staining rather than a defect in LPS trafficking, as the internalization of LPS itself was not affected. This observation underscores the specific impact of ARF6 deficiency on lysosomal function rather than on the upstream endocytic processes.

Lastly, we investigated the dynamics of lysosomal activity during necroptosis stimulation. While both WT and *Arf6*$^{-/-}$ cells showed an increase in overall lysosomal staining upon LPS+EMR treatment, the *Arf6*-deficient cells consistently displayed reduced levels of LysoView fluorescence **(Figure 22 J)**. This persistent impairment in lysosomal staining during necroptosis further emphasizes the critical role of ARF6 in maintaining lysosomal homeostasis under various cellular conditions.

In conclusion, our detailed analysis reveals that *Arf6* deficiency specifically impairs lysosomal function and acidification in both unstimulated and necroptosis-stimulated cells. Importantly, this impairment does not extend to early endosomes or LPS internalization, highlighting the selective role of Arf6 in late endosomal/lysosomal processes. The reduced colocalization of LPS with lysosomes in *Arf6*$^{-/-}$ cells is likely a consequence of impaired lysosomal function rather than a defect in LPS trafficking.

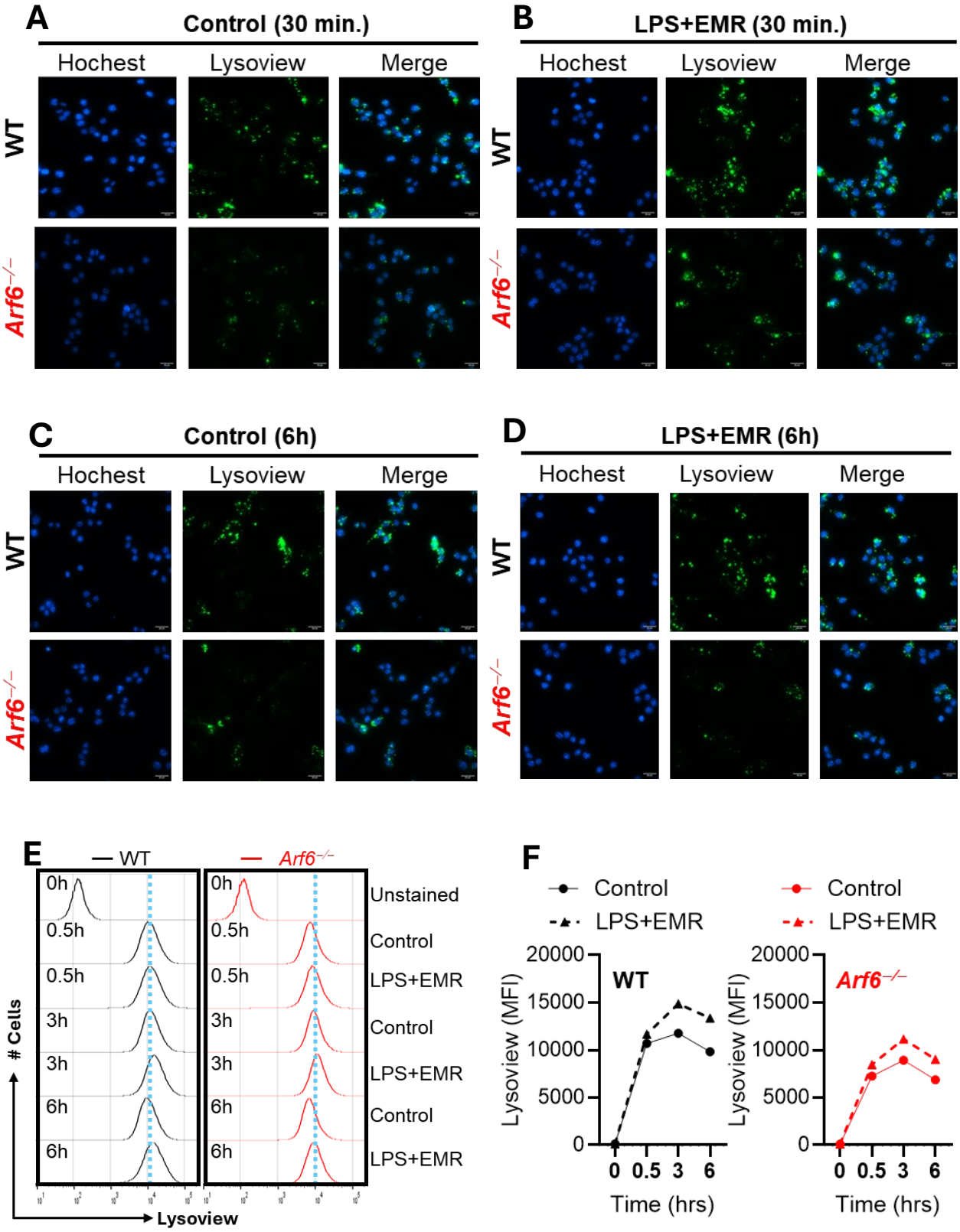
A
Control (30 min.)
Hochest
Lysoview
Merge
WT
Arf6−/−
B
LPS+EMR (30 min.)
C
Control (6h)
D
LPS+EMR (6h)
E
— WT
— Arf6−/−
0h
0.5h
3h
6h
Unstained
Control
LPS+EMR
Cells
Lysoview
F
Control
LPS+EMR
WT
Arf6−/−
Lysoview (MFI)
20000
15000
10000
5000
0
0 0.5 3 6
Time (hrs)

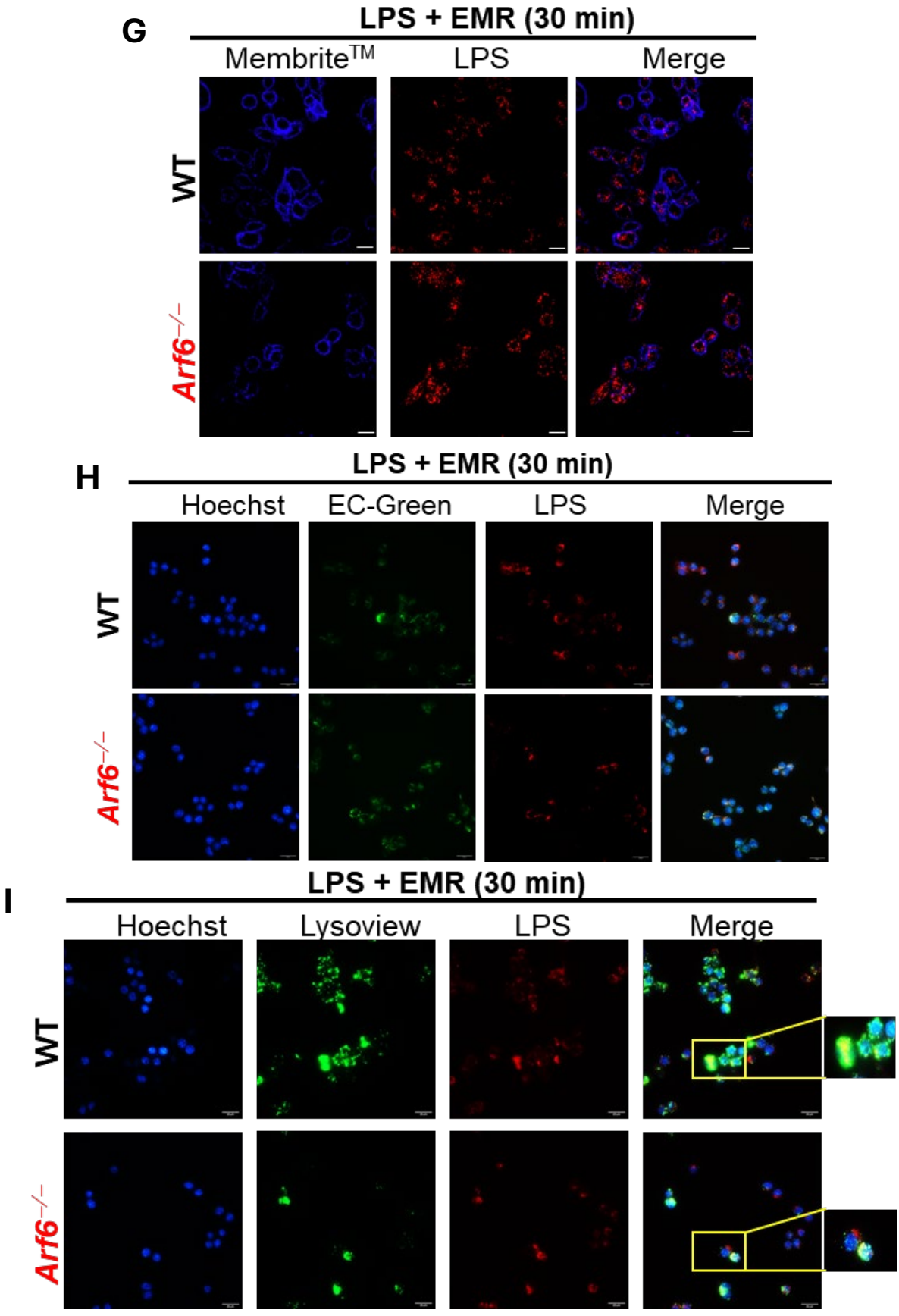
G
LPS + EMR (30 min)
Membrite™
LPS
Merge
WT
Arf6−/−
H
LPS + EMR (30 min)
Hoechst
EC-Green
LPS
Merge
WT
Arf6−/−
I
LPS + EMR (30 min)
Hoechst
Lysoview
LPS
Merge
WT
Arf6−/−

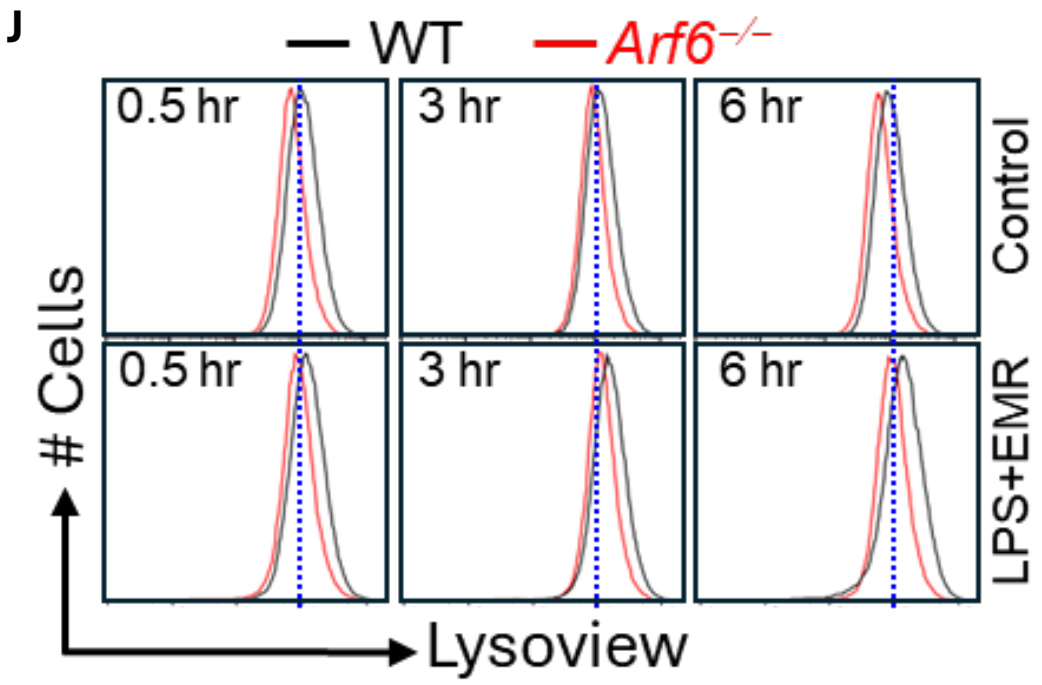

Figure 22. ARF6 promotes lysosomal homeostasis

A-F WT and *Arf6*$^{-/-}$ cells were treated with and without LPS (100ng/mL) + EMR (10µM) for different intervals and labelled with LysoView 405 (Live Lysosome Stain) (Green) and Hoechst (Nucleus Stain) (Blue) at the same time **(A-D)**. Histograms depict the LysoView uptake by cells over time **(E).** The MFI values of LysoView uptake are depicted in panel **(F)**. **G** WT and *Arf6*$^{-/-}$ cells were treated with Alexa Fluor 594 (Red) conjugated LPS 100ng/mL. Cell membranes were stained with Membrite 405/430 (Blue). **H, I** WT, and *Arf6*$^{-/-}$ cells were treated with LPS (100ng/mL) and EMR (10µM) for 30 minutes and labelled with Hoechst (Nuclear Stain) (Blue). In addition, cells were labelled with EC-Green 405 (Live Endosomal stain) (Green) **(H)** and LysoView- 405 (Live Lysosomal Stain) (Green) **(I)**. **J** WT and *Arf6*$^{-/-}$ cells were treated with and without LPS (100ng/mL) + EMR (10µM) for different intervals and labelled with LysoView 405 (Live Lysosome Stain) at the same time. The graph represents the histogram of LysoView uptake by cells over time. Each experiment was repeated at least three times. Graphs depict mean ± SEM. The scale bar is 20µm. (*P< 0.05, **P< 0.01).

4.1.5. ARF6 promotes Ripoptosome activation without impacting apoptosis

We probed the mechanism through which ARF6 promotes necroptosis by first evaluating whether ARF6 impacts other pathways of cell death. Induction of apoptosis by treatment of cells with Etoposide (**Figure 23 A**), or Gliotoxin (**Figure 23 B**), and other known inhibitors of the NF-kB pathway (**Figure C, D**) did not reveal any impact of ARF6. We then treated cells with the SMAC mimetic Birinapant, which induces ripoptosome-dependent cell death through the degradation of IAPs. WT cells treated with SMAC resulted in potent cell death (ripoptosis) which was rescued by the RipK1 inhibitor Nec-1, but not by the RipK3 inhibitor GSK872 (**Figure 23 E**). *Arf6*$^{-/-}$ cells displayed significant resistance against this form of cell death (**Figure 23 E**), suggesting that a common pathway may be modulated by ARF6 in ripoptosome and necrosome activation. Activation of RipK1 is a common signaling mechanism that participates in both these forms of cell death. Since ripoptosome activation is dependent on TNF-R1 signaling, we evaluated the internalization of TNF-R1 following SMAC treatment of cells. There was a progressive decrease in cell surface TNF-R1 in both WT and *Arf6*$^{-/-}$ cells (**Figure 23 F**), suggesting that the endocytosis of TNF-R1 is not impacted by ARF6. While the degradation of cIAP1/2 by SMAC treatment was sustained in WT cells, the levels of cIAP1/2 were transiently reduced in *Arf6*$^{-/-}$ cells (**Figure 23 G**). The activation of caspase-8 and caspase-3 was compromised in *Arf6*$^{-/-}$ cells treated with SMAC (**Figure 23 G**), confirming that ARF6-signaling promotes ripoptosome signaling.

Overall, these results suggest that ARF6 plays a specific role in programmed cell death pathways that are dependent on RipK1. While having no significant impact on apoptosis, ARF6 promotes ripoptosome-mediated cell death by sustaining cIAP1/2 degradation, leading to enhanced caspase activation. Importantly, this function is independent of TNF-R1 internalization. These findings highlight the selective modulation of cell death pathways, specifically in ripoptosome-mediated processes by ARF6.

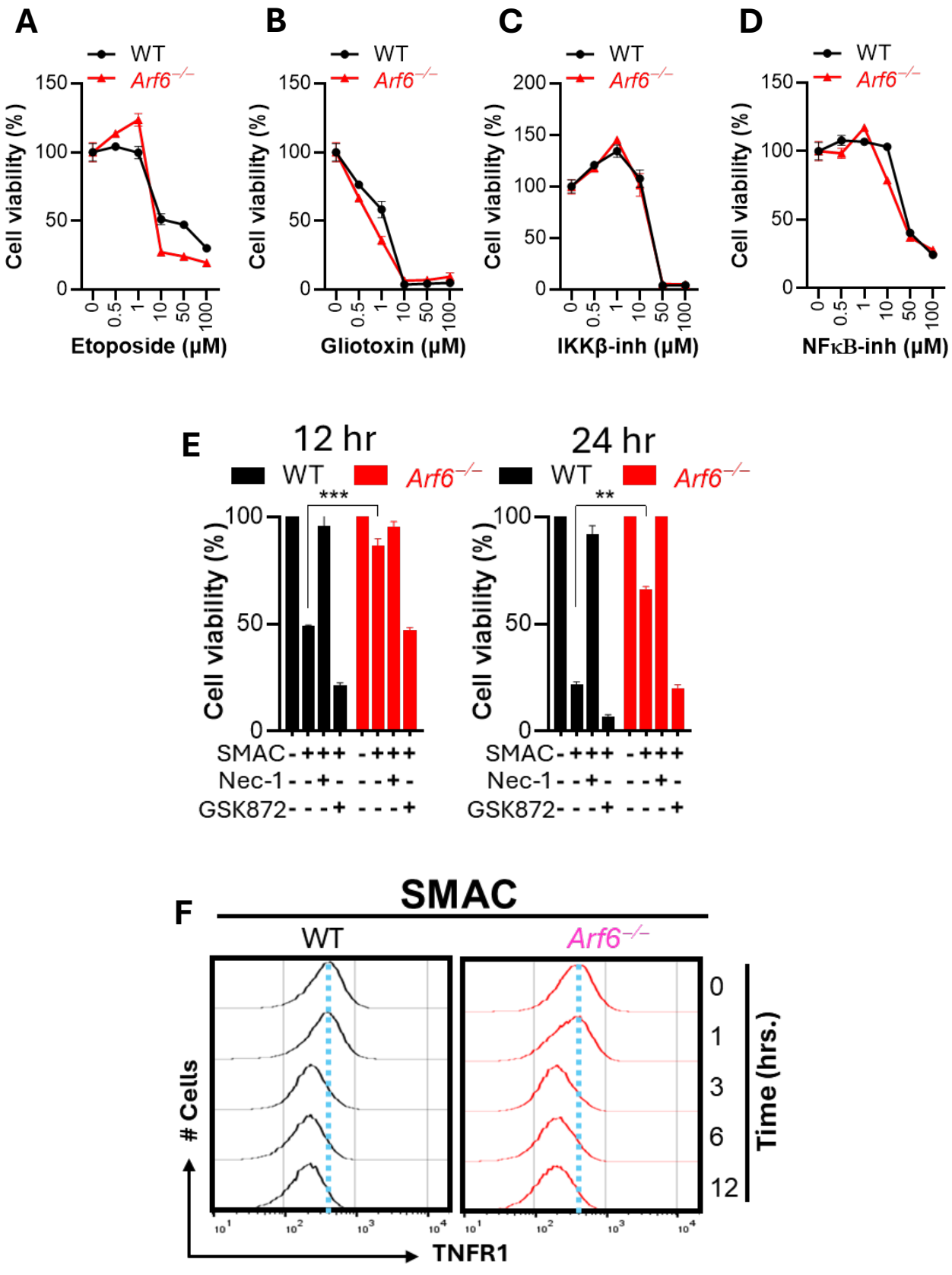
A
B
C
D
WT
Arf6−/−
Cell viability (%)
Etoposide (μM)
Gliotoxin (μM)
IKKβ-inh (μM)
NFκB-inh (μM)
E
12 hr
24 hr
***
**
SMAC
Nec-1
GSK872
F
SMAC
Cells
TNFR1
Time (hrs.)

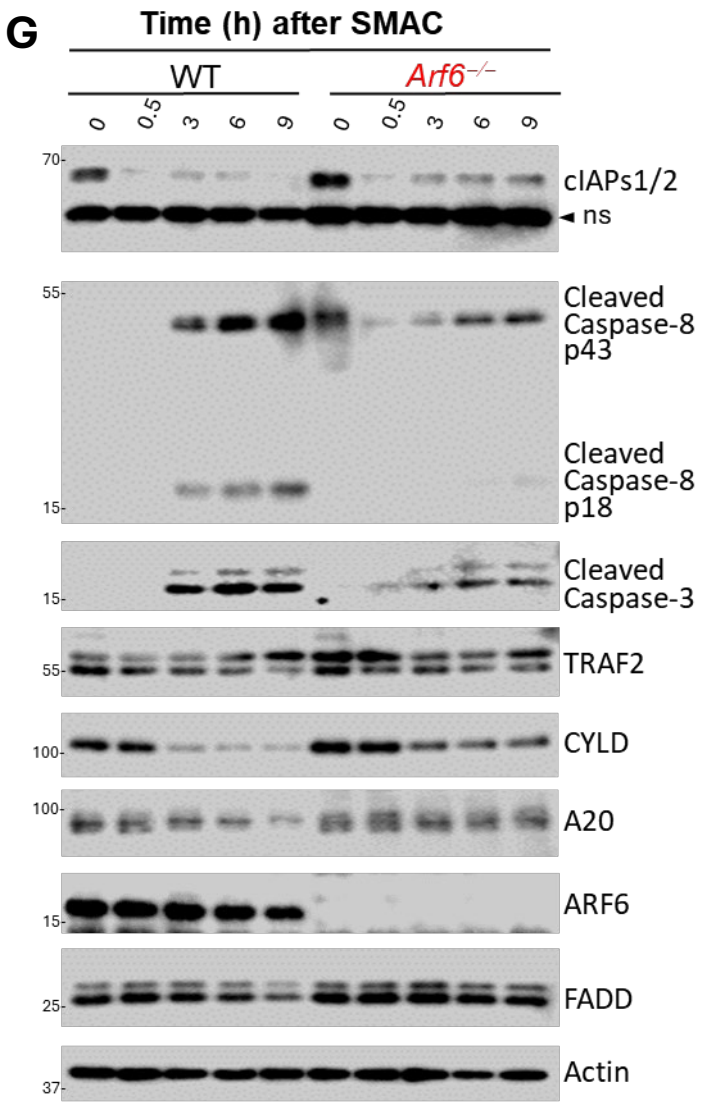

Figure 23. ARF6 promotes ripoptosome activation without impacting apoptosis

A-D WT and *Arf6*$^{-/-}$ cells were treated with different concentrations of Topoisomerase II inhibitor- Etoposide **(A)**, DNA synthesis inhibitor- Gliotoxin **(B)**, Iκκ2 inhibitor **(C)**, and NF-κB activation inhibitor II **(D)** and the impact on cell viability was evaluated at 24h by Neutral Red uptake. **E** WT and *Arf6*$^{-/-}$ cells were treated with the SMAC-mimetic Birinapant (10μM), Nec-1 (10 μM), and GSK872 (10 μM), and the impact on cell viability was evaluated at 12h and 24h by Neutral Red uptake. **F, G** WT, and *Arf6*$^{-/-}$ cells were treated with SMAC- Birinapant (10μM) for different time intervals as indicated. After that, cells were stained with an anti-TNFR1 Ab. The graph represents the histogram of surface TNFR1 expression over time **(F)**. Cell extracts were collected at various time intervals and the activation of signaling proteins was evaluated by western blot analysis **(G)**. Graphs depict mean ± SEM. Each experiment was repeated at least three times. (**P< 0.01, ***P< 0.001).

4.1.6. ARF6 promotes the degradation of cIAPs during necroptosis signaling

To further investigate the potential involvement of ARF6 in the ripoptosome and necrosome signaling pathways, we explored the possibility of a direct interaction between ARF6 and RipK1, given that both pathways were affected by ARF6 and required RipK1 activation. We conducted a comprehensive series of immunoprecipitation experiments to examine this potential interaction under various conditions.

Initially, we performed RipK1 immunoprecipitations in unstimulated control cells **(Figure 24 A)** to establish a baseline for protein-protein interactions in the absence of external stimuli. Subsequently, we extended our investigation to include multiple time points following the stimulation of cells with LPS+EMR **(Figure 24 B-D)**. This time-course analysis allowed us to capture any transient or dynamic interactions that might occur during the activation and progression of necrosome signaling. We were unable to detect any interaction between RipK1 and ARF6 at any of the time points analyzed. This consistent lack of interaction suggests that ARF6 does not directly associate with RipK1 in these pathways.

In WT cells, we were able to detect the interaction of RipK1 with RipK3 as expected, confirming the validity of our experimental approach and the formation of the necrosome complex under stimulated conditions. Interestingly, this interaction was significantly diminished in *Arf6*$^{-/-}$ cells **(Figure 24 D)**, indicating that while ARF6 may not directly interact with RipK1, its presence is crucial for facilitating or stabilizing the RipK1-RipK3 interaction. This observation provides valuable insight into the potential regulatory role of ARF6 in necrosome formation. Furthermore, we examined the interaction between RipK3 and MLKL, a key effector protein in the necroptosis pathway. Consistent with our findings on the RipK1-RipK3 interaction, we observed robust RipK3-MLKL association in WT cells, which was notably reduced in *Arf6*$^{-/-}$ cells **(Figure 24 E)**. This result further supports the hypothesis that ARF6 plays a significant role in promoting or maintaining the integrity of the necrosome complex, even in the absence of direct binding to its core components.

To complete our investigation of potential protein-protein interactions, we also probed for any direct interaction between RipK3 and ARF6. However, we failed to detect any such interaction

(Figure 24 E), further reinforcing the notion that if ARF6 influences the necrosome pathway, it likely does so through indirect mechanisms rather than direct binding to core necrosome components. This finding suggests that ARF6 may exert its effects on the ripoptosome and necrosome pathways through an alternative mechanism.

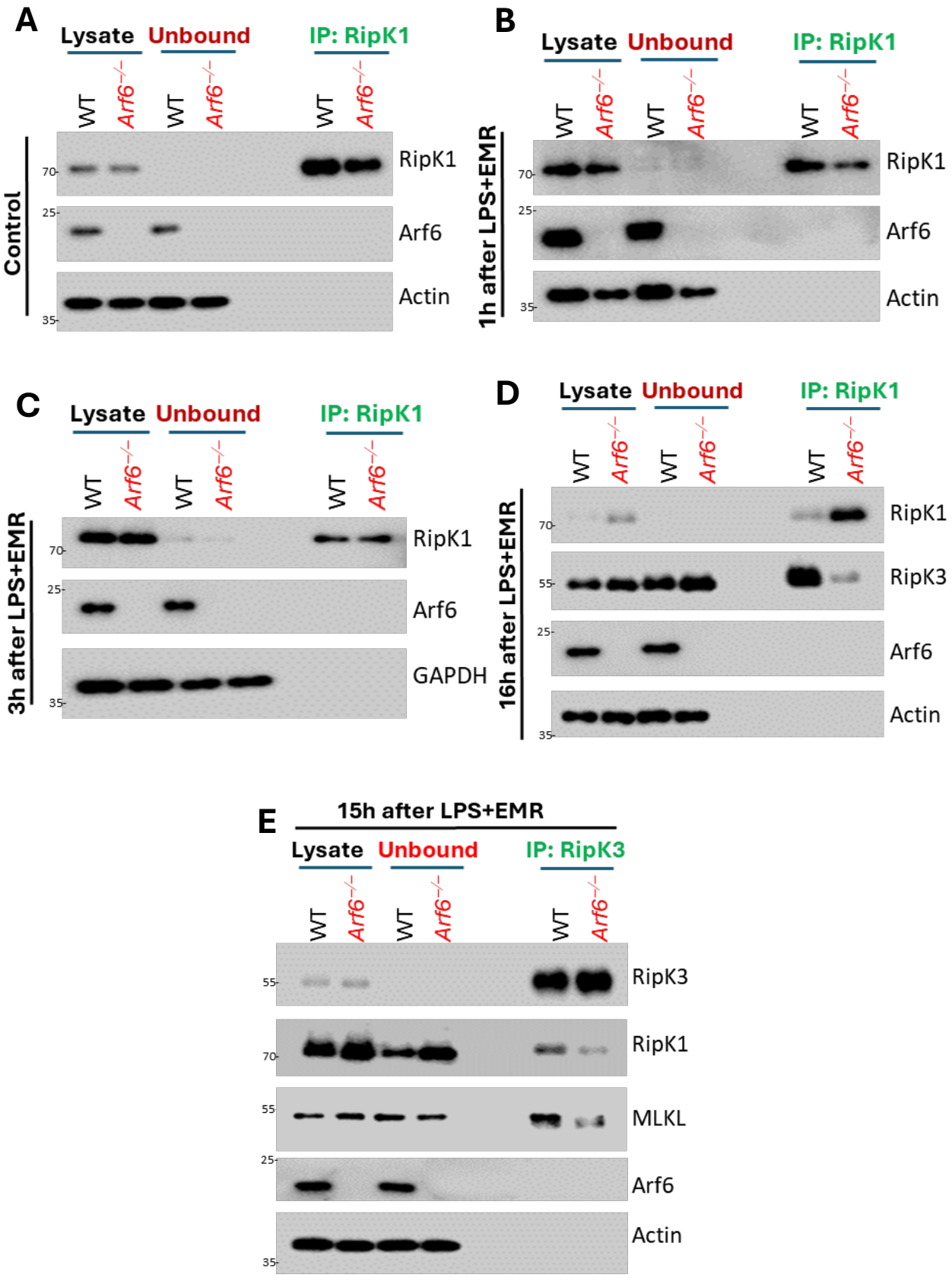
A
Lysate
Unbound
IP: RipK1
WT
Arf6−/−
Control
70
25
35
RipK1
Arf6
Actin
B
1h after LPS+EMR
C
3h after LPS+EMR
GAPDH
D
16h after LPS+EMR
55
RipK3
E
15h after LPS+EMR
IP: RipK3
MLKL

Figure 24. RipK1 and RipK3 do not interact with ARF6

A-D WT and *Arf6*$^{-/-}$ cells were treated with LPS (100ng/mL) + EMR (10μM), and RipK1 was immunoprecipitated at different time intervals as indicated. The expression of various proteins in the immunoprecipitates and the cell lysates was examined by western blotting. **E** WT and *Arf6*$^{-/-}$ cells were treated with LPS (100ng/mL) + EMR (10μM). RipK3 was immunoprecipitated at 15h post-stimulation. The expression of various proteins in the immune precipitates and the cell lysates was examined by western blotting. Each experiment was repeated at least three times.

Since ARF6 plays a crucial role in facilitating protein trafficking between the plasma membrane and other cellular compartments, we conducted a comprehensive analysis of the relative localization of ARF6 and other key proteins during necroptosis stimulation. To achieve this, we isolated membrane and cytosolic fractions at various time intervals. Our findings revealed intriguing dynamics in protein distribution and activation patterns.

Prior to necroptosis stimulation, ARF6 was predominantly localized in the membrane fraction. However, a significant shift in its distribution was observed at 9 hours post-stimulation, with a substantial proportion of ARF6 becoming detectable in the cytosolic fraction **(Figure 25 A, B)**. This translocation of ARF6 coincided with other notable changes in the localization and activation states of other proteins. Activated RipK1 (pS166) exhibited a primarily cytoplasmic distribution, with its highest levels correlating with the increased cytoplasmic presence of ARF6 at 9-hour post-stimulation **(Figure 25 A)**. Interestingly, when compared to WT cells, *Arf6*$^{-/-}$ cells displayed markedly reduced levels of activated RipK1 in the cytoplasm. This observation suggests a potential regulatory role for ARF6 in RipK1 activation or localization during necroptosis.

The activation pattern of RipK3 also showed distinct differences between WT and *Arf6*$^{-/-}$ cells. In *Arf6*$^{-/-}$ cells, the levels of activated RipK3 in the cytoplasm were notably reduced compared to WT cells **(Figure 25 A)**. Surprisingly, we detected high levels of activated RipK3 in the membrane fraction of WT cells at 9 hours post-stimulation with LPS+EMR. Phosphorylated MLKL, a crucial effector of necroptosis, showed a preferential distribution in the membrane fraction of WT cells, with higher levels compared to the cytosolic fraction. Strikingly, both the membrane and cytosolic fractions of *Arf6*$^{-/-}$ cells exhibited significantly reduced levels of phosphorylated MLKL **(Figure 25 A)**.

The levels of cIAP1/2, known regulators of RipK1-dependent cell death pathways, displayed contrasting trends in WT and *Arf6*$^{-/-}$ cells. In WT cells, cIAP1/2 levels decreased progressively in both the membrane and cytoplasmic fractions as necroptosis progressed. Conversely, *Arf6*$^{-/-}$ cells showed an increase in cIAP1/2 levels over time **(Figure 25 A)**. Notably, the decrease in cIAP1/2 levels in WT cells correlated with the increase in cytoplasmic ARF6 levels **(Figure 25 A, B)**, suggesting a potential regulatory relationship between ARF6 and cIAP1/2 during necroptosis.

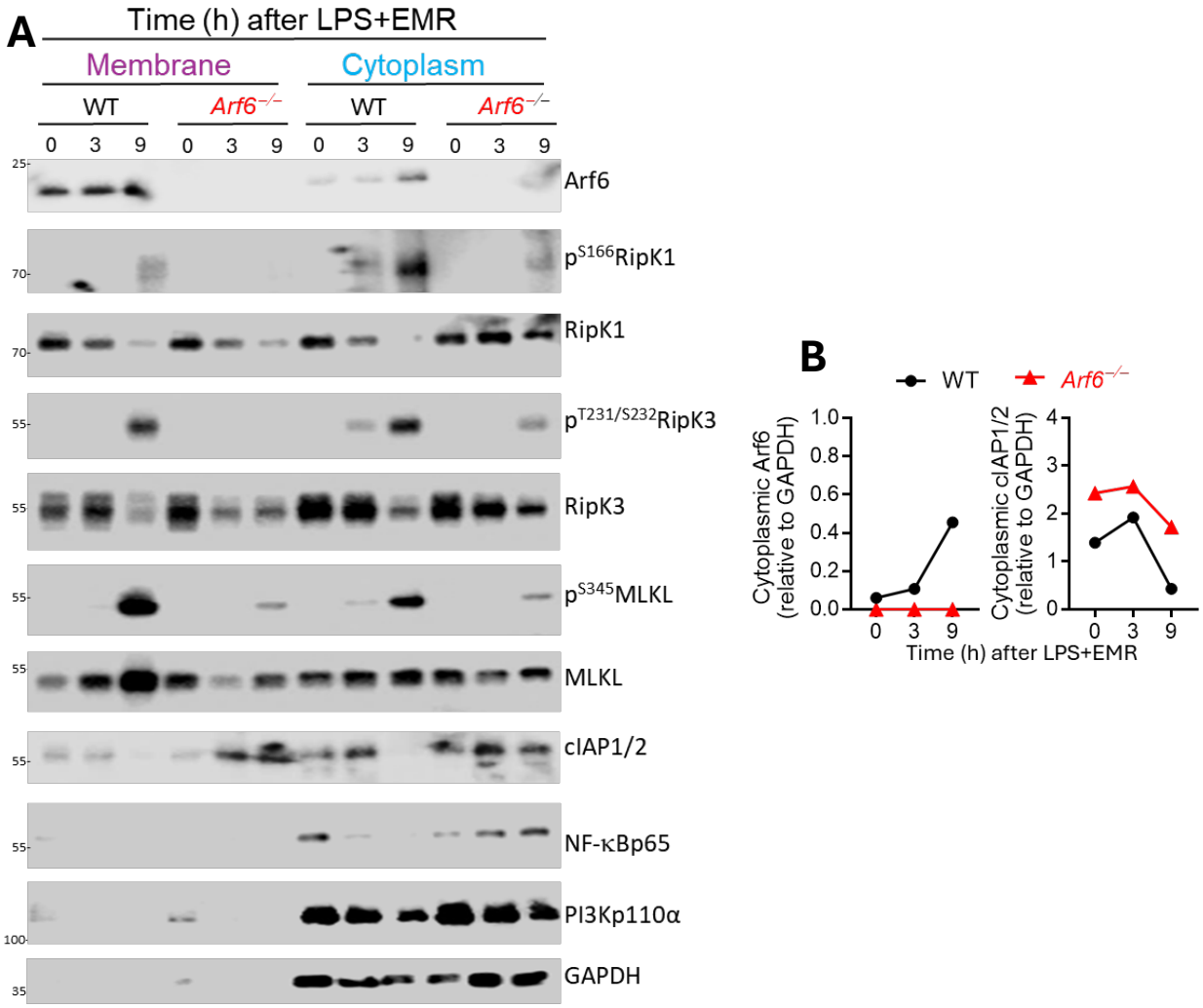

Figure 25. ARF6 promotes the partitioning of cIAPs during necroptosis signaling

A WT and *Arf6*$^{-/-}$ cells were treated with LPS (100ng/mL) and EMR (10μM) for different time intervals as indicated. Membrane and cytoplasmic cell extracts were separated. The expression of various signaling proteins in the membrane and cytoplasmic extracts was evaluated by western blot analysis. **B** Densitometric analysis of ARF6 and cIAPs relative to GAPDH in the cytoplasm was performed. Each experiment was repeated at least three times.

After observing a significant impact of ARF6 on the expression of cIAP1/2 and knowing that the degradation of cIAPs is essential for ripoptosis and necroptosis to proceed, we probed the role of cIAPs in the context of ARF6 further. Stimulation of cells with a SMAC mimetic Birinapant resulted in a transient degradation of cIAP1/2 in *Arf6*$^{-/-}$ cells in comparison to WT cells where the levels remained low (**Figure 26 A, B**). SMAC-mimetic treatment by itself did not induce the phosphorylation of RipK1 as expected (**Figure 26 A, B**). Differences in the levels of cIAP1/2 between WT versus *Arf6*$^{-/-}$ cells resulted in differential susceptibility of cells to ripoptosome-dependent cell death (**Figure 26 C**). Similar results were obtained when cells were stimulated with LPS+EMR to induce necroptosis (**Figure 26 D-F**). Treatment of cells with LPS+EMR resulted in progressive degradation of cIAP1/2 in WT but not in *Arf6*$^{-/-}$ cells (**Figure 26 D, E**). The decline in cIAP1/2 levels in WT cells correlated with the progressive increase in the S166 phosphorylation of RipK1 (**Figure 26 D, E**), which correlated with cell death (**Figure 26 F**). In contrast, *Arf6*$^{-/-}$ cells showed no degradation of cIAP1/2, which correlated with no phosphorylation of RipK1 and poor induction of necroptosis (**Figure 26 F**).

We observed that the treatment of cells with the SMAC mimetic caused a rapid degradation of cIAP1/2, in comparison to the treatment with LPS+EMR, which resulted in a protracted degradation of cIAP1/2 in WT cells (**Figure 26 A, B, D, E**). LPS by itself does not cause degradation of cIAP1/2. We therefore considered the possibility that the treatment of cells with SMAC+EMR, which also induces necroptosis, might break the "degradation resistance" of cIAP1/2 in *Arf6*$^{-/-}$ cells, and impact the resistance of these cells to necroptosis. Treatment of *Arf6*$^{-/-}$ cells with SMAC+EMR induced the S166 phosphorylation of RipK1, which was only slightly reduced in comparison to that observed in WT cells (**Figure 26 G, H**). This is in stark contrast to the situation with LPS+EMR, where the phosphorylation of RipK1 was undetectable in *Arf6*$^{-/-}$ cells (**Figure 26 G, H**). More importantly, treatment of cells with SMAC+EMR resulted in similar degradation of cIAP1/2 in both WT and *Arf6*$^{-/-}$ cells (**Figure 26 G, H**), and the resistance of *Arf6*$^{-/-}$ cells to necroptosis was blunted (**Figure 26 I**).

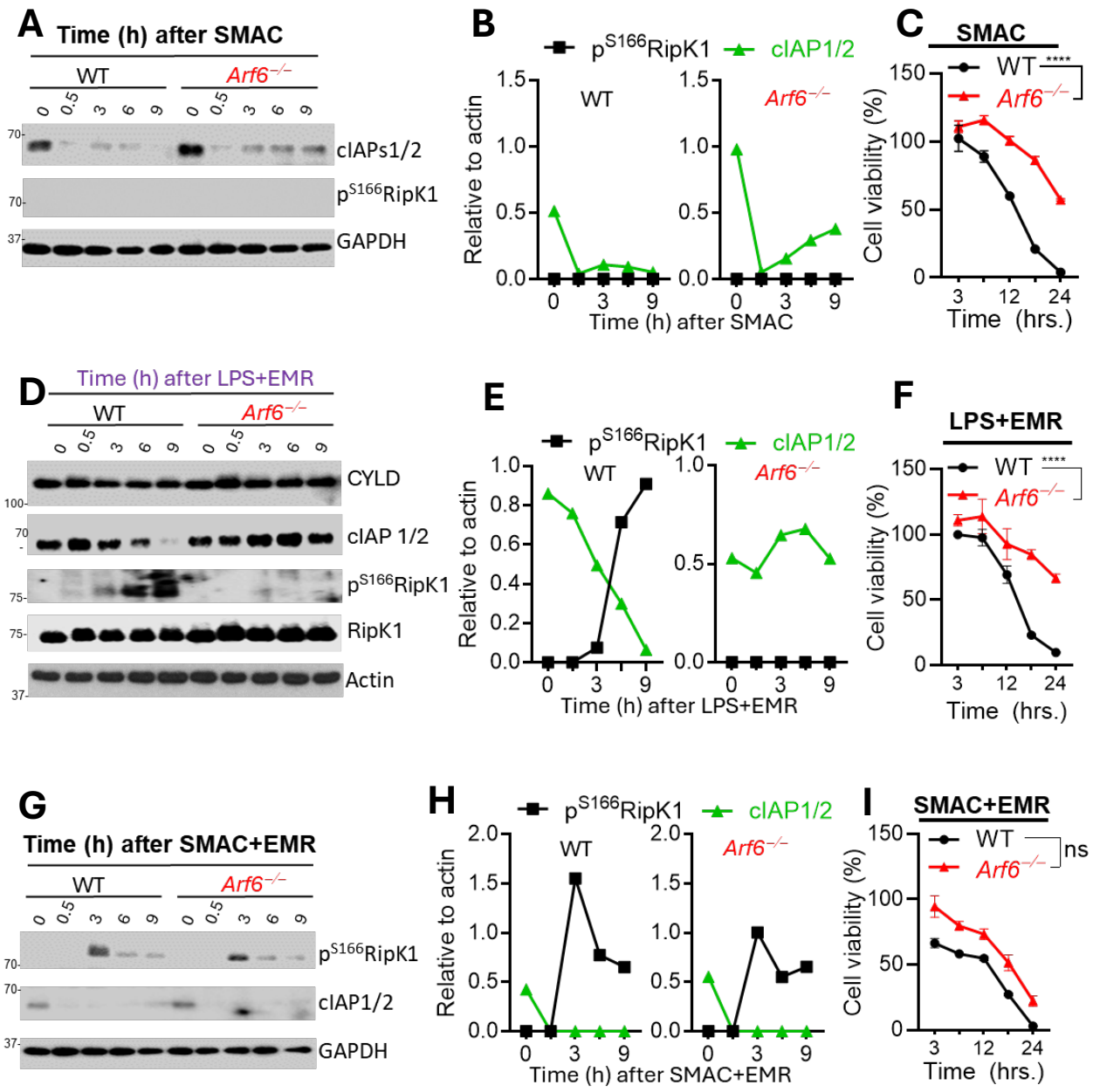

Figure 26. ARF6 promotes the degradation of cIAPs during necroptosis signaling

WT and *Arf6*$^{-/-}$ cells were treated with the SMAC-mimetic Birinapant (10µM) (**A-C**), LPS (100ng/mL) + EMR (10µM) (**D-F**), or Birinapant (10µM) + EMR (10µM) (**G-I**). Cell extracts were collected at various time intervals, and the activation of signaling proteins was evaluated by western blot analysis (**A, D, G**). Densitometric analysis of p^{S166}RipK1 and cIAPs1/2 relative to Actin and GAPDH were performed (**B, E, H**). Cell viability was evaluated by Neutral Red uptake **(C, F, I)**. Graphs depict mean ± SEM. Each experiment was repeated at least three times. (****P< 0.0001).

These findings collectively unveil a previously undiscovered role of ARF6 in regulating programmed cell death pathways. Specifically, our results demonstrate that ARF6 plays a crucial function in facilitating the compartmentalization and subsequent degradation of cIAP1/2, which are key inhibitors of apoptosis proteins. This process is essential for the proper activation and progression of both the ripoptosome and necrosome signaling cascades. By modulating the subcellular localization and breakdown of these inhibitory proteins, ARF6 effectively acts as a molecular switch, fine-tuning the decision between survival and death.

4.2.Aim 2: Delineating the role of necroptosis signaling on the inflammatory response.

4.2.1. Necroptosis stimulation induces an inflammatory storm

Necroptosis has been demonstrated to trigger the release of intracellular damage-associated molecular patterns (DAMPs), including S100 proteins, mitochondrial DNA, and high mobility group box 1 (HMGB1). The release of these molecules into the extracellular environment is considered to be the reason behind the exacerbation of the inflammatory response that is frequently observed following necrotic cell death. To investigate this phenomenon, we conducted a comprehensive transcriptomic analysis of bone marrow-derived macrophages (BMDMs) during necrosome stimulation at a 6-hour time point, when cell death is not yet detectable **(Figure 27 A)**. This approach allowed us to examine the early transcriptional changes associated with necroptosis induction prior to the onset of cell death.

We performed differential gene expression analysis on BMDMs at 6 hours following treatment with IFNβ alone and in combination with the pan-caspase inhibitor zVAD. The results are depicted using a 2D plot, with the X-axis representing the log2 fold-change (log2FC) of gene expression in cells treated with IFNβ relative to untreated wild-type (WT) BMDMs, and the Y-axis showing the log2FC of gene expression in cells treated with IFNβ+zVAD relative to untreated WT BMDMs **(Figure 27 B)**. This analysis revealed a significant upregulation of various pro-inflammatory genes, including tumor *Tnfα*, *Il1*, *Ifnβ*, and *Cxcl1* in cells stimulated with IFNβ+zVAD. These findings suggest that the combination of IFNβ and zVAD triggers a robust pro-inflammatory response in BMDMs, even before the onset of cell death.

To gain further insights into the biological processes affected by necroptosis stimulation, we conducted gene set enrichment analysis (GSEA). This analysis revealed the upregulation of various pathways related to the inflammatory response **(Figure 27 C-H)**. A detailed examination of the enriched leading edge gene sets uncovered an upregulation of the TNFα signaling pathway during necroptosis stimulation. This upregulation resulted in increased expression of various genes, including *Tnfα* itself, as well as the chemokines *Cxcl1* and *Cxcl2*, which are known to play crucial roles in the recruitment of inflammatory cells.

To further validate the specificity of the observed inflammatory response to necroptosis, we treated cells with Nec-1, a selective inhibitor of RipK1 that blocks its kinase activity and inhibits RipK1-RipK3 interaction. Nec-1 treatment significantly reduced the upregulation of the inflammatory response during necroptosis stimulation by IFNβ+zVAD **(Figure 27 C, D)**.

To contextualize our findings within the broader spectrum of inflammatory stimuli, we compared the GSEA results from cells treated with lipopolysaccharide (LPS) and zVAD (LPS+zVAD) relative to LPS alone. This comparison revealed a similar upregulation of inflammatory pathways during necroptosis stimulation **(Figure 27 I)**.

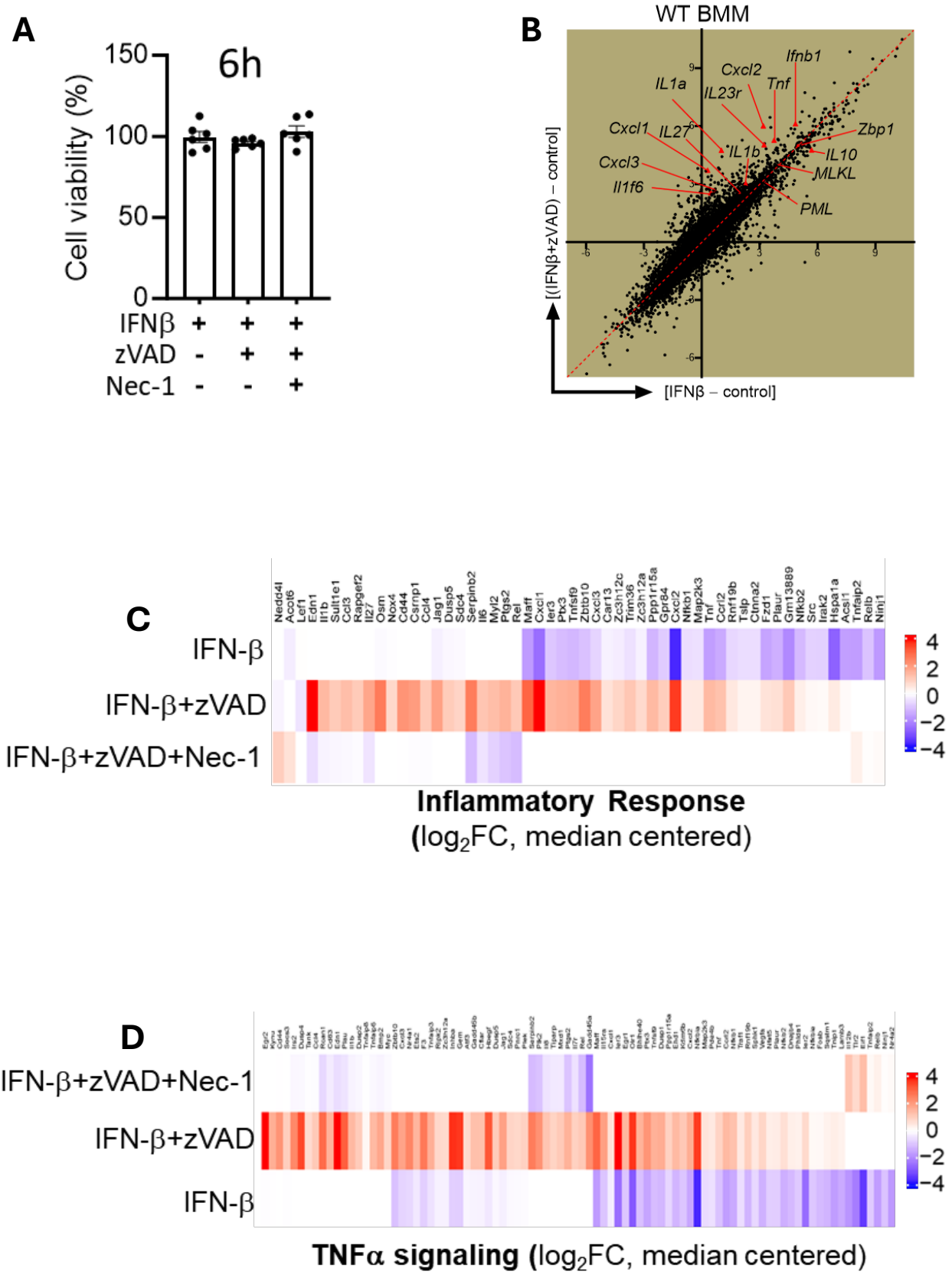
A
6h
Cell viability (%)
150
100
50
0
IFNβ + + +
zVAD - + +
Nec-1 - - +
B
WT BMM
Ifnb1
Cxcl2
IL1a
IL23r
Tnf
Cxcl1
IL27
Zbp1
IL1b
IL10
Cxcl3
MLKL
Il1f6
PML
[(IFNβ+zVAD) – control]
[IFNβ – control]
C
IFN-β
IFN-β+zVAD
IFN-β+zVAD+Nec-1
Inflammatory Response
(log2FC, median centered)
4
2
0
−2
−4
D
IFN-β+zVAD+Nec-1
IFN-β+zVAD
IFN-β
TNFα signaling (log2FC, median centered)
4
2
0
−2
−4

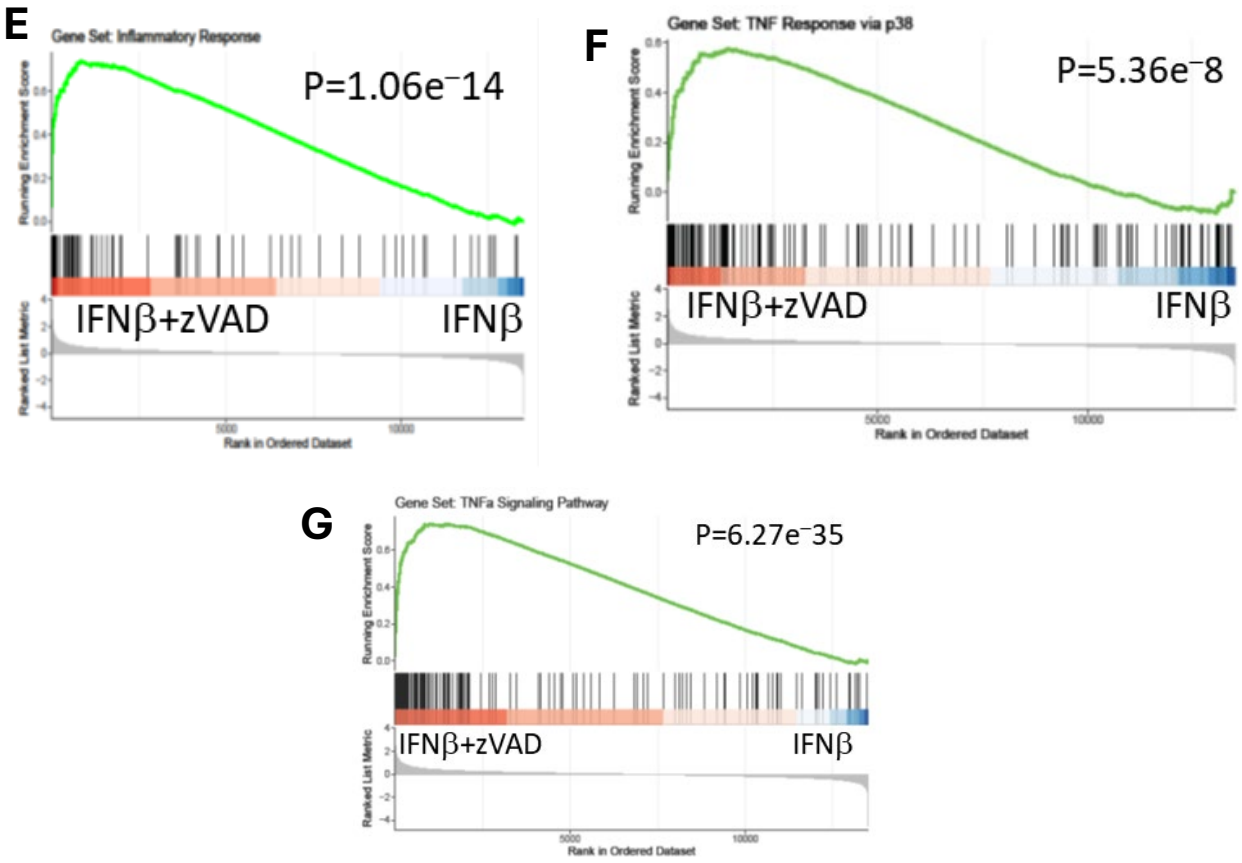
E
Gene Set: Inflammatory Response
P=1.06e⁻14
IFNβ+zVAD
IFNβ
Running Enrichment Score
Ranked List Metric
Rank in Ordered Dataset
F
Gene Set: TNF Response via p38
P=5.36e⁻8
IFNβ+zVAD
IFNβ
G
Gene Set: TNFa Signaling Pathway
P=6.27e⁻35
IFNβ+zVAD
IFNβ

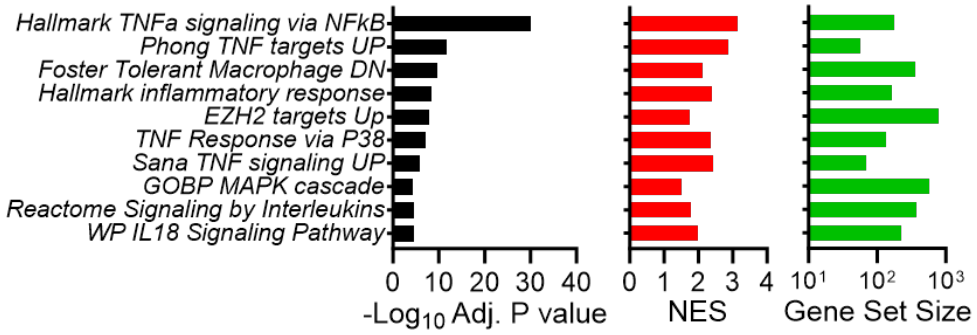
H [(IFNβ+zVAD) – control] relative to [(IFNβ – control)]
Hallmark TNFa signaling via NFkB
Phong TNF targets UP
Foster Tolerant Macrophage DN
Hallmark inflammatory response
EZH2 targets Up
TNF Response via P38
Sana TNF signaling UP
GOBP MAPK cascade
Reactome Signaling by Interleukins
WP IL18 Signaling Pathway
0 10 20 30 40
-Log10 Adj. P value
0 1 2 3 4
NES
10¹ 10² 10³
Gene Set Size

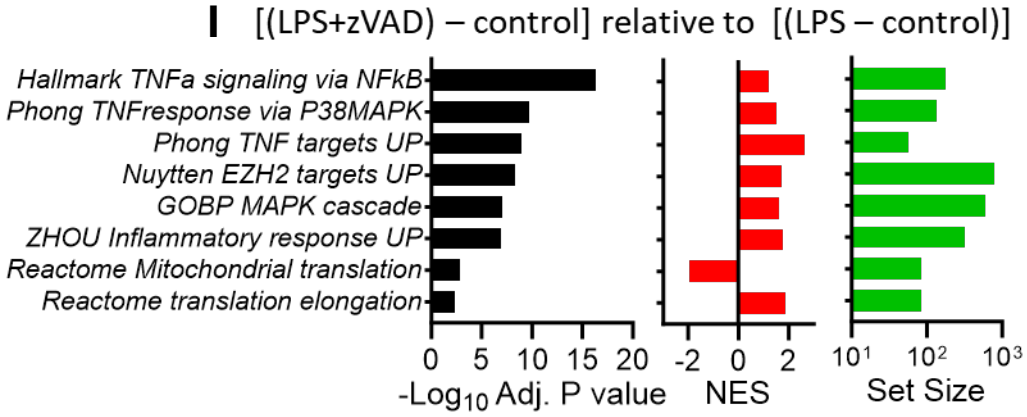
I [(LPS+zVAD) – control] relative to [(LPS – control)]
Hallmark TNFa signaling via NFkB
Phong TNFresponse via P38MAPK
Phong TNF targets UP
Nuytten EZH2 targets UP
GOBP MAPK cascade
ZHOU Inflammatory response UP
Reactome Mitochondrial translation
Reactome translation elongation
0 5 10 15 20
-Log10 Adj. P value
-2 0 2
NES
10¹ 10² 10³
Set Size

Figure 27. Necroptosis stimulation induces an inflammatory storm

A-H WT BMDMs were treated with IFNβ (100 U/mL), zVAD-fmk (50μM), and Nec-1 (10μM). Cell death was evaluated at 6 h by MTT (**A**). At 6h, differential gene expression, and GSEA were performed on microarray data comparing WT BMDMs treated with IFNβ, IFNβ+zVAD, and IFNβ+zVAD+Nec1 (**B-H**). **I** Differential gene expression and GSEA were performed in BMDMs stimulated with LPS (1 ng/mL), and zVAD-fmk (50μM). Graphs depict mean ± SEM.

As discussed previously in Aim 1, caspase inhibitor EMR promotes necroptosis at reduced concentrations due to its increased specificity towards caspase-8; therefore, we treated cells with LPS and EMR and measured the impact on cytokine expression and cell death. Treatment of cells with LPS+zVAD or LPS+EMR resulted in similar secretion of TNFα in cell supernatants (at 6h) and cell death (24h) (**Figure 28 A**). In correlation with increased transcription, the levels of secreted TNFα and IFNβ were increased in cells during necroptosis stimulation LPS+EMR (**Figure 28 B, C**). Necroptosis stimulation did not result in an upregulation of all cytokines since there was no impact on the expression of the anti-inflammatory cytokine IL-10 (**Figure 28 D**). On the contrary, the expression of IL-12p70 (**Figure 28 E**) and IL-6 (**Figure 28 F**) was significantly suppressed during necroptosis stimulation. These results indicate that while there is a global augmentation of the inflammatory response during necroptosis stimulation (**Figure 27 G**), the expression of some cytokines is selectively downregulated.

Nec-1 inhibited necroptosis induced by LPS, IFNβ, or TNFα. In contrast, IFNβ, treatment of cells with IFNγ did not induce necroptosis, implying the involvement of ISGF3 in necroptosis signaling (**Figure 28 G**). Interestingly, treatment of cells with Nec-1 during necroptosis stimulation resulted in a significant reduction in the levels of secreted TNFα (**Figure 28 H**), indicating that the activation of RipK1 is responsible for the augmentation of inflammatory responses. Western blotting of cell extracts at various time intervals post-necroptosis stimulation revealed that Nec-1 inhibited the phosphorylation of RipK1 and its downstream targets RipK3 and MLKL as expected (**Figure 28 I**). Since the S321 phosphorylation of RipK1 has been reported to be mediated by the MAPK-activated protein kinase 2 (MAPKAPK2, or MK2) (Jaco et al., 2017; Menon et al., 2017), and that MK2 promotes the stability of TNFα mRNA (Kotlyarov et al., 1999; Neininger et al., 2002), we tested the impact of Nec-1 on the activation (phosphorylation) of MK2. Our results indicate that Nec-1 also inhibited the activation of MK2 (**Figure 28 I**). In addition to the activation by p38MAPK (Winzen et al., 1999), MK2 has also been shown to be activated by ERK1/2 (Miguel et al., 2005; Stokoe et al., 1992). Our results indicate that the activation of ERK1/2 was also noticeably inhibited by Nec-1 during necrosome activation (**Figure 28 I**).

Overall, these results indicate that the RipK1-dependent $p38^{MAPK}$ pathway promotes inflammation during necrosome activation.

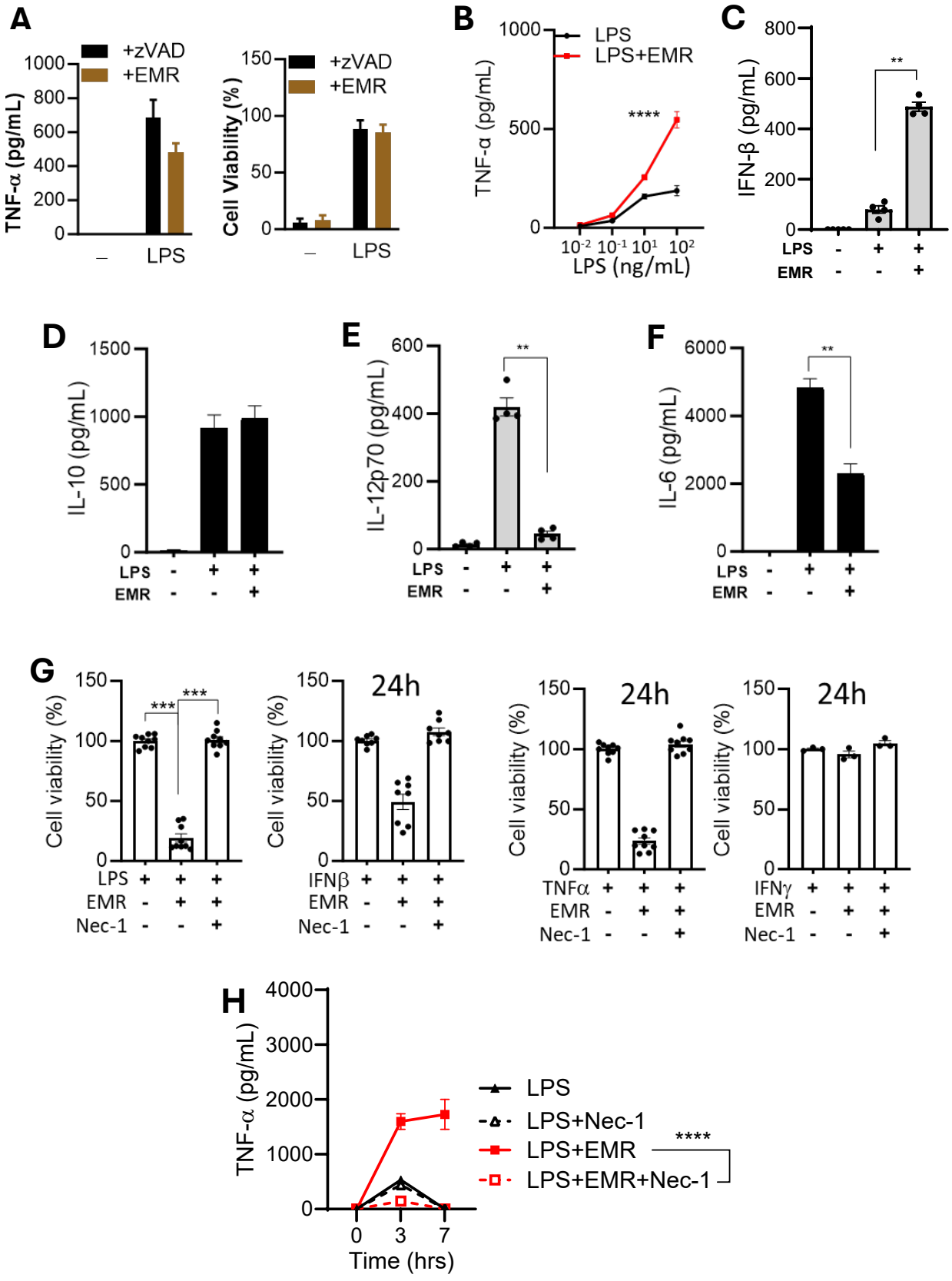
A
+zVAD
+EMR
TNF-α (pg/mL)
1000
800
600
400
200
0
–
LPS
Cell Viability (%)
150
100
50
0
B
LPS
LPS+EMR
TNF-α (pg/mL)
1000
500
0
****
10-2 10-1 101 102
LPS (ng/mL)
C
IFN-β (pg/mL)
800
600
400
200
0
**
LPS - + +
EMR - - +
D
IL-10 (pg/mL)
1500
1000
500
0
LPS - + +
EMR - - +
E
IL-12p70 (pg/mL)
600
400
200
0
**
LPS - + +
EMR - - +
F
IL-6 (pg/mL)
6000
4000
2000
0
**
LPS - + +
EMR - - +
G
Cell viability (%)
150
100
50
0
***
***
LPS + + +
EMR - + +
Nec-1 - - +
24h
IFNβ + + +
EMR - + +
Nec-1 - - +
TNFα + + +
EMR - + +
Nec-1 - - +
IFNγ + + +
EMR - + +
Nec-1 - - +
H
TNF-α (pg/mL)
4000
3000
2000
1000
0
0 3 7
Time (hrs)
LPS
LPS+Nec-1
LPS+EMR
LPS+EMR+Nec-1
****

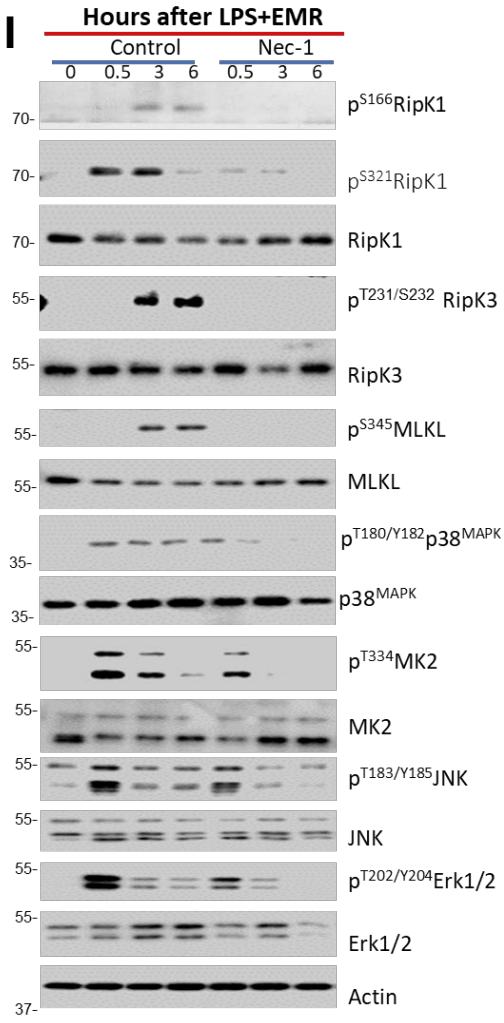

Figure 28. RipK1-dependent p38^{MAPK} pathway promotes inflammation during necrosome activation

A) Expression levels of TNFα were measured by ELISA in the supernatants collected at 6h post-stimulation of WT BMDMs with LPS (1ng/mL) + zVAD (50μM) or LPS (1ng/mL) + EMR (10μM). Cell death was measured by MTT assay at 24h post-stimulation. **B** Expression levels of TNFα were measured in the supernatants collected at 7h after treating the WT BMDMs with EMR (10μM) and different LPS concentrations. **C-F** Expression levels of IFNβ (**C**), IL-10 (**D**), IL-12p70 (**E**), and IL-6 **(F)** were measured in the supernatants collected at 7h after treating the WT BMDMs with LPS (1ng/mL) and EMR (10μM) at 7 h. **G** WT BMDMs were treated with LPS (1ng/mL), IFNβ (100U/mL), TNFα (50 ng/mL), IFN-γ (50 ng/mL), and EMR (10μM), and Nec1-s (10μM). Cell viability was evaluated by the MTT assay at 24 h post-stimulation. **H, I** WT BMDMs were stimulated with LPS (1ng/mL), EMR (10μM), and Nec1-s (10 μM). Secretion of TNFα was measured in supernatants collected at 7h (**H**), and the activation of various proteins was evaluated by performing western blotting of cell extracts collected at various time intervals (**I**). Graphs depict mean ± SEM. Each experiment was repeated at least three times. (**P< 0.01, ***P< 0.001, ****P< 0.0001).

4.2.2. ISGF3 restricts TNFα expression during necroptosis stimulation

Type I interferon has been shown to be a key driver of the cytokine storm during viral infections (F. McNab et al., 2015), and we have previously reported that *Ifnar1*$^{-/-}$ macrophages are significantly resistant to necroptosis (McComb et al., 2014). We, therefore, evaluated the impact of the TLR-adaptor proteins, MyD88 and TRIF, and the transcription factors downstream of IFNAR1 that might impact TNFα expression during necroptosis stimulation. *Trif*-deficient (*Ticam1*$^{-/-}$) BMDMs were highly resistant to necroptosis in response to TLR4 engagement, and this was bolstered further in macrophage deficient in both *MyD88* and *Ticam1* (**Figure 29 A-D**). In WT BMDMs, TNFα expression was detectable at 6h, which was strongly reduced at 24h (**Figure 29 A**). Since TNFα mRNA is highly susceptible to degradation at later time intervals (Kotlyarov et al., 1999; Tiedje et al., 2016), it is possible that the reduction of TNFα levels at 24h may be related to RNA decay. In *MyD88*$^{-/-}$ macrophages, TNFα expression was undetectable, indicating that MyD88 is indispensable for the transcription of TNFα during necroptosis stimulation (**Figure 29 B**). On the other hand, *Ticam1*$^{-/-}$ BMDMs displayed an augmentation in the expression of TNFα at 24h post-stimulation in comparison to WT or *MyD88*$^{-/-}$ macrophages, implying that TRIF-signaling may promote the degradation of TNFα (**Figure 29 C**). The upregulation of TNFα in *Ticam1*$^{-/-}$ BMDMs was abrogated by concomitant deletion of *MyD88* (**Figure 29 D**). In contrast to TNFα, the expression of type I interferon was promoted by TRIF signaling (**Figure 29 A-D**). These results indicate that the two key adaptor proteins, MyD88 and TRIF, that promote TLR4 signaling have opposite impacts on TNFα expression. MyD88 promotes the early expression of TNFα, whereas TRIF possibly compromises the maintenance of TNFα.

In response to LPS stimulation, *Ifnar1*$^{-/-}$ BMDMs displayed only a minor increase in TNFα expression in comparison to WT cells (**Figure 29 E**). On the other hand, necroptotic stimulation (LPS+EMR) of *Ifnar1*$^{-/-}$ BMDMs resulted in a substantial increase in TNFα expression in comparison to WT cells (**Figure 29 E**). *Ifnar1*$^{-/-}$ or *Ticam1*$^{-/-}$ macrophages displayed a similar augmentation in TNFα expression in contrast to WT cells, which was abrogated by treatment of cells with Nec-1 (**Figure 29 F**). Deficiency of the necrosome interacting protein RipK3 had no impact on TNFα expression (**Figure 29 F**). IFNAR1 signaling results in the phosphorylation-driven assembly of STAT1, STAT2, and IRF9, collectively called ISGF3, which promotes the transcription of genes that harbor an ISRE element in the promoter (K. Fink & Grandvaux, 2013;

Kessler et al., 1990). Our results indicate that *Stat1*$^{-/-}$, *Stat2*$^{-/-}$, or *Irf9*$^{-/-}$macrophages express increased levels of TNFα during necroptosis stimulation in comparison to WT macrophages (**Figure 29 G**). Interestingly, IFN-γ, which induces cell signaling by promoting the binding of STAT1 to the promoters of genes that harbor a GAS element (K. Fink & Grandvaux, 2013), did not impact the expression of TNFα (**Figure 29 G**). These results indicate that the IFNAR1-induced ISGF3 signaling is responsible for the reduction of TNFα levels during necroptosis stimulation.

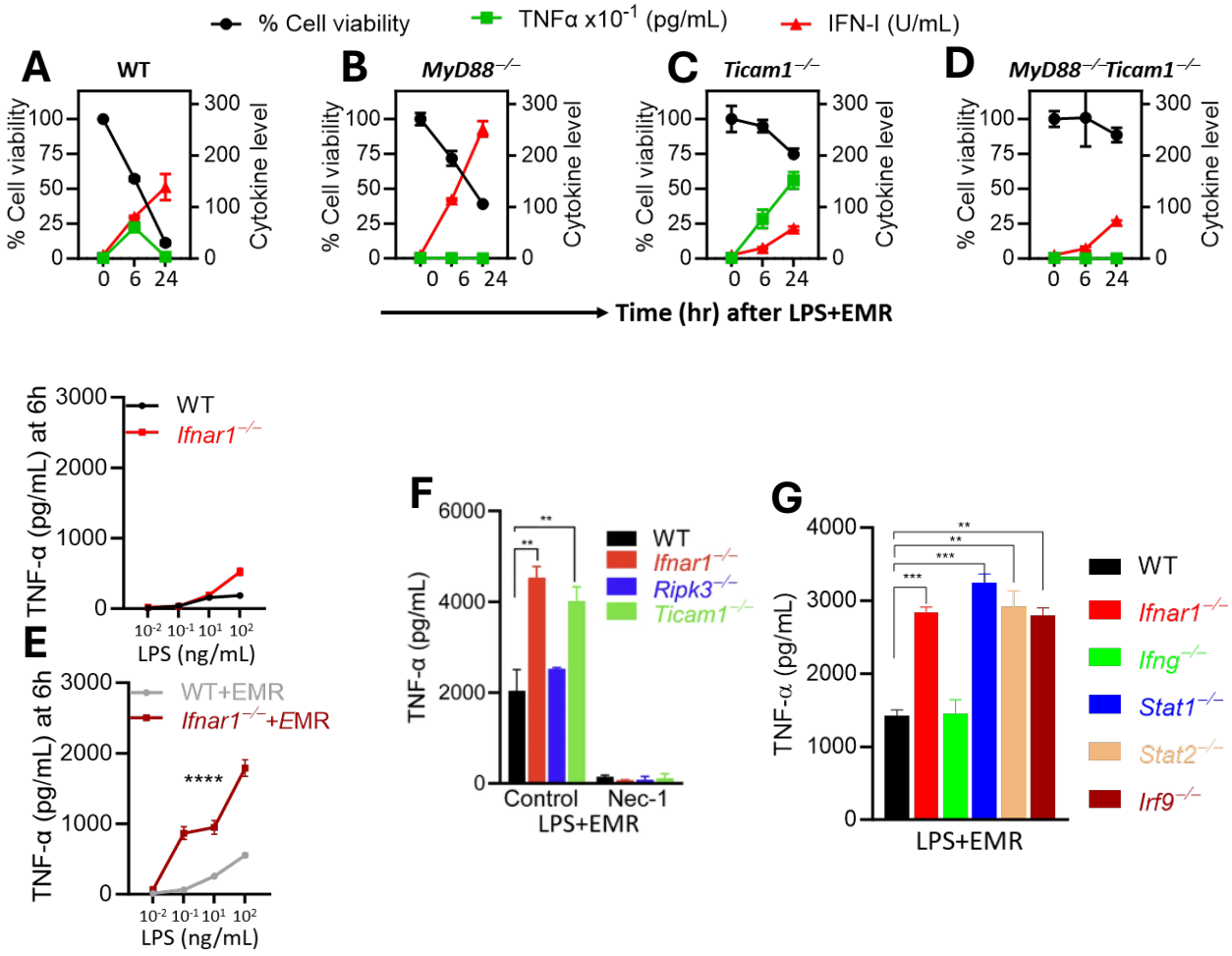

Figure 29. ISGF3 restricts TNFα expression during necroptosis stimulation

A-D WT, *MyD88*$^{-/-}$, *Ticam1*$^{-/-}$ and *Myd88*$^{-/-}$*Ticam1*$^{-/-}$ BMDMs were treated with LPS (1ng/mL) and EMR (10μM). At various time intervals, cell death was measured by MTT, and expression of TNFα and IFN-1 was measured in the supernatants by ELISA and bioassay respectively. **(E)** TNFα levels were measured in the supernatants of WT and *Ifnar1*$^{-/-}$ BMDMs at 7h following treatment with different concentrations of LPS and EMR (10μM). **F, G** TNFα levels were measured in the supernatants of BMDMs of various genotypes at 7h following treatment with LPS (1ng/mL), EMR (10μM), and Nec-1 (10μM). Graphs depict mean ± SEM. Each experiment was repeated at least three times. (**P< 0.01, ***P< 0.001, ****P< 0.0001).

In contrast to the inhibitory effect of ISGF3 on TNFα expression, ISGF3 demonstrated a promoting influence on the expression of IL-10 **(Figure 30 A and B)**. This differential regulation highlights the complex role of ISGF3 in modulating cytokine production during necroptosis signaling.

Both *Ifnar1*$^{-/-}$ and *Ticam1*$^{-/-}$ macrophages displayed a similar reduction in necroptosis following LPS+EMR stimulation when compared to WT cells. However, *RipK3*$^{-/-}$ macrophages demonstrated complete resistance to necroptosis under the same conditions **(Figure 30 C)**. Notably, *Ifnar1*$^{-/-}$ macrophages, but not *Ticam1*$^{-/-}$ macrophages, exhibited a significant reduction in necroptosis when stimulated with TNFα+EMR or IFNβ+EMR **(Figure 30 C)**. This finding suggests that IFNAR1 plays a crucial role in sensitizing cells to necroptosis induced by these specific stimuli. Macrophages deficient in the ISGF3 members (*Stat1, Stat2*, or *Irf9*) displayed enhanced resistance to necroptosis induced by both LPS+EMR and TNFα+EMR stimulation **(Figure 30 D)**. This observation indicates that the intact ISGF3 complex is necessary for full necroptotic sensitivity in macrophages under these conditions.

Collectively, these results indicate that ISGF3 signaling plays a multifaceted role in macrophage biology. It promotes necroptosis and enhances the expression of the anti-inflammatory cytokine IL-10, while simultaneously restricting the expression of the pro-inflammatory cytokine TNFα in macrophages. These findings highlight the intricate balance maintained by ISGF3 in regulating both cell death and inflammatory responses in the innate immune system.

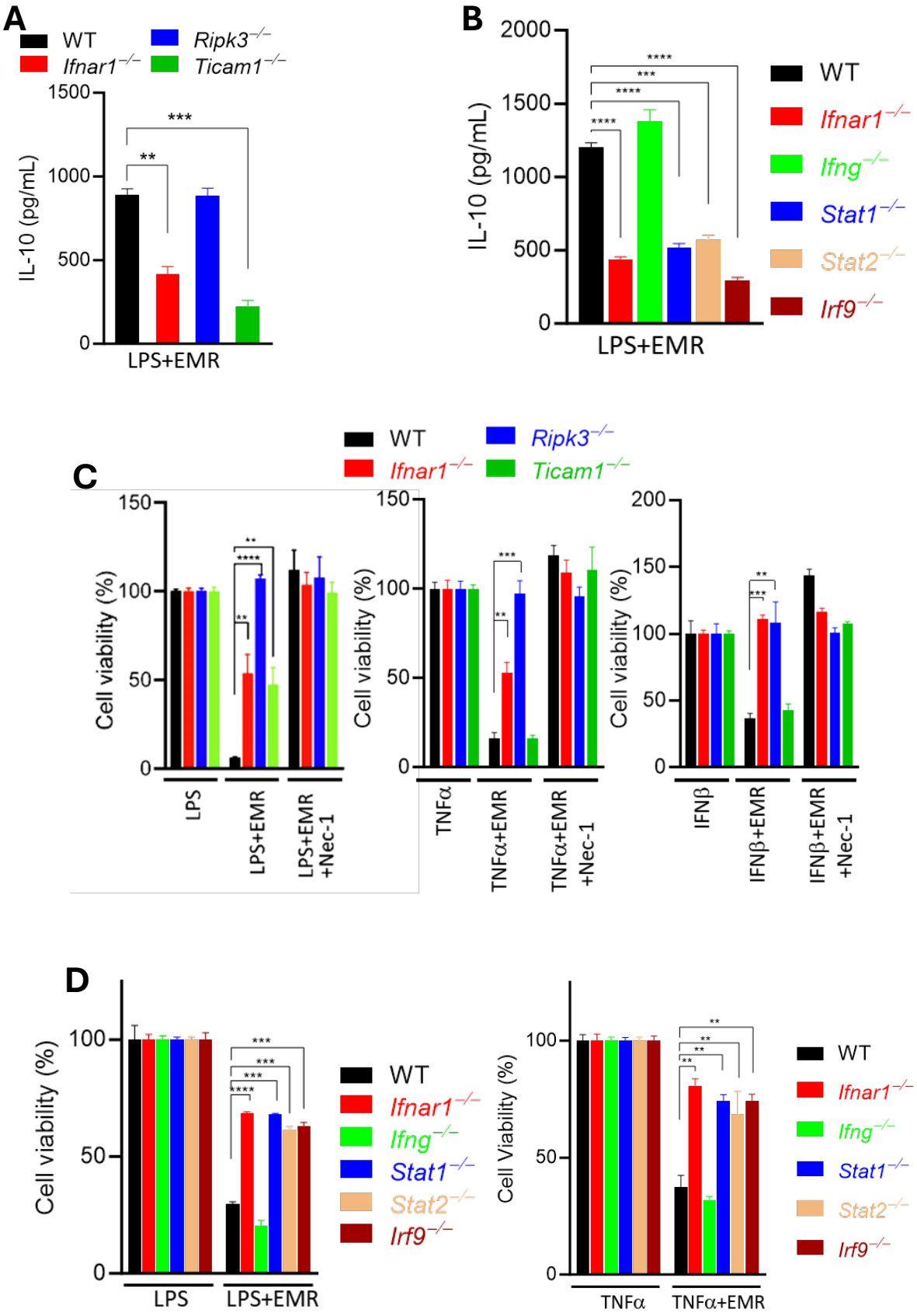
A
WT
Ifnar1−/−
Ripk3−/−
Ticam1−/−
IL-10 (pg/mL)
1500
1000
500
0
**
***
LPS+EMR
B
2000
1500
1000
500
0
IL-10 (pg/mL)
****
***
****
****
LPS+EMR
WT
Ifnar1−/−
Ifng−/−
Stat1−/−
Stat2−/−
Irf9−/−
C
WT
Ifnar1−/−
Ripk3−/−
Ticam1−/−
Cell viability (%)
150
100
50
0
LPS
LPS+EMR
LPS+EMR +Nec-1
TNFα
TNFα+EMR
TNFα+EMR +Nec-1
200
IFNβ
IFNβ+EMR
IFNβ+EMR +Nec-1
D
Cell viability (%)
100
50
0
LPS
LPS+EMR
WT
Ifnar1−/−
Ifng−/−
Stat1−/−
Stat2−/−
Irf9−/−
Cell Viability (%)
TNFα
TNFα+EMR

Figure 30. ISGF3 promotes necroptosis and IL-10 expression

A-B BMDMs of various genotypes were treated with LPS (1ng/mL) and EMR (10μM). Expression of IL-10 was measured in cell supernatants collected at 7 h post activation. **C** BMDMs of various genotypes were treated with LPS (1ng/mL), TNFα (50ng/ml), IFNβ (100U/mL), EMR (10μM), and Nec-1 (10μM). Cell death was measured by MTT assay at 24 h. **D** BMDMs of various genotypes were treated with LPS (1ng/mL), TNFα (50ng/ml), EMR (10μM), and Nec-1 (10μM). Cell death was measured by MTT assay at 24 h. Graphs depict mean ± SEM. Each experiment was repeated at least three times. (**P< 0.01, ***P< 0.001, ****P< 0.0001).

4.2.3. Modulation of the inflammatory response by IFNAR1- signaling during necroptosis stimulation

Analysis of the transcriptomic data unveiled a complex transcriptional landscape during necrosome activation of *Ifnar1*$^{-/-}$ macrophages, revealing the upregulation of various inflammatory genes **(Figure 31 A)**. As anticipated, gene set enrichment analysis demonstrated a significant downregulation of both type I and type II interferon responses in *Ifnar1*$^{-/-}$ macrophages when compared to their WT counterparts **(Figure 31 B)**. Intriguingly, WT cells exhibited a notable enrichment in the upregulation of the mRNA editing pathway relative to *Ifnar1*$^{-/-}$ cells, suggesting a potential role for interferon signaling in modulating RNA processing. In stark contrast, several other pathways showed enrichment in *Ifnar1*$^{-/-}$ macrophages compared to WT cells, including those related to reactive oxygen species (ROS) detoxification, RNA modification, cholesterol biosynthesis, and protein translation. These findings hint at potential compensatory mechanisms or altered cellular priorities in the absence of interferon signaling.

Further analysis revealed that a significant number of genes involved in inflammatory and MAPK pathways were differentially regulated by type I interferon signaling, underscoring the broad impact of this signaling cascade on cellular function **(Figure 31 C-E)**. To delve deeper into the functional consequences of these transcriptional changes, we conducted a kinetic evaluation of cytokine expression in WT versus *Ifnar1*$^{-/-}$ BMDMs under necroptosis stimulation. The results painted a nuanced picture of cytokine dynamics. At the 1-hour post-stimulation mark, TNFα secretion was diminished when cells were treated with LPS+EMR compared to LPS alone. However, this pattern reversed at later time intervals, revealing the temporal complexity of the cellular response **(Figure 31 F)**. Notably, while necroptosis stimulation with LPS+EMR led to increased TNFα expression in WT BMDMs at later time points, this effect was even more pronounced in *Ifnar1*$^{-/-}$ BMDMs, suggesting a potential regulatory role for interferon signaling in tempering the TNFα response.

The expression profile of IFNβ also showed interesting dynamics, with increased levels observed during necroptosis stimulation. However, WT cells consistently produced higher levels of IFNβ compared to *Ifnar1*$^{-/-}$ BMDMs, likely due to the absence of the feed-forward IFNAR1-signaling loop in the knockout cells. This observation highlights the importance of intact interferon signaling

for robust IFNβ production. Interestingly, the expression pattern of IL-6 diverged from that of TNFα and IFNβ, showing a slight reduction in both WT and *Ifnar1*$^{-/-}$ BMDMs under necroptosis stimulation **(Figure 31 F)**. This differential regulation of cytokines underscores the complexity of the inflammatory response and suggests that interferon signaling may have distinct modulatory effects on different cytokines during necroptosis.

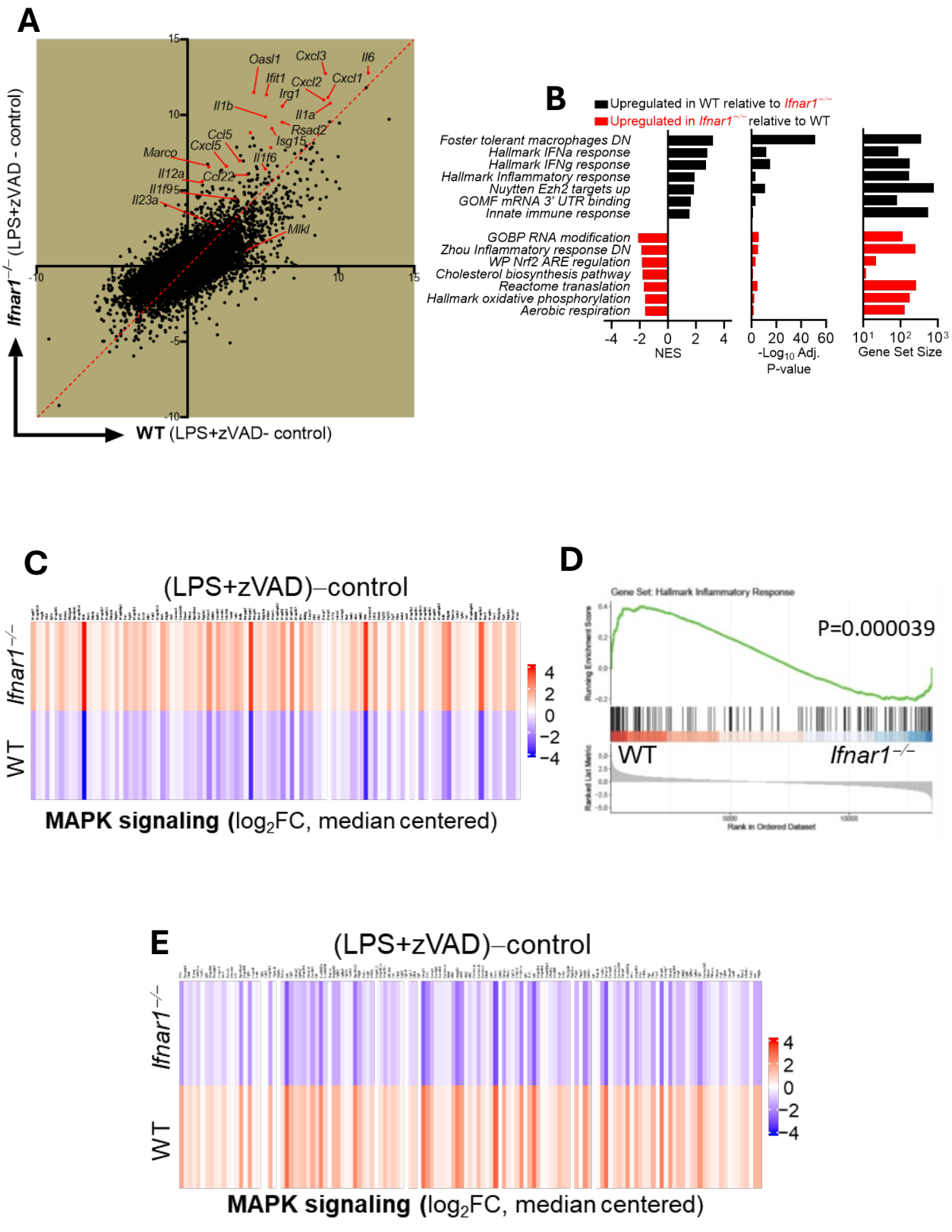
A
Ifnar1−/− (LPS+zVAD - control)
WT (LPS+zVAD- control)
Oasl1
Cxcl3
Il6
Ifit1
Cxcl2
Cxcl1
Irg1
Il1b
Il1a
Rsad2
Ccl5
Isg15
Cxcl5
Marco
Il1f6
Il12a
Ccl22
Il1f9
Il23a
Mlkl
B
Upregulated in WT relative to Ifnar1−/−
Upregulated in Ifnar1−/− relative to WT
Foster tolerant macrophages DN
Hallmark IFNa response
Hallmark IFNg response
Hallmark Inflammatory response
Nuytten Ezh2 targets up
GOMF mRNA 3' UTR binding
Innate immune response
GOBP RNA modification
Zhou Inflammatory response DN
WP Nrf2 ARE regulation
Cholesterol biosynthesis pathway
Reactome tranaslation
Hallmark oxidative phosphorylation
Aerobic respiration
NES
-Log10 Adj. P-value
Gene Set Size
C
(LPS+zVAD)−control
Ifnar1−/−
WT
MAPK signaling (log2FC, median centered)
D
Gene Set: Hallmark Inflammatory Response
P=0.000039
WT
Ifnar1−/−
Running Enrichment Score
Ranked List Metric
Rank in Ordered Dataset
E
(LPS+zVAD)−control
Ifnar1−/−
WT
MAPK signaling (log2FC, median centered)

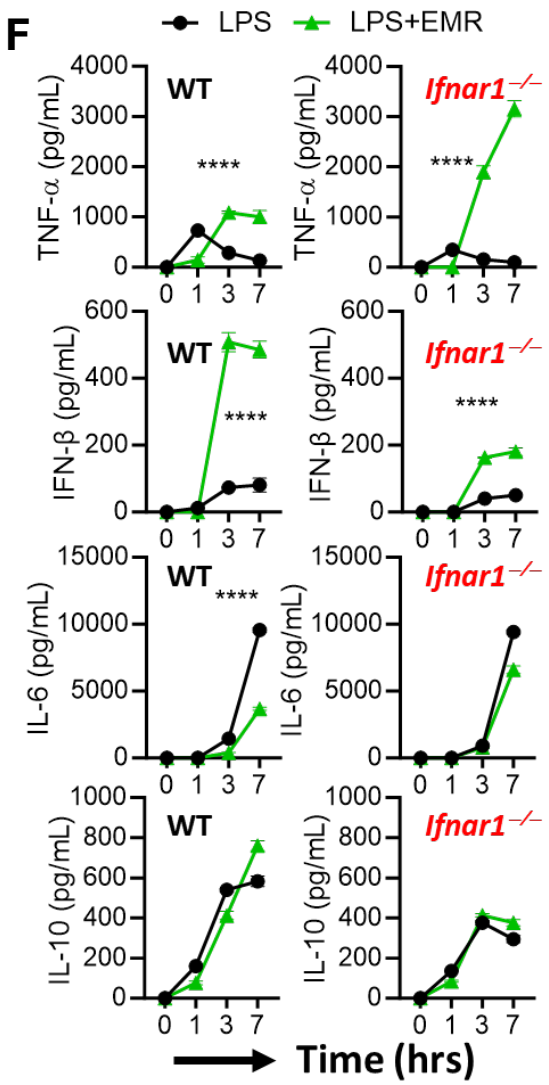

Figure 31. Modulation of the inflammatory response by IFNAR1 signaling during necroptosis stimulation

A-E WT and *Ifnar1*$^{-/-}$ BMDMs were treated with LPS (1ng/mL) in the presence of zVAD-fmk (50μM) for 6 h and differential gene expression and GSEA were performed on microarray data comparing WT BMDMs treated with LPS+zVAD with *Ifnar1*$^{-/-}$ BMDMs treated with LPS+zVAD. **(E)** Expression levels of TNFα, IFNβ, IL-6, and IL-10 were measured in the supernatants collected after treating WT and *Ifnar1*$^{-/-}$ BMDMs for 7 h with LPS (1ng/mL) and EMR (10μM). Graphs depict mean ± SEM. Experiment E was repeated at least three times. (****P< 0.0001).

Treatment of cells with Nec-1 at the time of LPS+EMR addition resulted in a reduction of TNFα levels in both WT and *Ifnar1*$^{-/-}$macrophages (**Figure 32 A**). Interestingly, *Ifnar1*$^{-/-}$BMDMs were resistant to Nec-1 when added at 1.5h post-LPS+EMR treatment in comparison to WT cells, which remained responsive to the inhibitory effect of Nec-1 (**Figure 32 A**). These results reveal significant differences in the role of RipK1 in promoting the kinetics of cytokine expression by WT versus *Ifnar1*$^{-/-}$macrophages.

Western blotting of cell extracts demonstrated that the activation of RipK3 and MLKL was highly reduced in *Ifnar1*$^{-/-}$ BMDMs, while the activation of RipK1 proceeded normally during necroptosis stimulation in *Ifnar1*$^{-/-}$ BMDMs (**Figure 32 B**). In cells treated with LPS without EMR, there was no activation of RipK1, RipK3, or MLKL (**Figure 32 C**). Thus, the increased expression of TNFα by *Ifnar1*$^{-/-}$ BMDMs does not appear to be mediated by the phosphorylation of RipK3 or MLKL. Various receptor-ligand interactions result in the amplification of metabolism which can promote cytokine expression (O'Neill et al., 2016; D. Wu et al., 2016). This is initiated by the activation of the PI3K-AKT pathway, which promotes cell survival and proliferation through the activation of various downstream targets such as mTORC1. The ribosomal protein S6 kinase (S6K) and 4E-BP1 are the two direct targets of mTORC1, which are phosphorylated by mTORC1 (Battaglioni et al., 2022). 4E-BP1 inhibits protein translation by binding to the translation initiation factor eIF4E, and phosphorylation of 4E-BP1 by mTORC1 leads to the dissociation of 4E-BP1 from eIF4A and reinitiation of protein translation (Gingras et al., 2001). We performed western blot analysis of cells stimulated with LPS (**Figure 32 D**) or LPS+EMR (**Figure 32 E**) and did not detect any modulation of AKT, S6K, 4E-BP1, or eIF4E by IFNAR1-signaling. These results imply that the upregulation of TNFα expression in *Ifnar1*$^{-/-}$ cells is not related to the modulation of translation or metabolism. One would also expect that an upregulation of metabolism might lead to an increased expression of numerous cytokines, which was not observed.

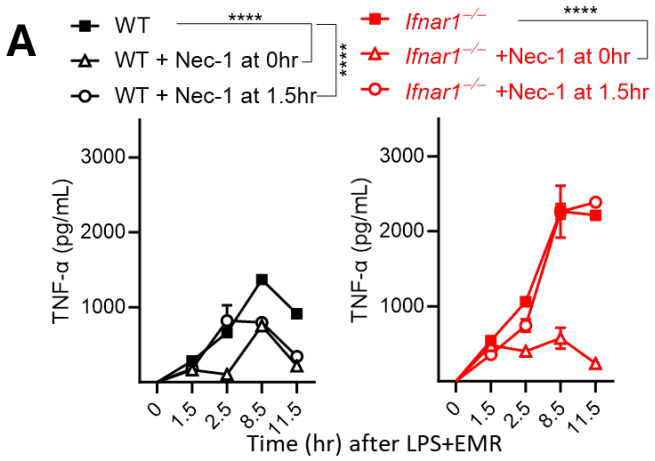
A
WT
WT + Nec-1 at 0hr
WT + Nec-1 at 1.5hr
Ifnar1−/−
Ifnar1−/− +Nec-1 at 0hr
Ifnar1−/− +Nec-1 at 1.5hr
****
****
****
TNF-α (pg/mL)
3000
2000
1000
0
1.5
2.5
8.5
11.5
Time (hr) after LPS+EMR

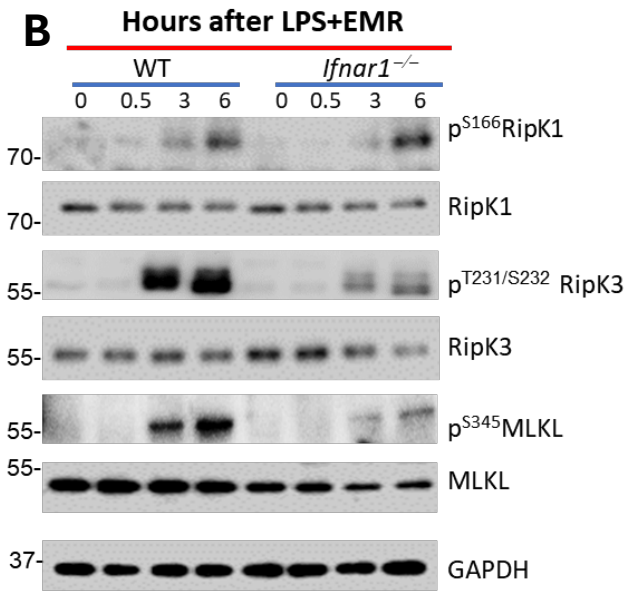
B
Hours after LPS+EMR
WT
Ifnar1−/−
0 0.5 3 6 0 0.5 3 6
70-
pS166RipK1
70-
RipK1
55-
pT231/S232 RipK3
55-
RipK3
55-
pS345MLKL
55-
MLKL
37-
GAPDH

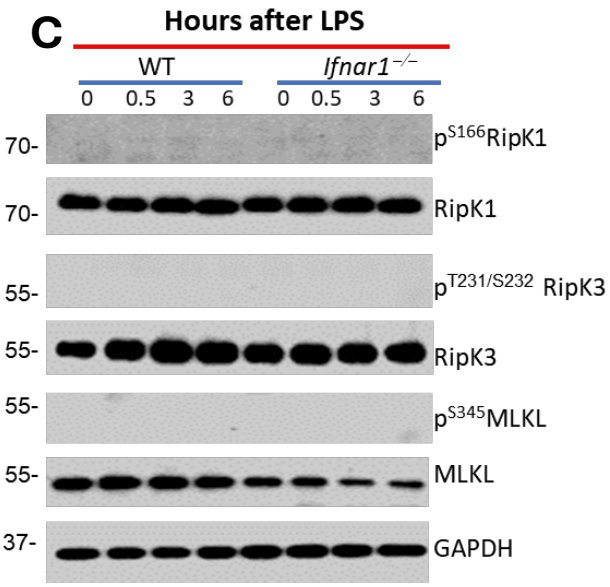
C
Hours after LPS
WT
Ifnar1−/−
0 0.5 3 6 0 0.5 3 6
70-
pS166RipK1
70-
RipK1
55-
pT231/S232 RipK3
55-
RipK3
55-
pS345MLKL
55-
MLKL
37-
GAPDH

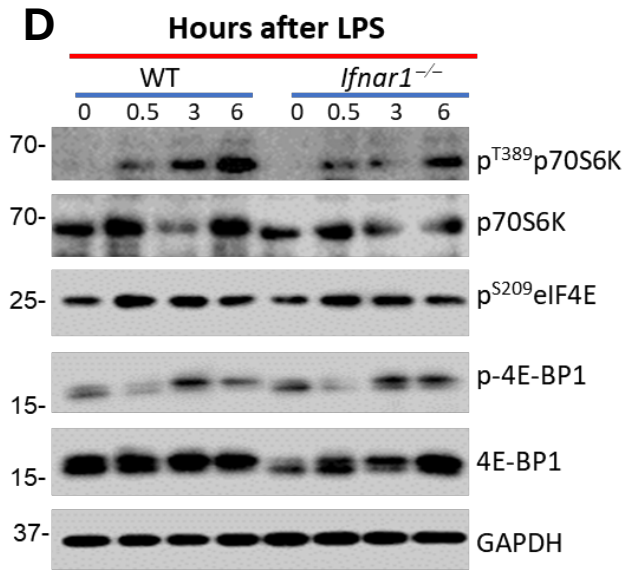
D
Hours after LPS
WT
Ifnar1−/−
0 0.5 3 6 0 0.5 3 6
70-
pT389p70S6K
70-
p70S6K
25-
pS209eIF4E
15-
p-4E-BP1
15-
4E-BP1
37-
GAPDH

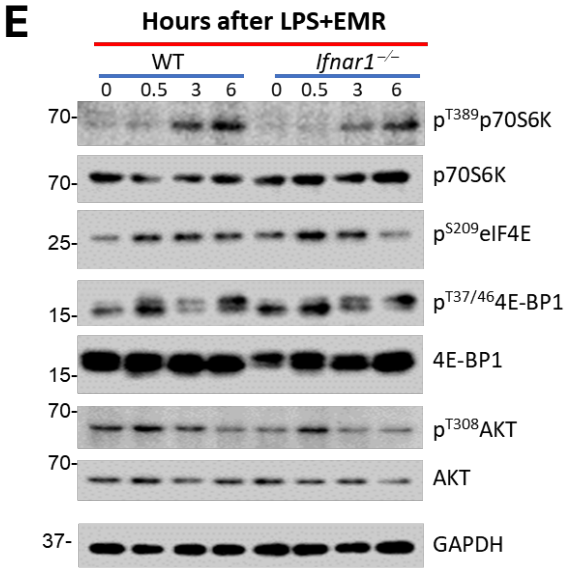
E
Hours after LPS+EMR
WT
Ifnar1−/−
0 0.5 3 6 0 0.5 3 6
70-
pT389p70S6K
70-
p70S6K
25-
pS209eIF4E
15-
pT37/464E-BP1
15-
4E-BP1
70-
pT308AKT
70-
AKT
37-
GAPDH

Figure 32. RipK1 has a differential impact on TNFα expression by WT versus *Ifnar1*$^{-/-}$ cells

A Expression of TNFα in the supernatants was collected at different time intervals following treatment of WT and *Ifnar1*$^{-/-}$ BMDMs with LPS (1ng/mL) and EMR (10μM). Nec1-s (10 μM) was added at the time or at 90 minutes post-treatment with LPS+EMR. Western blot analysis was performed in cell extracts collected from WT and *Ifnar1*$^{-/-}$ BMDMs at different time intervals following treatment with LPS (1ng/mL) and EMR (10μM) (**B, E)** and **(C, D)** LPS (1ng/mL). Each experiment was repeated at least three times. Graphs depict mean ± SEM. (****P< 0.0001).

4.2.4. Induction of Zfp36 (TTP) by IFNAR1 signaling regulates TNFα expression and necroptosis

The upregulation of inflammatory response during necroptosis signaling and its downregulation by type I interferon signaling and the downregulation of inflammatory gene transcripts led us to investigate the potential mechanisms underlying this phenomenon. GSEA of microarray results revealed an enrichment of mRNA destabilizing pathway (3'UTR binding) in WT cells compared to *Ifnar1*$^{-/-}$ cells **(Figure 31 B)**. Among the genes identified, Zfp36 emerged as a particularly intriguing candidate due to its well-established role in mRNA destabilization. Zfp36 encodes for Tristetraprolin (TTP), a protein that specifically targets mRNA transcripts containing AU-rich elements (AREs) in their 3' untranslated regions (3'UTRs). TTP facilitates the removal of poly(A) tails from these transcripts, ultimately leading to their degradation and the cessation of protein expression (Tiedje et al., 2016).

Our interest in TTP was further piqued by the observation that TNFα expression was significantly amplified in *Ifnar1*$^{-/-}$ macrophages during the later stages of necroptosis stimulation **(Figure 31 F)**. This finding led us to hypothesize that type I interferon signaling might promote the degradation of transcripts containing AREs. Notably, the mRNAs of various pro-inflammatory cytokines and chemokines, including *Tnfα*, *Il1b*, *Il6*, *Ifnβ*, *Il10*, and *Cxcl1*, harbor AREs in their 3'UTRs, making them potential targets for this regulatory mechanism.

To further investigate this hypothesis, we conducted a comprehensive bioinformatics analysis of a previously published ChIP-Seq dataset (GSE115435) from macrophages treated with IFNβ, available in the NCBI Sequence Read Archive (Platanitis et al., 2019). Our analysis revealed that IFNβ treatment induces the binding of ISGF3 members, namely STAT1, STAT2, and IRF9, to the ISRE site upstream of the *Zfp36* promoter **(Figure 33 A)**. This finding suggests that between type I interferon signaling promote the expression of and *Zfp36*.

To validate these bioinformatic predictions, we performed a series of in vitro experiments. Our results demonstrated a substantial reduction in *Zfp36* mRNA expression in *Ifnar1*$^{-/-}$ cells during necroptosis stimulation **(Figure 33 B, C)**. This observation was consistent across multiple time points and experimental replicates, highlighting the robustness of this regulatory relationship.

Furthermore, we examined the protein levels of TTP, the gene product of *Zfp36*, by western blot analysis. We observed that TTP expression was reduced during necroptosis stimulation in WT macrophages, and this reduction was even more pronounced in *Ifnar1*$^{-/-}$ macrophages **(Figure 33 D)**. These findings collectively support a model in which type I interferon signaling plays a crucial role in maintaining *Zfp36* expression and, consequently, in regulating the stability of ARE-containing inflammatory transcripts during necroptosis.

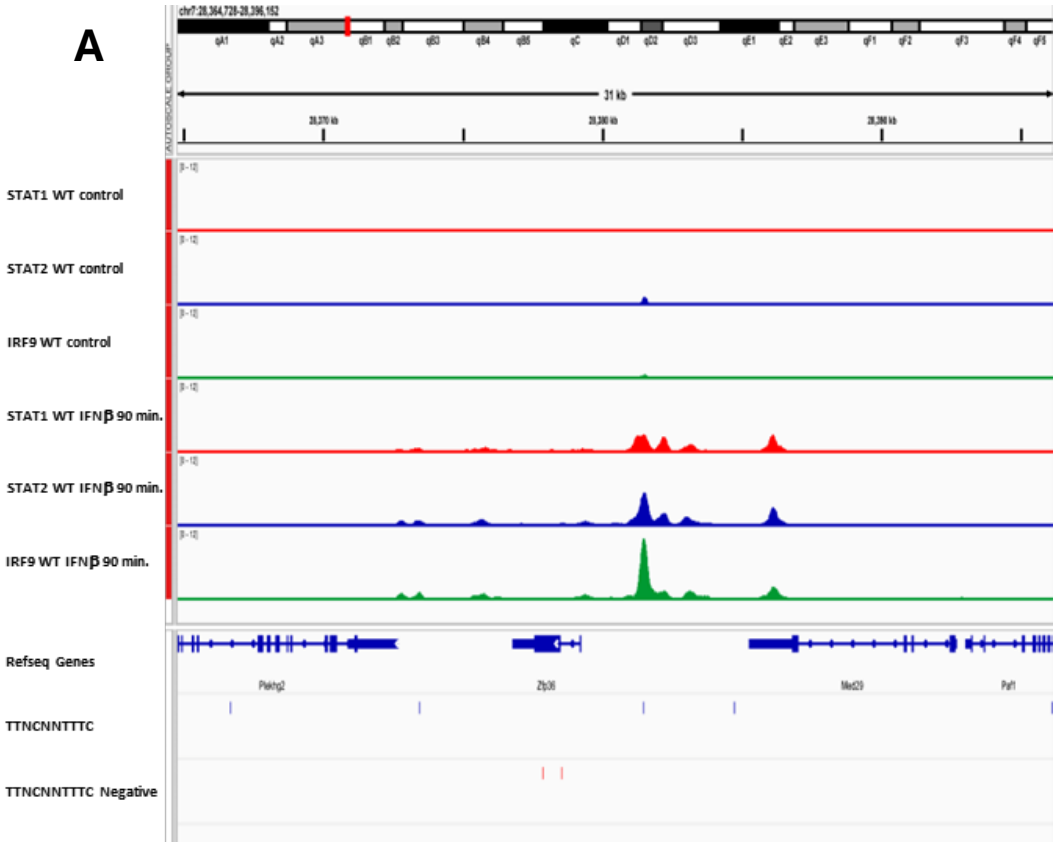
A
STAT1 WT control
STAT2 WT control
IRF9 WT control
STAT1 WT IFNβ 90 min.
STAT2 WT IFNβ 90 min.
IRF9 WT IFNβ 90 min.
Refseq Genes
TTNCNNTTTC
TTNCNNTTTC Negative

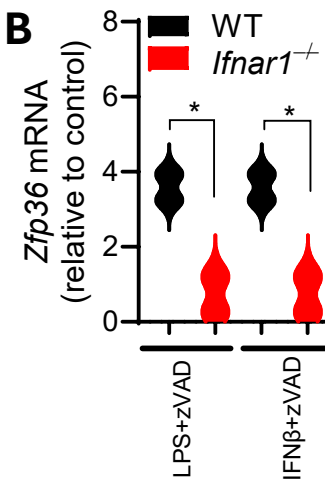
B
WT
Ifnar1−/−
Zfp36 mRNA (relative to control)
LPS+zVAD
IFNβ+zVAD

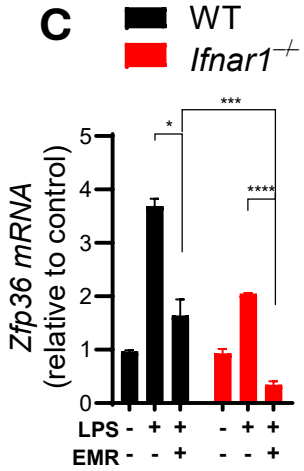
C
WT
Ifnar1−/−
Zfp36 mRNA (relative to control)
LPS
EMR

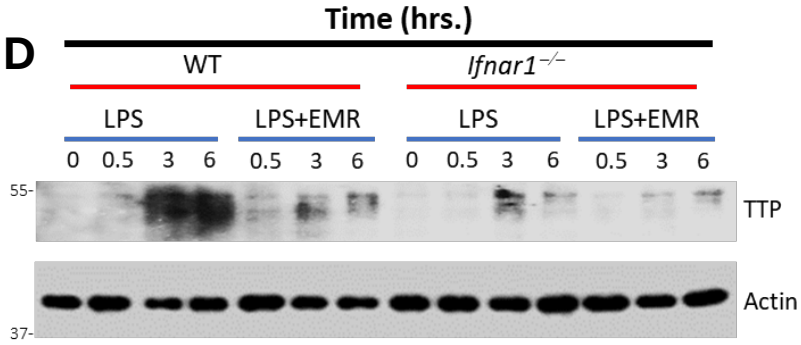
D
Time (hrs.)
WT
Ifnar1−/−
LPS
LPS+EMR
0 0.5 3 6 0.5 3 6 0 0.5 3 6 0.5 3 6
55-
TTP
37-
Actin

Figure 33. ISGF3 promotes Zfp36 transcription

A Genome Browser track was plotted from the ChiP-seq data retrieved from doi.org/10.1038/s41467-019-10970-y. The binding of STAT1 (red), STAT2 (blue), and IRF9 (green) is shown in untreated and IFNβ treated BMDMs at ISRE sites upstream of the *Zfp36* promoter. The integrative genomics viewer track represents a ChIP-seq experiment as described in doi.org/10.1038/s41467-019-10970-y. **B, C** Expression of *Zfp36* mRNA was measured in WT and *Ifnar1*$^{-/-}$ BMDMs by microarray with LPS (1ng/mL) + zVAD-fmk (50μM), and IFNβ (100 U/mL) + zVAD-fmk (50μM) (**B**) or with LPS (1ng/mL) + EMR (10μM) by qRT-PCR (**C**) at 6 h post-treatment. Each experiment was repeated at least three times. **D** Expression of TTP was analyzed by western blotting of cell extracts collected from WT and *Ifnar1*$^{-/-}$ BMDMs at various time intervals following treatment with LPS (1ng/mL) and/or EMR (10μM). Each experiment was repeated at least three times. Graphs depict mean ± SEM. (**P* <0.05, ****P*<0.001, *****P*<0.0001).

Zfp36$^{-/-}$ BMDMs exhibited significantly elevated levels of TNFα expression following stimulation with LPS **(Figure 34 A)** or LPS+EMR **(Figure 34 B)**, indicating that *Zfp36* is a major negative regulator of TNFα expression. The expression of IFNβ was dramatically upregulated, particularly during stimulation with LPS+EMR, and this upregulation was even more pronounced in *Zfp36*$^{-/-}$ macrophages compared to their WT counterparts **(Figure 34 B)**. This suggests a potential role for Zfp36 in regulating IFNβ production under specific stimulatory conditions. Interestingly, stimulation with IFNβ alone failed to induce TNFα expression in either WT or *Zfp36*$^{-/-}$ macrophages **(Figure 34 C)**. However, TNFα expression was notably induced by IFNβ specifically during necroptosis stimulation (i.e., treatment with IFNβ+EMR) in *Zfp36*$^{-/-}$ macrophages, but not in WT cells **(Figure 34 D, E)**. This observation underscores the potential involvement of *Zfp36* in modulating the necroptotic pathway and its associated inflammatory responses. The critical role of necroptosis in this process was further confirmed by the treatment of cells with Nec-1, a specific inhibitor of necroptosis, which effectively abrogated the induction of TNFα expression in *Zfp36*$^{-/-}$ cells **(Figure 34 E)**. Additionally, the expression levels of other important cytokines, namely IL-6 and IL-10, were also significantly upregulated in *Zfp36*$^{-/-}$ macrophages stimulated with IFNβ, regardless of co-treatment with EMR **(Figure 34 E)**. This suggests a broader impact of *Zfp36* deficiency on the overall cytokine profile of macrophages under various stimulatory conditions. A particularly intriguing finding was that *Zfp36*$^{-/-}$ BMDMs underwent increased necroptosis specifically when stimulated with the combination of IFNβ and EMR **(Figure 34 F, G, H)**, further emphasizing the complex interplay between *Zfp36*, cytokine signaling, and cell death pathways in macrophages.

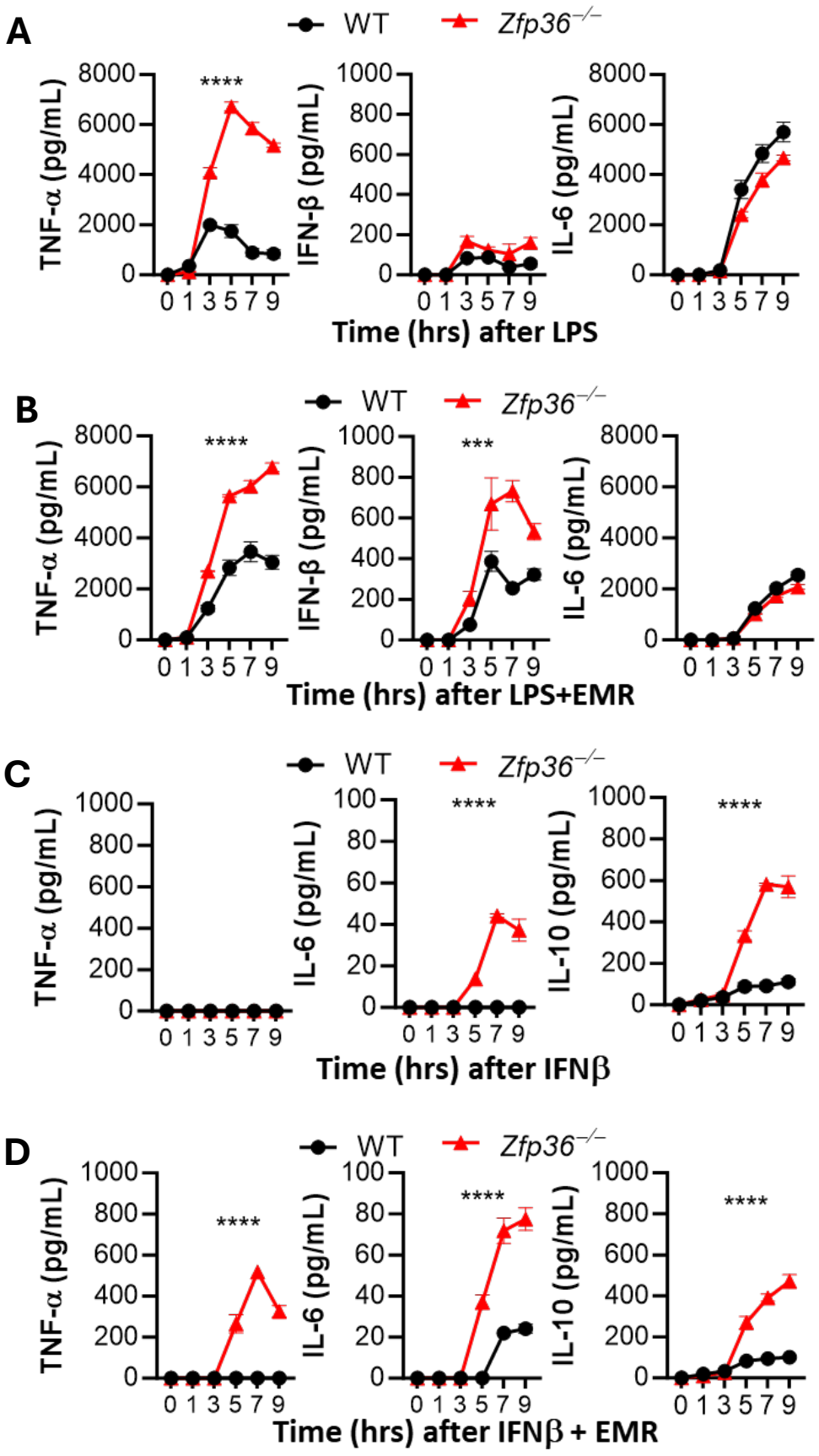
A
WT
Zfp36−/−
TNF-α (pg/mL)
IFN-β (pg/mL)
IL-6 (pg/mL)
****
Time (hrs) after LPS
B
WT
Zfp36−/−
TNF-α (pg/mL)
IFN-β (pg/mL)
IL-6 (pg/mL)
****
***
Time (hrs) after LPS+EMR
C
WT
Zfp36−/−
TNF-α (pg/mL)
IL-6 (pg/mL)
IL-10 (pg/mL)
****
Time (hrs) after IFNβ
D
WT
Zfp36−/−
TNF-α (pg/mL)
IL-6 (pg/mL)
IL-10 (pg/mL)
****
Time (hrs) after IFNβ + EMR

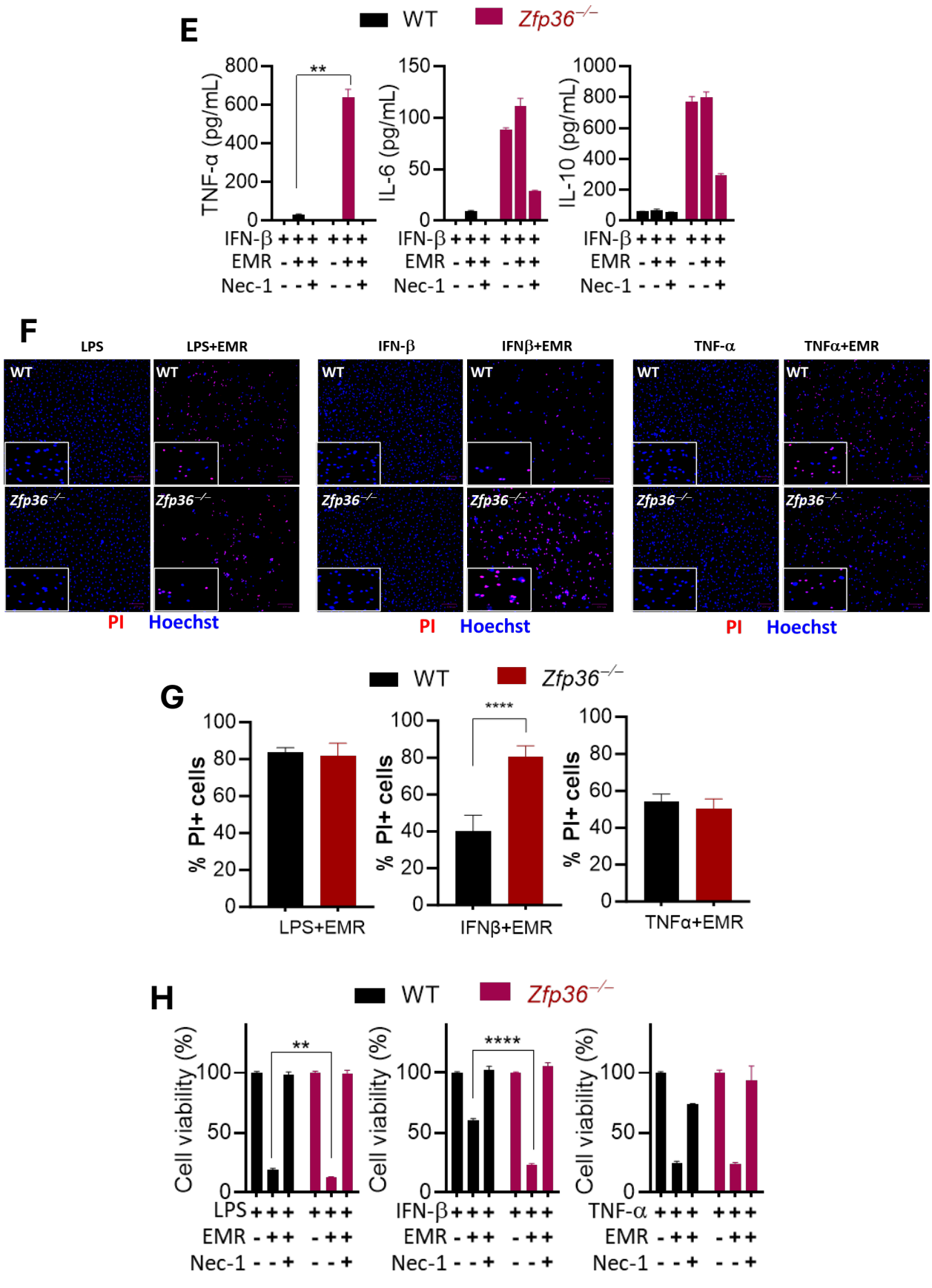
E
WT
Zfp36−/−
TNF-α (pg/mL)
IL-6 (pg/mL)
IL-10 (pg/mL)
**
****
IFN-β
EMR
Nec-1
F
LPS
LPS+EMR
IFN-β
IFNβ+EMR
TNF-α
TNFα+EMR
WT
Zfp36−/−
PI
Hoechst
G
% PI+ cells
LPS+EMR
IFNβ+EMR
TNFα+EMR
H
Cell viability (%)
LPS
IFN-β
TNF-α

Figure 34. Induction of *Zfp36* (TTP) by IFNAR1-signaling regulates TNFα expression and necroptosis

A-D Expression of TNFα, IFNβ, and IL-6 was measured in the supernatants collected at different time intervals after the treatment of WT and *Zfp36*$^{-/-}$ BMDMs with LPS (1ng/mL) **(A)**, LPS (1ng/mL) + EMR (10μM) **(B)**, IFNβ (10ng/mL) **(C)**, or IFNβ (10ng/mL) + EMR (10μM) **(D)**. **E** WT and *Zfp36*$^{-/-}$ BMDMs were treated with IFNβ (10ng/mL), EMR (10μM), and Nec1-s (10 μM). Expression of cytokines was measured in cell supernatants collected at 7h post-stimulation of cells. **F-H** Cell death was evaluated by staining of cells with Hoechst and PI at 18 h (**F, G**) and 24 by MTT **(H)** post-treatment with LPS (1ng/mL) +/- EMR (10μM), IFNβ(10ng/mL) +/- EMR (10μM), and TNFα (50ng/mL) +/- EMR (10μM), and Nec-1s (10μM). Each experiment was repeated at least three times. Graphs depict mean ± SEM. (**P <0.01, ***P<0.001, ****P<0.0001).

Western blotting analysis of cell extracts failed to reveal any significant modulation in the activation of NFκB or MAPK pathways by type I interferon signaling following LPS treatment **(Figure 35 A)**. This observation suggests that these pathways may not be directly influenced by type I interferon in the context of LPS stimulation. However, a notable increase in the activation of the MAPK pathway was observed during necroptosis stimulation of *Ifnar1*$^{-/-}$ macrophages **(Figure 35 B, E)**. This differential response indicates that the absence of type I interferon receptors may alter the cellular signaling dynamics during necroptotic events.

Furthermore, the induction of Tristetraprolin expression was found to be compromised in *Ifnar1*$^{-/-}$ macrophages **(Figure 35 C)**. Previous studies have demonstrated that MAPK-activated protein kinase 2 (MK2) phosphorylates TTP, leading to increased stability but reduced mRNA binding capacity (Manke et al., 2005). In line with this, our experiments revealed a reduction in TTP expression at 6 hours following necrosome activation in *Mk2*$^{-/-}$ macrophages (**Figure 35 D)**. This observation underscores the intricate relationship between MK2 and TTP in regulating cellular responses during necroptosis.

Collectively, these findings highlight the crucial role of TTP in modulating the expression of TNFα and regulating cell death by necroptosis, particularly during necroptosis stimulation mediated by type I interferon. The interplay between type I interferon signaling, MAPK pathway activation, and TTP expression appears to be a key determinant in the cellular response to necroptotic stimuli. These results not only shed light on the complex signaling networks involved in necroptosis but also emphasize the importance of type I interferon in fine-tuning the cellular death response.

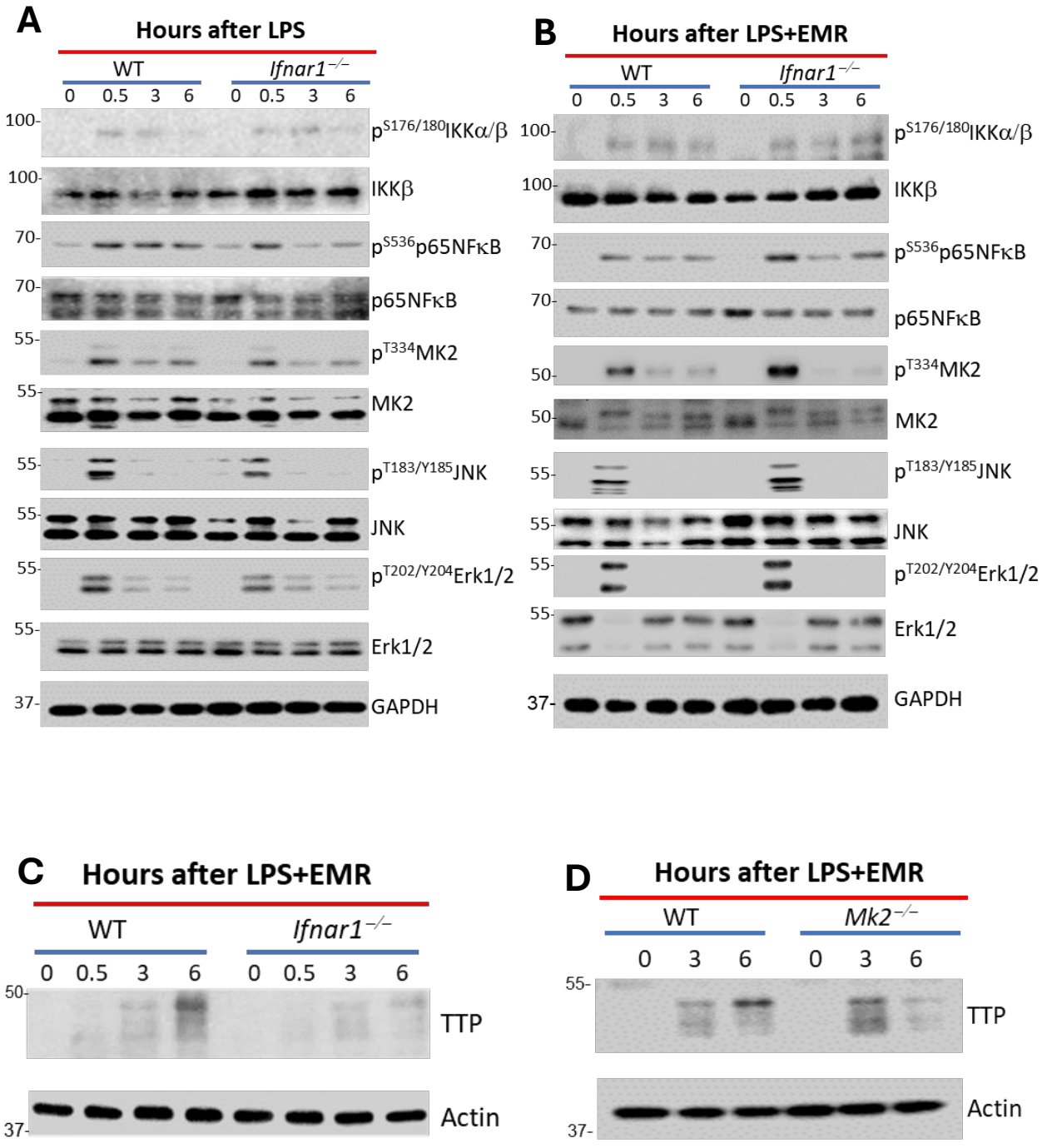
A
Hours after LPS
WT
Ifnar1−/−
0 0.5 3 6 0 0.5 3 6
100-
pS176/180IKKα/β
100-
IKKβ
70-
pS536p65NFκB
70-
p65NFκB
55-
pT334MK2
55-
MK2
55-
pT183/Y185JNK
55-
JNK
55-
pT202/Y204Erk1/2
55-
Erk1/2
37-
GAPDH
B
Hours after LPS+EMR
WT
Ifnar1−/−
0 0.5 3 6 0 0.5 3 6
100-
pS176/180IKKα/β
100-
IKKβ
70-
pS536p65NFκB
70-
p65NFκB
50-
pT334MK2
50-
MK2
55-
pT183/Y185JNK
55-
JNK
55-
pT202/Y204Erk1/2
55-
Erk1/2
37-
GAPDH
C
Hours after LPS+EMR
WT
Ifnar1−/−
0 0.5 3 6 0 0.5 3 6
50-
TTP
37-
Actin
D
Hours after LPS+EMR
WT
Mk2−/−
0 3 6 0 3 6
55-
TTP
37-
Actin

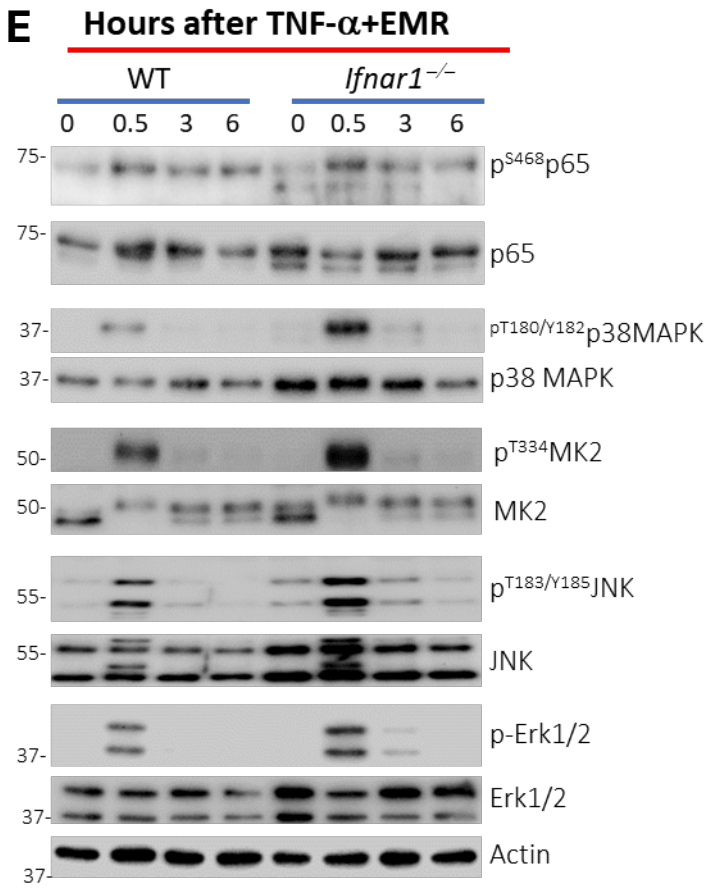

Figure 35. Modulation of MK2 and TTP by IFNAR1-signaling during necroptosis stimulation and upregulation of MAPK activation in *Ifnar1*$^{-/-}$ BMDMs

A-C WT and *Ifnar1*$^{-/-}$ BMDMs were stimulated with LPS (1ng/mL) (**A**) and LPS (1ng/mL) + EMR (10μM) (**B, C**). Cell extracts were collected at various time intervals and the activation of signaling proteins was evaluated by western blot analysis. **D** WT and *Mk2*$^{-/-}$ BMDMs were stimulated with LPS (1ng/mL) + EMR (10μM). Cell extracts were collected at various time intervals and the expression of TTP was evaluated by western blot analysis. **E** Western blot analysis was performed in cell extracts collected from WT and *Ifnar1*$^{-/-}$ BMDMs at different time intervals after treatment with TNFα (50ng/mL) and EMR (10μM). Each experiment was repeated at least three times.

4.2.5. Abrogation of MK2 restricts TNFα expression and augments necroptosis in *Ifnar1*$^{-/-}$ macrophages

Since MK2 plays a critical role in promoting the maintenance of TNFα expression through inactivating TTP (Kotlyarov et al., 1999; Neininger et al., 2002), and since we observed that the activation of MK2 and the expression of TTP is modulated during the necroptosis stimulation of *Ifnar1*$^{-/-}$ macrophages, we therefore, inhibited the p38MAPK pathway and evaluated its impact on TNFα expression and necroptosis to understand the intricate relationship between the p38MAPK-MK2-TTP signaling cascade and the regulation of cell death processes.

Treatment of cells with the MK2 inhibitor III led to a significant reduction in TNFα expression in both WT and *Ifnar1*$^{-/-}$ macrophages **(Figure 36 A)**. Surprisingly, despite this reduction in TNFα levels, we observed an enhancement of necroptosis in both cell types **(Figure 36 B)**. To further validate our findings, we employed an alternative approach using the p38MAPK inhibitor LY2228820. Consistent with our previous results, this inhibitor decreased TNFα expression **(Figure 36 C)** while simultaneously enhancing necroptosis **(Figure 36 D)**. The concordance between the effects of MK2 and p38MAPK inhibition underscores the importance of this signaling pathway in regulating both TNFα production and cell death processes. To confirm that the observed cell death was indeed necroptosis, we performed a crucial rescue experiment using the RipK3 inhibitor GSK872 **(Figure 36 E)**. This result not only validates the necroptotic nature of the observed cell death but also highlights the specificity of the p38MAPK-MK2 pathway's effect on this particular form of programmed cell death.

These findings reveal a complex interplay between the p38MAPK-MK2 signaling pathway, TNFα expression, and necroptosis, suggesting that this pathway may play a dual role in regulating cell death processes. The seemingly paradoxical enhancement of necroptosis despite reduced TNFα levels indicates that the p38MAPK-MK2 pathway might influence necroptosis through mechanisms independent of its effects on TNFα expression.

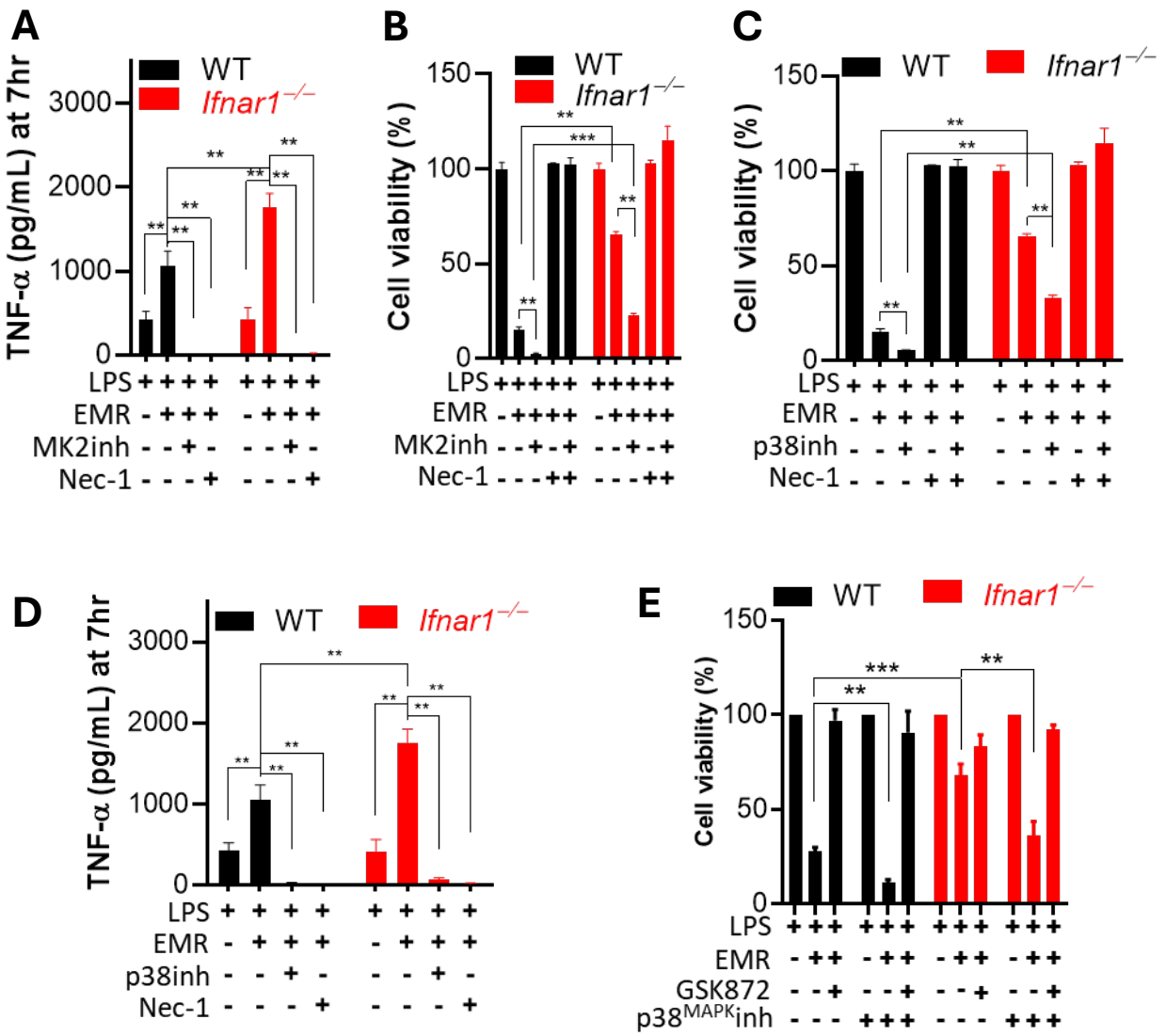

Figure 36. Inhibition of the p38^{MAPK} pathway reduces TNFα expression and increases cell death of *Ifnar1*$^{-/-}$ BMDMs

A, B WT and *Ifnar1*$^{-/-}$ BMDMs were stimulated with LPS (1ng/mL), EMR (10μM), and MK2 inhibitor (III, 5 μM), Nec1-s (10 μM), and the impact on TNFα secretion (**A**) and cell viability (**B**) was evaluated at 7 h and 24 h respectively. **C, D** WT and *Ifnar1*$^{-/-}$ BMDMs were stimulated with LPS (1ng/mL), EMR (10μM), p38^{MAPK} inhibitor (LY2228820, 4 μM), and Nec-1 (10μM). Expression of TNFα was measured in the supernatants at 7 h by ELISA (**A**), and cell death was measured at 24 h by MTT assay (**B**). **E** Cell viability was also measured in cells treated with the RipK3 inhibitor GSK872 (5 μM). Each experiment was repeated at least three times. Graphs depict mean ± SEM. (***P* <0.01, ****P*<0.001).

To investigate this pathway further, we generated mice that were deficient in both IFNAR1 and Mapkapk2 (*Mk2*- the endogenous inhibitor of TTP). The simultaneous deficiency of *Mk2* effectively eliminated the observed increase in TNFα expression during necrosome signaling in *Ifnar1*$^{-/-}$ macrophages **(Figure 37 A)**. This finding suggests a critical role for MK2 in regulating TNFα production within the context of IFNAR1 signaling. In *Mk2*$^{-/-}$macrophages, we observed an upregulation of the activating phosphorylation (S166) of RipK1, a key player in the necroptosis pathway. Interestingly, this upregulation was diminished in *Ifnar1*$^{-/-}$*Mk2*$^{-/-}$macrophages **(Figure 37 B)**, indicating that the increased S166 phosphorylation of RipK1 in *Mk2*$^{-/-}$macrophages is partially dependent on IFNAR1 signaling. We also examined the inhibitory (S321) phosphorylation of RipK1, which showed a slight increase in *Ifnar1*$^{-/-}$ macrophages. Notably, this inhibitory phosphorylation was completely abolished in both *Mk2*$^{-/-}$and *Ifnar1*$^{-/-}$*Mk2*$^{-/-}$macrophages **(Figure 37 B)**, highlighting the complex interplay between IFNAR1 and MK2 in regulating RipK1 phosphorylation. Furthermore, we investigated the downstream phosphorylation of RipK3 and MLKL, which are crucial for the execution of necroptosis. Our results revealed an upregulation of phosphorylation of RipK3 and MLKL in *Mk2*$^{-/-}$ macrophages, with a slight reduction observed in *Ifnar1*$^{-/-}$*Mk2*$^{-/-}$macrophages **(Figure 37 B)**. These findings collectively suggest an intricate regulatory network involving IFNAR1 and MK2 in the control of necroptosis signaling components.

Our experiments demonstrated that MK2 exerts an inhibitory effect on necroptosis during activation by LPS or IFNβ **(Figure 37 C-F)**. This inhibitory impact was consistently observed across different time points and stimuli. Interestingly, the inhibitory effect of MK2 during necroptosis stimulation by TNFα displayed a time-dependent pattern. It was detectable at 9 hours post-stimulation **(Figure 37 C, E)** but not at 18 hours post-stimulation **(Figure 37 D, F)**. This temporal difference in MK2's inhibitory effect suggests a dynamic regulation of necroptosis that evolves over time and varies depending on the specific stimulus. Furthermore, we found that the deficiency of *Mk2* in *Ifnar1*$^{-/-}$ macrophages resulted in increased necroptosis induced by both LPS and TNFα **(Figure 37 C-F)**. This observation underscores the importance of MK2 in modulating necroptosis, particularly in the context of IFNAR1 deficiency, and hints at a potential compensatory mechanism between these two pathways.

Taken together, these results indicate that the modulation of MK2 and Tristetraprolin by IFNAR1 signaling plays a crucial role in regulating the inflammatory cytokine milieu during necrosome activation. This intricate regulatory network involves complex phosphorylation patterns of key necroptosis mediators and exhibits stimulus-specific and time-dependent effects.

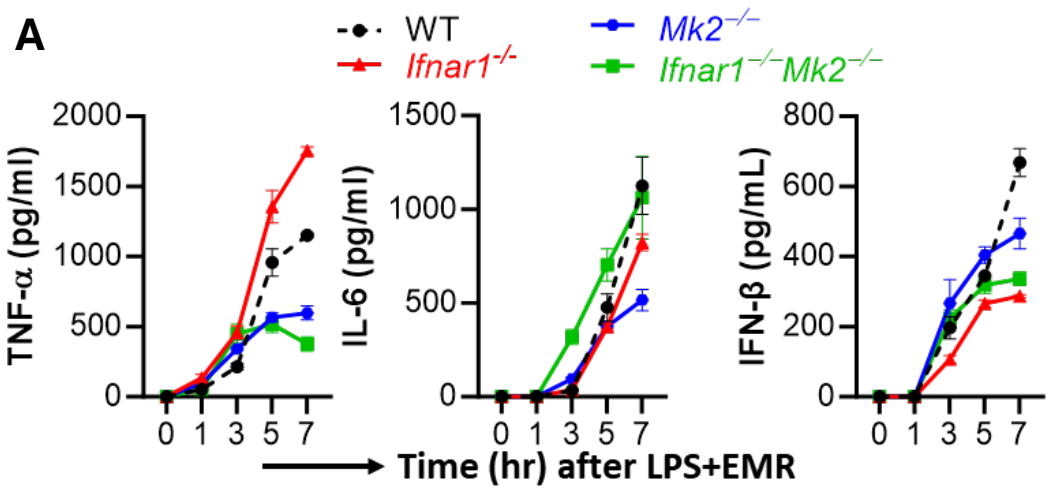
A
WT
Ifnar1-/-
Mk2-/-
Ifnar1-/-Mk2-/-
TNF-α (pg/ml)
IL-6 (pg/ml)
IFN-β (pg/mL)
Time (hr) after LPS+EMR

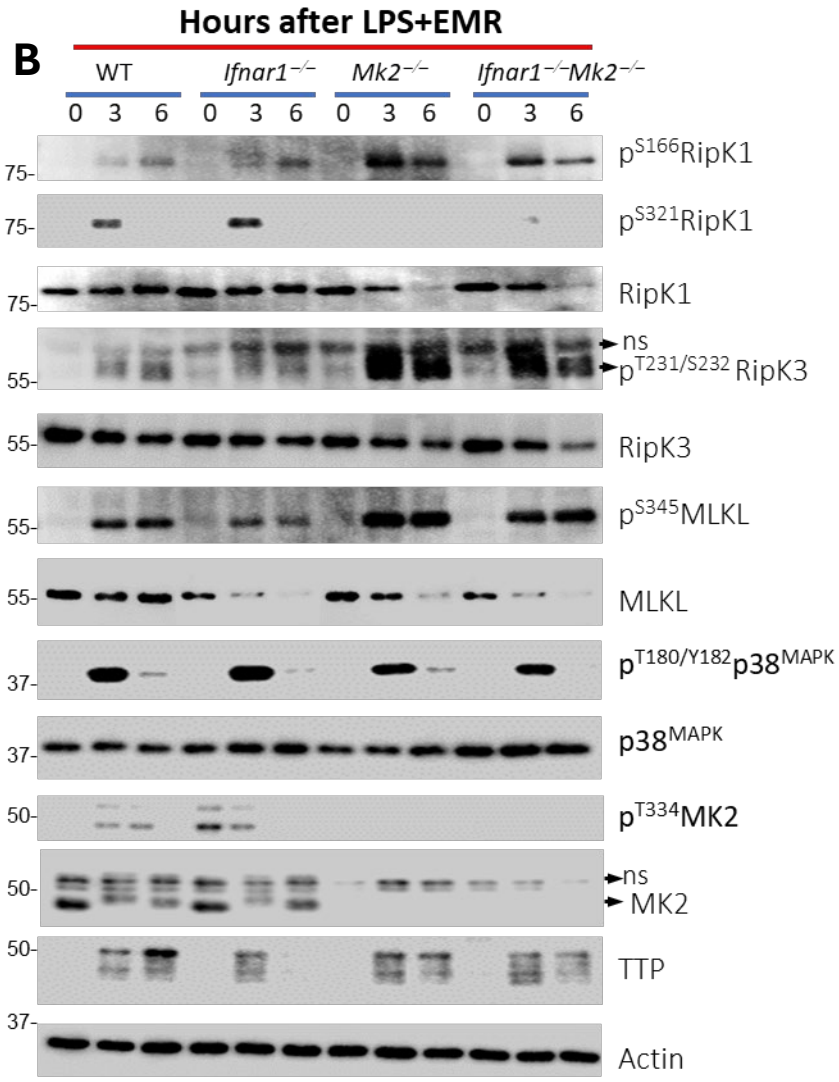
B
Hours after LPS+EMR
WT
Ifnar1-/-
Mk2-/-
Ifnar1-/-Mk2-/-
pS166RipK1
pS321RipK1
RipK1
ns
pT231/S232 RipK3
RipK3
pS345MLKL
MLKL
pT180/Y182p38MAPK
p38MAPK
pT334MK2
ns
MK2
TTP
Actin

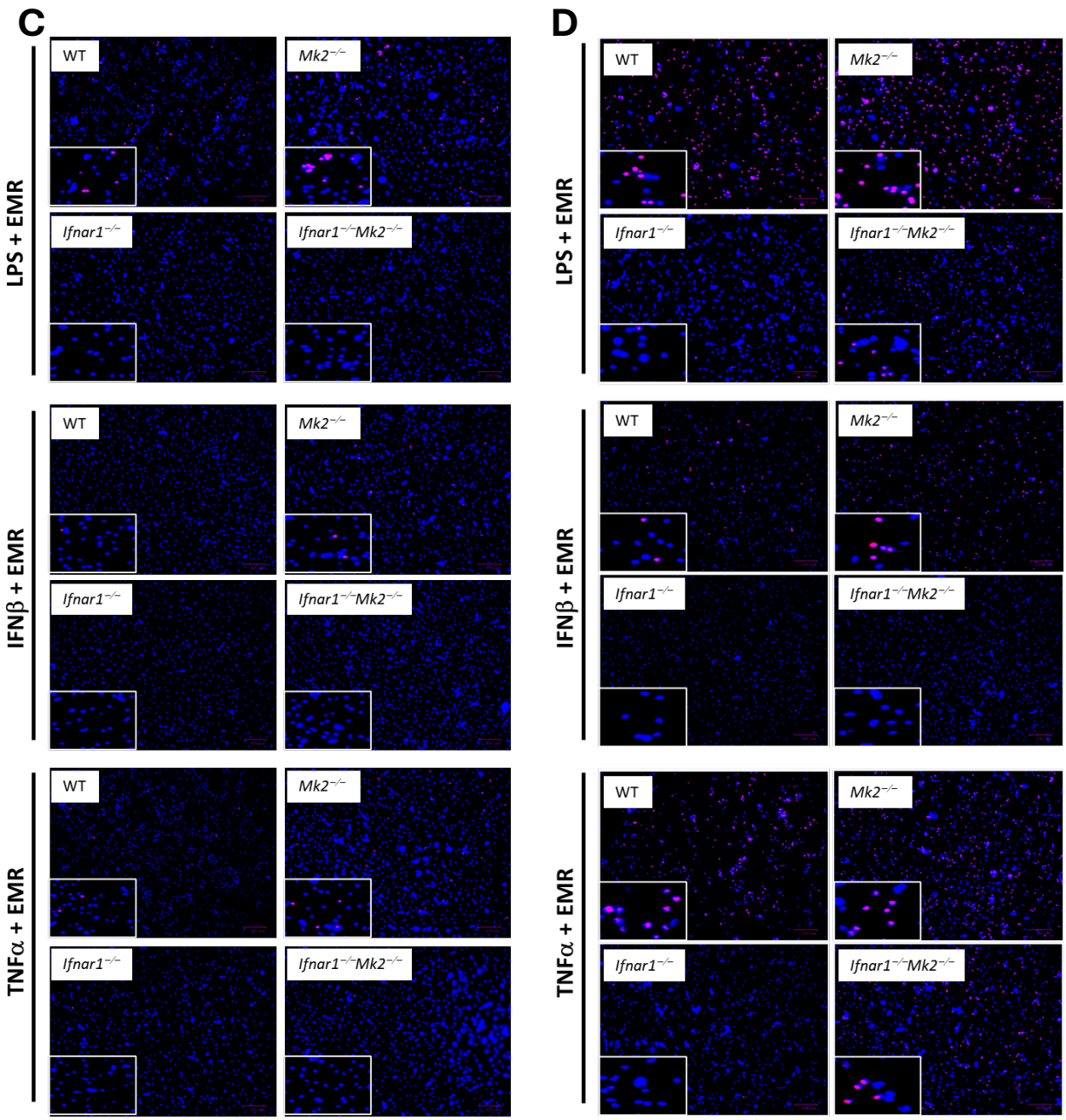
C
D
LPS + EMR
IFNβ + EMR
TNFα + EMR
WT
Mk2−/−
Ifnar1−/−
Ifnar1−/−Mk2−/−

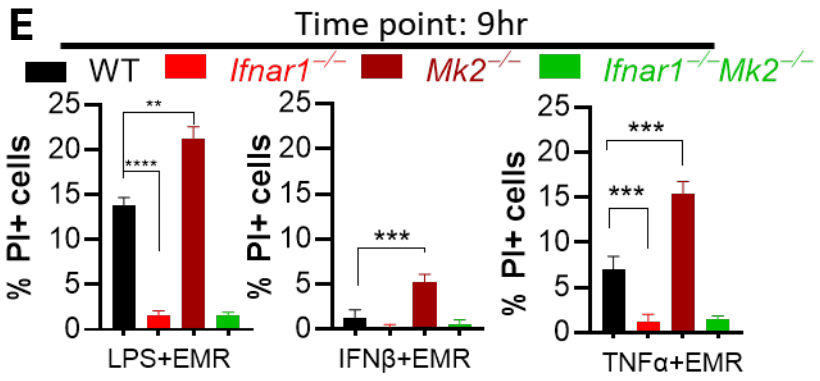
E
Time point: 9hr
WT
Ifnar1−/−
Mk2−/−
Ifnar1−/−Mk2−/−
% PI+ cells
LPS+EMR
IFNβ+EMR
TNFα+EMR

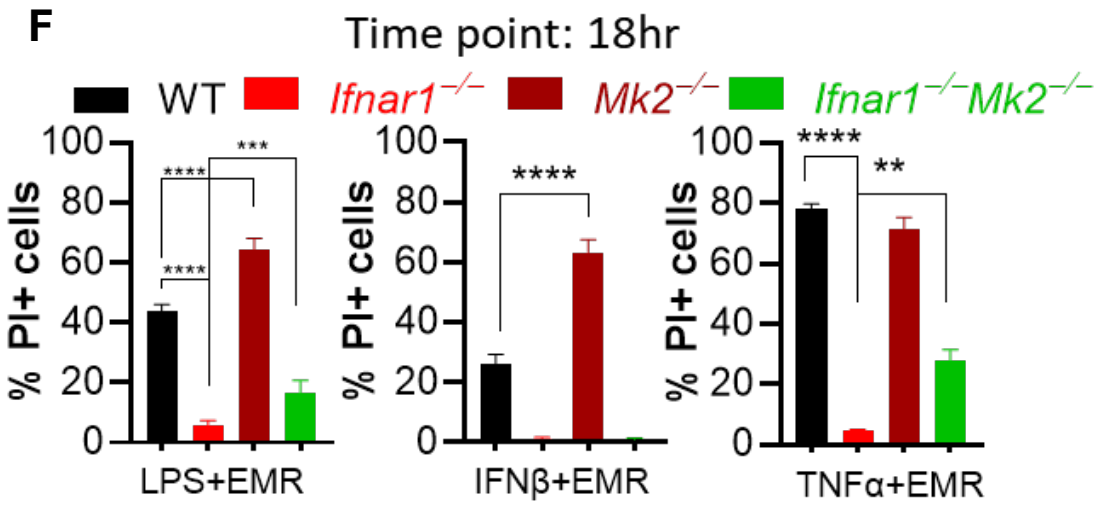

Figure 37. Abrogation of MK2 restricts TNFα expression and augments necroptosis in *Ifnar1*$^{-/-}$ macrophages

A-F WT, *Ifnar1*$^{-/-}$, *Mk2*$^{-/-}$, and *Ifnar1*$^{-/-}$*Mk2*$^{-/-}$ BMDMs were stimulated with LPS (1 ng/mL) + EMR (10μM). Cytokine expression was evaluated at various time intervals by ELISA (**A**). Activation of signaling proteins was evaluated by western blot analysis of cell extracts collected at various time intervals (**B**). Cell death was evaluated by staining cells with Hoechst and PI following stimulation of WT, *Ifnar1*$^{-/-}$, *Mk2*$^{-/-}$, and *Ifnar1*$^{-/-}$*Mk2*$^{-/-}$ BMDMs with LPS (1ng/mL) + EMR (10μM), IFNβ (10ng/mL) + EMR (10μM), and TNFα (50ng/mL) + EMR (10μM) at 9h (**C, E**) or 18h (**D, F**). Each experiment was repeated at least three times. Graphs depict mean ± SEM. (**P<0.01, ***P<0.001, ****P<0.0001).

4.2.6. IFNAR1 signaling promotes the degradation of TNFα mRNA

We conducted qRT-PCR analysis to measure the transcript levels of selected genes that exhibited upregulation (*Cxcl1, Ifnb1, Tnfα*) or downregulation (*IL-12*) during necroptosis stimulation. The results revealed intriguing patterns of gene expression in WT and *Ifnar1*$^{-/-}$ macrophages. The mRNA level of *IL-12p35* and *IL12-12p40* showed a notable reduction during necroptosis stimulation, with *Ifnar1*$^{-/-}$ macrophages displaying an even more pronounced decrease compared to their WT counterparts **(Figure 38 A, B)**. This observation suggests a potential role for IFNAR1 signaling in maintaining IL-12 expression during necroptotic conditions.

In contrast to *IL-12*, the transcript level of *Cxcl1* exhibited significant upregulation during necrosome activation. Interestingly, *Ifnar1*$^{-/-}$ macrophages demonstrated a more robust upregulation of *Cxcl1* compared to WT cells **(Figure 38 C)**. This enhanced expression in the absence of IFNAR1 signaling implies a possible negative regulatory role of the interferon pathway on *Cxcl1* transcription during necroptosis. The expression of the *Ifnβ1* transcript also showed enhancement during necroptosis stimulation. However, in this case, WT cells displayed greater upregulation relative to *Ifnar1*$^{-/-}$ cells **(Figure 38 D)**. This differential response could be attributed to the absence of feedforward signaling by IFNβ in *Ifnar1*$^{-/-}$ macrophages, highlighting the importance of intact interferon signaling for optimal Ifnβ1 expression during necroptosis. *Tnfα* mRNA levels were also enhanced during necrosome activation, with *Ifnar1*$^{-/-}$ macrophages exhibiting an even greater increase compared to WT cells **(Figure 38 E)**. To further investigate the role of IFNβ in regulating *Tnfα* expression, we treated cells with IFNβ and observed a reduction in both transcription **(Figure 38 F)** and translation **(Figure 38 G)** of *Tnfα* in WT macrophages. Notably, this effect was absent in *Ifnar1*$^{-/-}$ macrophages, underscoring the specific involvement of IFNAR1 signaling in modulating *Tnfα* expression.

Increase in the TNFα levels in *Ifnar1*$^{-/-}$ cells could be due to increased transcription or reduced degradation of mRNA transcripts. To discriminate between these scenarios, we treated cells with Actinomycin D at 1.5 hours post necrosome activation to inhibit gene transcription. Subsequently, we evaluated the impact on *Tnfα* transcript levels at various time intervals. This approach revealed that *Tnfα* transcripts underwent reduced degradation in *Ifnar1*$^{-/-}$ macrophages **(Figure 38 H)**,

suggesting a role for IFNAR1 signaling in promoting the maintenance of *Tnfα* mRNA possibly through the expression of *Zfp36*.

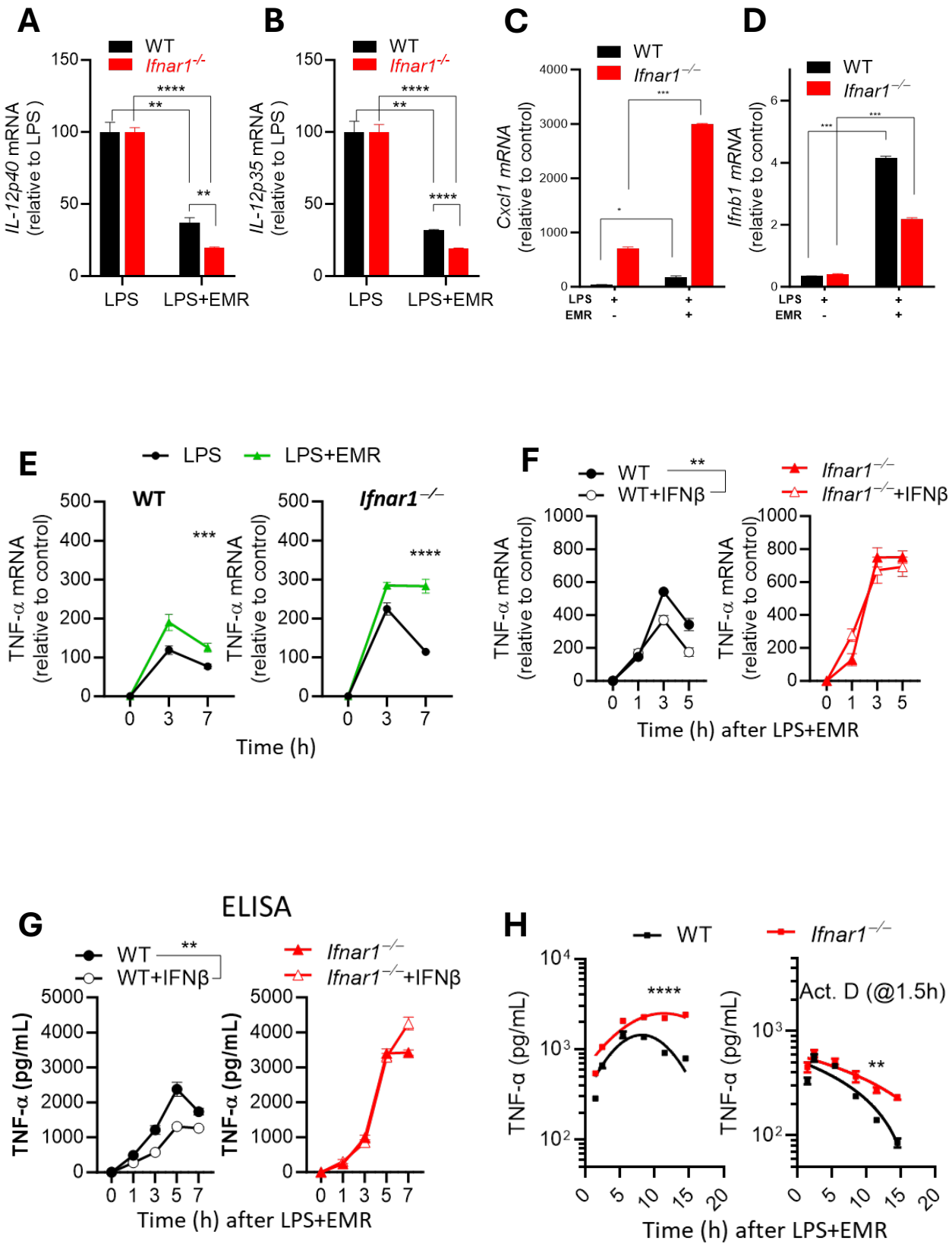
A
B
C
D
WT
Ifnar1-/-
IL-12p40 mRNA (relative to LPS)
IL-12p35 mRNA (relative to LPS)
Cxcl1 mRNA (relative to control)
Ifnb1 mRNA (relative to control)
LPS
LPS+EMR
EMR
E
F
LPS
LPS+EMR
WT
Ifnar1-/-
TNF-α mRNA (relative to control)
Time (h)
WT+IFNβ
Ifnar1-/-+IFNβ
Time (h) after LPS+EMR
G
H
ELISA
TNF-α (pg/mL)
Act. D (@1.5h)

Figure 38. IFNAR1-signaling promotes the degradation of TNFα mRNA

A-D Expression of *Il-12*, *Cxcl11*, and *Ifnb1* mRNA were measured by qRT-PCR analysis at 3 h following treatment of WT and *Ifnar1*$^{-/-}$ BMDMs with LPS (1ng/mL) and EMR (10μM). **E, F** Expression of *Tnfα* mRNA was measured by qRT-PCR analysis at various time intervals post-treatment of WT and *Ifnar1*$^{-/-}$ BMDMs with LPS (1ng/mL), EMR (10μM), and IFNβ (10ng/mL). **G, H** Expression of TNFα was measured by ELISA in the supernatants collected at different time intervals following treatment of WT and *Ifnar1*$^{-/-}$ BMDMs with LPS (1ng/mL), EMR (10μM), and IFNβ (10ng/mL), or Actinomycin D (2 μM). Each experiment was at least repeated three times. Graphs depict mean ± SEM. (**P* <0.05, ***P*<0.01, ****P*<0.001, *****P*<0.0001).

Collectively, these results indicate that necroptosis stimulation promotes RipK1-dependent activation of the $p38^{MAPK}$ pathway, which in turn drives an inflammatory response independently of cell death. The excessive upregulation of inflammation during necroptosis stimulation is partially suppressed by IFNAR1-signaling through ISGF3, which promotes the transcription of the RNA-destabilizing protein TTP. These findings shed light on the complex interplay between necroptosis, interferon signaling, and inflammatory gene regulation in macrophages, offering new insights into the molecular mechanisms underlying the inflammatory response during programmed necrotic cell death.

4.3. Aim 3: Deciphering the mechanism of necroptosis induction by IFNAR1 signaling.

4.3.1. IFNAR1 signaling promotes necroptosis in macrophages

Recent research has illuminated the intricate relationship between type I interferon signaling and necroptosis, revealing a critical dependency of necroptosis on IFN-1 receptor signaling for its full manifestation. To investigate this connection, we conducted a comprehensive study using WT and *Ifnar1*$^{-/-}$ BMDMs. These cells were subjected to PI and Hoechst staining to assess cell viability and death at two distinct time points: 6- and 24-hour post-stimulation with LPS alone or in combination with EMR. At the earlier time point of 6 hours post-stimulation, minimal cell death was observed only in WT cells, suggesting that the necroptotic process had not yet fully engaged **(Figure 39 A)**. However, the 24-hour time point revealed a dramatic difference between the WT and *Ifnar1*$^{-/-}$ macrophages. The *Ifnar1*$^{-/-}$ macrophages displayed a remarkable resistance to necroptosis, highlighting the crucial role of type I interferon receptor signaling in this cell death pathway **(Figure 39 B)**. To further elucidate the role of type I interferon receptor signaling in necroptosis, we treated WT and *Ifnar1*$^{-/-}$ BMDMs with various necroptosis-inducing conditions. This was achieved by activating different receptors known to trigger necroptosis. Specifically, the cells were treated with LPS, TNFα, and IFNβ to initiate necroptosis through the TLR4, TNFR1, and Ifnar1 signaling pathways, respectively. To ensure specificity for necroptosis, these treatments were administered in the presence of EMR and GSK872, which are inhibitors of apoptosis and RipK3, respectively. The cell death analysis from these experiments yielded compelling results, further emphasizing the critical role of IFNAR1 signaling in necroptosis. Regardless of whether necroptosis was initiated through LPS, TNFα, or IFN-β pathways, IFNAR1 signaling proved to be a crucial component in the full manifestation of necroptotic cell death **(Figure 39 C)**. These findings collectively highlight the paramount importance of type I interferon receptor signaling in the complete execution of necroptosis, irrespective of the initial triggering receptor or pathway. This discovery suggests that type I interferon receptor signaling serves as a key component in the necroptotic pathway, potentially acting as a common downstream mediator for various necroptosis-inducing signals in BMDMs.

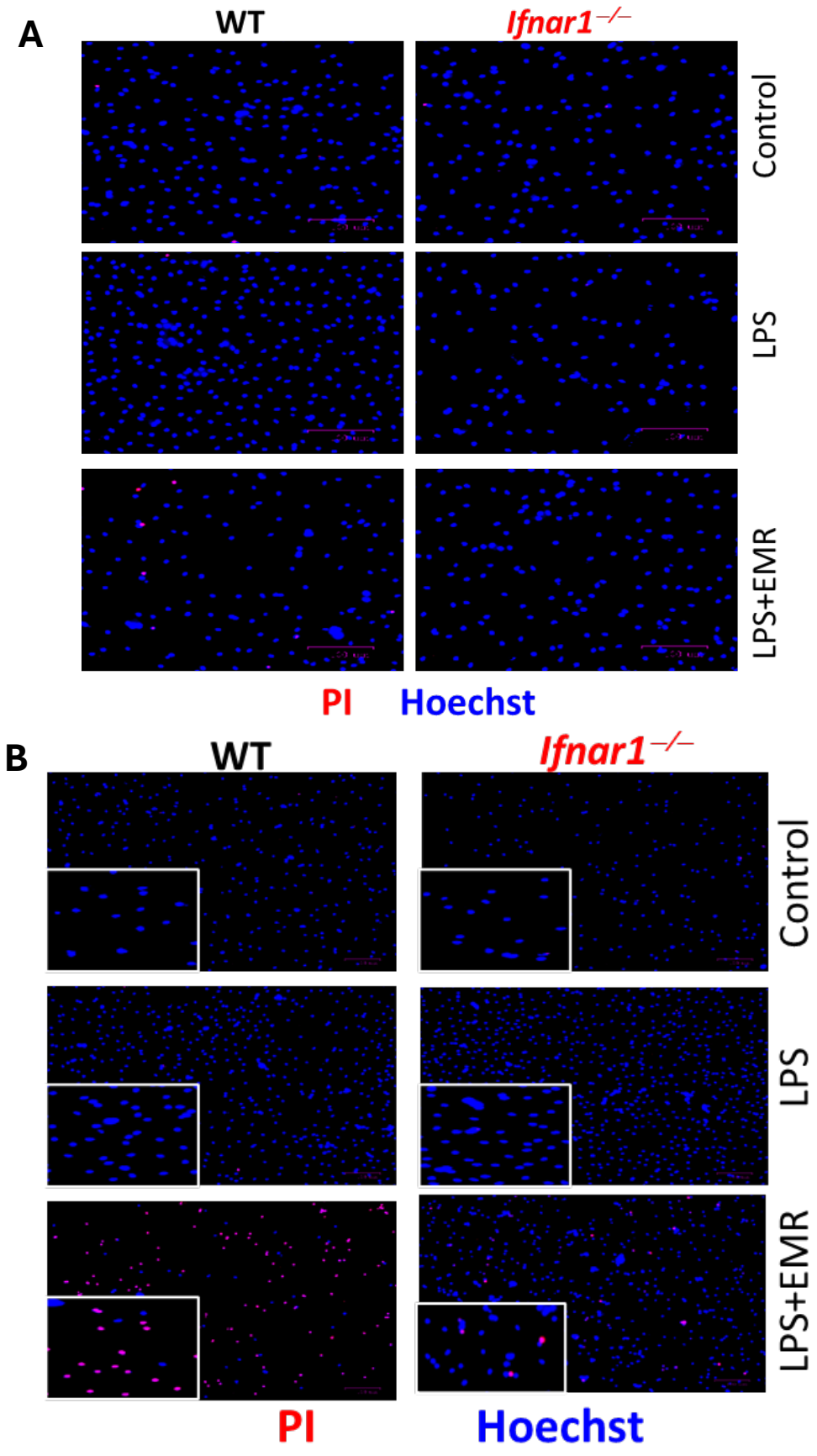
A
WT
Ifnar1−/−
Control
LPS
LPS+EMR
PI
Hoechst
B
WT
Ifnar1−/−
Control
LPS
LPS+EMR
PI
Hoechst

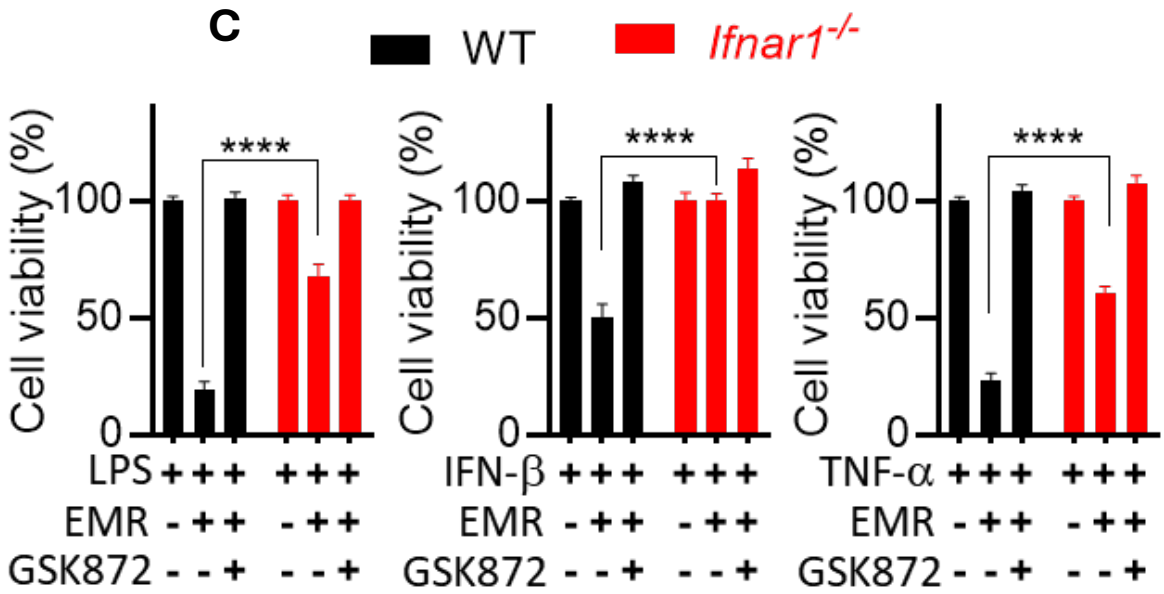

Figure 39. IFNAR1 signaling promotes necroptosis in macrophages

A, B Cell death was evaluated by staining cells with Hoechst and PI following stimulation of WT and *Ifnar1*$^{-/-}$ BMDMs with LPS (1 ng/mL) and EMR (10μM) at 6 hours **(A)** and 24 hours **(B)**. **C** After 24 hours cell death was evaluated by treating the WT and *Ifnar1*$^{-/-}$ cells with LPS (1ng/mL) +/- EMR (10μM), IFNβ(10ng/mL) +/- EMR (10μM), and TNFα (50ng/mL) +/- EMR (10μM), and GSK872 (10μM) by MTT. Each experiment was repeated at least three times. Graphs depict mean ± SEM. (****P<0.0001).

4.3.2. Signaling bridge between IFNAR1 and TNFR signaling

Activation of TLR4 leads to the expression of multiple cytokines, including TNFα. To investigate the potential roles of TNF receptor 1 (TNFR1) and TNF receptor 2 (TNFR2) in LPS-induced necroptosis of macrophages, *Tnfr1*- and *Tnfr2*-deficient BMDMs were generated and subjected to treatment with LPS in combination with EMR for 24 hours. Subsequent cell death analysis revealed significant protection from LPS-induced necroptosis, specifically in *Tnfr2*-deficient macrophages **(Figure 40 A)**. Intriguingly, a similar pattern of resistance was also observed when these *Tnfr2*-deficient BMDMs were exposed to IFNβ- and TNFα-mediated necroptosis **(Figure 40 A)**. This compelling observation suggests that TNFR2 plays a crucial role in promoting necroptosis within macrophages, potentially serving as a key mediator in the cell death signaling cascade. Given that LPS stimulation is known to activate the expression of type-I interferons and considering our previous findings indicating that IFNAR1 signaling promotes necroptosis, we sought to further elucidate the potential relationship between IFNAR1 signaling and TNFR2 expression. To address this question, we conducted a comprehensive evaluation of TNFR2 expression in both WT and *Ifnar1*$^{-/-}$ cells. Bioinformatics analysis showed that treatment of macrophages with either LPS or type-I interferons with zVAD does not lead to a significant upregulation of *Tnfr2* (Tnfrsf1b) at the transcriptional level **(Figure 40 B)**. This finding was further corroborated by Western blot analysis, which demonstrated that IFNAR1 signaling does not substantially influence TNFR2 expression in *Ifnar1*$^{-/-}$ BMDMs under normal physiological conditions. To further validate these intriguing findings and ensure their robustness, we conducted additional experiments to examine TNFR2 expression under various stimulatory conditions. Notably, we observed no significant increase in TNFR2 expression following stimulation with either LPS+EMR or IFNβ+EMR **(Figure 40 C)**. These comprehensive and multi-faceted results, obtained through a combination of genetic, biochemical, and bioinformatic approaches, provide strong evidence that while TNFR2 plays a crucial role in promoting necroptosis, the resistance to necroptosis observed in *Ifnar1*$^{-/-}$ macrophages cannot be attributed to alterations in TNFR2 expression levels.

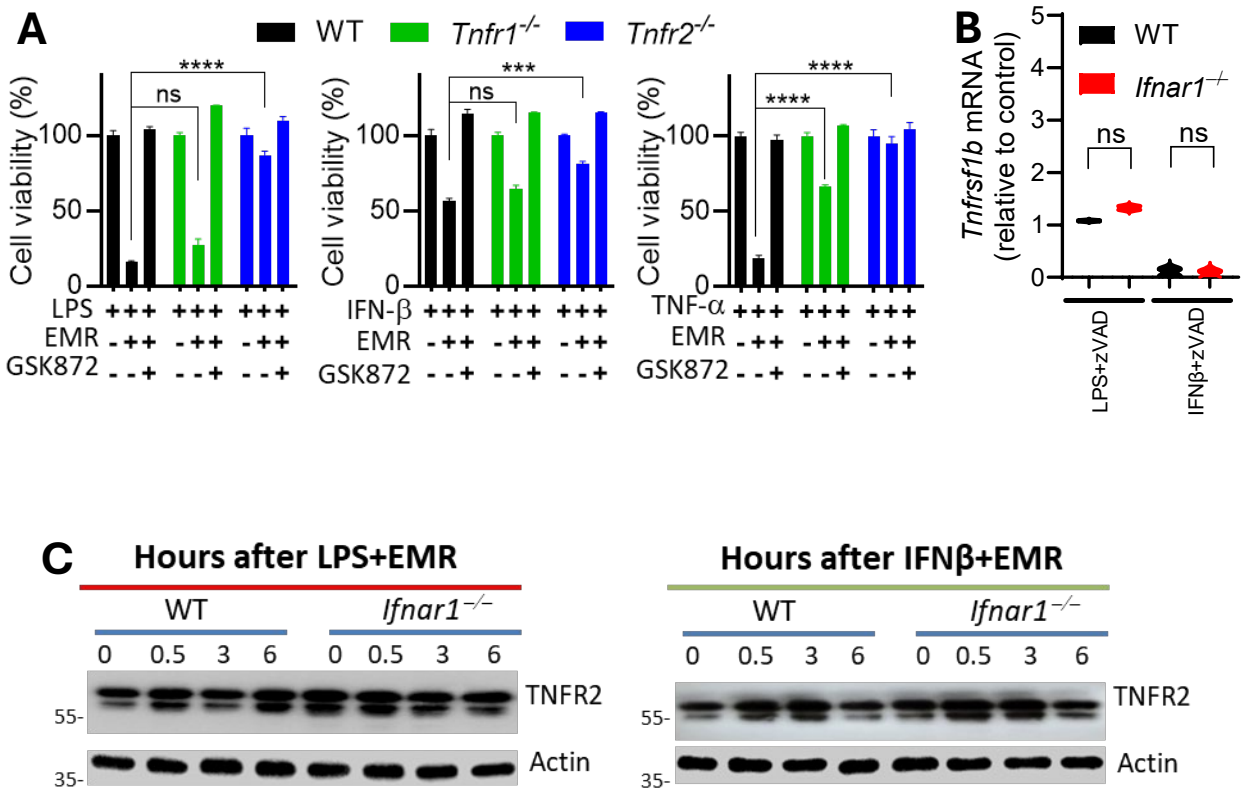

Figure 40. TNFR2 Promotes Necroptosis in macrophages independently of IFNAR1 signaling

A After 24 hours cell death was evaluated by treating the WT and *Ifnar1*$^{-/-}$ cells with LPS (1ng/mL) +/- EMR (10μM), IFNβ(10ng/mL) +/- EMR (10μM), and TNFα (50ng/mL) +/- EMR (10μM), and GSK872 (10μM) by MTT. **B** Expression of *Zfp36* mRNA was measured in WT, *Tnfr1*$^{-/-}$, and *Tnfr2*$^{-/-}$ BMDMs by microarray after treating the cells with LPS (1ng/mL) + zVAD-fmk (50μM), and IFNβ (100 U/mL) + zVAD-fmk (50μM). **C** Expression of TNFR2 was analyzed by western blotting of cell extracts collected from WT and *Ifnar1*$^{-/-}$ BMDMs at various time intervals following treatment with LPS (1ng/mL) + EMR (10μM), and IFNβ (10ng/mL) + EMR (10μM). Each experiment was repeated at least three times. Graphs depict mean ± SEM. (***P<0.001, ****P<0.0001).

4.3.3. Phosphorylated vs Unphosphorylated ISGF3 complex

Upon engagement of IFNAR1 by type-I interferon, a trimeric transcriptional complex known as ISGF3 is formed, consisting of STAT1, STAT2, and IRF9. ISGF3 then translocates to the nucleus and activates the transcription of numerous genes that contain an ISRE in their promoter region (Au-Yeung et al., 2013). This process is crucial for the interferon-mediated immune response. Interestingly, macrophages deficient in the ISGF3 members (Stat1, Stat2, or Irf9) displayed enhanced resistance to necroptosis induced by both LPS+EMR and TNFα+EMR stimulation **(Figure 30 D)**. This observation suggests a potential link between the ISGF3 complex and necroptotic cell death pathways. As expected, in *Ifnar1*$^{-/-}$ macrophages, both the phosphorylation and total levels of STAT1, STAT2, and IRF9 proteins were significantly reduced compared to WT macrophages **(Figure 41 A, B)**. This finding highlights the importance of the phosphorylation of ISGF3 complex proteins and their dependence on IFNAR1 signaling. The reduced levels of these proteins in *Ifnar1*$^{-/-}$ macrophages further emphasize the critical role of type-I interferon signaling in maintaining the ISGF3 complex. Taken together, these observations indicate that the intact ISGF3 complex is necessary for full necroptotic sensitivity in macrophages under these conditions.

Recent studies have shed light on the dynamic nature of the ISGF3 complex. It has been shown that the components of the ISGF3 complex are initially phosphorylated, but the unphosphorylated complex can remain intact for extended periods and transcribe a different set of genes (Nowicka et al., 2023). This finding adds a layer of complexity to our understanding of ISGF3 function and suggests that both phosphorylated and unphosphorylated forms of the complex may have distinct roles in cellular processes, including necroptosis. To understand the role of phosphorylated and unphosphorylated forms of the ISGF3 complex in necroptosis, we conducted a series of experiments. First, we treated WT BMDMs with a low concentration of IFN-β overnight and then added EMR at later time intervals. When EMR was added at 24 hours post IFNβ treatment, we did not observe any cell death **(Figure 41 C)**. This result suggested that prolonged exposure to low levels of IFNβ might not be sufficient to sensitize macrophages to necroptosis. Based on these findings, we then treated WT macrophages with IFN-β to induce the phosphorylation and assembly of ISGF3 and added EMR at various time points to induce necroptosis. Interestingly, treatment of WT macrophages with EMR at 6 hours post IFNβ treatment revealed an attenuation in necroptosis induction **(Figure 41 D)**. Addition of EMR after 12 hours of treatment with IFNβ failed to induce

significant necroptosis. This result correlates with the expression pattern of ISGF3 complex proteins, which peaks at early time points and starts to dephosphorylate around 6 hours in the IFN-β mediated necroptosis state **(Figure 41 B)**. The temporal relationship between ISGF3 phosphorylation status and necroptotic sensitivity suggests a critical role for the phosphorylated form of the complex in promoting necroptosis. On the other hand, treatment of macrophages with LPS and the addition of EMR at various time points showed that the cells remained sensitive to necroptosis induction for prolonged periods **(Figure 41 E)**. This prolonged sensitivity of cells to necroptosis induction in response to LPS can be attributed to the fact that induction of IFNAR1 signaling by TLR4 receptor engagement requires the transcription and translation of IFN-1 which can occur for prolonged periods in comparison to treatment of cells with IFNβ **(Figure 41 A)**.

Collectively, these results suggest that the phosphorylated form of ISGF3 may be essential for necroptosis. The temporal correlation between ISGF3 phosphorylation status and necroptotic sensitivity, along with the differential responses to IFN-β and LPS stimulation, indicates the important role of phosphorylated ISGF3 in promoting necroptotic cell death in macrophages.

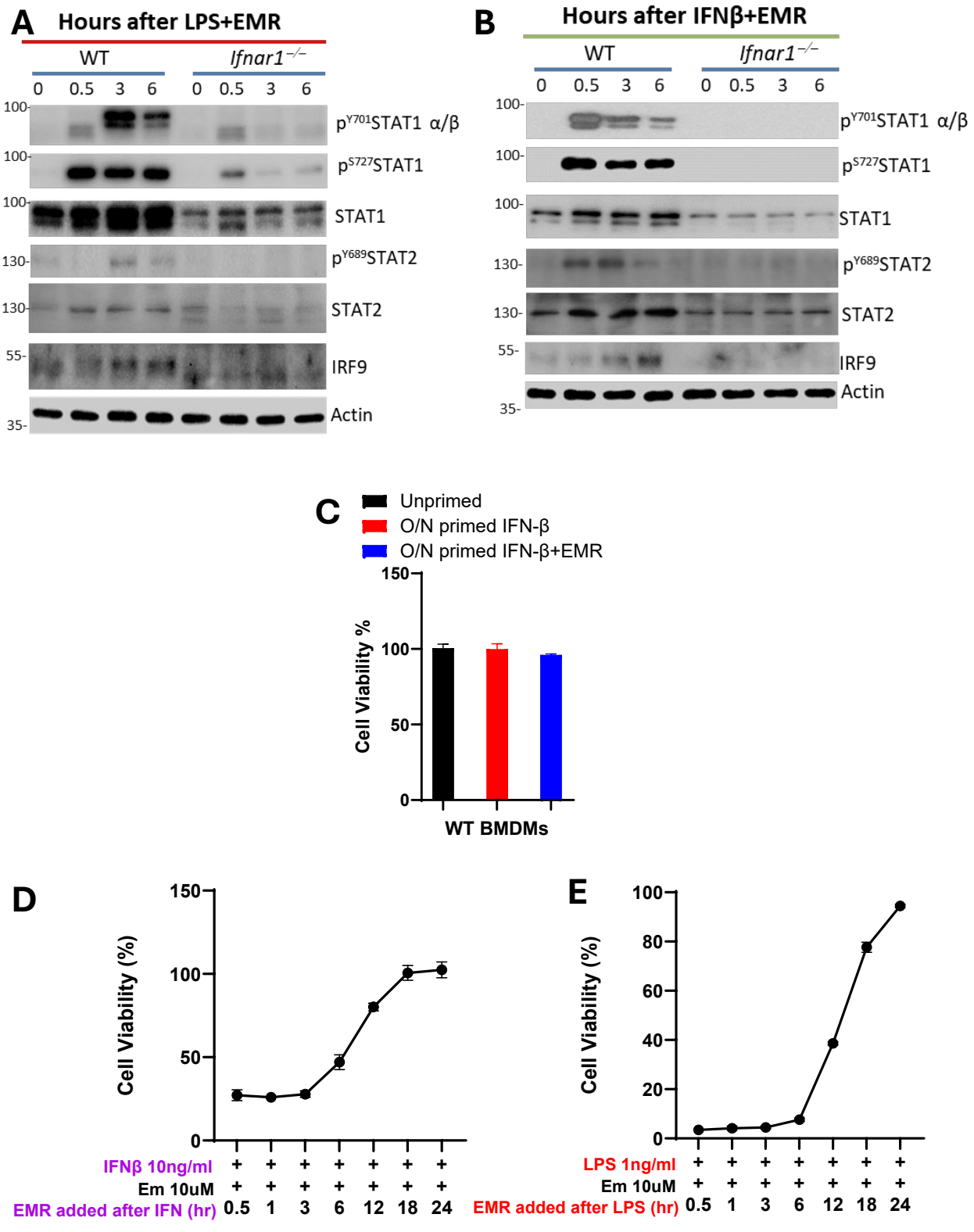
A
Hours after LPS+EMR
WT
Ifnar1−/−
0 0.5 3 6 0 0.5 3 6
100-
pY701STAT1 α/β
pS727STAT1
STAT1
130-
pY689STAT2
STAT2
55-
IRF9
35-
Actin
B
Hours after IFNβ+EMR
C
Unprimed
O/N primed IFN-β
O/N primed IFN-β+EMR
Cell Viability %
150
100
50
0
WT BMDMs
D
Cell Viability (%)
IFNβ 10ng/ml
Em 10uM
EMR added after IFN (hr) 0.5 1 3 6 12 18 24
E
Cell Viability (%)
LPS 1ng/ml
Em 10uM
EMR added after LPS (hr) 0.5 1 3 6 12 18 24

Figure 41. The role of phosphorylated ISGF3 complex in macrophage necroptosis

A, B Expression of ISGF3 complex proteins were analyzed by western blotting of cell extracts collected from WT and *Ifnar1*$^{-/-}$ BMDMs at various time intervals following treatment with LPS (1ng/mL) + EMR (10μM) **(A)**, and IFNβ (10ng/mL) + EMR (10μM) **(B)**. **C** WT BMDMs were treated with IFN (1ng/mL) overnight, and then EMR (10μM) was added. After 24 hours of EMR addition, cell death was measured by MTT. **D, E** WT BMDMs were treated with IFNβ (10ng/mL) **(D)**, LPS (10ng/mL) **(E)**, and EMR (10μM) was added at different time points, and then cell death was measured by MTT after 24 hours of each time point. Each experiment was repeated at least three times. Graphs depict mean ± SEM.

4.3.4. Role of the IFNAR1 stimulated downstream genes

Interferons (IFNs) are a family of potent cytokines that exhibit diverse functions, profoundly impacting cellular physiology, particularly in cells of the immune system. These signaling proteins mediate most of their effects through the induction of Interferon-Stimulated Genes (ISGs), which are transcriptionally regulated by IFN signaling pathways. To elucidate the molecular mechanisms underlying IFN-mediated cellular responses, we conducted a comprehensive microarray analysis. This analysis revealed the transcriptional modulation of several target genes that are highly upregulated or downregulated during necrosome activation in *Ifnar1*$^{-/-}$ macrophages, with genes such as X-linked inhibitor of apoptosis-associated factor 1 (XAF1) and Mixed Lineage Kinase Domain-Like Protein (MLKL) being of particular interest **(Figure 42 A).**

XAF1, an IFN-stimulated gene, has been shown to promote IFN-induced apoptosis and plays a crucial role in IFN-mediated cellular sensitization to the pro-apoptotic actions of TNF-related apoptosis-inducing ligand (TRAIL) (Leaman et al., 2002). Our experiments demonstrated that XAF1 mRNA levels were significantly elevated in WT macrophages following treatment with IFNβ alone and in combination with EMR **(Figure 42 B)**. To further investigate the potential role of XAF1 in necroptosis, we performed a series of necroptosis assays using LPS, TNFα, and IFN-β on *Xaf1*$^{+/-}$ BMDMs and *Xaf1*$^{-/-}$ RAW macrophages (which were previously generated in the lab by the CRISPR-Cas9 approach). Interestingly, we observed no significant differences in necroptosis susceptibility between *Xaf1*$^{-/-}$ and WT macrophages **(Figure 42 C, D)**. These findings suggest that XAF1, despite its upregulation in response to IFN-1 signaling, is not essential for the execution of necroptosis.

To gain further insights into the molecular mechanism involved in IFN-1 induced necroptosis, we performed qRT-PCR analysis to measure the transcript levels of MLKL, a key executioner of necroptosis. Our qRT-PCR results revealed that IFNβ alone and in combination with EMR induced MLKL expression in WT cells **(Figure 42 E)**, highlighting the direct link between IFN-1 signaling and MLKL regulation. Furthermore, when we treated the BMDMs with LPS, IFNβ, and TNFα in combination with EMR, we observed that the levels of phosphorylated and total MLKL were reduced in *Ifnar1*$^{-/-}$ macrophages relative to their WT counterparts **(Figure 42 F)**. This observation is particularly noteworthy because previous studies have demonstrated that *Mlkl*-

deficient macrophages are resistant to necroptosis (Murphy et al., 2013). Therefore, the reduced MLKL expression observed in the *Ifnar1*$^{-/-}$ BMDMs likely contributes substantially to their resistance to necroptosis, underscoring the critical role of IFN-1 signaling in modulating cellular susceptibility to this form of programmed cell death.

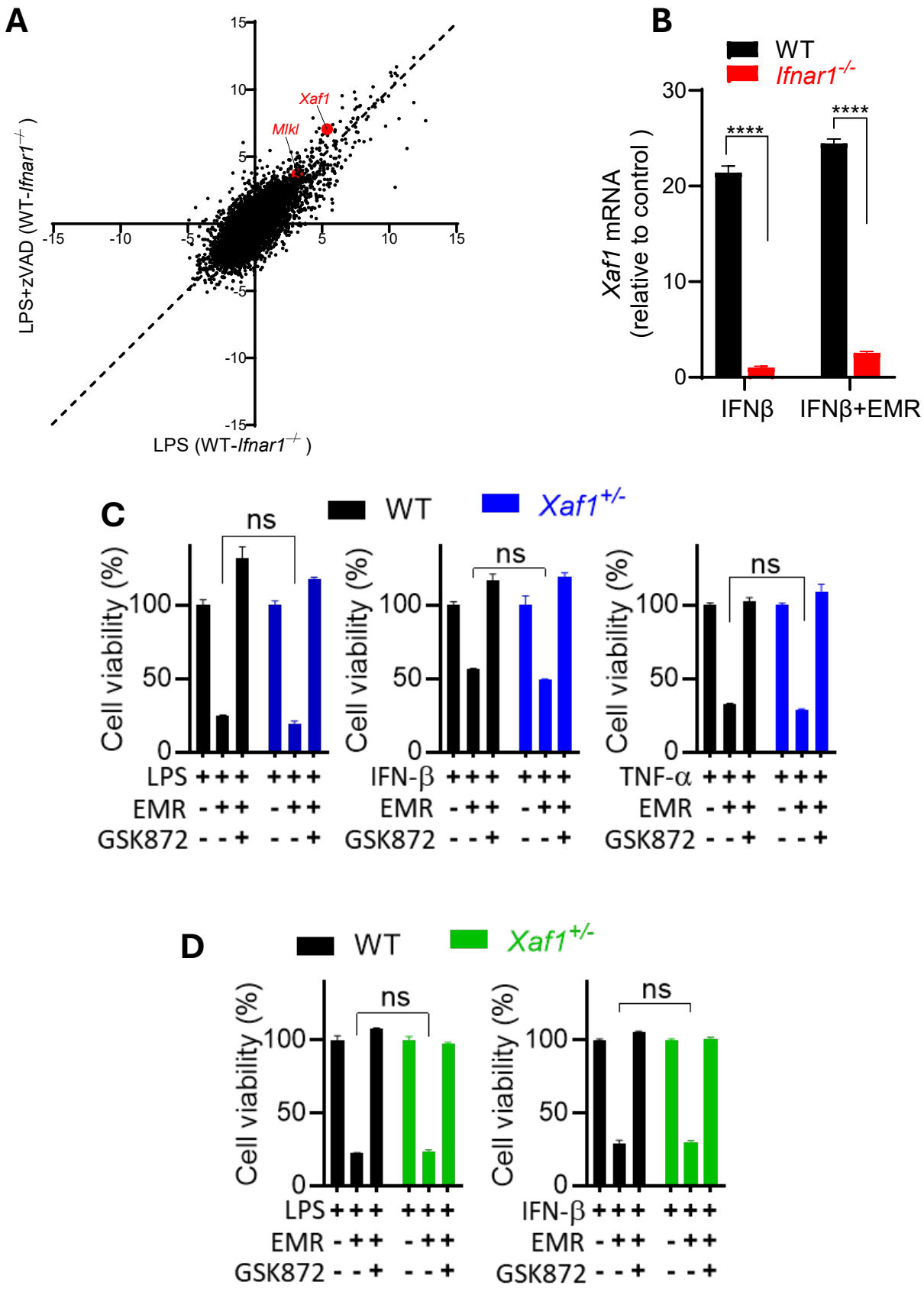
A
Xaf1
Mlkl
LPS+zVAD (WT-Ifnar1−/−)
LPS (WT-Ifnar1−/−)
B
WT
Ifnar1-/-
Xaf1 mRNA (relative to control)
****
****
IFNβ
IFNβ+EMR
C
WT
Xaf1+/-
ns
Cell viability (%)
LPS
IFN-β
TNF-α
EMR
GSK872
D
WT
Xaf1+/-
ns
Cell viability (%)
LPS
IFN-β
EMR
GSK872

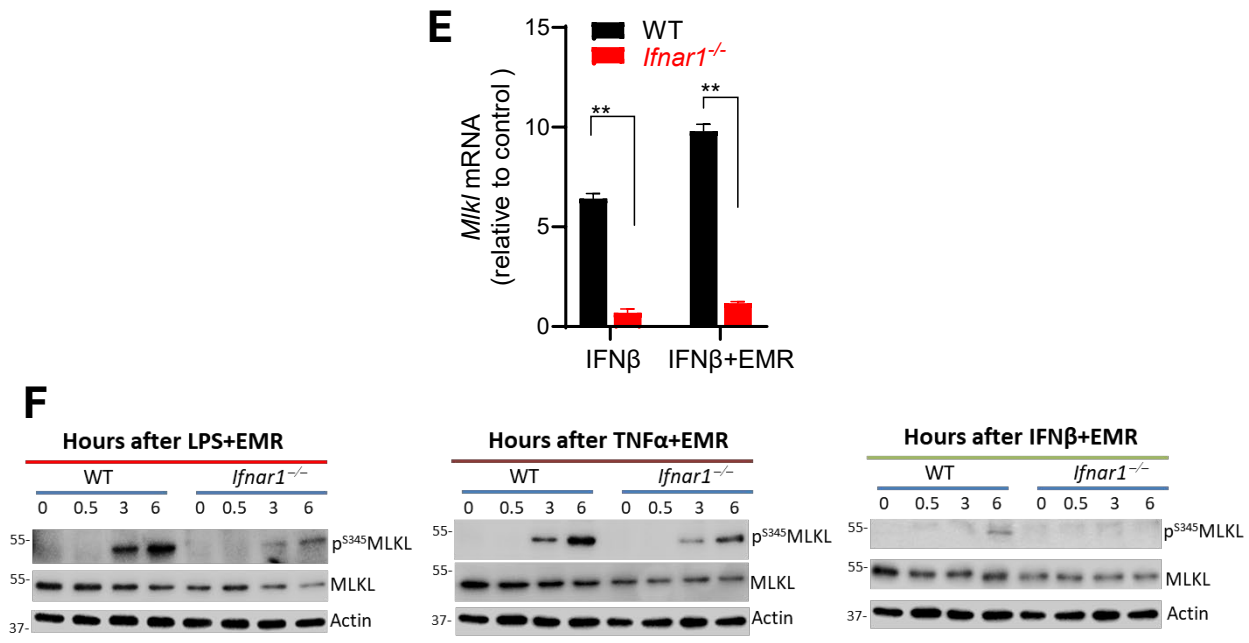

Figure 42. IFN signaling modulates necroptosis susceptibility through regulation of the MLKL expression

A WT and *Ifnar1*$^{-/-}$ BMDMs were treated with LPS (1ng/mL) in the presence of zVAD-fmk (50μM) for 6 h and differential gene expression was performed on microarray data comparing WT and *Ifnar1*$^{-/-}$ BMDMs treated with LPS and LPS+zVAD. **B, E** Expression of *Xaf1* **(B)**, and *Mlkl* **(E)** mRNA were measured by qRT-PCR analysis at 3 h following treatment of WT and *Ifnar1*$^{-/-}$ BMDMs with IFNβ (10ng/mL) alone and in combination with EMR (10μM). **C, D** After 24 hours cell death was evaluated by treating the WT and *Xaf*$^{+/-}$ BMDMs **(C)**, WT and *Xaf1*$^{-/-}$ RAW macrophages **(D)** with LPS (1ng/mL) +/- EMR (10μM), IFNβ (10ng/mL) +/- EMR (10μM), and TNFα (50ng/mL) +/- EMR (10μM), and GSK872 (10μM) by MTT. **F** Expression of MLKL was analyzed by western blotting of cell extracts collected from WT and *Ifnar1*$^{-/-}$ BMDMs at various time intervals following treatment with LPS (1ng/mL) + EMR (10μM), TNFα (50ng/mL) + EMR (10μM), and IFNβ (10ng/mL) + EMR (10μM). Each experiment was repeated at least three times. Graphs depict mean ± SEM. (**P<0.01, ****P<0.0001).

4.3.5. Reconstitution of MLKL in *Ifnar1*$^{-/-}$ macrophages

To investigate whether reduced MLKL expression is responsible for the enhanced necroptosis resistance of *Ifnar1*$^{-/-}$ BMDMs, we utilized RAW *Ifnar1*$^{-/-}$ macrophages previously generated previously in the lab through CRISPR-Cas9 approach. Our experimental approach began with the validation of the *Ifnar1*$^{-/-}$ cells by comparing IFNAR1 receptor expression in WT and *Ifnar1*$^{-/-}$ RAW macrophages following treatment with LPS and IFNβ at various time points. The results demonstrated a markedly lower level of Ifnar1 receptor in *Ifnar1*$^{-/-}$ cells compared to their WT counterparts. Furthermore, we observed a time-dependent decrease in cell surface expression of IFNAR1 in WT cells, likely due to receptor internalization following stimulation. In contrast, *Ifnar1*$^{-/-}$ cells showed no changes in receptor expression over time, confirming their knockout status **(Figure 43 A-C).**

Having validated the *Ifnar1*$^{-/-}$ cells, we proceeded to induce necroptosis in both WT and *Ifnar1*$^{-/-}$ RAW macrophages by treating them with LPS and IFNβ and EMR. Consistent with our observations in BMDMs, *Ifnar1*$^{-/-}$ RAW macrophages exhibited significant resistance to necroptosis compared to WT cells **(Figure 43 D)**. This finding further supports the protective role of IFNAR1 deficiency against necroptotic cell death across different macrophage types. To explore the molecular basis of this protection, we examined MLKL expression levels in both cell types. We found that RAW *Ifnar1*$^{-/-}$ macrophages expressed reduced levels of MLKL compared to WT cells **(Figure 43 E)**, mirroring our earlier observations in BMDMs. This consistent pattern of reduced MLKL expression in *Ifnar1*$^{-/-}$ cells across different macrophage models strengthens the hypothesis that lower MLKL levels may be a key factor in conferring protection against necroptosis in *Ifnar1*-deficient macrophages.

Given the significantly lower levels of MLKL observed in *Ifnar1*$^{-/-}$ BMDMs and RAW macrophages, we hypothesized that this reduction might be responsible for the resistance of *Ifnar1*$^{-/-}$ macrophages to necroptosis. To test this hypothesis, we decided to complement *Ifnar1*$^{-/-}$ RAW macrophages with MLKL. Using retroviral transduction, we successfully enhanced MLKL expression in these cells. The resulting cell line was designated as *Ifnar1*$^{-/-}$G418 (the antibiotic resistance marker- G418). The retroviral transduction of MLKL in RAW *Ifnar1*$^{-/-}$ macrophages resulted in increased expression of MLKL in these cells **(Figure 43 F-H)**. However, contrary to

our expectations, the reconstitution of MLKL in RAW *Ifnar1*$^{-/-}$ macrophages did not have any significant impact on their resistance to necroptotic cell death **(Figure 43 I)**. This unexpected result suggests that the resistance of *Ifnar1*$^{-/-}$ macrophages to necroptosis is not solely due to reduced MLKL expression. Instead, it implies that other molecules and mechanisms, beyond the reduced expression of MLKL, may play crucial roles in conferring resistance to necroptosis in *Ifnar1*$^{-/-}$ macrophages.

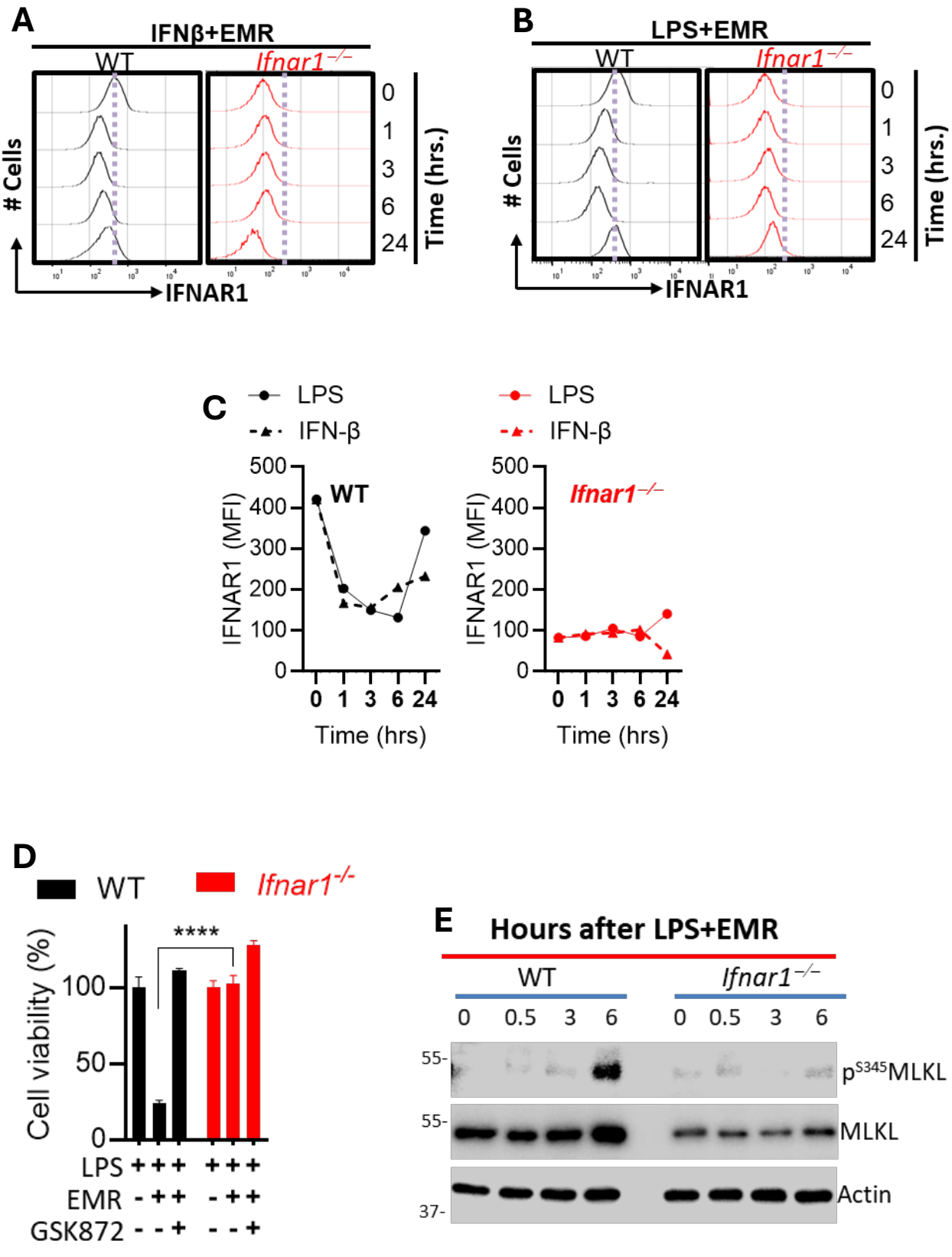
A
IFNβ+EMR
WT
Ifnar1−/−
Cells
IFNAR1
0
1
3
6
24
Time (hrs.)
B
LPS+EMR
WT
Ifnar1−/−
Cells
IFNAR1
0
1
3
6
24
Time (hrs.)
C
LPS
IFN-β
WT
IFNAR1 (MFI)
500
400
300
200
100
0
0 1 3 6 24
Time (hrs)
LPS
IFN-β
Ifnar1−/−
IFNAR1 (MFI)
500
400
300
200
100
0
0 1 3 6 24
Time (hrs)
D
WT
Ifnar1-/-
****
Cell viability (%)
100
50
0
LPS + + + + + +
EMR - + + - + +
GSK872 - - + - - +
E
Hours after LPS+EMR
WT
Ifnar1−/−
0 0.5 3 6 0 0.5 3 6
55-
pS345MLKL
55-
MLKL
37-
Actin

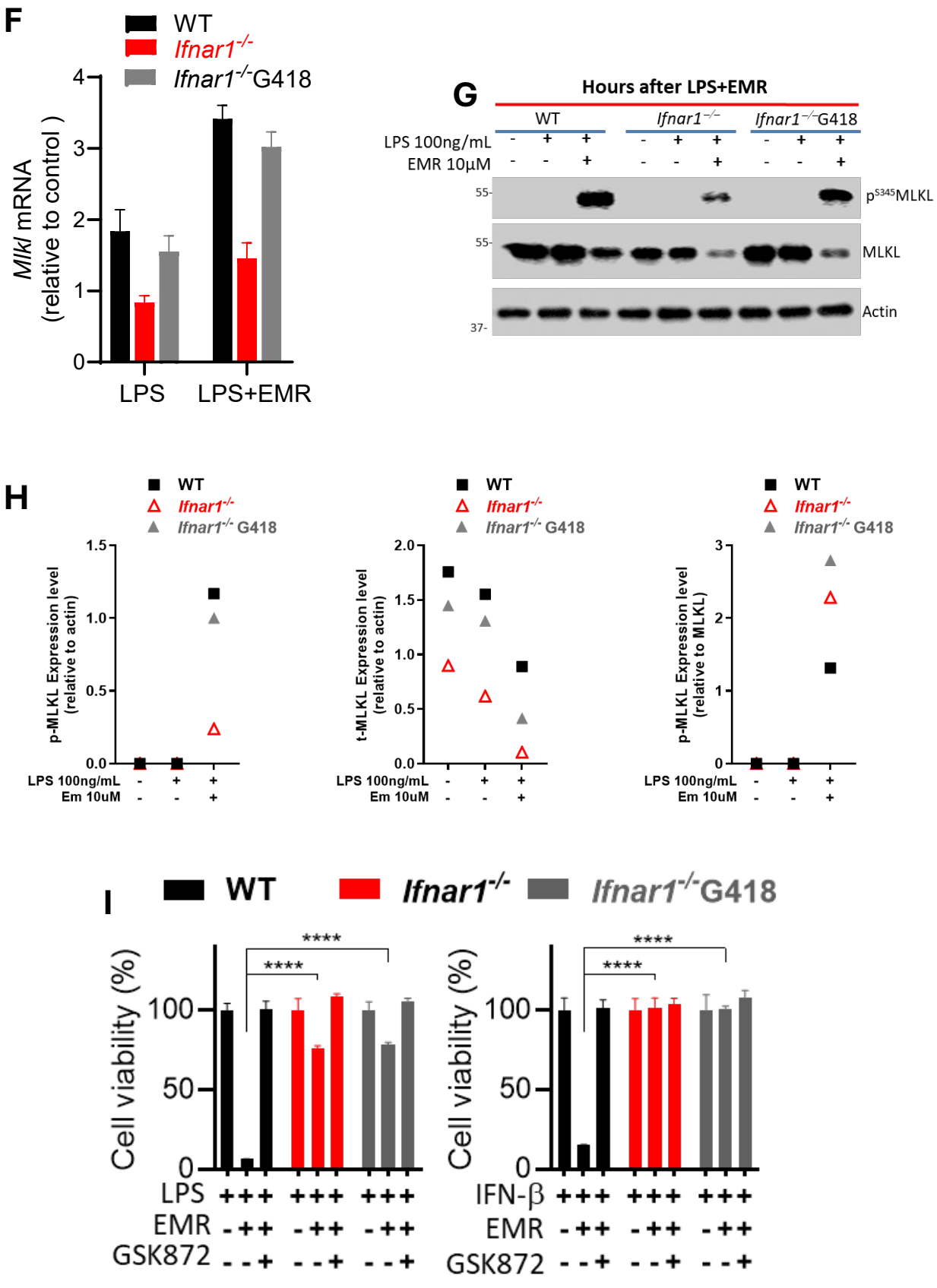
F
WT
Ifnar1-/-
Ifnar1-/-G418
Mlkl mRNA (relative to control)
LPS
LPS+EMR
G
Hours after LPS+EMR
WT
Ifnar1-/-
Ifnar1-/-G418
LPS 100ng/mL
EMR 10μM
pS345MLKL
MLKL
Actin
H
p-MLKL Expression level (relative to actin)
t-MLKL Expression level (relative to actin)
p-MLKL Expression level (relative to MLKL)
LPS 100ng/mL
Em 10uM
I
Cell viability (%)
LPS
EMR
GSK872
IFN-β

Figure 43. MLKL complementation in *Ifnar1*$^{-/-}$ RAW macrophages

A-C WT and *Ifnar1*$^{-/-}$ RAW macrophages were treated with LPS (100ng/mL) **(A**) and IFNβ (10ng/mL) **(B**) for different time intervals as shown. After that cells were stained with an anti-IFNAR1 antibody. Histograms depict the IFNAR1 receptor movement. The MFI values of IFNAR1 receptors are plotted using a line graph **(C**). **D** After 24 hours cell death was evaluated by treating the WT and *Ifnar1*$^{-/-}$ RAW with LPS (100ng/mL) +/- EMR (10μM), and GSK872 (10μM) by MTT. **E** Expression of MLKL was analyzed by western blotting of cell extracts collected from WT and *Ifnar1*$^{-/-}$ RAW macrophages at various time intervals following treatment with LPS (100ng/mL) + EMR (10μM). **F, G** Expression of *Mlkl* mRNA was measured by qRT-PCR analysis at 4 h **(F)**, and protein was measured by western blotting at 8 h **(G)** following the treatment of WT, *Ifnar1*$^{-/-}$, and *Ifnar1*$^{-/-}$G418 RAW macrophages with LPS (100ng/mL) alone and in combination with EMR (10μM). **H** Densitometric analysis of p^{S343}MLKL and MLKL relative to Actin was performed. **I** After 24 hours cell death was evaluated by treating the WT, *Ifnar1*$^{-/-}$ and *Ifnar1*$^{-/-}$G418 RAW macrophages with LPS (100ng/mL) +/- EMR (10μM), IFNβ (10ng/mL) +/- EMR (10μM), and GSK872 (10μM) by MTT. Each experiment was repeated at least three times. Graphs depict mean ± SEM. (****$P<0.0001$).

4.3.6. IFNAR1 signaling impact on necroptosis effector translocation

We evaluated whether the transfection of MLKL in *Ifnar1*$^{-/-}$ macrophages impacts necroptosis signaling following treatment with LPS + EMR. Our results revealed the enforced expression of MLKL in *Ifnar1*$^{-/-}$ macrophages does not impact the activation of STAT1 or STAT2 **(Figure 44 A)**. However, we observed a significant increase in the phosphorylation of RipK3 in *Ifnar1*$^{-/-}$G418 RAW macrophages compared to their *Ifnar1*$^{-/-}$ counterparts, **(Figure 44 A)**. Furthermore, our analysis revealed a striking and statistically significant elevation in the levels of phosphorylated MLKL in *Ifnar1*$^{-/-}$G418 RAW macrophages when compared to *Ifnar1*$^{-/-}$ RAW macrophages **(Figure 44 A)**. Furthermore, we observed that the phosphorylation of MLKL was increased in *Ifnar1*$^{-/-}$G418 RAW relative to *Ifnar1*$^{-/-}$ cells (**Figure 44 A**), yet this did not result in increased necroptosis (**Figure 43 I**). This unexpected outcome suggests that the increased accumulation of phosphorylated MLKL alone is insufficient to trigger necroptosis in *Ifnar1*$^{-/-}$ macrophages. This finding challenges the conventional understanding of the relationship between MLKL phosphorylation and necroptotic cell death, indicating that additional factors or regulatory mechanisms may be involved in determining the ultimate fate of these cells.

After the phosphorylation of MLKL and its subsequent oligomerization, this protein complex is translocated to the cell membrane, where it induces necroptosis. To investigate the role of IFNAR1 signaling in these molecular processes, we conducted a series of experiments using WT and *Ifnar1*$^{-/-}$G418 RAW macrophages. Following treatment with LPS and EMR, we isolated the membrane and cytosolic fractions of these cells for analysis **(Figure 44 B)**. In WT cells, we observed a dynamic shift in the localization of STAT1, STAT2, and IRF9 proteins. At the 3-hour mark, these proteins moved from the membrane to the cytoplasm, and their levels began to decrease as necroptosis progressed to later time points **(Figure 44 B)**. This pattern suggests the movement of the ISGF3 complex from the cytoplasm to the nucleus, a key step in the interferon signaling pathway. *Ifnar1*$^{-/-}$G418 cells showed no detectable ISGF3 complex proteins, highlighting the critical role of IFNAR1 in this process **(Figure 44 B)**. Activated RipK1 (pS166) exhibited a primarily cytoplasmic distribution in both WT and *Ifnar1*$^{-/-}$G418 cells, indicating that IFNAR1 signaling may not significantly affect RipK1 activation and localization. However, the activation pattern of RipK3 showed distinct differences between WT and *Ifnar1*$^{-/-}$G418 cells. In *Ifnar1*$^{-/-}$G418 cells, the levels of activated RipK3 in the cytoplasm were slightly reduced

compared to WT cells **(Figure 44 B)**. Surprisingly, we detected high levels of activated RipK3 in the membrane fraction of WT cells at 9 hours post-stimulation with LPS+EMR, which was not observed to the same extent in *Ifnar1*$^{-/-}$G418 cells. This finding suggests that IFNAR1 signaling may play a role in the membrane recruitment or retention of activated RipK3 during necroptosis.

Phosphorylated MLKL, a crucial effector of necroptosis, showed a preferential distribution in the membrane fraction of WT cells, with higher levels compared to the cytosolic fraction. This observation aligns with the current understanding of MLKL's role in membrane permeabilization during necroptosis. Strikingly, membrane fractions of *Ifnar1*$^{-/-}$G418 cells exhibited significantly reduced levels of phosphorylated MLKL **(Figure 44 B)**. The observed stark contrast in MLKL localization between WT and *Ifnar1*$^{-/-}$G418 cells offers compelling evidence for the crucial role of IFNAR1 signaling in facilitating the appropriate translocation of activated MLKL to the plasma membrane. This finding provides a mechanistic explanation for the heightened resistance of *Ifnar1*$^{-/-}$ cells to necroptosis.

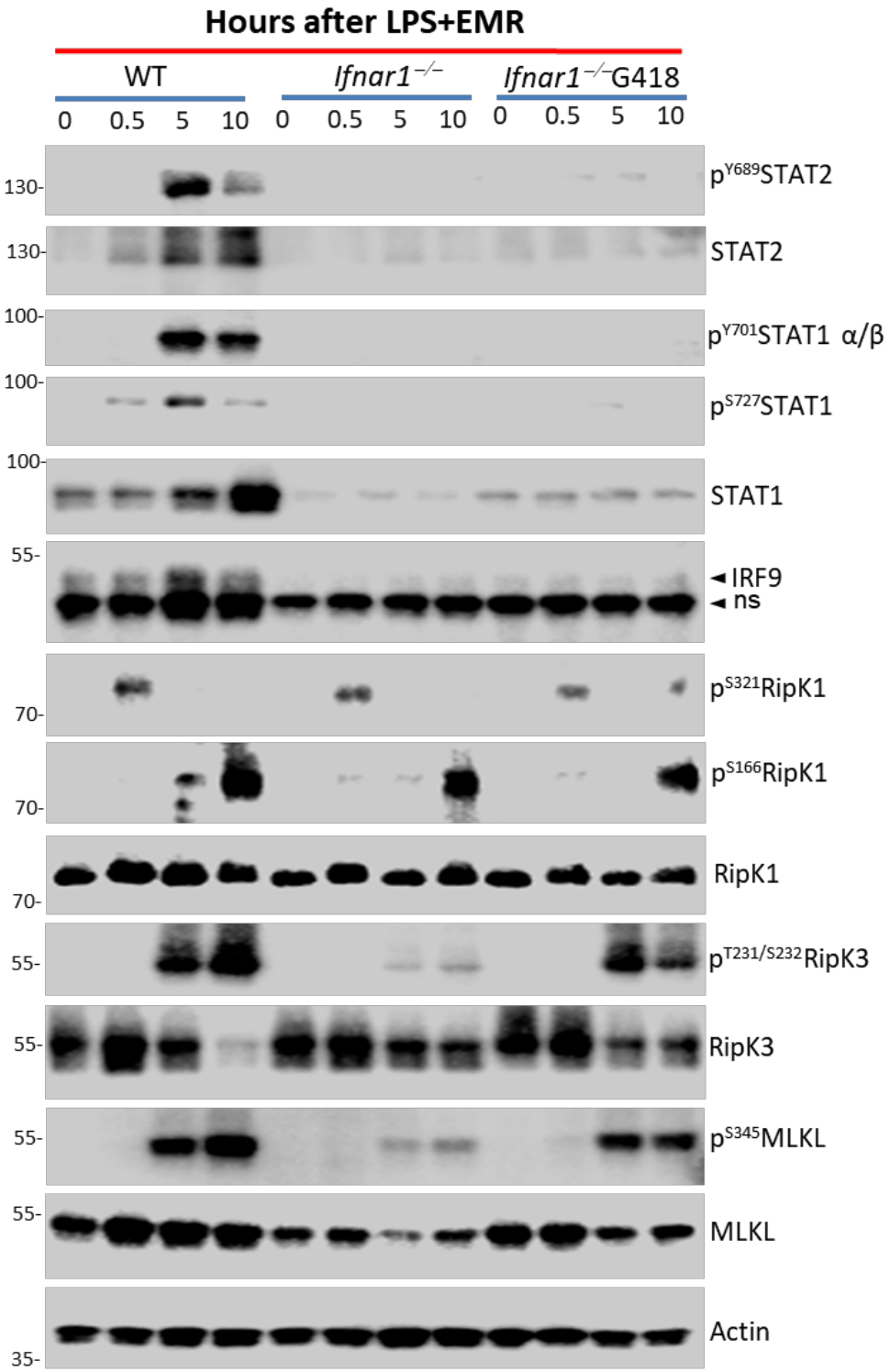
Hours after LPS+EMR
WT
Ifnar1−/−
Ifnar1−/−G418
0 0.5 5 10 0 0.5 5 10 0 0.5 5 10
130-
pY689STAT2
130-
STAT2
100-
pY701STAT1 α/β
100-
pS727STAT1
100-
STAT1
55-
◄IRF9
◄ns
70-
pS321RipK1
70-
pS166RipK1
70-
RipK1
55-
pT231/S232RipK3
55-
RipK3
55-
pS345MLKL
55-
MLKL
35-
Actin

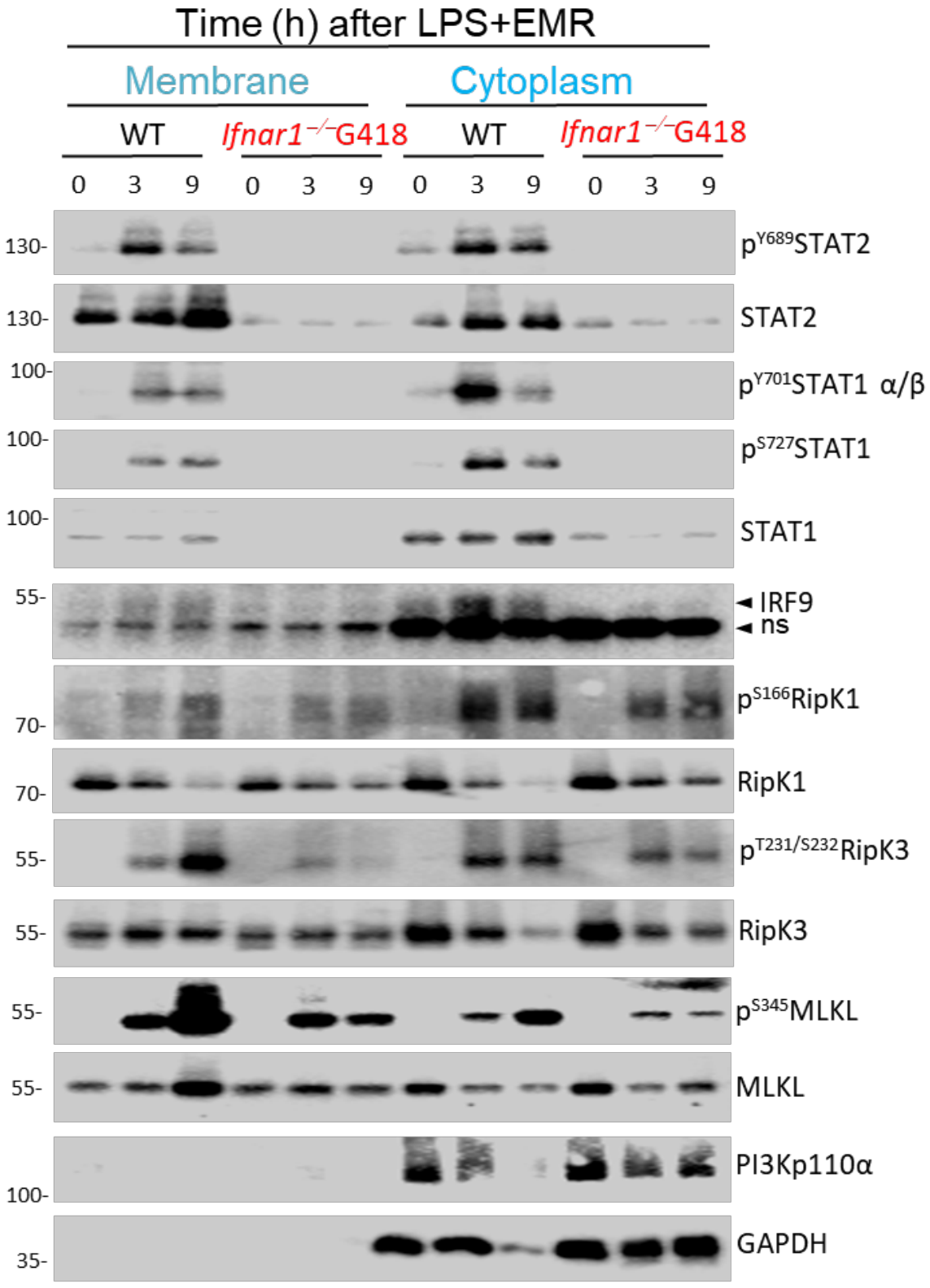
Time (h) after LPS+EMR
Membrane
Cytoplasm
WT
Ifnar1−/−G418
WT
Ifnar1−/−G418
0 3 9 0 3 9 0 3 9 0 3 9
130-
pY689STAT2
130-
STAT2
100-
pY701STAT1 α/β
100-
pS727STAT1
100-
STAT1
55-
◄ IRF9
◄ ns
70-
pS166RipK1
70-
RipK1
55-
pT231/S232RipK3
55-
RipK3
55-
pS345MLKL
55-
MLKL
100-
PI3Kp110α
35-
GAPDH

Figure 44. MLKL translocation and membrane localization

A WT, *Ifnar1*$^{-/-}$, and *Ifnar1*$^{-/-}$G418 RAW macrophages were treated with LPS (100ng/mL) and EMR (10μM). Cell extracts were collected at various time intervals and the activation of signaling proteins was evaluated by western blot analysis. **B** WT and *Ifnar1*$^{-/-}$G418 RAW macrophages were treated with LPS (100ng/mL) and EMR (10μM) for different time intervals as indicated. Membrane and cytoplasmic cell extracts were separated. Expression of various signaling proteins in the membrane and cytoplasmic extracts was evaluated by western blot analysis. Each experiment was repeated at least three times.

These findings collectively suggest that IFNAR1 signaling plays a pivotal role in the localization of key necroptosis mediators, particularly the translocation of activated MLKL from the cytoplasm to the membrane in macrophages. The inability of MLKL to properly localize to the cell membrane in the absence of IFNAR1 signaling likely impairs its pore-forming function, which is essential for the execution of necroptosis. The absence of IFNAR1 signaling appears to disrupt this crucial step in the necroptosis pathway. Thus, this observation not only highlights the importance of interferon signaling in the necroptotic pathway but also elucidates a key reason behind the necroptosis-resistant phenotype observed in *Ifnar1*-deficient cells. This discovery also opens new avenues for potential therapeutic interventions in diseases characterized by dysregulated cell death processes. Further research is warranted to elucidate the precise mechanisms by which IFNAR1 signaling influences the subcellular localization of necroptosis effectors and to explore the potential implications of this relationship in various pathological conditions.

5. DISCUSSION

Necroptosis, a form of programmed cell death, plays a dual role in the immune system. While it serves as a crucial defense mechanism to protect against virulent pathogens, the persistent rupture of host cells by necroptosis in response to sterile triggers during chronic inflammatory conditions can lead to undesirable outcomes. The ubiquitous presence of macrophages and macrophage-like cells, such as Kupffer cells in the liver and microglia in the brain, across diverse non-lymphoid organs has sparked intense research interest in understanding the mechanisms that initiate and regulate macrophage necroptosis.

On one hand, necroptotic macrophages have the potential to act as potent effector cells of the innate immune system, capable of combating a wide range of viral and bacterial infections. This highlights their importance in the body's defense against pathogens. On the other hand, the activation of necroptosis in these cells can contribute to tissue damage and inflammation in various disease states.

Despite significant advancements in our understanding of necroptosis signaling pathways, the intricate molecular mechanisms underlying this process remain elusive. The complex interplay between pro-survival and pro-death signals and the context-dependent nature of necroptosis activation continues to challenge researchers in the field.

As our knowledge of necroptosis expands, it becomes increasingly clear that a delicate balance must be struck between harnessing its protective potential and mitigating its harmful effects. Further research is needed to fully elucidate the precise molecular mechanisms governing necroptosis in macrophages and other immune cells, aiming to develop targeted therapies for both infectious and inflammatory diseases.

5.1. ARF6: A Novel Regulator of Programmed Cell Death Initiation

RipK1, is a multifaceted enzyme that participate in several signaling complexes and plays a pivotal role in governing cell fate decisions. This versatile kinase exhibits remarkable functional plasticity, integrating into diverse signaling complexes within the cell. Depending on the cellular context and specific molecular interactions, RipK1 can either promote cell survival or trigger cell death by

multiple pathways (Festjens et al., 2007). Following TNF-R engagement polyubiquitylated RipK1 recruits TGFβ-activated kinase 1 (TAK1) and MAP3K7-binding protein 2 (TAB2)/TAB3, which phosphorylates JUN N-terminal kinase (JNK) and $p38^{MAPK}$, as well as the IκB kinase (IKK) complex, leading to the activation of MAPK and NF-κB which promotes cell survival (McMahon & Boucrot, 2011). The ubiquitination of RipK1 status serves as a critical switch, altering its functional role within cellular signaling networks. When the ubiquitination of RipK1 is modified, whether through deubiquitination or changes in ubiquitin chain types, it triggers the dissociation of RipK1 from the pro-survival signaling complex. This detachment event marks a significant shift in the function of RipK1 (McComb et al., 2012). Consequently, RipK1 participates in the "ripoptosome" or "necrosome" complex. A20 and CYLD mediate ubiquitin editing of RipK1 (Onizawa et al., 2015; Schworer et al., 2014) to modulate RipK1-RipK3 interaction. The interplay between active caspase-8 and RipK1 signaling gives rise to a distinct form of programmed cell death known as ripoptosis. Inhibition of caspase-8 activity endogenously by cFLIP (Feoktistova et al., 2011) or exogenously by caspase inhibitors such as zVAD or Emricasan (EMR) (Brumatti et al., 2016; Ito et al., 2016) results in the phosphorylation of RipK3, which in turn phosphorylates the pseudo kinase MLKL (He et al., 2009; Vandenabeele et al., 2010; Vanlangenakker, Vanden Berghe, et al., 2011). This leads to the formation of MLKL-trimers, which relocate to the cell membrane and interact with PtdIns(4,5)P2, leading to the leakage of the cell membrane (Xia et al., 2022) and consequent release of intracellular DAMPs (McComb et al., 2014; Robinson et al., 2012; Shutinoski et al., 2016). The initial molecular events that precede RipK1 activation and drive cells toward necroptosis remain largely enigmatic. This gap in our understanding prompted an exploration of alternative mechanisms that might orchestrate the early stages of this cell death pathway. So, we considered the possibility that proteins that are involved in endosomal sorting might mediate the early signaling events that promote cell death. Since ARF6 is located at the plasma membrane and the endosomal compartments (D'Souza-Schorey & Chavrier, 2006), we evaluated its role in the cell signaling pathways that promote cell death. *In silico* analysis of the amino acid sequence of ARF6 indicates the presence of the myristoylation site at the N-terminal followed by a polybasic site (**Figure 4 B**) that is typical of proteins involved in shuttling cargo between different compartments in the cell. Our findings demonstrate that ARF6 plays a crucial role in initiating the formation of both the ripoptosome and necrosome, two key signaling

complexes involved in RipK1-dependent cell death. ARF6 achieves this by orchestrating the degradation of cIAP1/2.

5.1.1. Role of ARF6 in Receptor Endocytosis and Post-Endocytic Cytokine Regulation during Necroptosis Signaling

While receptor-endocytosis can proceed through various pathways (Barbieri et al., 2016), endocytosis of TLR4 was reported to be mediated by the large GTPase dynamin, which promoted the phosphorylation of IRF3 and expression of IFN-β (Kagan et al., 2008; Rajaiah et al., 2015). It was also reported that the endocytosis of IFNAR1 occurs through classical clathrin- and dynamin-dependent endocytosis (Marchetti et al., 2006). While our preliminary results indicate that the inhibition of dynamin with inhibitors leads to a reduction in the secretion of IFN-β, we show that ARF6 plays a significant role in the expression of cytokines, particularly during necroptosis stimulation. In contrast to the reported role of dynamin in facilitating the endocytosis of TLR4 (Kagan et al., 2008) we did not observe any impact of ARF6 in the endocytosis of TLR4 upon engagement with LPS. Since internalization of cargo can occur through multiple mechanism it is likely that that ARF6 plays a key role in facilitating the downstream trafficking of the cargo after endocytosis. The functional relationship between dynamin and ARF6 in clathrin-mediated endocytosis has been well established as ARF6 was shown to be activated by dynamin in clathrin-mediated endocytosis through various guanine nucleotide exchange factors (Okada et al., 2015; Palacios et al., 2002).

It has been previously observed that ARF6 promotes the endocytosis of TLR4, which impacts the activation of IRF3. Our recent results have shown that during necroptosis stimulation, the secretion of TNFα is dependent on the MyD88 adapter protein, whereas the secretion of IFN-β relies on TRIF signaling. While we observed that the activation of IRF3 was reduced in *Arf6*$^{-/-}$ cells, the levels of both TNFα and IFN-β were reduced to the same degree during the necroptosis stimulation of *Arf6*$^{-/-}$ cells, suggesting the involvement of a different mechanism. It has been reported that the endocytosis of TLR4 and TRIF signaling in macrophages are under separate mechanistic control (Palacios et al., 2002). We have shown that the activation of the MAPK pathway is significantly impacted by ARF6, which could potentially explain the reduction in the levels of cytokines in *Arf6*$^{-/-}$ cells. Since the endocytosis of TLR4 was not impacted in *Arf6*$^{-/-}$ cells, yet the downstream

pathways of cell death were impacted, these results implicate the involvement of ARF6 at a step that occur post receptor endocytosis.

It has been reported that ARF6-mediated internalization of TLR4 promotes the expression of TNFα, IL-6, and IFN-β (Murase et al., 2018; Van Acker et al., 2014). In contrast to these results, we failed to detect any impact of ARF6 on the endocytosis of TLR4, and the impact on cytokine expression in response to LPS stimulation was negligible. However, in response to TLR4 engagement during necroptosis stimulation, we observed that the expression of the two key inflammatory cytokines TNFα and IFN-β which are relevant in necroptosis was reduced in *Arf6*$^{-/-}$ cells, but the levels were not reduced substantially to explain the degree of necroptosis resistance observed in *Arf6*$^{-/-}$ cells. Furthermore, necroptosis resistance was also observed when *Arf6*$^{-/-}$ cells were stimulated with IFN-β+EMR, implying that the resistance of *Arf6*$^{-/-}$ cells to necroptosis cannot be due to impaired TRIF-signaling.

It was reported that the inhibition of dynamin with the inhibitor Dynasore, which inhibited the endocytosis of TLR4, did not have any impact on p38^{MAPK} activation (Kagan et al., 2008). In contrast, our results indicate that ARF6 promotes the activation of the various members of the MAPK pathway during necroptosis stimulation by LPS+EMR, and this effect was more pronounced during necroptosis stimulation by IFN-β+EMR. Type I interferon signaling has been shown to promote the activation of p38^{MAPK} through the engagement of the small GTPase Rac1 (Uddin et al., 2000). The Ras superfamily of small GTPases includes Ras, Rho, Ran, Rab, and Arf GTPases, with different members of the subfamily controlling cell proliferation, morphology, nuclear transport, and vesicle transport (Wennerberg et al., 2005). ARF6 has been shown to modulate Rac1 activity through the engagement of various exchange factors (Radhakrishna et al., 1999; Santy et al., 2005), and it is conceivable that some of those exchange factors are involved in necroptosis signaling.

5.1.2. Regulation of Endo-Lysosomal Function and Cell Death by ARF6

Recent studies have highlighted the importance of endosomal and lysosomal biogenesis in regulating cellular homeostasis and immune responses (Yang & Wang, 2021). Our findings suggest that ARF6 regulates lysosomal homeostasis, as evidenced by compromised lysosomal maturation

and reduced lysosome numbers in *Arf6*$^{-/-}$ cells. This is consistent with previous reports demonstrating that ARF6 promotes autophagy, a process closely linked to lysosomal function (Moreau et al., 2012). Notably, lysosomal degradation of key regulators of cell survival, such as the cIAP1-TRAF2 complex, has been implicated in the modulation of TNFα-induced apoptosis (Vince et al., 2008). The reduced lysosome numbers and compromised autophagic flux in *Arf6*$^{-/-}$ cells may render them more susceptible to infection and compromise their ability to maintain cellular homeostasis. Furthermore, our data indicates that *Arf6*$^{-/-}$ cells exhibit impaired activation of RipK1-dependent cell death pathways, which are normally inhibited by cIAP1/2 (McComb et al., 2012). These findings collectively underscore the critical role of ARF6 in regulating endo-lysosomal homeostasis, autophagy, and cell death pathways.

5.1.3. ARF6 Modulates RipK1 Ubiquitination and Interferon Signaling

RipK1 is subject to extensive ubiquitin editing by ubiquitin ligases and deubiquitinases, which allows RipK1 to participate in multiple cell-signaling complexes that promote cell survival, apoptosis, ripoptosis, and necroptosis (de Almagro et al., 2015). Ubiquitination of RipK1 by cIAPs and LUBAC in response to TNF-R engagement promotes NF-kB activation and cell survival (Dynek et al., 2010; Peltzer et al., 2016; Silke & Vucic, 2014). While the transition of RipK1 away from the cell survival complex requires deubiquitination of RipK1 (Vucic et al., 2011), necroptosis signaling is facilitated by K63 and linear ubiquitination of necroptosis proteins (de Almagro et al., 2015; S.-K. Hsu et al., 2020; Lawlor et al., 2015; Moriwaki & Chan, 2016). Ubiquitination of RipK1 coincides with its involvement in the necrosome complex and the phosphorylation of RipK3 (de Almagro et al., 2015). In the necrosome complex, IAPs do not impact the ubiquitination of RipK1 but facilitate the recruitment of RipK1 to the complex (de Almagro et al., 2015, 2017). HOIP and HOIL1 mediate linear ubiquitination of RipK1 in the necrosome but are not essential for necrosome formation. RipK1 was shown to be conjugated with the M1-/K63-linked ubiquitin chains during necroptosis (de Almagro et al., 2017). The E3 ubiquitin ligase PELI1 was reported to mediate K63 ubiquitination of RipK1 to promote necroptosis (H. Wang et al., 2017). It was reported that RipK3 undergoes K5-linked ubiquitination, which promotes the formation of the RipK1-RipK3 complex that is inhibited by A20 (Onizawa et al., 2015). Our results indicate that the degradation of IAPs correlates inversely with the phosphorylation of RipK1 in an ARF6-dependent manner. It is therefore, conceivable that the ubiquitination of RipK1 and RipK3 is

reduced in *Arf6*$^{-/-}$ cells stimulated with LPS+EMR. Preliminary results indicate that there is reduced ubiquitination of RipK1 and RipK3 in *Arf6*$^{-/-}$ cells (results not shown).

It has been previously reported that in addition to the activation of STAT1 and STAT2, type I interferon signaling promotes the activation of STAT3 (K. Fink & Grandvaux, 2013) which acts in a negative capacity to inhibit the STAT1-mediated transcription of genes (Bhatt et al., 2012). We observed that during stimulation of cells with LPS+EMR the activation of STAT3 is dependent on the activation of the p38^{MAPK} pathway. Furthermore, stimulation of cells with IFN-β+EMR promoted the activation of STAT3, possibly through the activation of the p38^{MAPK} pathway. However, the activation of STAT3 does not play a role in the activation of necroptosis as inhibition of STAT3 does not influence cell death. In contrast to the effect on TLR4, we observed that the internalization of Ifnar1 is partially modulated by ARF6. It has been reported that type I interferon signaling is modulated by the endo-lysosomal recycling of Ifnar1 (Qian et al., 2011). The RhoA GTPase has been shown to regulate type I interferon signaling (Fan et al., 2023). While the endocytosed receptors are mainly viewed as being targeted for degradation, more evidence suggests that cytokine receptors use the endosomal pathway primarily as a signaling platform (Cendrowski et al., 2016).

5.2. Necroptosis Signaling Amplifies Inflammation via ISGF3-MK2-TTP Axis

Necroptosis is a regulated form of necrotic cell death that plays a significant role in inflammation and various inflammatory diseases. This programmed cell death pathway is closely intertwined with the immune system and can both promote and exacerbate inflammatory responses. Necroptosis of cells has been shown to exacerbate various acute and chronic inflammatory diseases (Afonso et al., 2015; Duprez et al., 2011; Günther et al., 2011; Jun et al., 2020; Karunakaran et al., 2016; Z. Lu et al., 2021; Ofengeim et al., 2015; Re et al., 2014), and it has been suggested that this is perpetuated by the spillage of intracellular contents to the extracellular milieu, which engages additional signaling pathways that promote inflammation (G. Y. Chen & Nuñez, 2010). Our findings demonstrate that the inflammatory response is significantly enhanced during necroptosis signaling, occurring independently and before the onset of actual cell death. This suggests that the pro-inflammatory effects of necroptosis are not solely due to the release of cellular contents upon cell rupture but are an integral part of the signaling process itself.

While the premature cell death of macrophages can impact the expression of cytokines (Phuong et al., 2021), the augmentation in the expression of inflammatory cytokines during necroptosis signaling that we have shown here is not related to cell death for the following reasons: (1) an increase in cytokine expression occurred prior to the commencement of cell death, (2) cytokine expression was augmented in *RipK3*$^{-/-}$ cells that were completely resistant to cell death, (3) *Ifnar1*$^{-/-}$ or *Ticam1*$^{-/-}$ cells displayed reduced cell death but the cytokine expression was still augmented, and (4) Increased expression of inflammatory cytokines was also observed in *Mlkl*$^{-/-}$ cells that are resistant to necroptosis(Najjar et al., 2016).

5.2.1. RipK1 and MyD88 drive TNFα in Necroptosis

It was previously reported that the activation of necroptosis signaling promotes the expression of several inflammatory cytokines and chemokines independently of cell death, which was dependent on the kinase activity of RipK1 and RipK3 (Najjar et al., 2016). While we also observed that the expression of TNFα during necroptosis signaling was dependent on the kinase activity of RipK1, we failed to detect any involvement of RipK3 in the augmentation of TNFα production. In our experiments, the expression of TNFα was increased in both WT and *RipK3*$^{-/-}$ cells to the same degree. Interestingly, the elevation of TNFα expression during necroptosis signaling was not dependent on MLKL (Najjar et al., 2016), implying that the complete necrosome platform is not required for the augmentation of inflammation. Since the necrosome formation is compromised in the absence of RipK3, this indicates that the translocation and phosphorylation of RipK1 towards the necrosome pathway may be responsible for the upregulation of inflammation. In the absence of necroptosis signaling, RipK1 has been shown to promote cell survival and inflammation (Dondelinger et al., 2015; Ito et al., 2016; Kondylis et al., 2017; Lukens et al., 2013; Meylan et al., 2004; Roderick et al., 2014). RipK1 undergoes K63 ubiquitination, creating binding sites for TAB2. This interaction facilitates the recruitment and activation of TAK1, which subsequently phosphorylates IκB. Phosphorylated IκB is then targeted for degradation, releasing NFκB and enabling its translocation to the nucleus, where it activates the transcription of target genes (Lee et al., 2003; Ofengeim & Yuan, 2013). While the exact mechanism of RipK1-mediated MAPK activation remains unclear, evidence suggests that TAK1 activation plays a crucial role in this process. Once activated, TAK1 is thought to initiate a phosphorylation cascade that ultimately leads to the activation of various MAPK family members, thus linking RipK1 signaling to MAPK

pathway stimulation (Lee et al., 2003; Ofengeim & Yuan, 2013). It has also been suggested that RipK1 may mediate the $p38^{MAPK}$ activation by recruiting the MEKK3 (Lee et al., 2003).

In TLR4 signaling, the adapter protein MyD88 plays a critical role in inducing TNFα expression, while the TRIF adapter is essential for triggering type I interferon production. This division of labor between MyD88 and TRIF in mediating distinct cytokine responses downstream of TLR4 is a well-established paradigm in innate immune signaling (Akira & Takeda, 2004). Our results uphold this paradigm during stimulation of cells with LPS or LPS + EMR. Surprisingly, it was reported that the upregulation of TNFα during TLR4- or TLR4-induced necroptosis signaling was abrogated in *Ticam1*$^{-/-}$ cells (Najjar et al., 2016). Considering that MyD88 is indispensable for the TLR4-induced expression of TNFα, it is unclear how this role can be taken over by TRIF during necroptosis signaling. In contrast, a later study reported that the activation of necroptosis signaling results in increased expression of TNFα in cells with compromised TRIF signaling (Muendlein et al., 2020), indicative of an inhibitory role of TRIF in the elevation of TNFα expression. It has also been reported that the kinase activities of RipK1 and RipK3 promote the production of IFNβ during necroptosis signaling through the IRF/TBK1 axis (Saleh et al., 2017). Our experiments revealed that TNFα expression was similarly elevated during necroptosis signaling in both *Ifnar1*-deficient and *Ticam1*-deficient cells. This observation suggests that TRIF signaling may play an inhibitory role in TNFα expression, rather than enhancing it as previously thought.

5.2.1.1. RipK1-Independent Elevation of TNFα Expression in Necroptosis

Our prior research demonstrated that during necrosome signaling in macrophages, RipK1 phosphorylation remains consistent between wild-type and *Ifnar1*-deficient cells. However, *Ifnar1*-deficient cells exhibit reduced phosphorylation (activation) of RipK3 and MLKL, leading to enhanced resistance against necroptosis compared to their wild-type counterparts (McComb et al., 2014). The comparable RipK1 phosphorylation in wild-type and *Ifnar1*-deficient cells, coupled with the heightened inflammatory response during necroptosis signaling in *Ifnar1*-deficient cells, indicates that RipK1 kinase activity may not be the primary driver of increased TNFα expression in these cells. This hypothesis is further supported by our observation that *Ifnar1*-deficient cells showed resistance to the inhibitory effects of Nec-1 when administered 1.5 hours after stimulation,

suggesting alternative mechanisms are at play in regulating TNFα production during necroptosis in *Ifnar1*-deficient cells.

5.2.2. Necroptosis Regulates Cytokines via ISGF3-MK2-TTP

Since TNFα signaling is an important mediator of inflammatory responses that influences various disease outcomes (Jang et al., 2021), we evaluated how the expression of TNFα is modulated during necroptosis signaling. Our investigation into the modulation of TNFα expression during necroptosis signaling revealed a complex regulatory landscape of inflammatory responses. While necroptosis signaling led to the upregulation of numerous genes associated with TNFα signaling and the MAPK pathway, it simultaneously exerted a suppressive effect on other cytokines, notably IL-12 and IL-6. Particularly the expression of IL-12 was dramatically inhibited during necroptosis signaling, raising the intriguing possibility that reduced IL-12 levels could serve as a potential biomarker for necrosome activation *in vivo*—a hypothesis that warrants further investigation. Interestingly, previous research has reported an upregulation of the anti-inflammatory cytokine IL-10 during necroptosis signaling in *Ifnβ*-deficient cells, adding another layer of complexity to the cytokine regulation in this context (Muendlein et al., 2020). In contrast, we observed that the expression of IL-10 was downregulated in *Ifnar1*$^{-/-}$ cells that were stimulated with LPS or LPS + EMR. It is well established that type I interferon promotes the expression of IL-10 (F. W. McNab et al., 2014). We analyzed the published ChiP-Seq data of BMMs stimulated with IFNβ (Platanitis et al., 2019) and observed that there are multiple ISRE sites in the promoter region of IL-10, which explains the reduced expression of IL-10 by *Ifnar1*$^{-/-}$ cells. Thus, the impact of necroptosis signaling on the upregulation of cytokines does not appear to be global, and additional mechanisms exist that modulate the expression of various cytokines separately. We have shown here that ISGF3 signaling induces the expression of TTP, which promotes the degradation of TNFα. It has been previously reported that TTP promotes the degradation of various cytokines/chemokine mRNAs that harbor the AU-rich elements (AREs) at the 3-UTR (e.g., *Tnfα, Il1a, Il1b, Il6, Ifnβ, Il10, Cxcl1, Ccl4, Ccl2, Ccl3*) (Tiedje et al., 2016).

5.2.2.1. Necroptosis Regulates TNFα Expression through a Post-Transcriptional Mechanism

Our results indicate that the transcription and translation of TNFα are upregulated during necrosome activation of macrophages. There have been contradictory reports regarding the translation of TNFα during the necrosome activation of WT macrophages, with one report indicating that the TNFα protein levels are upregulated (Najjar et al., 2016), whereas the other report showed that the translation of *Tnfα* mRNA is not upregulated (Muendlein et al., 2020). The later report indicated that the IFNAR1-signaling in WT cells, downstream of TRIF, is responsible for the suppression of the translation of *Tnfα* mRNA. The reasons for these contradictory results in WT cells are not clear but could be related to differences in basal type I interferon levels, which might exert their impact through tonic IFNAR1 signaling to suppress the protein levels. We have observed that the *Tnfα* mRNA and protein levels are upregulated in *Ifnar1*$^{-/-}$ cells; however, our results indicate that this is due to a post-transcriptional and pre-translational mechanism that involves the expression of the mRNA degrading protein TTP (*Zfp36*) downstream of ISGF3.

GSEA of *Ifnar1*$^{-/-}$ cells revealed a major downregulation of the innate immune response, including the type I and type II interferon responses, which is expected since type I interferon is a major mediator of innate immune response (F. W. McNab et al., 2014). On the other hand, there was an upregulation of various pathways, such as RNA modification, antioxidant defense, and mitochondrial metabolism in *Ifnar1*$^{-/-}$ cells, which can influence the expression of cytokines. A prior report indicated that the upregulation of cytokines during the necrosome activation of *Ifnar1*$^{-/-}$ cells is related to increased protein translation (Muendlein et al., 2020). Necroptosis stimulation was shown to result in increased puromycin incorporation by cells. However, the uptake of puromycin was similar in WT versus *Ifnβ*$^{-/-}$ cells (Muendlein et al., 2020). While the GSEA of our data indicated the enrichment of the mitochondrial translation in *Ifnar1*$^{-/-}$ cells, we did not observe any enrichment in the eIF2 pathway and there was no detectable increase in the activators (p70S6K, eIF4E, AKT) or inhibitor (4E-BP1) of protein translation in *Ifnar1*$^{-/-}$ cells during necrosome activation. Furthermore, if increased protein translation was responsible for the elevated inflammatory response in *Ifnar1*$^{-/-}$ cells, then one would expect a global upregulation of protein expression, which is not the case. Type I interferon signaling has been shown to promote, rather than inhibit, the core metabolism in myeloid cells (D. Wu et al., 2016).

5.2.2.2. IFNAR1 Signaling Modulates Cytokines Expression via p38^{MAPK}-TTP Pathway During Necroptosis Activation

Our results indicate that IFNAR1 signaling impacts cytokine expression during necroptosis stimulation through the modulation of the p38^{MAPK}-TTP axis. We have shown that ISGF3 signaling promotes the expression of TTP, which is an RNA-binding protein that controls the stability of mRNA of various transcripts that contain an ARE in the 3' UTR (Tiedje et al., 2016). Downstream of p38^{MAPK} activation, MK2 and MK3 phosphorylate TTP at various sites, leading to increased stability but compromised activity of TTP (Ronkina et al., 2019). This phosphorylation negatively affects the ability of TTP to regulate TNFα, which results in increased TNFα levels (Clement et al., 2011; Ronkina et al., 2019). When the p38^{MAPK} is inhibited, the phosphorylation and stability of TTP are compromised, which results in poor TNFα levels. We have previously reported that TTP inhibits necroptosis only when cells are stimulated with an LPS+zVAD+p38^{MAPK} inhibitor (Ariana et al., 2020). We now show that TTP inhibits necroptosis only when cells are stimulated with IFNβ + EMR. This suggests a context-dependent regulation of necroptosis by TTP. In addition to modulating the activity and stability of TTP, MK2 mediates the inhibitory phosphorylation (S321) and inhibits the necrosome activating phosphorylation (S166) of RipK1, which is in agreement with previous studies (Dondelinger et al., 2017; Jaco et al., 2017; Menon et al., 2017). The combined absence of IFNAR1 and MK2 leads to an unexpected outcome: a decrease in the pro-death S166 phosphorylation of RipK1 while leaving its inhibitory phosphorylation unchanged. This selective effect effectively dissociates the inhibitory and stimulatory phosphorylation events on RipK1 during the activation of cell death signaling complexes.

Interferons have been previously reported to promote the induction of TTP to limit the expression of inflammatory cytokines (Sauer et al., 2006). A gamma-activating sequence (GAS) was reported in the promoter of *Zfp36* (Sauer et al., 2006). However, this induction of TTP required the concomitant addition of the p38^{MAPK} agonist anisomycin. While we observed that the addition of the caspase inhibitor EMR results in the activation of the p38^{MAPK} pathway in cells treated with IFNβ or LPS, the induction of TTP was reduced during necroptosis activation of WT cells and reduced even further during necroptosis activation of *Ifnar1*-deficient cells. We did not detect any role of IFN-γ in inducing necroptosis and show that the upregulation of TNFα during necroptosis stimulation is compromised in cells that are deficient in type I interferon signaling (e.g., *Ifnar1*$^{-/-}$,

Stat1$^{-/-}$, *Stat2*$^{-/-}$, and *Irf9*$^{-/-}$) but not in type II interferon signaling (*IFNγ*$^{-/-}$). In support of this, we have revealed an ISRE in the promoter of *Zfp36*. It was reported that IL-10 promotes TTP induction through the activation of STAT3 which impacted the expression of IL-6, IL-12, and IL-23, but not TNFα (Gaba et al., 2012). Our research revealed that during cell death signaling, the expression of TNFα but not IL-6 and IL-12 was increased. This selective cytokine response suggests that the IL-10/STAT3 pathway is likely not the primary driver of the enhanced inflammatory response observed under these conditions.

We have revealed the dichotomous role of type I interferon signaling in necroptosis. While IFNβ induces the transcription of MLKL to promote necroptosis (Sarhan et al., 2019), it also induces the expression of TTP to inhibit necroptosis. Interestingly, IFNβ signaling has been previously reported to inhibit inflammasome signaling (Guarda et al., 2011), and a later study reported that TTP inhibits NLRP3-dependent inflammasome signaling (Haneklaus et al., 2017).

We have highlighted the complex relationship between TNFα and IFNβ signaling in the regulation of inflammatory response during necroptosis signaling. While necroptosis signaling by multiple TLRs is dependent on TNFα- (Kaiser et al., 2013) and- Ifnar1- (McComb et al., 2014) signaling, the molecular relationship between these two pathways in necroptosis induction in response to the same TLR engagement is still not clear. We have shown here that *Ifnar1*-deficient macrophages remain significantly resistant to necroptosis despite expressing higher levels of TNFα relative to WT cells. A key downstream signaling pathway of necroptosis is likely blocked in *Ifnar1*-deficient cells.

5.3. IFNAR1-Necroptosis Axis- From Receptor to Executioner

The relationship between type I interferon (IFN-I) signaling and necroptosis in macrophages has emerged as a critical area of research in cell death mechanisms. Recent studies have revealed that IFN-I receptor signaling plays a crucial role in promoting necroptosis in macrophages, acting as a key mediator in the execution of this programmed cell death pathway. Studies have demonstrated that IFNAR1 signaling is essential for the induction of necroptosis in macrophages stimulated by various pathways. *Ifnar1*-deficient macrophages show remarkable resistance to necroptosis induced by LPS, poly I:C, TNF-α, and IFN-β in the presence of caspase inhibitors (Legarda et al., 2016; McComb et al., 2014). This resistance highlights the central role of type I IFN signaling in

the necroptotic process. The temporal pattern of necroptosis suggests that IFN-1 receptor signaling may be crucial for the sustained activation or amplification of the necroptotic pathway, rather than its initial triggering. IFNAR1 signaling is essential for necroptosis induced by various stimuli and acts as a common downstream mediator for diverse necroptosis-inducing signals in BMDMs. This convergence on IFNAR1 signaling could represent a critical node in the necroptotic pathway.

5.3.1. IFNAR1 Signaling and Necroptosis: Beyond TNFR2 Regulation

The observation that *Tnfr2*-deficient macrophages show significant protection against LPS-, IFNβ-, and TNFα-induced necroptosis is an important finding. This suggests that TNFR2 plays a crucial role in promoting necroptosis in macrophages, which is somewhat unexpected given that TNFR1 has traditionally been considered the primary mediator of TNF-induced cell death (C. Liu et al., 2018; Saveljeva et al., 2015; Vanlangenakker, Bertrand, et al., 2011; Wajant & Siegmund, 2019; Xu et al., 2021). TNFR1 contains a death domain in its cytoplasmic region, which is essential for triggering cell death pathways which is absent in TNFR2 (Wajant & Siegmund, 2019). Intriguingly, the relationship between IFNAR1 signaling and TNFR2 expression appears to be more complex than initially anticipated. Our results correlate with previous findings that *Tnfr2*$^{-/-}$ BMDMs were resistant to necroptosis induced by murine TNF, confirming the requirement for TNFR2 (Legarda et al., 2016). Unlike their findings, our bioinformatics analysis and Western blot results indicate that neither LPS nor type-I interferons significantly upregulate TNFR2 expression at the transcriptional or protein level. TNFR2 and Fn14 play crucial roles in modulating TNFR1-induced cell death by efficiently recruiting TRAF2 and associated proteins cIAP1/2 (Siegmund et al., 2023). This recruitment limits the availability of these proteins for TNFR1 signaling. As a result, TNFR2 and Fn14 activation can enhance TNFR1-induced apoptosis and necroptosis by sensitizing cells to TNFR1-induced death. This sensitization occurs independently of effects on NFκB signaling (Siegmund et al., 2023). The observation that *Ifnar1*$^{-/-}$ macrophages are resistant to necroptosis, despite showing no significant alterations in TNFR2 expression, suggests that IFNAR1 signaling contributes to necroptosis through mechanisms independent of TNFR2 regulation. The interplay between IFNAR1 and TNFR2 signaling pathways might involve complex feedback loops or crosstalk mechanisms that are not immediately apparent from

expression analysis alone. Furthermore, IFNAR1 signaling does not appear to directly regulate TNFR2 expression, these two pathways may synergize at a downstream point in the necroptotic signaling cascade. For instance, IFNAR1 signaling might enhance the pro-necroptotic effects of TNFR2 activation by modulating shared downstream effectors or by altering the cellular metabolic state in a way that favors necroptosis.

5.3.2. The ISGF Complex: A Key Player in Necroptosis Sensitivity

Our results provide compelling evidence for the critical role of the ISGF3 complex, particularly in its phosphorylated form, in promoting necroptosis in macrophages. The observation that macrophages deficient in STAT1, STAT2, or IRF9 display enhanced resistance to necroptosis induced by both LPS+EMR and TNFα+EMR stimulation aligns with previous research highlighting the importance of these factors in cellular responses to type I interferons (McComb et al., 2014). ISGF3 complex is crucial for the full spectrum of ISG expression (Majoros et al., 2017). Our findings extend this concept, suggesting that ISGF3 not only regulates gene expression but also plays a direct role in sensitizing cells to necroptotic death. The temporal correlation between ISGF3 phosphorylation and necroptotic sensitivity is a key finding in our study. We observed that ISGF3 complex protein expression peaks early and dephosphorylates around 6 hours in the IFN-β mediated necroptosis state, aligning with the window of necroptotic sensitivity. This observation builds upon the work, that showed that phosphorylated and unphosphorylated ISGF3 can transcribe different gene sets (Nowicka et al., 2023). Our results specifically implicate the phosphorylated ISGF3 in promoting necroptosis, suggesting a novel role for this complex in regulating programmed cell death. STAT1 can be phosphorylated at two key residues: tyrosine 701 (Y701) and serine 727 (S727) (Barnholt et al., 2009; Sadzak et al., 2008). Y701 phosphorylation is essential for STAT1 dimerization and nuclear translocation, while S727 phosphorylation enhances transcriptional activity (Kovarik et al., 2001). Our results, showing the importance of phosphorylated ISGF3 in necroptosis, suggest that both phosphorylation sites may be involved in this process. Investigating the precise function of STAT1 phosphorylation in the necroptosis pathway would be a valuable research endeavor. Interestingly, it has been reported that protein kinase C-δ (PKC-δ) can phosphorylate STAT1 at S727 in response to type I IFNs *in vitro* (Uddin et al., 2002). Another study reported that in PKC-δ-deficient cells, STAT1 phosphorylation on Ser727 still occurred in response to IFN-β, IFN-γ, and LPS stimulation *in vivo* (Pilz et al., 2003).

These findings suggest that while PKC-δ can phosphorylate STAT1 at Ser727 *in vitro*, but not *in vivo.* There are other kinases, such as other PKC isoforms or calcium/calmodulin-dependent protein kinase II, that might also be involved in STAT1 Ser727 phosphorylation (Pilz et al., 2003). These results highlight the complexity of STAT1 phosphorylation regulation and suggest that multiple kinases may contribute to this process in response to different stimuli. The role and another mechanism that lead to the activation of different phosphorylation sites on STAT1 in this process warrant further discussion.

5.3.3. Transcriptional Landscape of Necrosome Signaling in the Absence of IFNAR1

Analysis of microarray data revealed numerous genes exhibiting altered expression in *Ifnar1*-deficient macrophages during necrosome signaling. Type-I IFN signaling activation induces numerous ISGs, suggesting that unidentified proteins might contribute to MLKL phosphorylation and translocation to the plasma membrane **(Figure 45)**. Several of these genes were selected for further screening and validation experiments. The downregulation of TRAIL in *Ifnar1*-deficient macrophages prompted an investigation into its role in necroptosis. TRAIL, known for inducing apoptosis in tumor cells via DR4 and DR5 receptors (Gonzalvez & Ashkenazi, 2010), has also been reported to trigger necroptosis in various cell types through RipK1-RipK3-PARP-1 activation (Jouan-Lanhouet et al., 2012; Voigt et al., 2014). However, supplementation of *Ifnar1*-deficient macrophages with recombinant TRAIL by a previous student neither enhanced LPS-induced necroptosis in WT macrophages nor reversed the necroptosis resistance in *Ifnar1*-deficient cells. These findings suggest that while TRAIL expression is influenced by IFNAR1 signaling, it does not appear to be a critical factor in explaining the necroptosis resistance observed in *Ifnar1*-deficient cells.

In addition to looking at the expression of pro-cell death genes, we also analyzed the expression of anti-cell death genes. Interestingly, we observed that the expression of XAF1 (XIAP-associated factor 1), an XIAP interacting protein that is known to antagonize XIAP function by suppressing its anti-caspase activity (Liston et al., 2001) was potently impacted by *Ifnar1*-deficiency. Furthermore, XAF1 is a known transcriptional coactivator of interferon regulatory factor-1 (IRF-1) which is required for TNF-induced IFNβ production (Venkatesh et al., 2013; Yarilina et al., 2008). Lastly, a previous study from our lab showed that *Irf1*-deficient cells are protected against TNF-, LPS-induced necroptosis (McComb et al., 2014). Taken together, these studies indicated

that XAF1 may be a relevant gene that promotes type-I interferon-induced necroptosis of macrophages.

XAF1 upregulation in response to IFNβ treatment, both alone and combined with EMR, confirmed its status as an ISG. This finding aligns with previous research demonstrating XAF1's role in enhancing IFN-induced apoptosis and increasing cellular sensitivity to TRAIL-mediated apoptosis. (Micali et al., 2007). However, necroptosis assays conducted on *Xaf1*$^{+/-}$ BMDMs and *Xaf1*$^{-/-}$ RAW macrophages showed no significant differences in necroptosis susceptibility compared to WT cells. This suggests that while XAF1 responds to IFN signaling, it does not play a crucial role in necroptosis execution.

OAS1 (2'-5'-oligoadenylate synthetase 1) which is downregulated in *Ifnar1*$^{-/-}$ cells during necroptosis is an ISG that plays a crucial role in the innate immune response against viral infections (Torices et al., 2023). While OAS1 is not directly involved in the core necroptosis machinery it may contribute to necroptosis through activation leading to the production of 2'-5' oligoadenylates, which activate RNase L. This process can further enhance type I IFN production, creating a positive feedback loop (Pulit-Penaloza et al., 2012). So, it will be interesting to figure out the role of OAS1 in the resistance nature of *Ifnar1*$^{-/-}$ cells against necroptosis. When type I interferons (IFN-α/β) trigger a signaling cascade that leads to the upregulation of ISGs, including MX1 and MX2 (Betancor, 2023) which are also downregulated in *Ifnar1*$^{-/-}$ cells during necroptosis. MX1 and MX2, are GTPases that contribute to the antiviral state of the cell. MX2, in particular, has been shown to inhibit HIV-1 nuclear entry (Betancor, 2023). ARF6, another small GTPase, plays a role in vesicular trafficking and actin remodeling (Van Acker et al., 2019). In the context of viral infections, ARF6 may facilitate viral entry or assembly (Mirabelli et al., 2023) and we have discussed the role of ARF6 in necroptosis in our first Aim. So maybe prolonged IFNAR1 signaling, possibly in conjunction with ARF6 and MX protein activities, sensitizes cells to necroptosis. It will be interesting to check if a complex interplay where IFNAR1 signaling not only induces antiviral factors like MX proteins but also primes cells for necroptosis. ARF6 may serve as a regulatory node, potentially influenced by MX proteins, to fine-tune the balance between antiviral defense and cell death. Further work would be needed to elucidate the specific interactions between MX proteins and ARF6, and how these interactions might influence the progression from antiviral response to necroptosis.

Recent publications have indicated that constitutive IFN signaling is vital for maintaining the MLKL threshold necessary for rapid necroptosis response. (Sarhan et al., 2019). Given MLKL's reported role as an essential terminal step in necroptosis signaling, we examined the expression of MLKL in *Ifnar1*$^{-/-}$ cells. Our observations revealed that impaired type-I IFN signaling resulted in reduced MLKL expression. This reduced level of MLKL might explain the resistant nature of *Ifnar1*-deficient cells against necroptosis. However, it has been recently reported that overexpression of MLKL in *Ifnar1*-deficient macrophages does not sensitize cells to necroptosis (Legarda et al., 2016; Sarhan et al., 2019). Given that previous studies did not examine MLKL phosphorylation and translocation in-depth, mechanisms beyond reduced MLKL expression may contribute to the impaired necroptosis observed in *Ifnar1*-deficient macrophages. To further explore this hypothesis, we opted to overexpress MLKL in *Ifnar1*-deficient RAW macrophages. This approach would allow us to investigate whether restoring MLKL levels alone is sufficient to rescue the necroptosis phenotype or if additional factors are involved in the resistance mechanism.

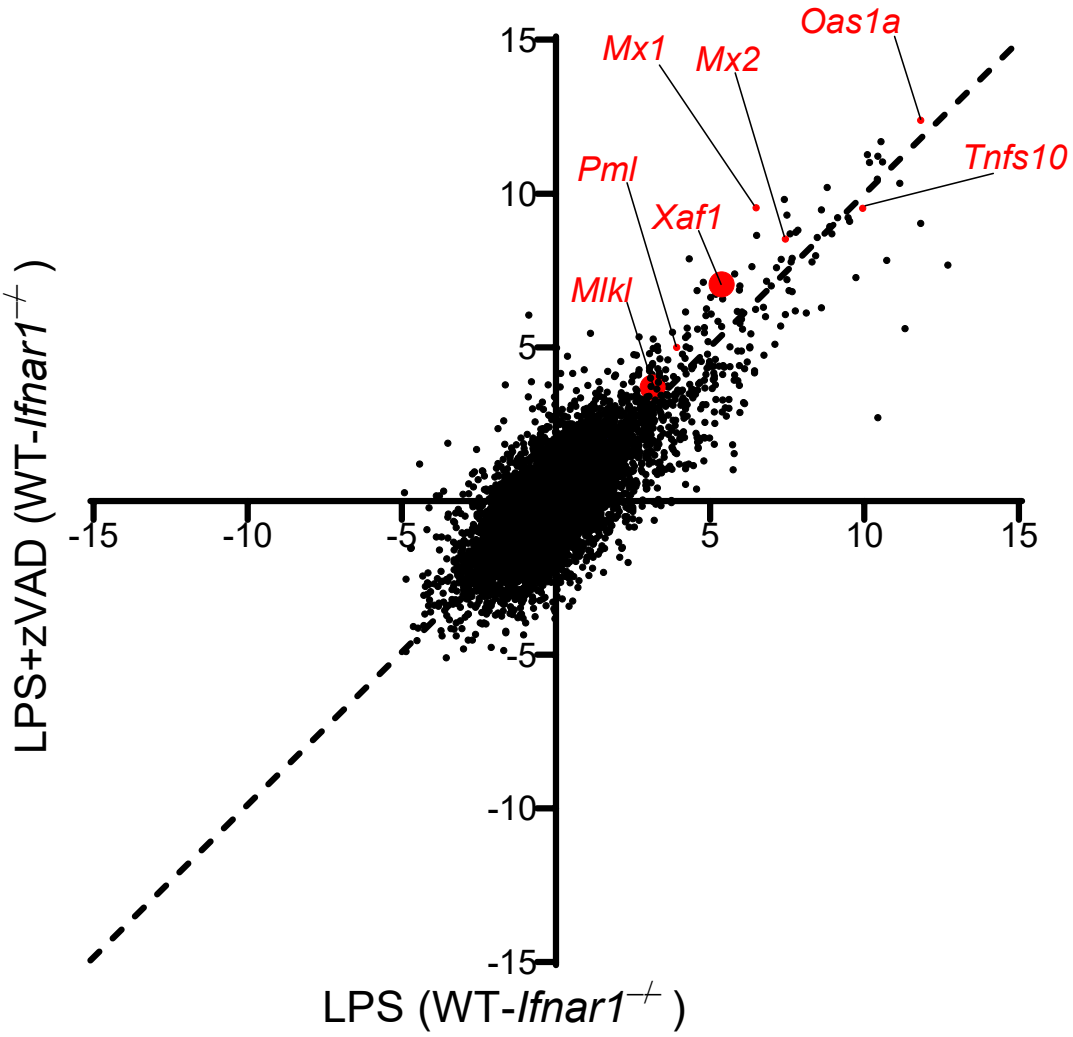

Figure 45. Altered Gene Expression in *Ifnar1*-deficient macrophages during necrosome activation

Microarray analysis of the change in gene expression following LPS (10 ng/mL) alone versus in combination with zVAD (50 μM) treatment in *Ifnar1*$^{-/-}$ macrophages compared to WT.

5.3.4. Beyond MLKL Expression: Multiple Facets of IFNAR1-Mediated Necroptosis Regulation

Recently it has been reported that the Promyelocytic Leukemia (PML) protein inhibits MK2 to promote necroptosis (I. Chen et al., 2021). We observed a low level of PML in *Ifnar1*-deficient macrophages indicating PML's potential role in mediating these cells' resistant phenotype. In addition to this, it has been demonstrated that MK2 induces the inhibitory S321 phosphorylation on RipK1, which restricts necroptosis. (Jaco et al., 2017). This inhibitory phosphorylation was completely abolished in both *Mk2*$^{-/-}$and *Ifnar1*$^{-/-}$*Mk2*$^{-/-}$ BMDMs**.** Moreover, this led to a significant increase in the phosphorylation of MLKL, a crucial protein for the execution of necroptosis. Interestingly, despite these molecular changes, we did not observe a substantial difference in cell death between *Ifnar1*$^{-/-}$ BMDMs and *Ifnar1*$^{-/-}$*Mk2*$^{-/-}$ BMDMs. These findings collectively indicate that while the deletion of *Mk2* in *Ifnar1*$^{-/-}$ macrophages leads to an increase in the phosphorylation of necroptosis-inducing proteins, the resistance of *Ifnar1*$^{-/-}$ macrophages to necroptosis is not solely attributable to higher levels of MK2 phosphorylation. This observation underscores the complex interplay between IFNAR1 and Mk2 in the regulation of necroptosis, suggesting that additional factors may be involved in this intricate cellular process.

Our initial hypothesis that reduced MLKL expression in *Ifnar1*$^{-/-}$ macrophages was solely responsible for their resistance to necroptosis was not supported by the data. While *Ifnar1*$^{-/-}$ RAW macrophages showed lower MLKL expression and resistance to necroptosis, reconstitution of MLKL levels through retroviral transduction did not restore necroptosis sensitivity. This unexpected result suggests that MLKL expression alone is insufficient to determine necroptosis susceptibility in the absence of IFNAR1 signaling. Interestingly, MLKL reconstitution in *Ifnar1*$^{-/-}$ cells led to increased RipK3 phosphorylation and MLKL phosphorylation. This observation indicates that MLKL may play a role in regulating RipK3 kinase activity, potentially through a feedback mechanism (McComb et al., 2014). However, the increased phosphorylation of MLKL did not correlate with increased necroptosis, challenging the conventional view that MLKL phosphorylation is the ultimate determinant of necroptotic cell death (Hildebrand et al., 2014). Perhaps the most striking observation was the difference in membrane localization of activated RipK3 and phosphorylated MLKL between WT and *Ifnar1*$^{-/-}$ cells. The reduced presence of these key necroptosis effectors in the membrane fraction of *Ifnar1*$^{-/-}$ cells provides a potential

mechanistic explanation for their resistance to necroptosis. This finding suggests that IFNAR1 signaling may play a crucial role in facilitating the translocation or retention of activated RipK3 and MLKL at the plasma membrane, a critical step in necroptosis execution (Dai et al., 2020; Martinez-Osorio et al., 2023).

MLKL is a key protein in the necroptosis pathway, and its interaction with phosphatidylinositol phosphates (PIPs) plays a crucial role in executing cell death (H. Wang et al., 2014). MLKL consists of an N-terminal four-helix bundle (4HB), a two-helix brace or linker, and a C-terminal pseudo kinase domain (Zhan et al., 2021). Activation occurs when RipK3 phosphorylates MLKL at specific residues in the pseudo-kinase domain, triggering conformational changes that expose the 4HB domain (Garnish et al., 2021). The exposed 4HB domain binds to PIP polar head groups with a low affinity that facilitates MLKL oligomerization and plasma membrane localization (Quarato et al., 2016). MLKL undergoes a "rolling over" mechanism at the membrane exposing additional high-affinity PIP-binding sites. Phosphatidylinositol 4-phosphate 5-kinase (PI(4,5)P2) shows particularly strong binding to MLKL. Increased PI(4,5)P2 concentrations lead to more frequent and larger MLKL-mediated currents (Xia et al., 2022). ARF6 directly activates (PIP5K), which leads to the production of phosphatidylinositol 4,5-bisphosphate (PIP2) (Moreau et al., 2012; Van Acker et al., 2019) which is critical for many cellular processes such as membrane trafficking, cytoskeletal organization, and secretion. Therefore, investigating the expression levels and activity of PIP5K and ARF6 in necroptosis-resistant cells could provide insights into potential resistance mechanisms. Alterations in these proteins might affect PI(4,5)P2 production, subsequently impacting MLKL's ability to execute necroptosis effectively.

6. CONCLUSION

Our research demonstrates that ARF6 does not influence cellular susceptibility to apoptotic cell death. Instead, ARF6 specifically targets RipK1-dependent ripoptosome and necrosome cell death pathways. Our findings indicate that ARF6 does not affect TLR4 or TNF-R internalization during RipK1-dependent cell death signaling, suggesting a post-endocytic mechanism. We have uncovered that Arf6 regulates endo-lysosomal compartment maturation, promoting cIAP1/2 degradation, which removes inhibition on RipK1 and facilitates its phosphorylation towards cell death pathways. This study reveals a novel signaling event preceding RipK1 phosphorylation, which is crucial for activating RipK1-dependent cell death pathways **(Figure 46)**. We have also demonstrated that the initiation of necroptosis leads to RipK1 activation, resulting the upregulation of the MAPK pathway that leads to increased expression of various inflammatory cytokines, independent of cell death. This inflammatory response upregulation is counterbalanced by type I interferon expression during necrosome activation. The interplay between IFNAR1 signaling, the MAPK pathway, and post-transcriptional regulation via ZFP36 plays a vital role in balancing inflammatory responses and cell death. While type I interferon induces necroptosis, it also promotes the expression of TTP through ISGF3 signaling, which leads to post-transcriptional degradation of important inflammatory cytokines like TNFα. Without this preventative mechanism, necrosome signaling could potentially lead to even more potent inflammatory response leading to tissue toxicity **(Figure 47)**. Our study provides compelling evidence for the critical role of IFNAR1 signaling in necroptosis. We have shown that Ifnar1-deficient macrophages exhibit significant resistance to necroptosis induced by various stimuli. We show that IFNAR1 signaling is crucial for the proper functioning of the ISGF3 complex (STAT1, STAT2, and IRF9) and the expression and activation of MLKL, a key necroptosis executioner. Intriguingly, restoring MLKL expression in *Ifnar1*-deficient cells does not impact their resistance to necroptosis, suggesting the existence of additional mechanisms. Further investigation demonstrated that IFNAR1 signaling is essential for the appropriate translocation of phosphorylated MLKL to the plasma membrane, a critical step in necroptosis execution. These findings significantly advance our understanding of the molecular mechanisms underlying necroptosis and highlight the complex interplay between interferon signaling and programmed cell death pathways in macrophages. We anticipate that this study will contribute to future discoveries

of potential prognostic biomarkers and aid in developing treatments for inflammatory diseases involving necroptosis.

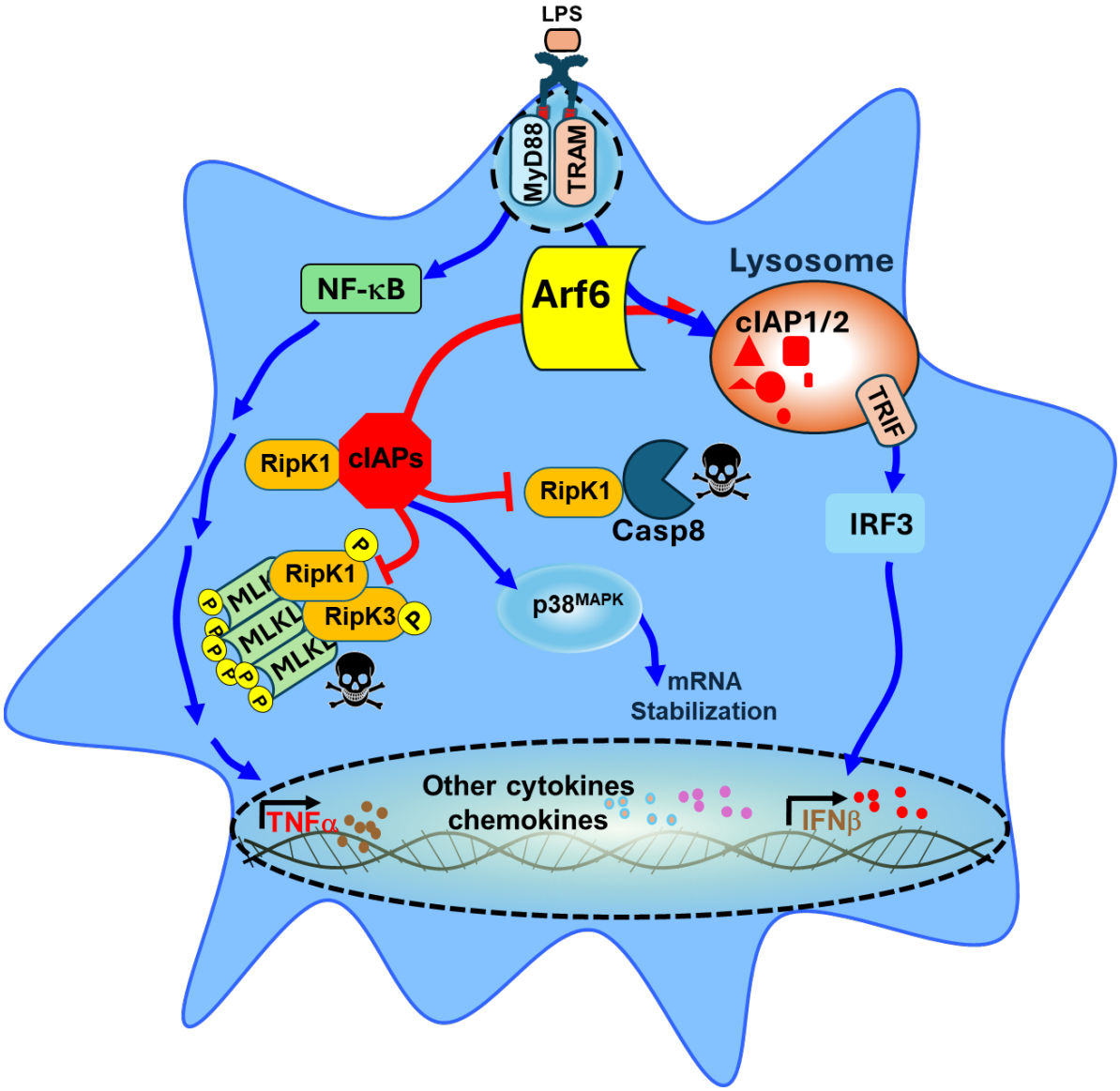

Figure 46. The role of ARF6 in RipK1-dependent cell death

ARF6 regulates RipK1-dependent ripoptosome and necrosome cell death pathways. It facilitates the maturation of endo-lysosomal compartments, leading to cIAP1/2 degradation. This process removes inhibition on RipK1, promoting its phosphorylation and subsequent activation of cell death pathways.

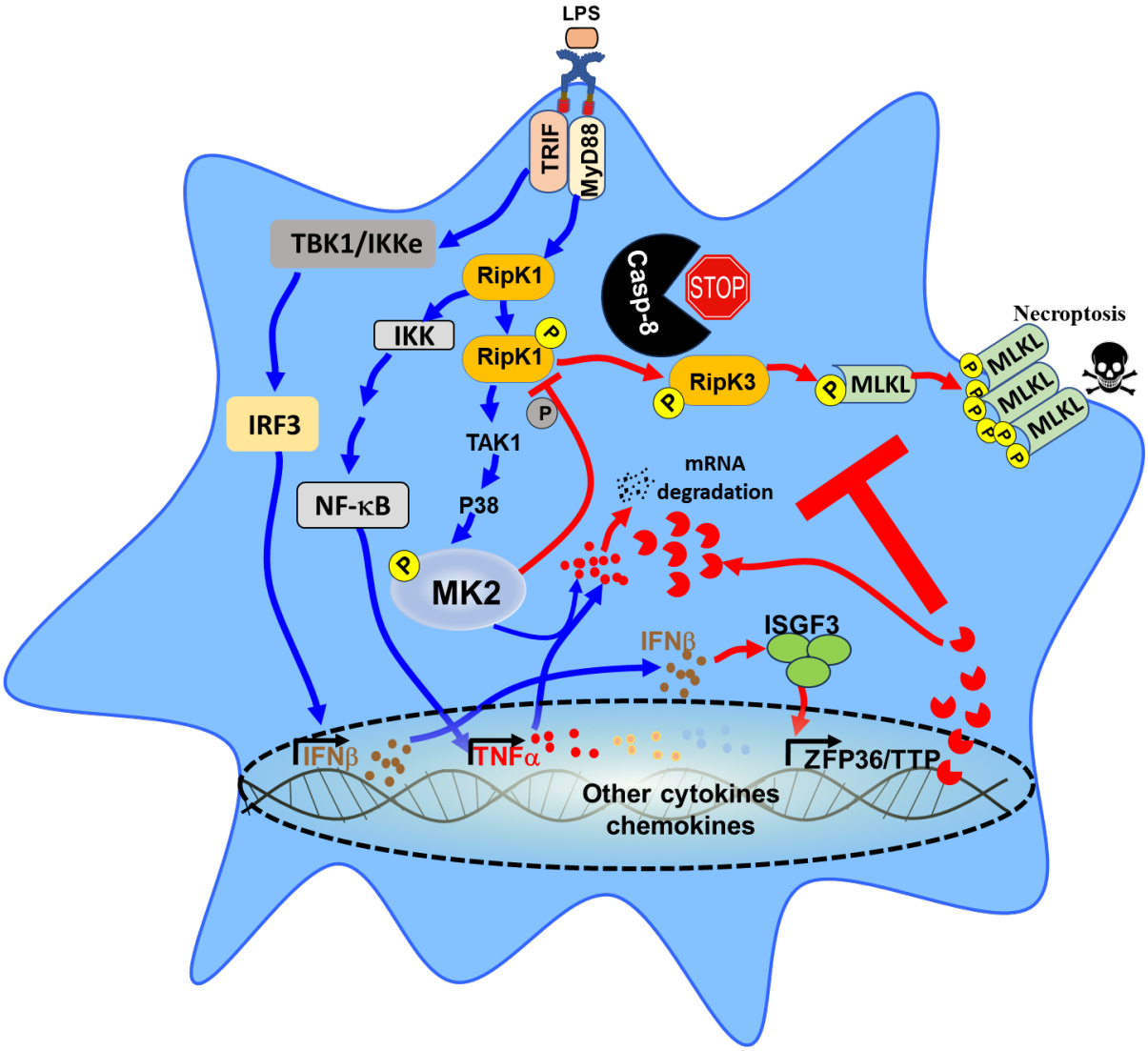

Figure 47. IFNAR1 Signaling: A double-edged sword in necroptosis and inflammation

Necrosome activation triggers RipK1 phosphorylation, leading to MAPK pathway stimulation and enhanced inflammatory response, independent of cell death. Concurrently, TRIF-mediated type I interferon expression activates the ISGF3 transcriptional complex, inducing TTP expression. TTP promotes mRNA degradation of various inflammatory cytokines and chemokines. This mechanism demonstrates how IFNAR1 signaling simultaneously promotes necroptosis while limiting excessive inflammation.

7. REFERENCES

1. Chaplin, D. D. 1. Overview of the immune response. *J Allergy Clin Immunol* **111**, S442-459 (2003).
2. O'Neill, L. A. J., Kishton, R. J. & Rathmell, J. A guide to immunometabolism for immunologists. *Nat Rev Immunol* **16**, 553–565 (2016).
3. Platanitis, E. *et al.* A molecular switch from STAT2-IRF9 to ISGF3 underlies interferon-induced gene transcription. *Nat Commun* **10**, 2921 (2019).
4. Platanitis, E. *et al.* A molecular switch from STAT2-IRF9 to ISGF3 underlies interferon-induced gene transcription. *Nat Commun* **10**, 2921 (2019).
5. A molecular switch from STAT2-IRF9 to ISGF3 underlies interferon-induced gene transcription - PMC. https://pmc.ncbi.nlm.nih.gov/articles/PMC6606597/.
6. A molecular switch from STAT2-IRF9 to ISGF3 underlies interferon-induced gene transcription - PMC. https://pmc.ncbi.nlm.nih.gov/articles/PMC6606597/.
7. Dai, J. *et al.* A necroptotic-independent function of MLKL in regulating endothelial cell adhesion molecule expression. *Cell Death Dis* **11**, 1–16 (2020).
8. Sun, L. & Wang, X. A new kind of cell suicide: mechanisms and functions of programmed necrosis. *Trends Biochem Sci* **39**, 587–593 (2014).
9. Tartaglia, L. A., Ayres, T. M., Wong, G. H. W. & Goeddel, D. V. A novel domain within the 55 kd TNF receptor signals cell death. *Cell* **74**, 845–853 (1993).
10. Taylor, G. A. *et al.* A pathogenetic role for TNF alpha in the syndrome of cachexia, arthritis, and autoimmunity resulting from tristetraprolin (TTP) deficiency. *Immunity* **4**, 445–454 (1996).
11. Bonham, K. S. *et al.* A promiscuous lipid-binding protein diversifies the subcellular sites of Toll-like Receptor signal transduction. *Cell* **156**, 705–716 (2014).
12. Zulkefli, K. L. *et al.* A role for Rab30 in retrograde trafficking and maintenance of endosome-TGN organization. *Exp Cell Res* **399**, 112442 (2021).
13. Sun, S.-C. & Liu, Z.-G. A special issue on NF-κB signaling and function. *Cell Res* **21**, 1–2 (2011).
14. Brandt, P. W. A study of the mechanism of pinocytosis. *Exp Cell Res* **15**, 300–313 (1958).
15. Gurung, P., Man, S. M. & Kanneganti, T.-D. A20 is a regulator of necroptosis. *Nat Immunol* **16**, 596–597 (2015).
16. Gallucci, S., Meka, S. & Gamero, A. M. "Abnormalities of the Type I Interferon signaling pathway in Lupus autoimmunity". *Cytokine* **146**, 155633 (2021).
17. Loiben, A., Friedman, C., Chen, W.-M., Chao, L. & Yang, K. C. Abstract P2110: Myosin-7 E848G Mutation Reduces Contractility And Activates P53-associated Intrinsic Apoptosis In Patient-derived Induced Pluripotent Stem Cell Model Of Hypertrophic Cardiomyopathy. *Circulation Research* **131**, (2022).
18. Rohn, J. L. & Baum, B. Actin and cellular architecture at a glance. *J Cell Sci* **123**, 155–158 (2010).
19. Cargnello, M. & Roux, P. P. Activation and function of the MAPKs and their substrates, the MAPK-activated protein kinases. *Microbiol Mol Biol Rev* **75**, 50–83 (2011).
20. Ofengeim, D. *et al.* Activation of Necroptosis in Multiple Sclerosis. *Cell Reports* **10**, 1836–1849 (2015).

21. Ofengeim, D. *et al.* Activation of necroptosis in multiple sclerosis. *Cell Rep* **10**, 1836–1849 (2015).
22. Pulit-Penaloza, J. A., Scherbik, S. V. & Brinton, M. A. Activation of Oas1a gene expression by type I IFN requires both STAT1 and STAT2 while only STAT2 is required for Oas1b activation. *Virology* **425**, 71–81 (2012).
23. Hildebrand, J. M. *et al.* Activation of the pseudokinase MLKL unleashes the four-helix bundle domain to induce membrane localization and necroptotic cell death. *Proceedings of the National Academy of Sciences* **111**, 15072–15077 (2014).
24. Okada, R. *et al.* Activation of the Small G Protein Arf6 by Dynamin2 through Guanine Nucleotide Exchange Factors in Endocytosis. *Sci Rep* **5**, 14919 (2015).
25. Okada, R. *et al.* Activation of the Small G Protein Arf6 by Dynamin2 through Guanine Nucleotide Exchange Factors in Endocytosis. *Sci Rep* **5**, 14919 (2015).
26. Barnholt, K. E., Kota, R. S., Aung, H. H. & Rutledge, J. C. Adenosine Blocks IFN-γ-Induced Phosphorylation of STAT1 on Serine 727 to Reduce Macrophage Activation. *J Immunol* **183**, 6767–6777 (2009).
27. Han, M. *et al.* Ameliorative effects of epigallocatechin-3-gallate nanoparticles on 2,4-dinitrochlorobenzene induced atopic dermatitis: A potential mechanism of inflammation-related necroptosis. *Front Nutr* **9**, 953646 (2022).
28. Marshall, J. S., Warrington, R., Watson, W. & Kim, H. L. An introduction to immunology and immunopathology. *Allergy, Asthma & Clinical Immunology* **14**, 49 (2018).
29. Kowalski, S. *et al.* An overview of programmed cell death: Apoptosis and pyroptosis-Mechanisms, differences, and significance in organism physiology and pathophysiology. *J Cell Biochem* **124**, 765–784 (2023).
30. Kaiser, W. J. & Offermann, M. K. Apoptosis induced by the toll-like receptor adaptor TRIF is dependent on its receptor interacting protein homotypic interaction motif. *J Immunol* **174**, 4942–4952 (2005).
31. Fink, S. L. & Cookson, B. T. Apoptosis, Pyroptosis, and Necrosis: Mechanistic Description of Dead and Dying Eukaryotic Cells. *Infect Immun* **73**, 1907–1916 (2005).
32. Elmore, S. Apoptosis: a review of programmed cell death. *Toxicol Pathol* **35**, 495–516 (2007).
33. D'Souza-Schorey, C. & Chavrier, P. ARF proteins: roles in membrane traffic and beyond. *Nat Rev Mol Cell Biol* **7**, 347–358 (2006).
34. Nakai, W. *et al.* ARF1 and ARF4 regulate recycling endosomal morphology and retrograde transport from endosomes to the Golgi apparatus. *Mol Biol Cell* **24**, 2570–2581 (2013).
35. Sumiyoshi, M. *et al.* Arf1 and Arf6 Synergistically Maintain Survival of T Cells during Activation. *The Journal of Immunology* **206**, 366–375 (2021).
36. George, A. A., Hayden, S., Stanton, G. R. & Brockerhoff, S. E. Arf6 and the 5'phosphatase of synaptojanin 1 regulate autophagy in cone photoreceptors. *Bioessays* **38 Suppl 1**, S119-135 (2016).
37. Mirabelli, C. *et al.* ARF6 is a host factor for SARS-CoV-2 infection in vitro. *J Gen Virol* **104**, 001868 (2023).
38. Macia, E., Partisani, M., Paleotti, O., Luton, F. & Franco, M. Arf6 negatively controls the rapid recycling of the β2 adrenergic receptor. *Journal of Cell Science* **125**, 4026–4035 (2012).
39. Arf6 negatively controls the rapid recycling of the β2 adrenergic receptor | Journal of Cell Science | The Company of Biologists. https://journals.biologists.com/jcs/article/125/17/4026/32543/Arf6-negatively-controls-the-

rapid-recycling-of.
40. Moreau, K., Ravikumar, B., Puri, C. & Rubinsztein, D. C. Arf6 promotes autophagosome formation via effects on phosphatidylinositol 4,5-bisphosphate and phospholipase D. *Journal of Cell Biology* **196**, 483–496 (2012).
41. Moreau, K., Ravikumar, B., Puri, C. & Rubinsztein, D. C. Arf6 promotes autophagosome formation via effects on phosphatidylinositol 4,5-bisphosphate and phospholipase D. *Journal of Cell Biology* **196**, 483–496 (2012).
42. Arf6 promotes autophagosome formation via effects on phosphatidylinositol 4,5-bisphosphate and phospholipase D | Journal of Cell Biology | Rockefeller University Press. https://rupress.org/jcb/article/196/4/483/36778/Arf6-promotes-autophagosome-formation-via-effects.
43. Radhakrishna, H., Al-Awar, O., Khachikian, Z. & Donaldson, J. G. ARF6 requirement for Rac ruffling suggests a role for membrane trafficking in cortical actin rearrangements. *J Cell Sci* **112 (Pt 6)**, 855–866 (1999).
44. Radhakrishna, H., Al-Awar, O., Khachikian, Z. & Donaldson, J. G. ARF6 requirement for Rac ruffling suggests a role for membrane trafficking in cortical actin rearrangements. *Journal of Cell Science* **112**, 855–866 (1999).
45. Palacios, F., Schweitzer, J. K., Boshans, R. L. & D'Souza-Schorey, C. ARF6-GTP recruits Nm23-H1 to facilitate dynamin-mediated endocytosis during adherens junctions disassembly. *Nat Cell Biol* **4**, 929–936 (2002).
46. Schweitzer, J. K., Sedgwick, A. E. & D'Souza-Schorey, C. ARF6-mediated endocytic recycling impacts cell movement, cell division and lipid homeostasis. *Semin Cell Dev Biol* **22**, 39–47 (2011).
47. Wohlfromm, F. *et al.* Arginine methylation of caspase-8 controls life/death decisions in extrinsic apoptotic networks. *Oncogene* **43**, 1955–1971 (2024).
48. Yonekawa, T. & Thorburn, A. Autophagy and Cell Death. *Essays Biochem* **55**, 105–117 (2013).
49. Marongiu, L., Gornati, L., Artuso, I., Zanoni, I. & Granucci, F. Below the surface: The inner lives of TLR4 and TLR9. *J Leukoc Biol* **106**, 147–160 (2019).
50. Lu, L. L., Suscovich, T. J., Fortune, S. M. & Alter, G. Beyond binding: antibody effector functions in infectious diseases. *Nat Rev Immunol* **18**, 46–61 (2018).
51. Venkatesh, V., Brown, S. A. & Bala, H. Bridging the Qualitative-Quantitative Divide: Guidelines for Conducting Mixed Methods Research in Information Systems. *MIS Quarterly* **37**, 21–54 (2013).
52. Dynek, J. N. *et al.* c-IAP1 and UbcH5 promote K11-linked polyubiquitination of RIP1 in TNF signalling. *EMBO J* **29**, 4198–4209 (2010).
53. Dynek, J. N. *et al.* c-IAP1 and UbcH5 promote K11-linked polyubiquitination of RIP1 in TNF signalling. *EMBO J* **29**, 4198–4209 (2010).
54. Yarza, R., Vela, S., Solas, M. & Ramirez, M. J. c-Jun N-terminal Kinase (JNK) Signaling as a Therapeutic Target for Alzheimer's Disease. *Front Pharmacol* **6**, 321 (2016).
55. Zhang, C. *et al.* Calcium- and dynamin-independent endocytosis in dorsal root ganglion neurons. *Neuron* **42**, 225–236 (2004).
56. Majoros, A. *et al.* Canonical and Non-Canonical Aspects of JAK-STAT Signaling: Lessons from Interferons for Cytokine Responses. *Front Immunol* **8**, 29 (2017).
57. Günther, C. *et al.* Caspase-8 regulates TNF-alpha induced epithelial necroptosis and terminal ileitis. *Nature* **477**, 335–339 (2011).

58. Oberst, A. *et al.* Catalytic activity of the caspase-8-FLIP(L) complex inhibits RIPK3-dependent necrosis. *Nature* **471**, 363–367 (2011).
59. Yu, B. & Wright, S. D. Catalytic properties of lipopolysaccharide (LPS) binding protein. Transfer of LPS to soluble CD14. *J Biol Chem* **271**, 4100–4105 (1996).
60. Rajaiah, R., Perkins, D. J., Ireland, D. D. C. & Vogel, S. N. CD14 dependence of TLR4 endocytosis and TRIF signaling displays ligand specificity and is dissociable in endotoxin tolerance. *Proc Natl Acad Sci U S A* **112**, 8391–8396 (2015).
61. Rossatti, P. *et al.* Cdc42 Couples T Cell Receptor Endocytosis to GRAF1-Mediated Tubular Invaginations of the Plasma Membrane. *Cells* **8**, 1388 (2019).
62. Lockshin, R. A. & Zakeri, Z. Cell death in health and disease. *Journal of Cellular and Molecular Medicine* **11**, 1214–1224 (2007).
63. Kanduc, D. *et al.* Cell death: apoptosis versus necrosis (review). *Int J Oncol* **21**, 165–170 (2002).
64. Voigt, N. *et al.* Cellular and molecular mechanisms of atrial arrhythmogenesis in patients with paroxysmal atrial fibrillation. *Circulation* **129**, 145–156 (2014).
65. de Almagro, M. C., Goncharov, T., Newton, K. & Vucic, D. Cellular IAP proteins and LUBAC differentially regulate necrosome-associated RIP1 ubiquitination. *Cell Death Dis* **6**, e1800 (2015).
66. de Almagro, M. C., Goncharov, T., Newton, K. & Vucic, D. Cellular IAP proteins and LUBAC differentially regulate necrosome-associated RIP1 ubiquitination. *Cell Death Dis* **6**, e1800–e1800 (2015).
67. Mani, I. & Singh, V. Chapter One - An overview of receptor endocytosis and signaling. in *Progress in Molecular Biology and Translational Science* (eds. Mani, I. & Singh, V.) vol. 194 1–18 (Academic Press, 2023).
68. Rodriguez, D. A. *et al.* Characterization of RIPK3-mediated phosphorylation of the activation loop of MLKL during necroptosis. *Cell Death Differ* **23**, 76–88 (2016).
69. Degterev, A. *et al.* Chemical inhibitor of nonapoptotic cell death with therapeutic potential for ischemic brain injury. *Nat Chem Biol* **1**, 112–119 (2005).
70. Degterev, A. *et al.* Chemical inhibitor of nonapoptotic cell death with therapeutic potential for ischemic brain injury. *Nat Chem Biol* **1**, 112–119 (2005).
71. Degterev, A. *et al.* Chemical inhibitor of nonapoptotic cell death with therapeutic potential for ischemic brain injury. *Nat Chem Biol* **1**, 112–119 (2005).
72. Bertrand, M. J. M. *et al.* cIAP1 and cIAP2 facilitate cancer cell survival by functioning as E3 ligases that promote RIP1 ubiquitination. *Mol Cell* **30**, 689–700 (2008).
73. Bertrand, M. J. M. *et al.* cIAP1 and cIAP2 facilitate cancer cell survival by functioning as E3 ligases that promote RIP1 ubiquitination. *Mol Cell* **30**, 689–700 (2008).
74. McComb, S. *et al.* cIAP1 and cIAP2 limit macrophage necroptosis by inhibiting Rip1 and Rip3 activation. *Cell Death Differ* **19**, 1791–1801 (2012).
75. Vanlangenakker, N. *et al.* cIAP1 and TAK1 protect cells from TNF-induced necrosis by preventing RIP1/RIP3-dependent reactive oxygen species production. *Cell Death Differ* **18**, 656–665 (2011).
76. Feoktistova, M. *et al.* cIAPs Block Ripoptosome Formation, a RIP1/Caspase-8 Containing Intracellular Cell Death Complex Differentially Regulated by cFLIP Isoforms. *Mol Cell* **43**, 449–463 (2011).
77. Feoktistova, M. *et al.* cIAPs Block Ripoptosome Formation, a RIP1/Caspase-8 Containing Intracellular Cell Death Complex Differentially Regulated by cFLIP Isoforms. *Mol Cell* **43**,

449–463 (2011).
78. Mayer-Barber, K. D. & Yan, B. Clash of the Cytokine Titans: counter-regulation of interleukin-1 and type I interferon-mediated inflammatory responses. *Cell Mol Immunol* **14**, 22–35 (2017).
79. Sandvig, K., Pust, S., Skotland, T. & van Deurs, B. Clathrin-independent endocytosis: mechanisms and function. *Curr Opin Cell Biol* **23**, 413–420 (2011).
80. Mayor, S., Parton, R. G. & Donaldson, J. G. Clathrin-Independent Pathways of Endocytosis. *Cold Spring Harb Perspect Biol* **6**, a016758 (2014).
81. Hughes, M. A. *et al.* Co-operative and Hierarchical Binding of c-FLIP and Caspase-8: A Unified Model Defines How c-FLIP Isoforms Differentially Control Cell Fate. *Mol Cell* **61**, 834–849 (2016).
82. Sadh, S. *et al.* Coating M-CSF on plastic surface results in the generation of increased numbers of macrophages in vitro. *J Immunol Methods* **481–482**, 112788 (2020).
83. Garnish, S. E. *et al.* Conformational interconversion of MLKL and disengagement from RIPK3 precede cell death by necroptosis. *Nat Commun* **12**, 2211 (2021).
84. Muendlein, H. I. *et al.* Constitutive Interferon Attenuates RIPK1/3-Mediated Cytokine Translation. *Cell Rep* **30**, 699-713.e4 (2020).
85. Sarhan, J. *et al.* Constitutive interferon signaling maintains critical threshold of MLKL expression to license necroptosis. *Cell Death Differ* **26**, 332–347 (2019).
86. Cook, S. J., Stuart, K., Gilley, R. & Sale, M. J. Control of cell death and mitochondrial fission by ERK1/2 MAP kinase signalling. *FEBS J* **284**, 4177–4195 (2017).
87. de Almagro, M. C. *et al.* Coordinated ubiquitination and phosphorylation of RIP1 regulates necroptotic cell death. *Cell Death Differ* **24**, 26–37 (2017).
88. Gaba, A. *et al.* Cutting edge: IL-10-mediated tristetraprolin induction is part of a feedback loop that controls macrophage STAT3 activation and cytokine production. *J Immunol* **189**, 2089–2093 (2012).
89. Cutting edge: IL-10-mediated tristetraprolin induction is part of a feedback loop that controls macrophage STAT3 activation and cytokine production - PubMed. https://pubmed.ncbi.nlm.nih.gov/22865915/.
90. Giri, B. *et al.* CXCL12-induced partitioning of flotillin-1 with lipid rafts plays a role in CXCR4 function. *Eur J Immunol* **37**, 2104–2116 (2007).
91. Moquin, D. M., McQuade, T. & Chan, F. K.-M. CYLD Deubiquitinates RIP1 in the TNFα-Induced Necrosome to Facilitate Kinase Activation and Programmed Necrosis. *PLoS One* **8**, e76841 (2013).
92. Trompouki, E. *et al.* CYLD is a deubiquitinating enzyme that negatively regulates NF-kappaB activation by TNFR family members. *Nature* **424**, 793–796 (2003).
93. Legarda, D. *et al.* CYLD Proteolysis Protects Macrophages from TNF-Mediated Auto-necroptosis Induced by LPS and Licensed by Type I IFN. *Cell Reports* **15**, 2449–2461 (2016).
94. Legarda, D. *et al.* CYLD Proteolysis Protects Macrophages from TNF-Mediated Auto-necroptosis Induced by LPS and Licensed by Type I IFN. *Cell Reports* **15**, 2449–2461 (2016).
95. Upton, J. W., Kaiser, W. J. & Mocarski, E. S. DAI/ZBP1/DLM-1 Complexes with RIP3 to Mediate Virus-Induced Programmed Necrosis that Is Targeted by Murine Cytomegalovirus vIRA. *Cell Host Microbe* **26**, 564 (2019).
96. Gong, T., Liu, L., Jiang, W. & Zhou, R. DAMP-sensing receptors in sterile inflammation and inflammatory diseases. *Nat Rev Immunol* **20**, 95–112 (2020).
97. Igney, F. H. & Krammer, P. H. Death and anti-death: tumour resistance to apoptosis. *Nat Rev*

Cancer **2**, 277–288 (2002).
98. Bittner, S., Knoll, G. & Ehrenschwender, M. Death receptor 3 mediates necroptotic cell death. *Cell Mol Life Sci* **74**, 543–554 (2016).
99. Lomphithak, T. & Fadeel, B. Die hard: cell death mechanisms and their implications in nanotoxicology. *Toxicol Sci* **192**, 141–154 (2023).
100. Park, M. Y. *et al.* Differences of Key Proteins between Apoptosis and Necroptosis. *Biomed Res Int* **2021**, 3420168 (2021).
101. Park, M. Y. *et al.* Differences of Key Proteins between Apoptosis and Necroptosis. *Biomed Res Int* **2021**, 3420168 (2021).
102. Shen, S., Shao, Y. & Li, C. Different types of cell death and their shift in shaping disease. *Cell Death Discov.* **9**, 1–12 (2023).
103. Rijal, D. *et al.* Differentiated macrophages acquire a pro-inflammatory and cell death–resistant phenotype due to increasing XIAP and p38-mediated inhibition of RipK1. *J Biol Chem* **293**, 11913–11927 (2018).
104. Hervas-Stubbs, S. *et al.* Direct effects of type I interferons on cells of the immune system. *Clin Cancer Res* **17**, 2619–2627 (2011).
105. Shlomovitz, I., Zargarian, S., Erlich, Z., Edry-Botzer, L. & Gerlic, M. Distinguishing Necroptosis from Apoptosis. *Methods Mol Biol* **1857**, 35–51 (2018).
106. Gaschet, J. & Hsu, V. W. Distribution of ARF6 between membrane and cytosol is regulated by its GTPase cycle. *J Biol Chem* **274**, 20040–20045 (1999).
107. Chen, W. *et al.* Diverse sequence determinants control human and mouse receptor interacting protein 3 (RIP3) and mixed lineage kinase domain-like (MLKL) interaction in necroptotic signaling. *J Biol Chem* **288**, 16247–16261 (2013).
108. Park, W. *et al.* Diversity and complexity of cell death: a historical review. *Exp Mol Med* **55**, 1573–1594 (2023).
109. Park, W. *et al.* Diversity and complexity of cell death: a historical review. *Exp Mol Med* **55**, 1573–1594 (2023).
110. Ross, E. A. *et al.* Dominant Suppression of Inflammation via Targeted Mutation of the mRNA Destabilizing Protein Tristetraprolin. *J Immunol* **195**, 265–276 (2015).
111. Macia, J. *et al.* Dynamic signaling in the Hog1 MAPK pathway relies on high basal signal transduction. *Sci Signal* **2**, ra13 (2009).
112. Hinshaw, J. E. Dynamin and its role in membrane fission. *Annu Rev Cell Dev Biol* **16**, 483–519 (2000).
113. Singh, M., Jadhav, H. R. & Bhatt, T. Dynamin Functions and Ligands: Classical Mechanisms Behind. *Mol Pharmacol* **91**, 123–134 (2017).
114. Gundu, C. *et al.* Dynamin-Independent Mechanisms of Endocytosis and Receptor Trafficking. *Cells* **11**, 2557 (2022).
115. Henley, J. R., Krueger, E. W. A., Oswald, B. J. & McNiven, M. A. Dynamin-mediated Internalization of Caveolae. *J Cell Biol* **141**, 85–99 (1998).
116. Heymann, J. A. W. & Hinshaw, J. E. Dynamins at a glance. *J Cell Sci* **122**, 3427–3431 (2009).
117. Yuan, R., Ma, Y., Yang, C. & Li, L. Editorial: Plasticity of monocytes/macrophages: phenotypic changes during disease progression. *Front. Immunol.* **14**, (2023).
118. Cendrowski, J., Mamińska, A. & Miaczynska, M. Endocytic regulation of cytokine receptor signaling. *Cytokine Growth Factor Rev* **32**, 63–73 (2016).
119. Hemalatha, A., Prabhakara, C. & Mayor, S. Endocytosis of Wingless via a dynamin-independent pathway is necessary for signaling in Drosophila wing discs. *Proc Natl Acad Sci*

U S A **113**, E6993–E7002 (2016).
120. Saveljeva, S., Mc Laughlin, S. L., Vandenabeele, P., Samali, A. & Bertrand, M. J. M. Endoplasmic reticulum stress induces ligand-independent TNFR1-mediated necroptosis in L929 cells. *Cell Death Dis* **6**, e1587–e1587 (2015).
121. Xia, B., Qie, J., Shen, X., Wang, S. & Gao, Z. Enhanced channel activity by PI(4,5)P2 ignites MLKL-related pathogenic processes. *Cell Discov* **8**, 1–4 (2022).
122. Miguel, S. M. S., Namdar-Attar, M., Noh, T., Frenkel, B. & Bab, I. ERK1/2-activated de novo Mapkapk2 synthesis is essential for osteogenic growth peptide mitogenic signaling in osteoblastic cells. *J Biol Chem* **280**, 37495–37502 (2005).
123. Yamamoto, M. *et al.* Essential role for TIRAP in activation of the signalling cascade shared by TLR2 and TLR4. *Nature* **420**, 324–329 (2002).
124. Ge, L. *et al.* Flotillins play an essential role in Niemann-Pick C1-like 1-mediated cholesterol uptake. *Proc Natl Acad Sci U S A* **108**, 551–556 (2011).
125. Siegmund, D., Zaitseva, O. & Wajant, H. Fn14 and TNFR2 as regulators of cytotoxic TNFR1 signaling. *Front Cell Dev Biol* **11**, 1267837 (2023).
126. Siegmund, D., Zaitseva, O. & Wajant, H. Fn14 and TNFR2 as regulators of cytotoxic TNFR1 signaling. *Front Cell Dev Biol* **11**, 1267837 (2023).
127. Ichijo, H. From receptors to stress-activated MAP kinases. *Oncogene* **18**, 6087–6093 (1999).
128. Meng, J., Gong, M., Björkbacka, H. & Golenbock, D. T. Genome-Wide Expression Profiling and Mutagenesis Studies Reveal that Lipopolysaccharide Responsiveness Appears To Be Absolutely Dependent on TLR4 and MD-2 Expression and Is Dependent upon Intermolecular Ionic Interactions. *The Journal of Immunology* **187**, 3683–3693 (2011).
129. Genome-Wide Expression Profiling and Mutagenesis Studies Reveal that Lipopolysaccharide Responsiveness Appears To Be Absolutely Dependent on TLR4 and MD-2 Expression and Is Dependent upon Intermolecular Ionic Interactions | The Journal of Immunology | American Association of Immunologists. https://journals.aai.org/jimmunol/article/187/7/3683/85254/Genome-Wide-Expression-Profiling-and-Mutagenesis.
130. Virolainen, M. HEMATOPOIETIC ORIGIN OF MACROPHAGES AS STUDIED BY CHROMOSOME MARKERS IN MICE. *J Exp Med* **127**, 943–952 (1968).
131. Roderick, J. E. *et al.* Hematopoietic RIPK1 deficiency results in bone marrow failure caused by apoptosis and RIPK3-mediated necroptosis. *Proc Natl Acad Sci U S A* **111**, 14436–14441 (2014).
132. Gingras, A. C. *et al.* Hierarchical phosphorylation of the translation inhibitor 4E-BP1. *Genes Dev* **15**, 2852–2864 (2001).
133. Aggarwal, B. B., Gupta, S. C. & Kim, J. H. Historical perspectives on tumor necrosis factor and its superfamily: 25 years later, a golden journey. *Blood* **119**, 651–665 (2012).
134. Peltzer, N., Darding, M. & Walczak, H. Holding RIPK1 on the Ubiquitin Leash in TNFR1 Signaling. *Trends Cell Biol* **26**, 445–461 (2016).
135. Enomoto, A., Fukasawa, T. & Yoshizaki, A. Hyperthermia-mediated cell death via deregulation of extracellular signal-regulated kinase and c-Jun NH2-terminal kinase signaling. *Front. Cell Death* **3**, 1465506 (2024).
136. Silke, J. & Vucic, D. IAP family of cell death and signaling regulators. *Methods Enzymol* **545**, 35–65 (2014).
137. Degterev, A. *et al.* Identification of RIP1 kinase as a specific cellular target of necrostatins. *Nat Chem Biol* **4**, 313–321 (2008).

138. Leaman, D. W. *et al.* Identification of X-linked Inhibitor of Apoptosis-associated Factor-1 as an Interferon-stimulated Gene That Augments TRAIL Apo2L-induced Apoptosis*. *Journal of Biological Chemistry* **277**, 28504–28511 (2002).
139. Liston, P. *et al.* Identification of XAF1 as an antagonist of XIAP anti-Caspase activity. *Nat Cell Biol* **3**, 128–133 (2001).
140. Phuong, M. S., Hernandez, R. E., Wolter, D. J., Hoffman, L. R. & Sad, S. Impairment in inflammasome signaling by the chronic Pseudomonas aeruginosa isolates from cystic fibrosis patients results in an increase in inflammatory response. *Cell Death Dis* **12**, 241 (2021).
141. Impairment in inflammasome signaling by the chronic Pseudomonas aeruginosa isolates from cystic fibrosis patients results in an increase in inflammatory response - PMC. https://pmc.ncbi.nlm.nih.gov/articles/PMC7933143/.
142. Davidovich, P., Kearney, C. J. & Martin, S. J. Inflammatory outcomes of apoptosis, necrosis and necroptosis. *Biol Chem* **395**, 1163–1171 (2014).
143. Chen, L. *et al.* Inflammatory responses and inflammation-associated diseases in organs. *Oncotarget* **9**, 7204–7218 (2017).
144. Riera Romo, M., Pérez-Martínez, D. & Castillo Ferrer, C. Innate immunity in vertebrates: an overview. *Immunology* **148**, 125–139 (2016).
145. Kessler, D. S., Veals, S. A., Fu, X. Y. & Levy, D. E. Interferon-alpha regulates nuclear translocation and DNA-binding affinity of ISGF3, a multimeric transcriptional activator. *Genes Dev* **4**, 1753–1765 (1990).
146. Pestka, S., Langer, J. A., Zoon, K. C. & Samuel, C. E. Interferons and their actions. *Annu Rev Biochem* **56**, 727–777 (1987).
147. Sauer, I. *et al.* Interferons limit inflammatory responses by induction of tristetraprolin. *Blood* **107**, 4790–4797 (2006).
148. Knuth, A.-K. *et al.* Interferons Transcriptionally Up-Regulate MLKL Expression in Cancer Cells. *Neoplasia* **21**, 74–81 (2018).
149. Pestka, S., Krause, C. D. & Walter, M. R. Interferons, interferon-like cytokines, and their receptors. *Immunol Rev* **202**, 8–32 (2004).
150. Freshney, N. W. *et al.* Interleukin-1 activates a novel protein kinase cascade that results in the phosphorylation of hsp27. *Cell* **78**, 1039–1049 (1994).
151. Loftus, L. V., Amend, S. R. & Pienta, K. J. Interplay between Cell Death and Cell Proliferation Reveals New Strategies for Cancer Therapy. *Int J Mol Sci* **23**, 4723 (2022).
152. Intravesicular Acidification Regulates Lipopolysaccharide Inflammation and Tolerance through TLR4 Trafficking. *CoLab* https://colab.ws/articles/10.4049%2Fjimmunol.1701390.
153. introduction to cell death. *Perplexity AI* https://www.perplexity.ai/search/introduction-to-cell-death-OzBDwRBuRDCWmrf8Z1MM3w.
154. Boldin, M. P., Goncharov, T. M., Goltsev, Y. V. & Wallach, D. Involvement of MACH, a novel MORT1/FADD-interacting protease, in Fas/APO-1- and TNF receptor-induced cell death. *Cell* **85**, 803–815 (1996).
155. Nowicka, H. *et al.* ISGF3 and STAT2/IRF9 Control Basal and IFN-Induced Transcription through Genome-Wide Binding of Phosphorylated and Unphosphorylated Complexes to Common ISRE-Containing ISGs. *Int J Mol Sci* **24**, 17635 (2023).
156. Shutinoski, B. *et al.* K45A mutation of RIPK1 results in poor necroptosis and cytokine signaling in macrophages, which impacts inflammatory responses in vivo. *Cell Death Differ* **23**, 1628–1637 (2016).
157. Saleh, D. *et al.* Kinase Activities of RIPK1 and RIPK3 Can Direct IFN-β Synthesis Induced

by Lipopolysaccharide. *J Immunol* **198**, 4435–4447 (2017).
158. Gerlach, B. *et al.* Linear ubiquitination prevents inflammation and regulates immune signalling. *Nature* **471**, 591–596 (2011).
159. Fitzgerald, K. A. *et al.* LPS-TLR4 signaling to IRF-3/7 and NF-kappaB involves the toll adapters TRAM and TRIF. *J Exp Med* **198**, 1043–1055 (2003).
160. Lu, Y.-C., Yeh, W.-C. & Ohashi, P. S. LPS/TLR4 signal transduction pathway. *Cytokine* **42**, 145–151 (2008).
161. Yang, C. & Wang, X. Lysosome biogenesis: Regulation and functions. *J Cell Biol* **220**, e202102001 (2021).
162. Yan, L. *et al.* Macrophage plasticity: signaling pathways, tissue repair, and regeneration. *MedComm (2020)* **5**, e658 (2024).
163. Alabdulaali, B. *et al.* Macrophages and the development and progression of non-alcoholic fatty liver disease. *Front Immunol* **14**, 1195699 (2023).
164. Kim, H.-R. *et al.* Mammalian dap3 is an essential gene required for mitochondrial homeostasis in vivo and contributing to the extrinsic pathway for apoptosis. *FASEB J* **21**, 188–196 (2007).
165. Lamkanfi, M. & Dixit, V. M. Manipulation of host cell death pathways during microbial infections. *Cell Host Microbe* **8**, 44–54 (2010).
166. Vanlangenakker, N., Vanden Berghe, T. & Vandenabeele, P. Many stimuli pull the necrotic trigger, an overview. *Cell Death Differ* **19**, 75–86 (2012).
167. Kotlyarov, A. *et al.* MAPKAP kinase 2 is essential for LPS-induced TNF-alpha biosynthesis. *Nat Cell Biol* **1**, 94–97 (1999).
168. Kotlyarov, A. *et al.* MAPKAP kinase 2 is essential for LPS-induced TNF-alpha biosynthesis. *Nat Cell Biol* **1**, 94–97 (1999).
169. Chrestensen, C. A. *et al.* MAPKAP kinase 2 phosphorylates tristetraprolin on in vivo sites including Ser178, a site required for 14-3-3 binding. *J Biol Chem* **279**, 10176–10184 (2004).
170. MAPKAP kinase-2 is a cell cycle checkpoint kinase that regulates the G2/M transition and S phase progression in response to UV irradiation - PubMed. https://pubmed.ncbi.nlm.nih.gov/15629715/.
171. Stokoe, D. *et al.* MAPKAP kinase-2; a novel protein kinase activated by mitogen-activated protein kinase. *EMBO J* **11**, 3985–3994 (1992).
172. Gaestel, M. MAPKAP kinases — MKs — two's company, three's a crowd. *Nat Rev Mol Cell Biol* **7**, 120–130 (2006).
173. Ronkina, N. *et al.* MAPKAP kinases MK2 and MK3 in inflammation: complex regulation of TNF biosynthesis via expression and phosphorylation of tristetraprolin. *Biochem Pharmacol* **80**, 1915–1920 (2010).
174. Krishna, S. & Overholtzer, M. Mechanisms and consequences of entosis. *Cell Mol Life Sci* **73**, 2379–2386 (2016).
175. Ellis, R. E., Yuan, J. Y. & Horvitz, H. R. Mechanisms and functions of cell death. *Annu Rev Cell Biol* **7**, 663–698 (1991).
176. Cuadrado, A. & Nebreda, A. R. Mechanisms and functions of p38 MAPK signalling. *Biochemical Journal* **429**, 403–417 (2010).
177. Cuadrado, A. & Nebreda, A. R. Mechanisms and functions of p38 MAPK signalling. *Biochem J* **429**, 403–417 (2010).
178. Cao, J. Y. & Dixon, S. J. Mechanisms of ferroptosis. *Cell Mol Life Sci* **73**, 2195–2209 (2016).
179. Ricketts, T. D., Prieto-Dominguez, N., Gowda, P. S. & Ubil, E. Mechanisms of Macrophage

Plasticity in the Tumor Environment: Manipulating Activation State to Improve Outcomes. *Front Immunol* **12**, 642285 (2021).
180. Wu, X., Nagy, L. E. & Gautheron, J. Mediators of necroptosis: from cell death to metabolic regulation. *EMBO Mol Med* **16**, 219–237 (2024).
181. Kolliniati, O., Ieronymaki, E., Vergadi, E. & Tsatsanis, C. Metabolic Regulation of Macrophage Activation. *J Innate Immun* **14**, 51–68 (2021).
182. Wu, X., Saito, T., Saido, T. C., Barron, A. M. & Ruedl, C. Microglia and CD206+ border-associated mouse macrophages maintain their embryonic origin during Alzheimer's disease. *eLife* **10**, e71879.
183. Abdul Rehman, S. A. *et al.* MINDY-1 Is a Member of an Evolutionarily Conserved and Structurally Distinct New Family of Deubiquitinating Enzymes. *Mol Cell* **63**, 146–155 (2016).
184. Galluzzi, L., Kepp, O. & Kroemer, G. Mitochondrial regulation of cell death: a phylogenetically conserved control. *Microb Cell* **3**, 101–108 (2016).
185. Cuschieri, J. & Maier, R. V. Mitogen-activated protein kinase (MAPK). *Crit Care Med* **33**, S417-419 (2005).
186. Sun, L. *et al.* Mixed lineage kinase domain-like protein mediates necrosis signaling downstream of RIP3 kinase. *Cell* **148**, 213–227 (2012).
187. Sun, L. *et al.* Mixed lineage kinase domain-like protein mediates necrosis signaling downstream of RIP3 kinase. *Cell* **148**, 213–227 (2012).
188. Wang, H. *et al.* Mixed Lineage Kinase Domain-like Protein MLKL Causes Necrotic Membrane Disruption upon Phosphorylation by RIP3. *Molecular Cell* **54**, 133–146 (2014).
189. Jaco, I. *et al.* MK2 Phosphorylates RIPK1 to Prevent TNF-Induced Cell Death. *Molecular Cell* **66**, 698-710.e5 (2017).
190. Dondelinger, Y. *et al.* MK2 phosphorylation of RIPK1 regulates TNF-mediated cell death. *Nat Cell Biol* **19**, 1237–1247 (2017).
191. Neininger, A. *et al.* MK2 targets AU-rich elements and regulates biosynthesis of tumor necrosis factor and interleukin-6 independently at different post-transcriptional levels. *J Biol Chem* **277**, 3065–3068 (2002).
192. Stoecklin, G. *et al.* MK2-induced tristetraprolin:14-3-3 complexes prevent stress granule association and ARE-mRNA decay. *EMBO J* **23**, 1313–1324 (2004).
193. Menon, M. B. & Gaestel, M. MK2–TNF–Signaling Comes Full Circle. *Trends in Biochemical Sciences* **43**, 170–179 (2018).
194. Lei, X., Chen, Y., Lien, E. & Fitzgerald, K. A. MLKL-Driven Inflammasome Activation and Caspase-8 Mediate Inflammatory Cell Death in Influenza A Virus Infection. *mBio* **14**, e00110-23.
195. Zhan, C., Huang, M., Yang, X. & Hou, J. MLKL: Functions beyond serving as the Executioner of Necroptosis. *Theranostics* **11**, 4759–4769 (2021).
196. Randazzo, P. A., Nie, Z., Miura, K. & Hsu, V. W. Molecular aspects of the cellular activities of ADP-ribosylation factors. *Sci STKE* **2000**, re1 (2000).
197. Nascimento, D. S. *et al.* Molecular cloning and expression analysis of sea bass (Dicentrarchus labrax L.) tumor necrosis factor-alpha (TNF-alpha). *Fish Shellfish Immunol* **23**, 701–710 (2007).
198. McMahon, H. T. & Boucrot, E. Molecular mechanism and physiological functions of clathrin-mediated endocytosis. *Nat Rev Mol Cell Biol* **12**, 517–533 (2011).
199. Casamento, A. & Boucrot, E. Molecular mechanism of Fast Endophilin-Mediated

Endocytosis. *Biochem J* **477**, 2327–2345 (2020).
200. Vandenabeele, P., Galluzzi, L., Vanden Berghe, T. & Kroemer, G. Molecular mechanisms of necroptosis: an ordered cellular explosion. *Nat Rev Mol Cell Biol* **11**, 700–714 (2010).
201. Gioannini, T. L., Teghanemt, A., Zhang, D., Levis, E. N. & Weiss, J. P. Monomeric endotoxin:protein complexes are essential for TLR4-dependent cell activation. *J Endotoxin Res* **11**, 117–123 (2005).
202. Battaglioni, S., Benjamin, D., Wälchli, M., Maier, T. & Hall, M. N. mTOR substrate phosphorylation in growth control. *Cell* **185**, 1814–1836 (2022).
203. Betancor, G. *et al.* MX2 Viral Substrate Breadth and Inhibitory Activity Are Regulated by Protein Phosphorylation. *mBio* **13**, e01714-22.
204. C, D.-S. & Pd, S. Myristoylation is required for the intracellular localization and endocytic function of ARF6. *Experimental cell research* **221**, (1995).
205. D'Souza-Schorey, C. & Stahl, P. D. Myristoylation is Required for the Intracellular Localization and Endocytic Function of ARF6. *Experimental Cell Research* **221**, 153–159 (1995).
206. Estlack, L. E., Roth, C. C., Thompson, G. L., Lambert, W. A. & Ibey, B. L. Nanosecond pulsed electric fields modulate the expression of Fas/CD95 death receptor pathway regulators in U937 and Jurkat Cells. *Apoptosis* **19**, 1755–1768 (2014).
207. Linkermann, A. & Green, D. R. Necroptosis. *N Engl J Med* **370**, 455–465 (2014).
208. Pasparakis, M. & Vandenabeele, P. Necroptosis and its role in inflammation. *Nature* **517**, 311–320 (2015).
209. Re, D. B. *et al.* Necroptosis drives motor neuron death in models of both sporadic and familial ALS. *Neuron* **81**, 1001–1008 (2014).
210. Jun, W., Benjanuwattra, J., Chattipakorn, S. C. & Chattipakorn, N. Necroptosis in renal ischemia/reperfusion injury: A major mode of cell death? *Arch Biochem Biophys* **689**, 108433 (2020).
211. Afonso, M. B. *et al.* Necroptosis is a key pathogenic event in human and experimental murine models of non-alcoholic steatohepatitis. *Clin Sci (Lond)* **129**, 721–739 (2015).
212. Seo, J., Nam, Y. W., Kim, S., Oh, D.-B. & Song, J. Necroptosis molecular mechanisms: Recent findings regarding novel necroptosis regulators. *Exp Mol Med* **53**, 1007–1017 (2021).
213. Lu, Z. *et al.* Necroptosis Signaling Promotes Inflammation, Airway Remodeling, and Emphysema in Chronic Obstructive Pulmonary Disease. *Am J Respir Crit Care Med* **204**, 667–681 (2021).
214. Liu, C. *et al.* Necroptosis: A novel manner of cell death, associated with stroke (Review). *International Journal of Molecular Medicine* **41**, 624–630 (2018).
215. Dhuriya, Y. K. & Sharma, D. Necroptosis: a regulated inflammatory mode of cell death. *Journal of Neuroinflammation* **15**, 199 (2018).
216. Chen, D., Yu, J. & Zhang, L. Necroptosis: an alternative cell death program defending against cancer. *Biochim Biophys Acta* **1865**, 228–236 (2016).
217. Kaczmarek, A., Vandenabeele, P. & Krysko, D. V. Necroptosis: the release of damage-associated molecular patterns and its physiological relevance. *Immunity* **38**, 209–223 (2013).
218. Gonzalvez, F. & Ashkenazi, A. New insights into apoptosis signaling by Apo2L/TRAIL. *Oncogene* **29**, 4752–4765 (2010).
219. Sun, S.-C. & Ley, S. C. New insights into NF-κB regulation and function. *Trends Immunol* **29**, 469–478 (2008).
220. Vicioso, Y. *et al.* NF-κB c-Rel Is Dispensable for the Development but Is Required for the

Cytotoxic Function of NK Cells. *Front Immunol* **12**, 652786 (2021).
221. Zhang, H. & Sun, S.-C. NF-κB in inflammation and renal diseases. *Cell Biosci* **5**, 63 (2015).
222. Zhang, H. & Sun, S.-C. NF-κB in inflammation and renal diseases. *Cell Biosci* **5**, 63 (2015).
223. Dondelinger, Y. *et al.* NF-κB-Independent Role of IKKα/IKKβ in Preventing RIPK1 Kinase-Dependent Apoptotic and Necroptotic Cell Death during TNF Signaling. *Mol Cell* **60**, 63–76 (2015).
224. Mulero, M. C., Huxford, T. & Ghosh, G. NF-κB, IκB, and IKK: Integral Components of Immune System Signaling. *Adv Exp Med Biol* **1172**, 207–226 (2019).
225. Kahn, R. A. *et al.* Nomenclature for the human Arf family of GTP-binding proteins: ARF, ARL, and SAR proteins. *J Cell Biol* **172**, 645–650 (2006).
226. Sun, S.-C. Non-canonical NF-κB signaling pathway. *Cell Res* **21**, 71–85 (2011).
227. Sun, S.-C. Non-canonical NF-κB signaling pathway. *Cell Res* **21**, 71–85 (2011).
228. Pan, B., Zheng, B., Xing, C. & Liu, J. Non-Canonical Programmed Cell Death in Colon Cancer. *Cancers (Basel)* **14**, 3309 (2022).
229. Ahmed, K. M., Dong, S., Fan, M. & Li, J. J. Nuclear Factor-K B p 65 Inhibits Mitogen-Activated Protein Kinase Signaling Pathway in Radioresistant Breast Cancer Cells. in (2006).
230. Torices, S. *et al.* Occludin Regulates HIV-1 Infection by Modulation of the Interferon Stimulated OAS Gene Family. *Mol Neurobiol* **60**, 4966–4982 (2023).
231. Shalini, S., Dorstyn, L., Dawar, S. & Kumar, S. Old, new and emerging functions of caspases. *Cell Death Differ* **22**, 526–539 (2015).
232. Bajgar, A. & Krejčová, G. On the origin of the functional versatility of macrophages. *Front Physiol* **14**, 1128984 (2023).
233. Zhang, W., Fan, W., Guo, J. & Wang, X. Osmotic stress activates RIPK3/MLKL-mediated necroptosis by increasing cytosolic pH through a plasma membrane Na+/H+ exchanger. *Sci Signal* **15**, eabn5881 (2022).
234. Keusekotten, K. *et al.* OTULIN Antagonizes LUBAC Signaling by Specifically Hydrolyzing Met1-Linked Polyubiquitin. *Cell* **153**, 1312–1326 (2013).
235. OTULIN Antagonizes LUBAC Signaling by Specifically Hydrolyzing Met1-Linked Polyubiquitin - PMC. https://pmc.ncbi.nlm.nih.gov/articles/PMC3690481/.
236. Heger, K. *et al.* OTULIN limits cell death and inflammation by deubiquitinating LUBAC. *Nature* **559**, 120–124 (2018).
237. Veldhuis, J. D., Garmey, J. C., Urban, R. J., Demers, L. M. & Aggarwal, B. B. Ovarian actions of tumor necrosis factor-alpha (TNF alpha): pleiotropic effects of TNF alpha on differentiated functions of untransformed swine granulosa cells. *Endocrinology* **129**, 641–648 (1991).
238. Peters, P. J. *et al.* Overexpression of wild-type and mutant ARF1 and ARF6: distinct perturbations of nonoverlapping membrane compartments. *J Cell Biol* **128**, 1003–1017 (1995).
239. Peters, P. J. *et al.* Overexpression of wild-type and mutant ARF1 and ARF6: distinct perturbations of nonoverlapping membrane compartments. *J Cell Biol* **128**, 1003–1017 (1995).
240. Goh, K. C., Haque, S. J. & Williams, B. R. p38 MAP kinase is required for STAT1 serine phosphorylation and transcriptional activation induced by interferons. *EMBO J* **18**, 5601–5608 (1999).
241. Menon, M. B. *et al.* p38MAPK/MK2-dependent phosphorylation controls cytotoxic RIPK1 signalling in inflammation and infection. *Nat Cell Biol* **19**, 1248–1259 (2017).

242. Chen, Y.-S. *et al.* Pan-Caspase Inhibitor zVAD Induces Necroptotic and Autophagic Cell Death in TLR3/4-Stimulated Macrophages. *Mol Cells* **45**, 257–272 (2022).
243. Fatokun, A. A., Dawson, V. L. & Dawson, T. M. Parthanatos: mitochondrial-linked mechanisms and therapeutic opportunities. *Br J Pharmacol* **171**, 2000–2016 (2014).
244. Akira, S., Uematsu, S. & Takeuchi, O. Pathogen recognition and innate immunity. *Cell* **124**, 783–801 (2006).
245. Akira, S., Uematsu, S. & Takeuchi, O. Pathogen recognition and innate immunity. *Cell* **124**, 783–801 (2006).
246. Kumar, H., Kawai, T. & Akira, S. Pathogen recognition by the innate immune system. *Int Rev Immunol* **30**, 16–34 (2011).
247. Qian, J. *et al.* Pathogen Recognition Receptor Signaling Accelerates Phosphorylation-Dependent Degradation of IFNAR1. *PLOS Pathogens* **7**, e1002065 (2011).
248. Pathogen Recognition Receptor Signaling Accelerates Phosphorylation-Dependent Degradation of IFNAR1 | PLOS Pathogens. https://journals.plos.org/plospathogens/article?id=10.1371/journal.ppat.1002065.
249. Li, D. & Wu, M. Pattern recognition receptors in health and diseases. *Sig Transduct Target Ther* **6**, 1–24 (2021).
250. Wang, H. *et al.* PELI1 functions as a dual modulator of necroptosis and apoptosis by regulating ubiquitination of RIPK1 and mRNA levels of c-FLIP. *Proc Natl Acad Sci U S A* **114**, 11944–11949 (2017).
251. Choi, S.-W. *et al.* PELI1 Selectively Targets Kinase-Active RIP3 for Ubiquitylation-Dependent Proteasomal Degradation. *Mol Cell* **70**, 920-935.e7 (2018).
252. Zeng, J. *et al.* Peptide-based allosteric inhibitor targets TNFR1 conformationally active region and disables receptor–ligand signaling complex. *Proc Natl Acad Sci U S A* **121**, e2308132121.
253. Perplexity. *Perplexity AI* https://www.perplexity.ai/search/new?q=pending&newFrontendContextUUID=a99421b2-0bb8-4b9a-a950-3c34ef9820ee&_rsc=1csqs.
254. Kagan, J. C. & Medzhitov, R. Phosphoinositide-mediated adaptor recruitment controls Toll-like receptor signaling. *Cell* **125**, 943–955 (2006).
255. Bhatt, S., Xiao, Z., Meng, Z. & Katzenellenbogen, B. S. Phosphorylation by p38 Mitogen-Activated Protein Kinase Promotes Estrogen Receptor α Turnover and Functional Activity via the SCFSkp2 Proteasomal Complex. *Mol Cell Biol* **32**, 1928–1943 (2012).
256. Liu, S. *et al.* Phosphorylation of innate immune adaptor proteins MAVS, STING, and TRIF induces IRF3 activation. *Science* **347**, aaa2630 (2015).
257. Phosphorylation of innate immune adaptor proteins MAVS, STING, and TRIF induces IRF3 activation | Science. https://www.science.org/doi/10.1126/science.aaa2630.
258. Pilz, A. *et al.* Phosphorylation of the Stat1 transactivating domain is required for the response to type I interferons. *EMBO Rep* **4**, 368–373 (2003).
259. Clement, S. L., Scheckel, C., Stoecklin, G. & Lykke-Andersen, J. Phosphorylation of tristetraprolin by MK2 impairs AU-rich element mRNA decay by preventing deadenylase recruitment. *Mol Cell Biol* **31**, 256–266 (2011).
260. Phosphorylation of tristetraprolin by MK2 impairs AU-rich element mRNA decay by preventing deadenylase recruitment - PubMed. https://pubmed.ncbi.nlm.nih.gov/21078877/.
261. Cai, Z. *et al.* Plasma membrane translocation of trimerized MLKL protein is required for TNF-induced necroptosis. *Nat Cell Biol* **16**, 55–65 (2014).

262. Cai, Z. *et al.* Plasma membrane translocation of trimerized MLKL protein is required for TNF-induced necroptosis. *Nat Cell Biol* **16**, 55–65 (2014).
263. Anderson, P. Post-transcriptional control of cytokine production. *Nat Immunol* **9**, 353–359 (2008).
264. Douglas, T. & Saleh, M. Post-translational Modification of OTULIN Regulates Ubiquitin Dynamics and Cell Death. *Cell Rep* **29**, 3652-3663.e5 (2019).
265. Chi, H., Pepper, M. & Thomas, P. G. Principles and therapeutic applications of adaptive immunity. *Cell* **187**, 2052–2078 (2024).
266. Raingeaud, J. *et al.* Pro-inflammatory Cytokines and Environmental Stress Cause p38 Mitogen-activated Protein Kinase Activation by Dual Phosphorylation on Tyrosine and Threonine (∗). *Journal of Biological Chemistry* **270**, 7420–7426 (1995).
267. Fuchs, Y. & Steller, H. Programmed Cell Death in Animal Development and Disease. *Cell* **147**, 742–758 (2011).
268. Chen, I.-T. *et al.* Promyelocytic leukemia protein targets MK2 to promote cytotoxicity. *EMBO Rep* **22**, e52254 (2021).
269. Uddin, S. *et al.* Protein kinase C-delta (PKC-delta) is activated by type I interferons and mediates phosphorylation of Stat1 on serine 727. *J Biol Chem* **277**, 14408–14416 (2002).
270. Mosmann, T. Rapid colorimetric assay for cellular growth and survival: application to proliferation and cytotoxicity assays. *J Immunol Methods* **65**, 55–63 (1983).
271. Zhao, T. *et al.* Reactive oxygen species-based nanomaterials for the treatment of myocardial ischemia reperfusion injuries. *Bioact Mater* **7**, 47–72 (2022).
272. He, S. *et al.* Receptor interacting protein kinase-3 determines cellular necrotic response to TNF-alpha. *Cell* **137**, 1100–1111 (2009).
273. He, S. *et al.* Receptor interacting protein kinase-3 determines cellular necrotic response to TNF-alpha. *Cell* **137**, 1100–1111 (2009).
274. Kaiser, W. J., Upton, J. W. & Mocarski, E. S. Receptor-interacting protein homotypic interaction motif-dependent control of NF-kappa B activation via the DNA-dependent activator of IFN regulatory factors. *J Immunol* **181**, 6427–6434 (2008).
275. Liu, B., Xie, C., Richardson, J. A., Turley, S. D. & Dietschy, J. M. Receptor-mediated and bulk-phase endocytosis cause macrophage and cholesterol accumulation in Niemann-Pick C disease. *J Lipid Res* **48**, 1710–1723 (2007).
276. Sadzak, I. *et al.* Recruitment of Stat1 to chromatin is required for interferon-induced serine phosphorylation of Stat1 transactivation domain. *Proc Natl Acad Sci U S A* **105**, 8944–8949 (2008).
277. Zhang, G. *et al.* Regulated necrosis, a proinflammatory cell death, potentially counteracts pathogenic infections. *Cell Death Dis* **13**, 637 (2022).
278. Conrad, M., Angeli, J. P. F., Vandenabeele, P. & Stockwell, B. R. Regulated necrosis: disease relevance and therapeutic opportunities. *Nat Rev Drug Discov* **15**, 348–366 (2016).
279. Regulated necrosis: disease relevance and therapeutic opportunities | Nature Reviews Drug Discovery. https://www.nature.com/articles/nrd.2015.6.
280. Vanden Berghe, T., Linkermann, A., Jouan-Lanhouet, S., Walczak, H. & Vandenabeele, P. Regulated necrosis: the expanding network of non-apoptotic cell death pathways. *Nat Rev Mol Cell Biol* **15**, 135–147 (2014).
281. Vallabhapurapu, S. & Karin, M. Regulation and function of NF-kappaB transcription factors in the immune system. *Annu Rev Immunol* **27**, 693–733 (2009).
282. Ofengeim, D. & Yuan, J. Regulation of RIP1 kinase signalling at the crossroads of

inflammation and cell death. *Nat Rev Mol Cell Biol* **14**, 727–736 (2013).
283. Ofengeim, D. & Yuan, J. Regulation of RIP1 kinase signalling at the crossroads of inflammation and cell death. *Nat Rev Mol Cell Biol* **14**, 727–736 (2013).
284. Geng, J. *et al.* Regulation of RIPK1 activation by TAK1-mediated phosphorylation dictates apoptosis and necroptosis. *Nat Commun* **8**, 359 (2017).
285. Moriwaki, K. & Chan, F. K.-M. Regulation of RIPK3- and RHIM-dependent Necroptosis by the Proteasome. *J Biol Chem* **291**, 5948–5959 (2016).
286. Brenner, D., Blaser, H. & Mak, T. W. Regulation of tumour necrosis factor signalling: live or let die. *Nat Rev Immunol* **15**, 362–374 (2015).
287. Regulation of tumour necrosis factor signalling: live or let die | Nature Reviews Immunology. https://www.nature.com/articles/nri3834.
288. Ivashkiv, L. B. & Donlin, L. T. Regulation of type I interferon responses. *Nat Rev Immunol* **14**, 36–49 (2014).
289. Ivashkiv, L. B. & Donlin, L. T. Regulation of type I interferon responses. *Nat Rev Immunol* **14**, 36–49 (2014).
290. Chen, K., Liu, J. & Cao, X. Regulation of type I interferon signaling in immunity and inflammation: A comprehensive review. *J Autoimmun* **83**, 1–11 (2017).
291. Zhao, F., Zhang, J., Liu, Y.-S., Li, L. & He, Y.-L. Research advances on flotillins. *Virol J* **8**, 479 (2011).
292. Duprez, L. *et al.* RIP kinase-dependent necrosis drives lethal systemic inflammatory response syndrome. *Immunity* **35**, 908–918 (2011).
293. Vivarelli, M. S. *et al.* RIP links TLR4 to Akt and is essential for cell survival in response to LPS stimulation. *J Exp Med* **200**, 399–404 (2004).
294. Meylan, E. *et al.* RIP1 is an essential mediator of Toll-like receptor 3-induced NF-kappa B activation. *Nat Immunol* **5**, 503–507 (2004).
295. Meylan, E. *et al.* RIP1 is an essential mediator of Toll-like receptor 3-induced NF-kappa B activation. *Nat Immunol* **5**, 503–507 (2004).
296. Meylan, E. *et al.* RIP1 is an essential mediator of Toll-like receptor 3-induced NF-kappa B activation. *Nat Immunol* **5**, 503–507 (2004).
297. Lukens, J. R. *et al.* RIP1-driven autoinflammation targets IL-1α independently of inflammasomes and RIP3. *Nature* **498**, 224–227 (2013).
298. Festjens, N., Vanden Berghe, T., Cornelis, S. & Vandenabeele, P. RIP1, a kinase on the crossroads of a cell's decision to live or die. *Cell Death Differ* **14**, 400–410 (2007).
299. RIP1, a kinase on the crossroads of a cell's decision to live or die | Cell Death & Differentiation. https://www.nature.com/articles/4402085.
300. Zhang, D.-W. *et al.* RIP3, an energy metabolism regulator that switches TNF-induced cell death from apoptosis to necrosis. *Science* **325**, 332–336 (2009).
301. Najjar, M. *et al.* RIPK1 and RIPK3 kinases promote cell death-independent inflammation by Toll-like receptor 4. *Immunity* **45**, 46–59 (2016).
302. Najjar, M. *et al.* RIPK1 and RIPK3 kinases promote cell death-independent inflammation by Toll-like receptor 4. *Immunity* **45**, 46–59 (2016).
303. Delanghe, T., Dondelinger, Y. & Bertrand, M. J. M. RIPK1 Kinase-Dependent Death: A Symphony of Phosphorylation Events. *Trends in Cell Biology* **30**, 189–200 (2020).
304. Ito, Y. *et al.* RIPK1 mediates axonal degeneration by promoting inflammation and necroptosis in ALS. *Science* **353**, 603–608 (2016).
305. Dondelinger, Y. *et al.* RIPK3 contributes to TNFR1-mediated RIPK1 kinase-dependent

apoptosis in conditions of cIAP1/2 depletion or TAK1 kinase inhibition. *Cell Death Differ* **20**, 1381–1392 (2013).
306. Lawlor, K. E. *et al.* RIPK3 promotes cell death and NLRP3 inflammasome activation in the absence of MLKL. *Nat Commun* **6**, 6282 (2015).
307. Atri, C., Guerfali, F. Z. & Laouini, D. Role of Human Macrophage Polarization in Inflammation during Infectious Diseases. *Int J Mol Sci* **19**, 1801 (2018).
308. Chen, Z., Tian, R., She, Z., Cai, J. & Li, H. Role of oxidative stress in the pathogenesis of nonalcoholic fatty liver disease. *Free Radic Biol Med* **152**, 116–141 (2020).
309. Safa, A. R. Roles of c-FLIP in Apoptosis, Necroptosis, and Autophagy. *J Carcinog Mutagen* **Suppl 6**, 003 (2013).
310. Quarato, G. *et al.* Sequential Engagement of Distinct MLKL Phosphatidylinositol–Binding Sites Executes Necroptosis. *Mol Cell* **61**, 589–601 (2016).
311. Hayden, M. S. & Ghosh, S. Shared principles in NF-kappaB signaling. *Cell* **132**, 344–362 (2008).
312. Nakamura, A., Goto, Y., Kondo, Y. & Aoki, K. Shedding light on developmental ERK signaling with genetically encoded biosensors. *Development* **148**, dev199767 (2021).
313. Hayden, M. S. & Ghosh, S. Signaling to NF-kappaB. *Genes Dev* **18**, 2195–2224 (2004).
314. Micali, O. C. *et al.* Silencing of the XAF1 gene by promoter hypermethylation in cancer cells and reactivation to TRAIL-sensitization by IFN-beta. *BMC Cancer* **7**, 52 (2007).
315. Karathanasis, C. *et al.* Single-molecule imaging reveals the oligomeric state of functional TNFα-induced plasma membrane TNFR1 clusters in cells. *Sci Signal* **13**, eaax5647 (2020).
316. Du, C., Fang, M., Li, Y., Li, L. & Wang, X. Smac, a mitochondrial protein that promotes cytochrome c-dependent caspase activation by eliminating IAP inhibition. *Cell* **102**, 33–42 (2000).
317. van Weering, J. R. T., Verkade, P. & Cullen, P. J. SNX-BAR proteins in phosphoinositide-mediated, tubular-based endosomal sorting. *Semin Cell Dev Biol* **21**, 371–380 (2010).
318. Kovarik, P. *et al.* Specificity of signaling by STAT1 depends on SH2 and C-terminal domains that regulate Ser727 phosphorylation, differentially affecting specific target gene expression. *EMBO J* **20**, 91–100 (2001).
319. Thottacherry, J. J., Sathe, M., Prabhakara, C. & Mayor, S. Spoiled for Choice: Diverse Endocytic Pathways Function at the Cell Surface. *Annu Rev Cell Dev Biol* **35**, 55–84 (2019).
320. Fink, K. & Grandvaux, N. STAT2 and IRF9: Beyond ISGF3. *JAKSTAT* **2**, e27521 (2013).
321. Chen, G. Y. & Nuñez, G. Sterile inflammation: sensing and reacting to damage. *Nat Rev Immunol* **10**, 826–837 (2010).
322. Sterile inflammation: sensing and reacting to damage - PMC. https://pmc.ncbi.nlm.nih.gov/articles/PMC3114424/.
323. Guo, X. *et al.* TAK1 regulates caspase 8 activation and necroptotic signaling via multiple cell death checkpoints. *Cell Death Dis* **7**, e2381–e2381 (2016).
324. Karunakaran, D. *et al.* Targeting macrophage necroptosis for therapeutic and diagnostic interventions in atherosclerosis. *Sci Adv* **2**, e1600224 (2016).
325. Li, Q., Li, H., Blitvich, B. J. & Zhang, J. The Aedes albopictus inhibitor of apoptosis 1 gene protects vertebrate cells from bluetongue virus-induced apoptosis. *Insect Mol Biol* **16**, 93–105 (2007).
326. Iovine, N., Eastvold, J., Elsbach, P., Weiss, J. P. & Gioannini, T. L. The carboxyl-terminal domain of closely related endotoxin-binding proteins determines the target of protein-lipopolysaccharide complexes. *J Biol Chem* **277**, 7970–7978 (2002).

327. Iovine, N., Eastvold, J., Elsbach, P., Weiss, J. P. & Gioannini, T. L. The carboxyl-terminal domain of closely related endotoxin-binding proteins determines the target of protein-lipopolysaccharide complexes. *J Biol Chem* **277**, 7970–7978 (2002).
328. Brumatti, G. *et al.* The caspase-8 inhibitor emricasan combines with the SMAC mimetic birinapant to induce necroptosis and treat acute myeloid leukemia. *Sci Transl Med* **8**, 339ra69 (2016).
329. Ji, L. *et al.* The crucial regulatory role of type I interferon in inflammatory diseases. *Cell & Bioscience* **13**, 230 (2023).
330. Lee, T. H. *et al.* The Death Domain Kinase RIP1 Is Essential for Tumor Necrosis Factor Alpha Signaling to p38 Mitogen-Activated Protein Kinase. *Mol Cell Biol* **23**, 8377–8385 (2003).
331. Pasrija, R. & Naime, M. The deregulated immune reaction and cytokines release storm (CRS) in COVID-19 disease. *Int Immunopharmacol* **90**, 107225 (2021).
332. Silke, J., Rickard, J. A. & Gerlic, M. The diverse role of RIP kinases in necroptosis and inflammation. *Nat Immunol* **16**, 689–697 (2015).
333. Santy, L. C., Ravichandran, K. S. & Casanova, J. E. The DOCK180/Elmo complex couples ARNO-mediated Arf6 activation to the downstream activation of Rac1. *Curr Biol* **15**, 1749–1754 (2005).
334. Ye, K., Chen, Z. & Xu, Y. The double-edged functions of necroptosis. *Cell Death Dis* **14**, 1–12 (2023).
335. Cooper, M. D. The early history of B cells. *Nat Rev Immunol* **15**, 191–197 (2015).
336. Wajant, H. The Fas signaling pathway: more than a paradigm. *Science* **296**, 1635–1636 (2002).
337. The Fas signaling pathway: more than a paradigm - PubMed. https://pubmed.ncbi.nlm.nih.gov/12040174/.
338. The function of the thymus and its impact on modern medicine | Science. https://www.science.org/doi/10.1126/science.aba2429.
339. Israël, A. The IKK Complex, a Central Regulator of NF-κB Activation. *Cold Spring Harb Perspect Biol* **2**, a000158 (2010).
340. Kondylis, V., Kumari, S., Vlantis, K. & Pasparakis, M. The interplay of IKK, NF-κB and RIPK1 signaling in the regulation of cell death, tissue homeostasis and inflammation. *Immunol Rev* **277**, 113–127 (2017).
341. Martinez-Osorio, V., Abdelwahab, Y. & Ros, U. The Many Faces of MLKL, the Executor of Necroptosis. *Int J Mol Sci* **24**, 10108 (2023).
342. Sun, S.-C. The noncanonical NF-κB pathway. *Immunol Rev* **246**, 125–140 (2012).
343. Winzen, R. *et al.* The p38 MAP kinase pathway signals for cytokine-induced mRNA stabilization via MAP kinase-activated protein kinase 2 and an AU-rich region-targeted mechanism. *EMBO J* **18**, 4969–4980 (1999).
344. Tiedje, C. *et al.* The p38/MK2-Driven Exchange between Tristetraprolin and HuR Regulates AU–Rich Element–Dependent Translation. *PLOS Genetics* **8**, e1002977 (2012).
345. Beamer, E. & Corrêa, S. A. L. The p38MAPK-MK2 Signaling Axis as a Critical Link Between Inflammation and Synaptic Transmission. *Front. Cell Dev. Biol.* **9**, (2021).
346. Murphy, J. M. *et al.* The Pseudokinase MLKL Mediates Necroptosis via a Molecular Switch Mechanism. *Immunity* **39**, 443–453 (2013).
347. Husebye, H. *et al.* The Rab11a GTPase controls Toll-like receptor 4-induced activation of interferon regulatory factor-3 on phagosomes. *Immunity* **33**, 583–596 (2010).

348. Uddin, S. *et al.* The Rac1/p38 mitogen-activated protein kinase pathway is required for interferon alpha-dependent transcriptional activation but not serine phosphorylation of Stat proteins. *J Biol Chem* **275**, 27634–27640 (2000).
349. Wennerberg, K., Rossman, K. L. & Der, C. J. The Ras superfamily at a glance. *J Cell Sci* **118**, 843–846 (2005).
350. Fan, W. *et al.* The RhoA GTPase regulates Type I Interferon Signaling in Systemic lupus erythematosus. *Res Sq* rs.3.rs-3320841 (2023) doi:10.21203/rs.3.rs-3320841/v1.
351. Li, J. *et al.* The RIP1/RIP3 Necrosome Forms a Functional Amyloid Signaling Complex Required for Programmed Necrosis. *Cell* **150**, 339–350 (2012).
352. Li, J. *et al.* The RIP1/RIP3 Necrosome Forms a Functional Amyloid Signaling Complex Required for Programmed Necrosis. *Cell* **150**, 339–350 (2012).
353. Li, J. *et al.* The RIP1/RIP3 Necrosome Forms a Functional Amyloid Signaling Complex Required for Programmed Necrosis. *Cell* **150**, 339–350 (2012).
354. The RIP1/RIP3 Necrosome Forms a Functional Amyloid Signaling Complex Required for Programmed Necrosis: Cell. https://www.cell.com/cell/fulltext/S0092-8674(12)00772-6?_returnURL=https%3A%2F%2Flinkinghub.elsevier.com%2Fretrieve%2Fpii%2FS0092867412007726%3Fshowall%3Dtrue.
355. Oberbeck, N. *et al.* The RIPK4–IRF6 signalling axis safeguards epidermal differentiation and barrier function. *Nature* **574**, 249–253 (2019).
356. Tenev, T. *et al.* The Ripoptosome, a Signaling Platform that Assembles in Response to Genotoxic Stress and Loss of IAPs. *Molecular Cell* **43**, 432–448 (2011).
357. Tenev, T. *et al.* The Ripoptosome, a Signaling Platform that Assembles in Response to Genotoxic Stress and Loss of IAPs. *Molecular Cell* **43**, 432–448 (2011).
358. Haneklaus, M., O'Neil, J. D., Clark, A. R., Masters, S. L. & O'Neill, L. A. J. The RNA-binding protein Tristetraprolin (TTP) is a critical negative regulator of the NLRP3 inflammasome. *J Biol Chem* **292**, 6869–6881 (2017).
359. Tiedje, C. *et al.* The RNA-binding protein TTP is a global post-transcriptional regulator of feedback control in inflammation. *Nucleic Acids Res* **44**, 7418–7440 (2016).
360. The RNA-binding protein TTP is a global post-transcriptional regulator of feedback control in inflammation - PMC. https://pmc.ncbi.nlm.nih.gov/articles/PMC5009735/.
361. Chen, Y. R., Wang, X., Templeton, D., Davis, R. J. & Tan, T. H. The role of c-Jun N-terminal kinase (JNK) in apoptosis induced by ultraviolet C and gamma radiation. Duration of JNK activation may determine cell death and proliferation. *J Biol Chem* **271**, 31929–31936 (1996).
362. Chen, Y.-R., Wang, X., Templeton, D., Davis, R. J. & Tan, T.-H. The Role of c-Jun N-terminal Kinase (JNK) in Apoptosis Induced by Ultraviolet C and γ Radiation. *Journal of Biological Chemistry* **271**, 31929–31936 (1996).
363. Schilperoort, M. *et al.* The role of efferocytosis-fueled macrophage metabolism in the resolution of inflammation. *Immunol Rev* **319**, 65–80 (2023).
364. Pidwill, G. R., Gibson, J. F., Cole, J., Renshaw, S. A. & Foster, S. J. The Role of Macrophages in Staphylococcus aureus Infection. *Front Immunol* **11**, 620339 (2020).
365. Hsu, S.-K. *et al.* The Role of Necroptosis in ROS-Mediated Cancer Therapies and Its Promising Applications. *Cancers (Basel)* **12**, 2185 (2020).
366. Yu, X., Deng, Q., Bode, A. M., Dong, Z. & Cao, Y. The role of necroptosis, an alternative form of cell death, in cancer therapy. *Expert Rev Anticancer Ther* **13**, 883–893 (2013).
367. Vandenabeele, P., Declercq, W., Van Herreweghe, F. & Vanden Berghe, T. The role of the kinases RIP1 and RIP3 in TNF-induced necrosis. *Sci Signal* **3**, re4 (2010).

368. Ronkina, N. *et al.* The Role of TTP Phosphorylation in the Regulation of Inflammatory Cytokine Production by MK2/3. *J Immunol* **203**, 2291–2300 (2019).
369. The Role of TTP Phosphorylation in the Regulation of Inflammatory Cytokine Production by MK2/3 - PubMed. https://pubmed.ncbi.nlm.nih.gov/31527197/.
370. Jang, D.-I. *et al.* The Role of Tumor Necrosis Factor Alpha (TNF-α) in Autoimmune Disease and Current TNF-α Inhibitors in Therapeutics. *Int J Mol Sci* **22**, 2719 (2021).
371. Basquin, C. *et al.* The signalling factor PI3K is a specific regulator of the clathrin-independent dynamin-dependent endocytosis of IL-2 receptors. *J Cell Sci* **126**, 1099–1108 (2013).
372. Van Acker, T., Tavernier, J. & Peelman, F. The Small GTPase Arf6: An Overview of Its Mechanisms of Action and of Its Role in Host–Pathogen Interactions and Innate Immunity. *Int J Mol Sci* **20**, 2209 (2019).
373. Park, B. S. *et al.* The structural basis of lipopolysaccharide recognition by the TLR4–MD-2 complex. *Nature* **458**, 1191–1195 (2009).
374. The structural basis of lipopolysaccharide recognition by the TLR4–MD-2 complex | Nature. https://www.nature.com/articles/nature07830.
375. Locksley, R. M., Killeen, N. & Lenardo, M. J. The TNF and TNF receptor superfamilies: integrating mammalian biology. *Cell* **104**, 487–501 (2001).
376. Hsu, H., Xiong, J. & Goeddel, D. V. The TNF receptor 1-associated protein TRADD signals cell death and NF-kappa B activation. *Cell* **81**, 495–504 (1995).
377. Shu, H. B., Takeuchi, M. & Goeddel, D. V. The tumor necrosis factor receptor 2 signal transducers TRAF2 and c-IAP1 are components of the tumor necrosis factor receptor 1 signaling complex. *Proc Natl Acad Sci U S A* **93**, 13973–13978 (1996).
378. Kovalenko, A. *et al.* The tumour suppressor CYLD negatively regulates NF-kappaB signalling by deubiquitination. *Nature* **424**, 801–805 (2003).
379. Kovalenko, A. *et al.* The tumour suppressor CYLD negatively regulates NF-kappaB signalling by deubiquitination. *Nature* **424**, 801–805 (2003).
380. Kwon, Y. T. & Ciechanover, A. The Ubiquitin Code in the Ubiquitin-Proteasome System and Autophagy. *Trends Biochem Sci* **42**, 873–886 (2017).
381. Hershko, A. & Ciechanover, A. The ubiquitin system. *Annu Rev Biochem* **67**, 425–479 (1998).
382. Onizawa, M. *et al.* The ubiquitin-modifying enzyme A20 restricts the ubiquitination of RIPK3 and protects cells from necroptosis. *Nat Immunol* **16**, 618–627 (2015).
383. Onizawa, M. *et al.* The ubiquitin-modifying enzyme A20 restricts ubiquitination of the kinase RIPK3 and protects cells from necroptosis. *Nat Immunol* **16**, 618–627 (2015).
384. Kalai, M. *et al.* Tipping the balance between necrosis and apoptosis in human and murine cells treated with interferon and dsRNA. *Cell Death Differ* **9**, 981–994 (2002).
385. Oshiumi, H. *et al.* TIR-containing adapter molecule (TICAM)-2, a bridging adapter recruiting to toll-like receptor 4 TICAM-1 that induces interferon-beta. *J Biol Chem* **278**, 49751–49762 (2003).
386. Oshiumi, H. *et al.* TIR-containing adapter molecule (TICAM)-2, a bridging adapter recruiting to toll-like receptor 4 TICAM-1 that induces interferon-beta. *J Biol Chem* **278**, 49751–49762 (2003).
387. Takeda, K. & Akira, S. TLR signaling pathways. *Semin Immunol* **16**, 3–9 (2004).
388. Yarilina, A., Park-Min, K.-H., Antoniv, T., Hu, X. & Ivashkiv, L. B. TNF activates an IRF1-dependent autocrine loop leading to sustained expression of chemokines and STAT1-

dependent type I interferon-response genes. *Nat Immunol* **9**, 378–387 (2008).
389. Wang, L., Du, F. & Wang, X. TNF-alpha induces two distinct caspase-8 activation pathways. *Cell* **133**, 693–703 (2008).
390. Wang, L., Du, F. & Wang, X. TNF-alpha induces two distinct caspase-8 activation pathways. *Cell* **133**, 693–703 (2008).
391. Vanlangenakker, N., Bertrand, M. J. M., Bogaert, P., Vandenabeele, P. & Vanden Berghe, T. TNF-induced necroptosis in L929 cells is tightly regulated by multiple TNFR1 complex I and II members. *Cell Death Dis* **2**, e230 (2011).
392. Vanlangenakker, N., Bertrand, M. J. M., Bogaert, P., Vandenabeele, P. & Vanden Berghe, T. TNF-induced necroptosis in L929 cells is tightly regulated by multiple TNFR1 complex I and II members. *Cell Death Dis* **2**, e230 (2011).
393. Vanlangenakker, N., Bertrand, M. J. M., Bogaert, P., Vandenabeele, P. & Vanden Berghe, T. TNF-induced necroptosis in L929 cells is tightly regulated by multiple TNFR1 complex I and II members. *Cell Death Dis* **2**, e230 (2011).
394. Xu, C. *et al.* TNF-α-dependent neuronal necroptosis regulated in Alzheimer's disease by coordination of RIPK1-p62 complex with autophagic UVRAG. *Theranostics* **11**, 9452–9469 (2021).
395. Wajant, H. & Scheurich, P. TNFR1-induced activation of the classical NF-κB pathway. *The FEBS Journal* **278**, 862–876 (2011).
396. TNFR1-induced activation of the classical NF-κB pathway - Wajant - 2011 - The FEBS Journal - Wiley Online Library. https://febs.onlinelibrary.wiley.com/doi/10.1111/j.1742-4658.2011.08015.x.
397. Kaiser, W. J. *et al.* Toll-like receptor 3-mediated necrosis via TRIF, RIP3, and MLKL. *J Biol Chem* **288**, 31268–31279 (2013).
398. Akira, S. & Takeda, K. Toll-like receptor signalling. *Nat Rev Immunol* **4**, 499–511 (2004).
399. Toll-like Receptor-mediated Down-regulation of the Deubiquitinase Cylindromatosis (CYLD) Protects Macrophages from Necroptosis in Wild-derived Mice - ScienceDirect. https://www.sciencedirect.com/science/article/pii/S0021925820387809.
400. Schworer, S. A. *et al.* Toll-like Receptor-mediated Down-regulation of the Deubiquitinase Cylindromatosis (CYLD) Protects Macrophages from Necroptosis in Wild-derived Mice*. *Journal of Biological Chemistry* **289**, 14422–14433 (2014).
401. Wicherska-Pawłowska, K., Wróbel, T. & Rybka, J. Toll-Like Receptors (TLRs), NOD-Like Receptors (NLRs), and RIG-I-Like Receptors (RLRs) in Innate Immunity. TLRs, NLRs, and RLRs Ligands as Immunotherapeutic Agents for Hematopoietic Diseases. *Int J Mol Sci* **22**, 13397 (2021).
402. He, S., Liang, Y., Shao, F. & Wang, X. Toll-like receptors activate programmed necrosis in macrophages through a receptor-interacting kinase-3-mediated pathway. *Proc Natl Acad Sci U S A* **108**, 20054–20059 (2011).
403. Xie, P. TRAF molecules in cell signaling and in human diseases. *Journal of Molecular Signaling* **8**, 7 (2013).
404. TRAF molecules in cell signaling and in human diseases - PMC. https://pmc.ncbi.nlm.nih.gov/articles/PMC3697994/.
405. TRAF molecules in cell signaling and in human diseases | Journal of Molecular Signaling. https://jmolecularsignaling.com/articles/10.1186/1750-2187-8-7.
406. Vince, J. E. *et al.* TRAF2 must bind to cellular inhibitors of apoptosis for tumor necrosis factor (tnf) to efficiently activate nf-{kappa}b and to prevent tnf-induced apoptosis. *J Biol*

Chem **284**, 35906–35915 (2009).
407. Jouan-Lanhouet, S. *et al.* TRAIL induces necroptosis involving RIPK1/RIPK3-dependent PARP-1 activation. *Cell Death Differ* **19**, 2003–2014 (2012).
408. Au-Yeung, N., Mandhana, R. & Horvath, C. M. Transcriptional regulation by STAT1 and STAT2 in the interferon JAK-STAT pathway. *JAKSTAT* **2**, e23931 (2013).
409. Chen, X. *et al.* Translocation of mixed lineage kinase domain-like protein to plasma membrane leads to necrotic cell death. *Cell Res* **24**, 105–121 (2014).
410. Ullah, M. O., Sweet, M. J., Mansell, A., Kellie, S. & Kobe, B. TRIF-dependent TLR signaling, its functions in host defense and inflammation, and its potential as a therapeutic target. *Journal of Leukocyte Biology* **100**, 27–45 (2016).
411. TRIF-dependent TLR signaling, its functions in host defense and inflammation, and its potential as a therapeutic target - Ullah - 2016 - Journal of Leukocyte Biology - Wiley Online Library. https://jlb.onlinelibrary.wiley.com/doi/full/10.1189/jlb.2ri1115-531r.
412. Ariana, A. *et al.* Tristetraprolin regulates necroptosis during tonic Toll-like receptor 4 (TLR4) signaling in murine macrophages. *J Biol Chem* **295**, 4661–4672 (2020).
413. Wajant, H., Pfizenmaier, K. & Scheurich, P. Tumor necrosis factor signaling. *Cell Death Differ* **10**, 45–65 (2003).
414. Tumor necrosis factor signaling | Cell Death & Differentiation. https://www.nature.com/articles/4401189.
415. Farajzadeh, D., Karimi-Gharigh, S. & Dastmalchi, S. Tumor necrosis factor-alpha and its inhibition strategies: review article. *Tehran University Medical Journal TUMS Publications* (2017).
416. Vince, J. E. *et al.* TWEAK-FN14 signaling induces lysosomal degradation of a cIAP1–TRAF2 complex to sensitize tumor cells to TNFα. *J Cell Biol* **182**, 171–184 (2008).
417. Montaner, L. J. *et al.* Type 1 and Type 2 Cytokine Regulation of Macrophage Endocytosis: Differential Activation by IL-4/IL-13 as Opposed to IFN-γ or IL-101. *The Journal of Immunology* **162**, 4606–4613 (1999).
418. Wu, D. *et al.* Type 1 interferons induce changes in core metabolism that are critical for immune function. *Immunity* **44**, 1325–1336 (2016).
419. Wu, D. *et al.* Type 1 Interferons Induce Changes in Core Metabolism that Are Critical for Immune Function. *Immunity* **44**, 1325–1336 (2016).
420. McNab, F. W. *et al.* Type I IFN Induces IL-10 Production in an IL-27–Independent Manner and Blocks Responsiveness to IFN-γ for Production of IL-12 and Bacterial Killing in Mycobacterium tuberculosis–Infected Macrophages. *J Immunol* **193**, 3600–3612 (2014).
421. Type I IFN Induces IL-10 Production in an IL-27–Independent Manner and Blocks Responsiveness to IFN-γ for Production of IL-12 and Bacterial Killing in Mycobacterium tuberculosis–Infected Macrophages - PMC. https://pmc.ncbi.nlm.nih.gov/articles/PMC4170673/.
422. Hos, N. J. *et al.* Type I interferon enhances necroptosis of Salmonella Typhimurium–infected macrophages by impairing antioxidative stress responses. *J Cell Biol* **216**, 4107–4121 (2017).
423. Robinson, N. *et al.* Type I interferon induces necroptosis in macrophages during infection with Salmonella enterica serovar Typhimurium. *Nat Immunol* **13**, 954–962 (2012).
424. Guarda, G. *et al.* Type I interferon inhibits interleukin-1 production and inflammasome activation. *Immunity* **34**, 213–223 (2011).
425. Fernandez-Ruiz, R. & Niewold, T. B. Type I Interferons in Autoimmunity. *J Invest Dermatol* **142**, 793–803 (2022).

426. Type I interferons in infectious disease - PMC. https://pmc.ncbi.nlm.nih.gov/articles/PMC7162685/.
427. Type I interferons in infectious disease | Nature Reviews Immunology. https://www.nature.com/articles/nri3787.
428. McComb, S. *et al.* Type-I interferon signaling through ISGF3 complex is required for sustained Rip3 activation and necroptosis in macrophages. *Proc Natl Acad Sci U S A* **111**, E3206-3213 (2014).
429. McComb, S. *et al.* Type-I interferon signaling through ISGF3 complex is required for sustained Rip3 activation and necroptosis in macrophages. *Proc Natl Acad Sci U S A* **111**, E3206–E3213 (2014).
430. Type-I interferon signaling through ISGF3 complex is required for sustained Rip3 activation and necroptosis in macrophages - PMC. https://pmc.ncbi.nlm.nih.gov/articles/PMC4128105/.
431. Swatek, K. N. & Komander, D. Ubiquitin modifications. *Cell Res* **26**, 399–422 (2016).
432. Dagar, G., Kumar, R., Yadav, K. K., Singh, M. & Pandita, T. K. Ubiquitination and deubiquitination: Implications on cancer therapy. *Biochimica et Biophysica Acta (BBA) - Gene Regulatory Mechanisms* **1866**, 194979 (2023).
433. Li, H., Kobayashi, M., Blonska, M., You, Y. & Lin, X. Ubiquitination of RIP is required for tumor necrosis factor alpha-induced NF-kappaB activation. *J Biol Chem* **281**, 13636–13643 (2006).
434. Vucic, D., Dixit, V. M. & Wertz, I. E. Ubiquitylation in apoptosis: a post-translational modification at the edge of life and death. *Nat Rev Mol Cell Biol* **12**, 439–452 (2011).
435. Clarke, M. C. H., Talib, S., Figg, N. L. & Bennett, M. R. Vascular smooth muscle cell apoptosis induces interleukin-1-directed inflammation: effects of hyperlipidemia-mediated inhibition of phagocytosis. *Circ Res* **106**, 363–372 (2010).
436. Ahn, J. *et al.* XAF1 is secreted from stressed tumor cells to activate T cell-mediated tumor surveillance via Lck-ERK signaling. *Neoplasia* **59**, 101094 (2025).
437. Betancor, G. You Shall Not Pass: MX2 Proteins Are Versatile Viral Inhibitors. *Vaccines (Basel)* **11**, 930 (2023).
438. Yuan, F. *et al.* Z-DNA binding protein 1 promotes heatstroke-induced cell death. *Science* **376**, 609–615 (2022).
439. Jiao, H. *et al.* Z-nucleic-acid sensing triggers ZBP1-dependent necroptosis and inflammation. *Nature* **580**, 391–395 (2020).